

Traces of disease in amyotrophic lateral sclerosis

Esther Verstraete

Cover design Happy Garaje (www.happygaraje.com) and Esther Verstraete
Layout Renate Siebes, Proefschrift.nu
Printed by Ipskamp Drukkers B.V.
ISBN 978-90-9027183-5

© 2012 **Esther Verstraete**

All rights reserved. No part of this publication may be reproduced or transmitted in any form or by any means, electronic or mechanical, including photocopy, recording, or any information storage or retrieval system, without permission in writing from the author.

Traces of disease in amyotrophic lateral sclerosis

Sporen van ziekte bij
amyotrofische laterale sclerose
(met een samenvatting in het Nederlands)

Proefschrift

ter verkrijging van de graad van doctor aan de
Universiteit Utrecht op gezag van de rector magnificus,
prof.dr. G.J. van der Zwaan, ingevolge het besluit van het
college voor promoties in het openbaar te verdedigen
op dinsdag 18 december 2012 des middags te 2.30 uur

door

Esther Verstraete

geboren op 19 juni 1981
te Gent, België

Promotor: Prof.dr. L.H. van den Berg

Co-promotoren: Dr. M.P. van den Heuvel
Dr. J.H. Veldink

The studies described in this thesis were performed at the Rudolf Magnus Institute of Neuroscience, Department of Neurology, University Medical Center Utrecht, The Netherlands.

Funding of the studies described in this thesis was kindly provided by The Netherlands Amyotrophic Lateral Sclerosis (ALS) foundation, 'Prinses Beatrix fonds', 'Zeldzame Ziekten Fonds', The Zabawas Foundation, Optimix Foundation, Jan Cornelia Foundation, Adessium Foundation, the Rudolf Magnus Institute of Neuroscience, the Dutch Brain Foundation and the European Community's Health Seven Framework Programme (FP7/2007-2013).

The publication of this thesis was financially supported by Roche Nederland BV, ChipSoft BV, GlaxoSmithKline BV, Genzyme Nederland BV, Boehringer Ingelheim BV and Caresharing BV.

CONTENTS

Chapter 1	General introduction	7
Chapter 2	Neuroimaging in amyotrophic lateral sclerosis	15
PART I SPREAD OF DISEASE		
Chapter 3	Symptom development in patients with motor neuron disease	59
Chapter 4	Motor network degeneration in ALS: a structural and functional connectivity study	75
Chapter 5	Impaired structural motor connectome in ALS	97
Chapter 6	Structural brain network imaging shows progressive disconnection of the motor system in ALS	119
PART II BIOMARKERS		
Chapter 7	Structural MRI reveals cortical thinning in ALS	139
Chapter 8	Multimodal tract-based analysis in ALS patients at 7T	153
Chapter 9	No evidence of microbleeds in ALS patients at 7 Tesla MRI	171
Chapter 10	TDP-43 plasma levels are higher in ALS	177
PART III CLINICAL TRIALS		
Chapter 11	Lithium lacks effect on survival in ALS: a phase IIb randomised sequential trial	191
Chapter 12	Would riluzole be efficacious in the new ALS trial design?	211
Chapter 13	General discussion	215
	References	227
	Summary	255
	Samenvatting (Summary in Dutch)	261
	Dankwoord (Acknowledgements)	269
	About the author	277



1

General introduction



INTRODUCTION

Amyotrophic lateral sclerosis (ALS) is a progressive disease of the motor system involving both upper motor neurons in the brain and lower motor neurons in the spinal cord (Kiernan et al., 2011). Onset and disease course in ALS is heterogeneous as each patient has their unique combination of upper and lower motor neuron involvement, site of onset and symptom development (Chio et al., 2011a; Ravits and La Spada, 2009). In The Netherlands, 400 to 500 persons are diagnosed each year with this destructive disease (2.77 per 100,000 person-years) (Huisman et al., 2011). ALS can occur at any age during adulthood with a median age at onset of 63 years and a median survival of three years (Huisman et al., 2011). Within this heterogeneous population it is a great challenge to identify patterns and uniform features in order to enhance our understanding and ultimately improve treatment.

ALS: a neuromuscular and neurodegenerative disease

The term neuromuscular disease is very broad; it encompasses many diseases and ailments that, either directly (through intrinsic muscle pathology) or indirectly (through nerve pathology), impair muscle functioning. ALS typically leads indirectly to muscle impairment due to degeneration of upper and lower motor neurons. The progressive loss of a subpopulation of neurons – motor neurons – makes it a neurodegenerative disease, similar to other neurodegenerative diseases such as Alzheimer’s disease, frontotemporal dementia (FTD) and Parkinson’s disease. One could say that from a patient’s perspective ALS is a neuromuscular disease, however, from a pathophysiological perspective it is a neurodegenerative disease.

OUTLINE OF THE THESIS

This thesis is entitled ‘traces of disease’ in ALS, referring to the search for a good biomarker by exploring both neuroimaging techniques and measurements in biological samples (**part II: Biomarkers**). In addition, it looks at the spread of disease; does the disease propagate in a predictable way, following a certain path or ‘trace’ (**part I: Spread of disease**)? The third part of this thesis is about clinical trials in which we depend on measurable markers (or traces) of disease to assess efficacy of the drug undergoing investigation or the intervention (**part III: Clinical trials**).

Spread of disease

1

'Social networks and spread of disease'

When one poses a question on the internet about “disease spread”, most hits are about infectious diseases; especially the spread of common viruses like influenza are the subject of the online forum. It is well known that ‘flu’ spreads via the social network of the world population. The most recent pandemic influenza outbreak in 2009 (H1N1) gave rise to a considerable amount of research into patterns of spread (Cauchemez et al., 2011). Insight into the spread of communicable diseases is crucial for the design of optimal control strategies like isolating a population (e.g. travel restrictions) or preventing transmission (e.g. wearing face masks). Network analysis helps in gaining such insights and prediction models can aid in assessing the efficacy of an intervention (The PLoS Medicine Editors, 2008).

During my years of research, a large number of patients with ALS has visited the outpatient clinic of the University Medical Center Utrecht for trial visits or scanning sessions. Following up on these patients, our interest was drawn to the spread of disease. Most patients initially had a focal presentation of symptoms, which during the course of disease spread to other body regions until, sooner or later, respiratory failure developed, the cause of death in most patients. We felt that it is important to know more about the underlying mechanisms of disease spread, just as it is essential to know, for example, how infectious diseases transmit from one person to another and how cancer cells spread throughout the body. More knowledge about the spread of disease could help in the development of effective treatment. Surprisingly little is known about this aspect of ALS (Ravits and La Spada, 2009; Kanouchi et al., 2012).

The following questions were asked:

1. Could we predict which body region would next become involved in the course of disease?
2. What is the role of the brain network or neural connectivity in spread of disease?

We assessed the development of symptoms clinically (**chapter 3**), and in addition, we studied the brain network using magnetic resonance imaging (MRI) as a tool to identify characteristics of patients with a faster or slower disease progression and to assess changes within the brain network over time (**chapters 4, 5 and 6**).

The field of neuroimaging is evolving quickly and an increasing number of advanced imaging measures is emerging to unravel how diseases affect brain structure and function. **Chapter 2** provides an overview of the full range of neuroimaging techniques as well as the insights this has brought into ALS. One may question to what extent neuroimaging has advantages over neuropathological assessment, as imaging is always a reconstruction of what is actually happening. Here, we indicate a few major advantages: (1) Imaging allows longitudinal measurements to be carried out while neuropathology is always an assessment at a single point in the disease process; (2) Besides structural measures, it is possible to assess functional characteristics; and (3) Automated neuroimaging measurements enable objective group comparison.

Biomarkers

'The rise of the biomarker'

The first citation including the term 'biomarker' in PubMed dates from 1980 in a report on a potential marker for breast cancer (Paone et al., 1980). Since 2000, the number of citations has increased from 99 to 1216 per year in 2011 (search term: "biomarker[title]"). On the whole these citations were reporting on measures in biological samples (e.g. blood, cerebrospinal fluid), but imaging techniques (e.g. MRI) are also an important source of biomarkers. The most accepted imaging marker in neurology is probably the MRI lesion activity in multiple sclerosis (MS), which is widely used in clinical trials studying the efficacy of new therapies (Barkhof et al., 2011). This imaging marker enables detection of treatment effects well before they can be appreciated clinically, thus allowing efficient drug screening. Despite the important contribution of this biomarker, clinical endpoints will rightly remain the gold standard for assessing efficacy of a new drug in definitive (phase III) trials. However, also in this phase of clinical research, imaging markers provide important additional information on subgroup performance and safety.

The term biomarker is a broad term encompassing virtually everything one can measure in a patient in relation to disease. The ideal biomarker is easily obtained, has a high specificity for disease and changes as the disease becomes more (or less) severe (Bowser et al., 2011). In this thesis, we focussed on finding an upper motor neuron marker for ALS.

Is ALS becoming a brain disease?

In the history of ALS, research has mainly concentrated on the lower motor neuron or spinal cord. There are several reasons for this: (1) On pathological examination changes within the spinal cord, such as sclerosis of the lateral columns, are much more pronounced than the changes in the brain (Kato, 2008). Atrophy of the primary motor region or precentral gyrus, is only rarely found (Brownell et al., 1970); (2) For many years, it has been possible to assess the lower motor neuron objectively using electromyography (EMG) (Eisen and Swash, 2001). This examination has become a routine part of the diagnosis of ALS and still is an important subject of ALS research (Schrooten et al., 2011); (3) The extensively studied mouse model of ALS is based on the first gene identified as a cause of familial ALS, the *SOD1*-gene (Rosen, 1993). This transgenic mouse carries a large number of the mutated human *SOD1*-gene copies and has a predominantly lower motor neuron phenotype (Gurney et al., 1994). An important difference compared to sporadic ALS, is that the *SOD1* familial ALS cases are largely resistant to the development of FTD (a dementia subtype), which is estimated to occur in about 5–15 % of the sporadic ALS cases (Wicks et al., 2009; Ringholz et al., 2005); (4) Lower motor neuron signs are usually more apparent when clinically assessing a patient with ALS as muscle atrophy and sometimes fasciculations can readily be seen while spasticity is present in only 4% of ALS patients at presentation (Tartaglia et al., 2007). The relative absence of spasticity might be due to masking of upper motor neuron signs by lower motor neuron loss, since the lower motor neuron needs to be largely intact to enable spasticity and hyperreflexia. Overall, the upper motor neuron or changes in the brain in general have received far less attention as they were less visible and measurable.

The discovery of 43 kDa transactive response DNA binding (TDP-43) protein as a major disease protein in intraneuronal aggregates in patients with ALS or FTD (Neumann et al., 2006), and more recently the identification of a hexanucleotide repeat expansion in the *C9ORF72*-gene as a common cause of both familial and sporadic ALS and FTD (DeJesus-Hernandez et al., 2011; Renton et al., 2011), have, however, definitely shifted attention towards the brain. In 2006, TDP-43 was discovered to be the main protein content of the inclusions found in the brain and spinal cord tissue on *post mortem* examination of patients with ALS (Neumann et al., 2006; Ince et al., 2011). These inclusions were known to be ubiquitin-positive, suggesting a role in the clearance of misfolded proteins, a process known as autophagy (Martinez-Vicente and Cuervo, 2007). The targeted protein was, however, not revealed until TDP-43 was discovered. Almost all ALS patients exhibit cytoplasmic

mislocalisation and TDP-43 aggregation on neuropathological examination (Neumann et al., 2006), except for a small number of familial ALS cases with *SOD1* or *FUS* mutations. These patients have protein aggregates containing *SOD1* or *FUS* protein (Kato, 2008; Deng et al., 2010). Protein aggregates are also found in FTD patients, the majority of whom have either TAU- or TDP-43-positive inclusions and – similar to ALS – a small number has protein inclusions positive for *FUS*. Since a subset of FTD patients develops a motor neuron disorder during the course of their disease and vice versa, it is clear that ALS and FTD belong to the same disease spectrum. The latter was further supported by the discovery of a hexanucleotide repeat expansion in the *C9ORF72*-gene as a shared genetic cause of ALS and FTD (DeJesus-Hernandez et al., 2011; Renton et al., 2011).

Currently, objective assessment of the upper motor neuron or extra-motor brain involvement in ALS is not available but would greatly improve the diagnosis of ALS (Turner et al., 2009). For example, in the spectrum of motor neuron diseases, it is impossible to differentiate between a pure lower motor neuron syndrome, progressive muscular atrophy (PMA), and PMA with subclinical upper motor neuron involvement. In addition, an objective assessment of extra-motor involvement might identify patients prone to developing cognitive deficits.

The following questions were asked:

1. Can we objectively assess the upper motor neuron using MRI measures?
2. How does upper motor neuron involvement – measured with MRI – relate to clinical impairment?
3. Can we find traces of TDP-43 ('disease protein') in blood samples of patients with ALS?

We studied the brain structure and more specifically the motor structures in order to quantify upper motor neuron involvement or learn more about changes within the brain tissue (**chapters 7, 8 and 9**). As TDP-43 is the key protein involved in neurodegeneration in ALS, we quantified this protein in blood (plasma) samples of patients compared to controls (**chapter 10**).

Clinical trials

1

'The first trial ever?'

The first description of an intervention trial dates from the second century BC and is described in the Bible (Daniël 1:12). This paragraph describes the effect of a dietary regime (only vegetables and water compared to royal dishes and wine) between two groups of healthy young men. After ten days the appearance of these young men was compared, revealing a stronger and healthier appearance for the group whose diet consisted of only vegetables and water. Unfortunately this diet has not been widely implemented in our Western dietary habits, but the principles of an intervention trial have been.

Improving treatment or obtaining a cure for ALS is the ultimate goal of all research activities. Performing a clinical trial is a crucial step towards reaching this goal and should, therefore, be carried out with great care. A false positive or negative outcome is detrimental to progress in the field.

Within a few months of 'getting started' as a PhD-student in 2008, a report on lithium appeared describing its potential to slow disease progression and increase survival in ALS (Fornai et al., 2008). Although the mood-stabilizing properties of lithium were already well known, more recently potential neuroprotective effects had been reported (Chuang et al., 2002). Patients with ALS, worldwide, rushed to their doctors to obtain this 'new drug'; however, the reported study was mainly about the effects of lithium in the SOD1-mutant mouse and included only 44 patients with ALS, 16 of whom had been given lithium. Apart from the small number, there were several methodological weaknesses, for example the lack of randomisation; this resulted in an uneven distribution of relevant prognostic factors in favour of the lithium group. It was, therefore, important to study the true effects of lithium in a larger, randomised controlled trial.

The following questions were asked:

1. Does lithium, compared with placebo, as an add-on treatment together with riluzole, increase survival in ALS?
2. What is the optimal trial design for studying candidate treatments for ALS?

We performed a randomised, placebo-controlled, double-blind, sequential trial studying the efficacy and safety of lithium in patients with ALS (**chapter 11**). As 'new' trial designs in ALS were emerging, we contemplated the potential pitfalls (**chapter 12**).

In summary, we have explored the mechanisms of spread of disease in ALS (**part I**), potential markers for upper motor neuron (or brain) involvement (**part II**) and strategies for clinical trials in ALS (**part III**). MRI-based, advanced neuroimaging techniques were the main research tool in our studies. Figure 1.1 illustrates how the sections of this thesis interfere with one another.

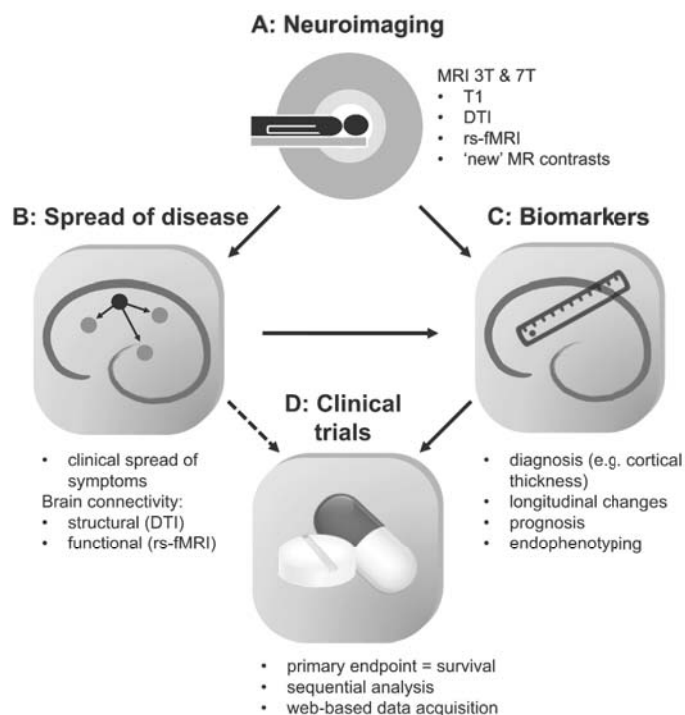


Figure 1.1 Schematic overview of the main topics in this thesis

This figure shows the main themes as further explored in each section within this thesis. (A) Our main study tool was neuroimaging using both 3T and 7T MRI. We performed structural brain imaging (T1, diffusion tensor imaging [DTI] and relative new, exploratory MR contrasts [e.g. T2*]) as well as functional imaging (resting state functional MRI [rs-fMRI]). The data acquired were used for studies on disease spread (**part I**) as well as for biomarker research (**part II**). (B) For the studies on disease spread we assessed the spread of symptoms clinically and studied brain connectivity, mainly using DTI and rs-fMRI data. (C) Our biomarker research focussed on structural MRI measures such as cortical thickness (T1), but other MR contrasts were also explored for their diagnostic potential, longitudinal changes, prognostic value and endophenotyping. (D) In this thesis we report on a clinical trial (**part III**) studying the efficacy of lithium on survival in ALS. We performed sequential analyses in order to be able to stop the trial as soon as the data showed efficacy of the studied drug or a lack thereof. For patient convenience, a web-based system was used for data acquisition. It is important to note that the connectivity profile of patients with ALS may also have potential as a biomarker (B > C). A good biomarker for ALS may in the future aid efficient drug screening in clinical trials (C > D). In addition, insights into disease spread may become a target for future disease modifying agents (B > D).

2

Neuroimaging in amyotrophic lateral sclerosis

Martin R. Turner
Federica Agosta
Peter Bede
Varan Govind
Dorothee Lulé
Esther Verstraete

Biomark Med 2012; 6(3): 319-37



ABSTRACT

The catastrophic system failure in amyotrophic lateral sclerosis (ALS) is characterised by progressive neurodegeneration within the corticospinal tracts, brainstem nuclei, and spinal cord anterior horns, with an extra-motor pathology that has overlap with frontotemporal dementia. The development of computer tomography and even more so magnetic resonance imaging (MRI) has brought insights into neurological disease, previously only available through *post mortem* study. Although largely research-based, radionuclide imaging has continued to provide mechanistic insights in neurodegenerative disorders. The evolution of MRI to use advanced sequences highly sensitive to cortical and white matter structure, parenchymal metabolites and blood flow, many of which are now applicable to the spinal cord as well as brain, make it a uniquely valuable tool for the study of a multi-system disorder like ALS. This comprehensive review considers the full range of neuroimaging applied to ALS over the last twenty-five years, the biomarkers they have revealed, and future developments.

INTRODUCTION

At the clinical core of amyotrophic lateral sclerosis (ALS) is a progressive and frequently rapid degeneration of a previously normally functioning motor system, comprising upper motor neurons (UMNs) of the primary motor cortex and corticospinal tract (CST), medullary brainstem nuclei, and the lower motor neurons (LMNs) arising from the anterior horns of the spinal cord (Kiernan et al., 2011). Whilst these structures bear the brunt of the neuropathology, it has been clear for over half a century that degeneration extends to involve extra-motor cerebral neuronal populations (Smith, 1960), most commonly those areas of the frontal and temporal lobes having clinical (Phukan et al., 2007), pathological (Neumann et al., 2006) and genetic (DeJesus-Hernandez et al., 2011; Renton et al., 2011) overlap with frontotemporal dementia (FTD) (Giordana et al., 2011). Thus involvement of the central nervous system is a core feature of ALS pathology, even in those cases with no clinical signs of UMN pathology termed progressive muscular atrophy (PMA) (Ince et al., 2003). The marked clinical heterogeneity, frequent diagnostic delay, and reliance of therapeutic trials on survival as the primary outcome measure, make the discovery of biomarkers in ALS a research priority (Turner et al., 2009).

The ability to study brain structure non-invasively has transformed the practise of clinical neurology and neurosurgery. Soon after the development of early computed tomography, functional as well as structural information began to emerge through the use of peripherally injectable radiotracers sensitive to blood flow and a range of neuronal receptors. Exponential increase in micro-processor speed translated the established non-clinical phenomenon of nuclear magnetic resonance into a routine, ionizing radiation-free form of medical tomography, namely magnetic resonance imaging (MRI). Whilst MRI forms a crucial part of the diagnostic process in ALS through its ability to exclude mimic pathology (Filippi et al., 2010), it is the development of advanced applications that has brought it to the forefront of the quest for much needed biomarkers (Turner, 2011). This review considers the full range of neuroimaging techniques that have been applied to ALS over the last quarter of a century.

RADIONUCLIDE IMAGING

Single photon emission computed tomography (SPECT) and the related positron emission tomography (PET) were the first neuroimaging techniques to be applied in ALS. Both rely on the detection and localisation of peripherally injected gamma-emitting radioisotopes

(incorporated within a tracer molecule) as they pass through the brain. In SPECT, gamma radiation is measured directly whereas PET relies on the detection of time-coincident gamma rays with exactly 180 degrees of separation occurring as a result of emitted positron annihilation with electrons. This permits significantly higher resolution in PET and allows the detection of tracers that are ligands for specific neuronal receptors (the original article contains a table [eTable 1] including all SPECT and PET studies applied to ALS and related disorders).

Single photon emission computed tomography

SPECT has become a routine nuclear medicine technique, though with limited application to neuroimaging to date. The commonly used tracer ^{99m}Tc -HMPAO (hexamethylpropyleneamine oxime) serves as a marker of blood flow, a surrogate for regional cerebral metabolism. The earliest SPECT studies in ALS used an alternative tracer N-isopropyl-p- ^{123}I -iodoamphetamine (^{123}I -IMP), revealing widespread cortical reductions that were more pronounced in those with longer disease duration (Ludolph et al., 1989). Shortly afterwards SPECT revealed frontotemporal changes in four ALS cases with dementia (Neary et al., 1990), later elegantly confirming the now-established concept of a continuum between ALS and FTD (Talbot et al., 1995a).

Positron emission tomography

Blood flow and activation studies

Early and longitudinal studies with PET in ALS using ^{18}F -fluorodeoxyglucose as a surrogate for cerebral metabolism (regional cerebral metabolic rate for glucose – rCMRGlc) confirmed widespread and progressive reductions in those ALS patients with clinical UMN signs (Dalakas et al., 1987). This was linked to neuropsychological deficits of a frontal lobe nature in ALS patients, particularly verbal fluency (Ludolph et al., 1992). Alternative tracers H_2^{15}O and C^{15}O_2 were used to measure similar reductions in regional cerebral blood flow (rCBF) in ALS patients with dementia (Tanaka et al., 1993), and later also linked to abnormalities of verbal fluency in ALS patients without overt dementia (Kew et al., 1993). The ‘boundary shift effect’ in cortical activation seen in response to a joystick task provided early evidence for a potential loss of inhibitory cortical influence (Kew et al., 1994).

Ligand studies

Radiotracers that bind selectively to receptors on specific neuronal populations have been used to reveal several aspects of pathogenesis in ALS (Figure 2.1). In keeping with the emerging theme of a multi-system cerebral degeneration, and the observation of overt extrapyramidal signs among some patients, a PET study using a ligand previously applied to Parkinson's disease patients, namely ^{18}F -6-fluorodopa, provided evidence for loss of nigral dopaminergic cells in ALS (Takahashi et al., 1993). The pivotal PET ligand study with respect to widespread extra-motor cortical changes arose through the use of the γ -amino-butyric acid (GABA)_A receptor ligand ^{11}C -flumazenil. The extensive decreases in cortical binding provided further evidence for loss of inhibitory interneuronal GABA-ergic influence (Lloyd et al., 2000), linking with an established theme of excitotoxicity in ALS through glutamate dysregulation (Turner and Kiernan, 2012). Subsequent comparative ^{11}C -flumazenil PET studies in those with a genetic mutation in the superoxide dismutase-1 gene (*SOD1*) linked to a consistently more slowly progressive form of ALS demonstrated relative preservation of tracer binding in motor regions, supporting the view that preservation of inhibitory influence might have prognostic significance (Turner et al., 2005a).

A key role for neuroinflammatory mechanisms in the pathogenesis of ALS remains the subject of active research (Philips and Robberecht, 2011). The PET ligand ^{11}C -PK11195 binds to the peripheral benzodiazepine receptor expressed by activated microglia. A study in ALS patients provided *in vivo* evidence of widespread corticospinal tract and extra-motor microglial activation (Turner et al., 2004), notably lateralised within the hemisphere contralateral to the most affected body side in individuals with rare forms of motor neuron disease (Turner et al., 2005b).

A serotonin 5-HT_{1A} receptor PET ligand ^{11}C -WAY100635 revealed very marked reductions in binding in a group of non-depressed ALS patients (Turner et al., 2005c). Loss of binding was located mainly in frontotemporal regions, and strikingly similar in distribution to a subsequent study in patients with FTD (Lanctot et al., 2007), confirmed histologically in addition (Bowen et al., 2008). Ostensibly assumed to be a surrogate marker of cerebral pyramidal cell loss in ALS (DeFelipe et al., 2001), this transmitter system has a number of other potential roles in ALS pathogenesis (Sandyk, 2006).

Limitations and opportunities

A major disadvantage of radionuclide imaging is the inherent exposure to ionizing radiation, and the need for arterial blood sampling in some cases. Ligand PET generally requires shorter-lived radionuclides entailing a local cyclotron for production, and so restricting access to few centres with appropriate experience. Moreover the precise pharmacodynamic properties required for a successful radioligand lie within a narrow range according to the receptor of interest, so that an active radiochemistry research and development programme with quality control processes places further restrictions on the availability of this kind of PET research.

Both SPECT and PET studies in ALS appear to have been ahead of their time, prescient of the current era in which ALS and FTD are generally accepted to have overlap. The subsequent discovery that expansions of the *C9ORF72* hexanucleotide repeat are associated with cases of both 'pure' FTD and ALS within the same kindred, offers renewed research potential for both techniques. SPECT has shown promise in the detection of FTD phenotypes (Talbot et al., 1995b) and would be a widely available, easily applied technique but may lack sensitivity to early change. Re-evaluation of the serotonergic system using PET in the post-FTD-linked era of ALS, as well as the application of novel neuroinflammatory and inhibitory PET ligands, should be considered with the aim of identifying novel therapeutic targets. PET ligands might serve as pharmacodynamic markers for drug discovery, providing proof of mechanism in the early stages of drug development.

VOXEL AND SURFACE-BASED MRI MORPHOMETRY

Whilst routine clinical MRI frequently demonstrates marked precentral gyrus atrophy in rare cases of the UMN-only motor neuron disease primary lateral sclerosis (PLS), it lacks sensitivity in ALS. Automated and unbiased whole brain analysis techniques have been developed that segment and quantify grey and white matter morphology using T1-weighted images. Current analysis techniques include voxel- and surface-based morphometry (VBM and SBM), the latter also known as cortical thickness measures. These techniques allow the study of regional differences in grey matter, and to a lesser extent white matter volume.

VBM and SBM classify each voxel as grey matter, white matter or (cerebrospinal) fluid. After normalisation of multiple brain volumes to standard templates, VBM compares the classification of each voxel in patients and controls resulting in a regional assessment of

grey or white matter ‘density’ (Ashburner and Friston, 2000) (not strictly equivalent to atrophy in the histological sense). SBM reconstructs the boundaries between grey and white matter, as well as grey matter and cerebrospinal fluid, allowing reconstruction of the cortical surface. Subsequently the cortex can be parcellated into units based on gyral and sulcal structure and a variety of surface-based parameters created including cortical thickness, curvature maps and sulcal depth (Fischl and Dale, 2000). SBM has several advantages over VBM as it allows decomposition of cortical volume into both thickness and surface area and respects the cortical topology, enhancing reliability and sensitivity (Pereira et al., 2011).

Voxel-based morphometry studies

VBM studies have been performed in ALS with group sizes ranging between 12–26 patients (Table 2.1). They have yielded inconsistent results, reporting grey matter changes confined to motor regions (Kassubek et al., 2005; Filippini et al., 2010; Senda et al., 2011), in other studies more widespread (Ellis et al., 2001; Mezzapesa et al., 2007; Tsujimoto et al., 2011) and white matter changes (Abrahams et al., 2005). The diverging results might reflect small and heterogeneous patient groups as well as methodological differences or limitations. A meta-analysis of VBM studies in ALS included a total of 84 patients. Group analysis demonstrated significant grey matter loss only in the right precentral gyrus (Chen and Ma, 2010), with extra-motor changes *not* found to be a consistent feature. This is in agreement with clinical observations, as at least half all ALS patients have no detectable cognitive impairment (Raaphorst et al., 2010). However in those with significant impairment or frank dementia, extra-motor grey matter changes are a clear feature across a range of techniques (Giordana et al., 2011). VBM studies in these patients have reported several features in ALS patients:

1. Poor performance of a cognitive task requiring understanding of verbs (rather than nouns), was linked to grey matter changes in the bilateral dorsolateral prefrontal and inferior frontal cortex (Grossman et al., 2008).
2. Apathy was related to regional atrophy of the bilateral orbitofrontal cortex, right dorsolateral prefrontal cortex and bilateral frontal pole (Tsujimoto et al., 2011).
3. ALS-dementia compared to ALS-only patients showed increased atrophy in frontal regions as well (left middle and inferior frontal and medial premotor cortex) (Chang et al., 2005a).

4. Involvement of similar frontal regions was found in a study comparing rapid versus slow-progressing ALS patients (Agosta et al., 2009a), reflecting the separate observations that early cognitive impairment is a poor prognostic factor (Elamin et al., 2011).

Longitudinal MRI studies in ALS are challenging as progressive bulbar and respiratory weakness complicates repeated scanning. Two longitudinal VBM studies have demonstrated progressive atrophy in extra-motor as well as motor regions (Senda et al., 2011; Agosta et al., 2009a). Patients with more rapidly progressive ALS showed frontal lobe as well as more extensive motor changes (Agosta et al., 2009a).

Surface-based morphometry studies

Studies of SBM in ALS have all revealed cortical thinning in the precentral gyrus. One study applied a region-of-interest (ROI) based analysis comparing the precentral, postcentral and lateral-occipital gyri, showing significant thinning in the precentral gyrus only (Roccatagliata et al., 2008). The other two studies revealed significant cortical thinning of the precentral gyrus in whole brain analysis (Verstraete et al., 2010; Verstraete et al., 2012) (Figure 2.2).

SBM measures (volume, thickness and surface area) showed thickness to be most sensitive to focal atrophy in cortical motor regions (Verstraete et al., 2012). Unlike VBM, this measure may be more promising as a marker of UMN involvement (unpublished data), which might then have value in the diagnostic pathway of PMA patients who have only LMN signs clinically. Although thickness of the precentral gyrus was not associated with clinical scores, a significant correlation was found between thinning within the temporal lobe cortex and rapid disease progression (Verstraete et al., 2012).

Limitations and opportunities

VBM in isolation has shown limited sensitivity for grey matter changes in ALS at group level. SBM (in time applicable to routine clinical images) might be able to deliver an UMN imaging marker to refine the diagnostic pathway. Patterns of cortical change may emerge to identify patients prone to develop dementia or have otherwise rapid progression, both of which are important for prognostication and effective care planning.

Table 2.1 Morphometric MRI studies in ALS (all are 1.5T field strength unless shown otherwise)

Analysis	Subjects/ Field strength	Motor changes	Extra-motor changes	Phenotype	Disability	Prognosis	Reference
VBM T1	16 ALS 8 HC	NS	GM: frontal (superior frontal gyrus; medial frontal gyrus; mid frontal gyrus) WM: increase in the right inferior frontal gyrus	Bulbar onset vs limb onset: GM: brainstem, cerebellum and fusiform gyrus WM: CST	-	-	(Ellis et al., 2001)
	23 ALS 12 HC	GM: NS WM: right internal capsule and left corona radiata	WM: corpus callosum forceps minor, left cingulum; posterior cingulate gyrus, posterior precuneus	Cognitive impairment (verbal fluency): WM: more extensive white matter loss GM: cerebellum	-	-	(Abrahams et al., 2005)
	20 ALS 22 HC	GM: bilateral motor/premotor cortex	GM: frontal (left middle and inferior frontal gyrus, bilateral frontal pole and ventromedial frontal cortex), temporal (bilateral superior temporal gyrus and temporal pole) and left posterior thalamus	ALS:FTLD (n=10) vs ALS (n=10): left middle frontal gyrus, left inferior frontal gyrus, and medial premotor cortex	-	-	(Chang et al., 2005)
	22 ALS 22 HC	GM: right precentral gyrus WM: increase in the bilateral internal capsule and corpus callosum	GM: left medial frontal gyrus WM: frontal, occipital, cerebellum	-	NS	-	(Kassubek et al., 2005)

Table 2.1 continues on next page

Table 2.1 Continued

Analysis	Subjects/ Field strength	Motor changes	Extra-motor changes	Phenotype	Disability	Prognosis	Reference
VBMT1	17 ALS 17 HC	GM: right pre-central gyrus WM: NS	GM: frontal (bilateral middle frontal gyrus; bilateral superior frontal gyrus); parietal (bilateral postcentral gyrus and inferior parietal lobule)	NS	ALSFRS-R: GM: right medial frontal gyrus (dorsolateral prefrontal cortex); Disease duration: NS	-	(Grosskreutz et al., 2006)
	16 ALS 9 HC	NS	GM: frontal (bilateral inferior frontal gyrus; insula; right superior frontal gyrus); temporal (bilateral middle temporal gyrus; subgyral, right superior temporal gyrus-uncus; right parahippocampal gyrus)	-	-	-	(Mezzapesa et al., 2007)
	25 ALS 18 HC	GM: right pre-central gyrus	GM: bilateral superior frontal gyrus; left inferior frontal gyrus	-	NS	-	(Agosta et al., 2007)
	15 ALS 25 HC	GM: bilateral precentral gyrus	GM: frontal (bilateral inferior frontal gyrus); temporal (bilateral hippocampal formation; bilateral temporal isthmus and left superior temporal gyrus and sulcus), left insula, parietal and occipital, bilateral thalamus and right cerebellum	-	-	-	(Thivard et al., 2007)

Analysis	Subjects/ Field strength	Motor changes	Extra-motor changes	Phenotype	Disability	Prognosis	Reference
VBMT1	23 ALS 7 hom 'D90A' SOD1 ALS 28 HC 0.5T	GM: greatest in midline motor/ pre-motor	GM: greatest in deep grey matter and midline frontal lobes	-	-	Distinct pat- tern of involve- ment in slower hom 'D90A' SOD1 disease patients de- spite similar disability	(Turner et al., 2007)
	26 ALS 16 HC 3T	GM: right motor	GM: frontal (bilateral inferior frontal, dorsolateral prefron- tal; right premotor; bilateral anterior cingulate); temporal (left anterior temporal); occipital (bilateral middle occipital)	Cognitive impairment (decreased action knowledge); GM: bilateral dorsolat- eral prefrontal cortex and inferior frontal cortex	-	-	(Grossman et al., 2008)
	16 ALS (FU 16) 10 HC (tensor based morphometry)	-	-	Rapidly progressing ALS: GM: left motor cortex, bilateral supplemen- tary motor area, right inferior and middle frontal gyri, left cau- date and right putamen	Follow-up after 9 months (sig- nificant decline in ALSFRS-R score): GM: left pre- motor cortex and right basal ganglia (i.e. putamen and caudate nuclei)	-	(Agosta et al., 2009)

Table 2.1 continues on next page

Table 2.1 Continued

Analysis	Subjects/ Field strength	Motor changes	Extra-motor changes	Phenotype	Disability	Prognosis	Reference
VBMT1	24 ALS 24 HC 3T	GM: bilateral precentral gyrus	GM: frontal (supplementary motor cortices, anterior cingulate gyrus); temporal (temporal lobe regions)	-	-	-	(Filippini et al., 2010)
	17 ALS (FU 17) 17 HC 3T	GM: bilateral paracentral lobule and precentral gyrus	GM: frontal (insula); temporal (right temporopolar area). WM: right inferior frontal gyrus	-	Follow-up after 6 months (significant decline in ALSFRS-score, no change in MMSE and FAB): GM: bilaterally in the frontal, temporal, and parietal lobes.	-	(Senda et al., 2011)
	21 ALS 21 HC 3T	WM: CST	GM: frontal lobe, limbic lobe, insula and occipital lobe	Apathy; GM: frontal (bilateral orbitofrontal cortex, right dorsolateral prefrontal cortex and bilateral frontal pole)	-	-	(Tsujiimoto et al., 2011)
VBMT1 versus VBR T2	12 ALS 12 HC	NS	WM: right middle cerebellar peduncle	-	Disease duration: GM: right cerebellum and lingual gyrus	-	(Minnerop et al., 2009)

Analysis	Subjects/ Field strength	Motor changes	Extra-motor changes	Phenotype	Disability	Prognosis	Reference
SBMT1	14 ALS 12 HC	precentral cortex	NS	-	-	-	(Roccatagliata et al., 2009)
	12 ALS 12 HC	bilateral precentral gyrus	NS	-	NS	Fast disease progression; precentral gyrus	(Verstraete et al., 2010)
	3T						
	45 ALS (FU 20) 25 HC	bilateral precentral gyrus	NS	NS	NS	Fast disease progression; right inferior temporal gyrus	(Verstraete et al., 2012)
	3T						

VBM = voxel-based morphometry; VBR = voxel-based relaxometry; SBM = surface-based morphometry; HC = healthy controls; NS = not significant; FU = follow-up; GM = grey matter; WM = white matter.

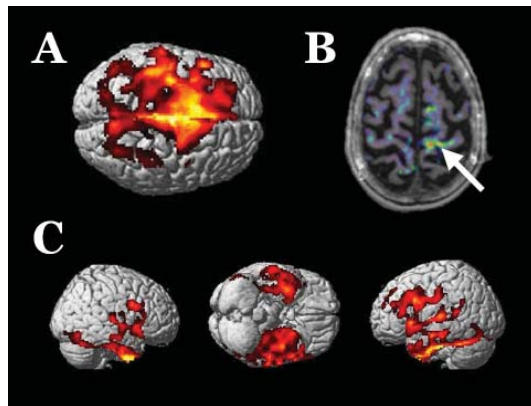


Figure 2.1 Composite image from ligand PET studies in ALS

This figure shows the potential of this technique to reveal mechanisms of pathogenesis. A large area of motor and pre-motor cortex showed reduced binding of the GABAA receptor ligand ^{11}C -flumazenil in ALS patients (A), supporting the concept of loss of interneuronal inhibitory circuits. Evidence of activated microglia, as demonstrated by binding of ^{11}C -PK11195 (B), was clearly localised to the left motor cortex (arrow) of a patient with weakness lateralised to the right sided limbs. Finally, right, inferior and left views of the brain show strikingly fronto-temporal localisation of significantly reduced binding of the serotonin $5\text{-HT}_{1\text{A}}$ receptor ligand ^{11}C -WAY100635 (C), in keeping with the pathological links between ALS and FTD.

to the right sided limbs. Finally, right, inferior and left views of the brain show strikingly fronto-temporal localisation of significantly reduced binding of the serotonin $5\text{-HT}_{1\text{A}}$ receptor ligand ^{11}C -WAY100635 (C), in keeping with the pathological links between ALS and FTD.

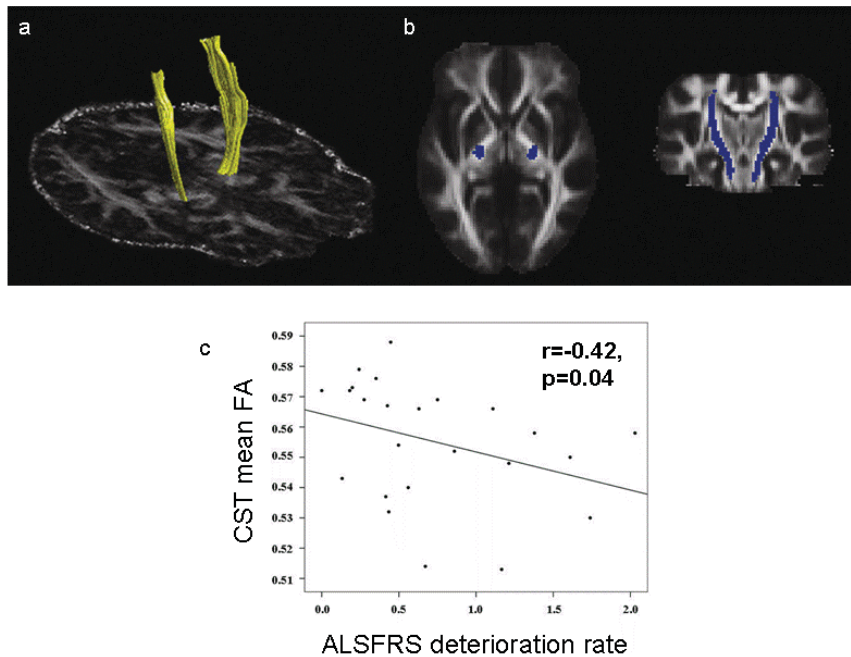


Figure 2.3 DTI of the corticospinal tracts

(a) Diffusion tensor imaging reconstruction of the corticospinal tracts (CST) (yellow) in a reference healthy control superimposed on the single subject's fractional anisotropy (FA) image. (b) Illustration of the CST probability maps (blue) obtained from reference healthy subjects. Probability map is superimposed on axial and coronal sections of the FA atlas. (c) Scatterplot of the correlation between the progression rate measured with the Amyotrophic Lateral Sclerosis Rating scale (ALSFRS) score and the mean FA of the CST in ALS patients.

Adapted from (Agosta et al., 2010a), with permission.

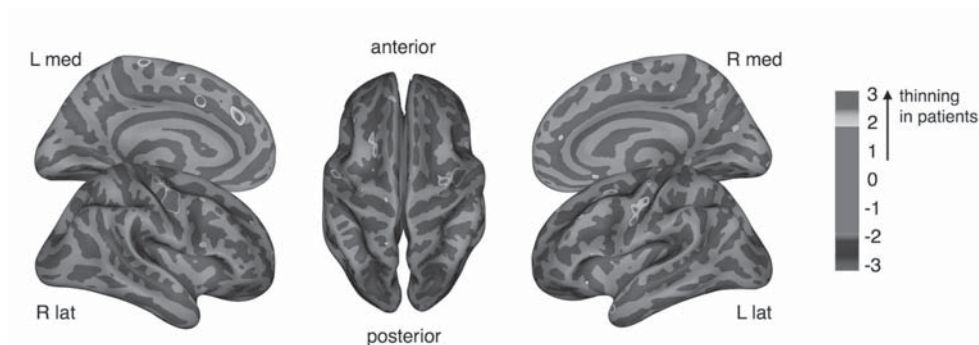


Figure 2.2 Surface based morphometry results in ALS

A surface based morphometry study showing significant cortical thinning in ALS compared with healthy control subjects. The differences in cortical thickness between patients and controls were projected onto an average brain template in a vertex-wise analysis. The precentral gyrus demonstrated significant cortical thinning on both sides.

Adapted from (Verstraete et al., 2012), with permission. See Figure 7.1 for full colour version.

DIFFUSION TENSOR IMAGING

Diffusion-weighted imaging measures the effect of brain white matter microstructure on the random translational motion of water molecules (Basser et al., 1994; Pierpaoli et al., 1996). A full characterization of diffusion can be provided by the so-called tensor, a 3×3 matrix that characterizes the measured diffusion in three orthogonal directions. Two scalar measures are most frequently derived. The mean diffusivity (MD) is calculated as one third of the tensor matrix trace and reflects the average diffusion in all three directions. Fractional anisotropy (FA) is derived from the eigenvalues of the tensor matrix and measures the extent to which diffusion is non-uniform. Analysis of directional diffusivities – axial and radial – provides additional information on the underlying mechanisms of white matter damage (Basser et al., 1994). Myelin breakdown is associated with increased perpendicular diffusivity (radial diffusivity), and axonal damage is reflected by diffusivity changes parallel (axial diffusivity) to the primary fibre orientation (Beaulieu, 2002; Pierpaoli et al., 2001).

The corticospinal tract

Multiple DTI studies have been performed in ALS (Table 2.2). They have most consistently reported decreased FA within the CST (Filippini et al., 2010; Roccatagliata et al., 2009; Abe et al., 2004; Agosta et al., 2010a; Ciccarelli et al., 2006; Cosottini et al., 2005; Ellis et al., 1999;

Table 2.2 Diffusion tensor imaging studies in ALS (all are 1.5T field strength unless shown otherwise)

Study type	Subjects/ Field strength	Analysis	Diagnosis	Phenotype	Disability	Prognosis	Reference
Cross-sectional	22 ALS 20 HC	ROI	Decreased CST FA and increased CST MD	CST damage most marked in bulbar- onset patients	Decreased CST FA vs. higher ALS severity scale and Ashworth spasticity scale scores Increased CST MD vs. longer disease duration	-	(Ellis et al., 1999)
	21 ALS 14 HC	ROI	Decreased CST FA and increased CST MD	-	NS	-	(Toosy et al., 2003)
	15 ALS 12 HC	Voxel-wise (SPM)	Decreased FA in the CST, CC, and thalamus	-	Decreased CST FA vs. delayed central motor conduction time.	DTI changes in patients without UMN signs, who developed UMN signs later in the course of the disease	(Sach et al., 2004)
	16 ALS 11 HC	ROI	Decreased FA and increased MD in the cerebral peduncles	-	Decreased CST FA vs. higher UMN score	-	(Hong et al., 2004)
	25 ALS 23 HC	ROI	Decreased CST FA	-	-	-	(Graham et al., 2004)
	18 ALS 8 PMA 20 HC	ROI	In ALS, decreased FA and increased MD in the CST	No CST DTI changes in PMA	Decreased CST FA vs. lower ALSFRS Increased CST MD vs. longer disease duration	-	(Cosottini et al., 2005)

Study type	Subjects/ Field strength	Analysis	Diagnosis	Phenotype	Disability	Prognosis	Reference
Cross-sectional	13 ALS 19 HC	Tractography	-	-	Decreased CST FA and connectivity measures in ALS with rapid disease progression	-	(Ciccarelli et al., 2006)
	15 ALS 10 HC	ROI	Decreased CST FA (PLIC)	-	Decreased CST FA vs. lower ALSFRS-R	-	(Wang et al., 2006)
	3T						
	10 ALS 20 HC	ROI	Maximum decrease in FA in causal internal capsule	-	NS	-	(Schimrigk et al., 2007)
	15 ALS 25 HC	Voxel-wise (SPM)	Decreased FA in the CST, premotor and parietal regions, thalamus. Increased MD in motor/premotor, hippocampal and temporal regions	-	Decreased FA in the CST, WM underneath the premotor cortex and precentral gyrus, cingulum, splenium of the CC	-	(Thi'vard et al., 2007)
	31 ALS 31 HC	ROI	Decreased CST FA	-	Decreased CST FA vs. higher UMN score and delayed central motor conduction time	-	(Iwata et al., 2008)
	18 ALS 34 HC	ROI	Decreased CST FA	-	-	-	(Nelles et al., 2008)
	3T						

Table 2.2 continues on next page

Table 2.2 Continued

Study type	Subjects/ Field strength	Analysis	Diagnosis	Phenotype	Disability	Prognosis	Reference
Cross-sectional	14 ALS 12 HC	ROI	Decreased CST FA and increased CST MD	-	Decreased CST FA vs. higher pyramidal and lower bulbar scores	-	(Roccatagliata et al., 2009)
	Cohort I: 13 ALS 20 HC	TBSS	-	In ALS vs. PLS, decreased FA adjacent to the superior frontal gyrus In PLS vs. ALS, decreased FA in the body of the CC and in the WM adjacent to the right PMC	In ALS, decreased CST and CC FA vs. more rapid disease progression rate In PLS, decreased FA in the WM adjacent to the PMC vs. more rapid disease progression rate	-	(Ciccarelli et al., 2009)
	Cohort II (3T): 13 ALS 6 PLS 21 HC						
	24 ALS 20 HC	Tractography	Decreased FA, increased MD & radial diffusivity in CST, and increased axial diffusivity in right uncinate fasciculus	-	Decreased CST FA vs. more rapid rate of disease progression	-	(Agosta et al., 2010a)
	24 ALS 24 HC 3T	TBSS	Decreased FA & increased radial diffusivity in CC & upper CSTs	-	Decreased CST FA vs. higher UMN score; Decreased CC FA vs. lower ALSFRS-R	Disease duration positively correlated with CST FA	(Filippini et al., 2010)

Study type	Subjects/ Field strength	Analysis	Diagnosis	Phenotype	Disability	Prognosis	Reference
Cross-sectional	24 ALS 18 HC	Tractography	Increased MD & decreased FA in the CST	No CST DTI differences between bulbar and limb-onset patients	-	Decreased CST FA vs. ALSFRS-R progression rate; decreased CST FA independent predictor of reduced survival (3.4 year FU)	(Agosta et al., 2010b)
	23 ALS 14 HC	Voxel-wise (SPM)	Accounting for brain volume, increased MD in orbitofrontal and frontotemporal regions, genu of the CC, and internal capsule, and decreased in the CST and left inferior frontal lobe	-	Increased orbitofrontal MD vs. longer disease duration	-	(Canu et al., 2011)
	15 ALS 9 HC	Tractography	Decreased uncinate FA	-	-	-	(Sato et al., 2010)
	16 ALS 15 HC	Tractography	-	-	Attention and executive function scores vs. DTI metrics of the CC, CST, and long association WM tracts bilaterally. Verbal learning and memory test scores vs. fornix DTI values. Visual-spatial abilities vs. left uncinate FA	-	(Sarro et al., 2011)

Table 2.2 continues on next page

Table 2.2 Continued

Study type	Subjects/ Field strength	Analysis	Diagnosis	Phenotype	Disability	Prognosis	Reference
Cross-sectional	15 ALS 20 HC 3T	Tractography; TBSS	Decreased FA in the CC & upper CSTs; Reduced FA in corticomotor connections	-	NS	-	(Rose et al., 2012)
	19PLS 18ALS 19HC 3T	Tractography; TBSS	FA reductions in CST and CC (linked)	FA reduction in PLS rostral near PMC and in ALS mainly distal; Clinical UMN involvement linked to FA in ALS and MD in PLS	NS	Disease duration positively correlated with CST FA in ALS	(Iwata et al., 2011)
Longitudinal	23 ALS (11 FU) 25 HC	ROI	Decreased FA & increased MD in the CST	-	No DTI changes at FU	-	(Blain et al., 2007)
	43 ALS (30 FU) 29 HC	ROI	-	-	No DTI changes at FU	-	(Mitsumoto et al., 2007)
	28 ALS (7 FU) 26 HC 3T	Tractography; voxel-wise (SPM)	Decreased FA in the precentral part of the CST; Decreased FA in the frontal, temporal and parietal lobes	-	Decreased CST FA vs. lower ALSFRS-R; No change at FU	ALSFRS-R progression correlated with global brain FA decrease	(Sage et al., 2007)

Study type	Subjects/ Field strength	Analysis	Diagnosis	Phenotype	Disability	Prognosis	Reference
Longitudinal	28 ALS (17 FU) 20 HC	Tractography; cervical cord	-	-	9-month decreased cord area and FA, and increased cord MD	NS	(Agosta et al., 2009)
	24 ALS (16 FU) 12 PLS 12 PMA (10 FU) 12 HC (12 FU)	Tractography; TBSS	Decreased CST FA in PLS and bulbar-onset ALS compared with HC. PLS vs. HC: decreased FA in the CST, CC, WM underneath primary sensory cortex, thalamus, fornix.	Decreased CST FA in PLS and bulbar-onset ALS compared with PMA	6-month FA changes in the CST, CC and several regions in the frontal and temporal lobes in bulbar-onset and limb- onset ALS and in PMA patients	-	(van der Graaff et al., 2011)
	3T		Bulbar-onset ALS vs. HC: decreased FA in the brainstem, internal capsule, WM underneath the PMC. Limb-onset ALS vs. HC: decreased FA in the WM underneath the PMC, fornix, thalamus. PMA vs. HC: decreased FA in the WM underneath the PMC, fornic, internal capsule				
Familial	8 ps SOD1 fALS 13 HC	Voxel-wise (SPM); ROI	Decreased FA in the PLIC	-	-	-	(Ng et al., 2008)

Table 2.2 continues on next page

Table 2.2 Continued

Study type	Subjects/ Field strength	Analysis	Diagnosis	Phenotype	Disability	Prognosis	Reference
Familial	6 hom 'D90A' <i>SOD1</i> fALS 21 HC	Voxel-wise (SPM)	-	Decreased FA in the CC and corona radiate bilaterally in sporadic compared with homD90A patients	In sporadic ALS, decreased FA in motor and extra-motor pathways vs. lower ALSFRS-R	-	(Stanton et al., 2009)
	7 hom 'D90A' <i>SOD1</i> fALS 21 ALS 20 HC	Tractography	-	Decreased CST FA in sporadic compared with homD90A patients	In sporadic ALS, decreased CST FA vs. higher UMN and Ashworth Spasticity Scale scores	-	(Blain et al., 2011)

fALS = familial amyotrophic lateral sclerosis; HC = healthy controls; PMA = progressive muscular atrophy; PLS = primary lateral sclerosis; ROI = region of interest; UMN = upper motor neuron; WM = white matter; CST = corticospinal tract; CC = corpus callosum; PLIC = posterior limb internal capsule; PMC = premotor cortex; FA = fractional anisotropy; MD = mean diffusivity; SPM = statistical parametric mapping; TBSS = tract-based statistical mapping; FU = follow-up; NS = not significant.

Graham et al., 2004; Iwata et al., 2008; Sach et al., 2004; Sage et al., 2007; Schimrigk et al., 2007; Senda et al., 2009; Toosy et al., 2003), in keeping with the involvement of the UMN in all cases of ALS, and many of those labeled as PMA clinically (Ince et al., 2003). Loss of pyramidal motor neurons in the primary motor cortex (PMC) and axonal degeneration of the CST, together with the proliferation of glial cells, extracellular matrix expansion, and intra-neuron abnormalities (Hughes, 1982), may all contribute to the observed DTI changes. A ‘sweet spot’ in the majority of ALS DTI studies appears to be in the region of the posterior limb of the internal capsule (PLIC), and a recent study suggests it may have prognostic value. This region contains descending fibre projections from the pre-motor and motor cortices (Zarei et al., 2007), consistent sites of ALS cerebral pathology. Patients with clinical PMA had FA values in the PLIC that were similar to those of ALS patients with clinical UMN signs (Graham et al., 2004), and in a study of presymptomatic individuals carrying a highly penetrant dominant *SOD1* mutation, decreased FA in the PLIC was seen when compared with healthy non-gene carriers (Ng et al., 2008). Meta-analysis of 8 DTI studies in ALS revealed FA decreases in the PLIC and cingulate gyrus (Li et al., 2012).

Many DTI studies have failed to show a clear relationship with clinical measures. In others, decreased CST FA in ALS patients has been found to correlate with disease severity (Cosottini et al., 2005; Ellis et al., 1999; Graham et al., 2004; Sage et al., 2007; Wang et al., 2006a; Sage et al., 2009), and rate of disease progression (Agosta et al., 2010a; Ciccarelli et al., 2006), along with clinical (Filippini et al., 2010; Abe et al., 2004; Ellis et al., 1999) and electrophysiological (Iwata et al., 2008; Sach et al., 2004) measures of UMN degeneration. Increased MD of the CST has been associated with longer disease duration (Cosottini et al., 2005; Ellis et al., 1999), but paradoxically also *higher* CST FA values which may reflect a higher baseline value or resistance to damage (Filippini et al., 2010; Iwata et al., 2011). One study has demonstrated independent prognostic value of CST FA (Figure 2.3) (Agosta et al., 2010b).

The corpus callosum

Several DTI studies in ALS have reported FA decrease in the CC (Filippini et al., 2010; Verstraete et al., 2010; Sach et al., 2004; Sage et al., 2007; Senda et al., 2009; Sage et al., 2009; Agosta et al., 2007; Ciccarelli et al., 2009; Zhang et al., 2011; Rose et al., 2012), in keeping with historical neuropathological observations (Smith, 1960). The strongest FA decreases seem to be found in the middle-posterior parts of the CC, linking the motor and premotor cortices (Filippini et al., 2010). CC involvement seems less consistently correlated with disease severity (Filippini et al., 2010; Bartels et al., 2008), and central motor conduction

time measured using transcranial magnetic stimulation (TMS) (Sach et al., 2004). Loss of CC integrity might reflect secondary Wallerian degeneration in response to neuronal death within the PMC (supported by the prominent radial diffusivity change (Filippini et al., 2010) or even be the conduit for interhemispheric spread of pathology (Eisen, 2009). CC involvement might be a very early feature, even before the onset of symptoms, reflected by the lack of a clear link between CC DTI measures and disease duration (Filippini et al., 2010). Marked and stereotyped patterns of CC involvement are a feature of other neurodegenerative disorders, including hereditary spastic paraparesis (Muller et al., 2012). Specific patterns of CC involvement may therefore serve as a ‘sign-post’ to phenotypes of extra-motor involvement within the range of ALS cases.

Extra-motor involvement

DTI studies that employed a voxel-wise approach to investigate differences in FA between ALS patients and controls, reported a decrease of FA values in regions outside the ‘classical’ motor network (Sach et al., 2004; Sage et al., 2007; Sage et al., 2009; Agosta et al., 2007; Ciccarelli et al., 2009; Canu et al., 2011). In keeping with clinicopathological overlap between ALS and FTD (Mackenzie and Feldman, 2005), FA decrease was found in the prefrontal (Sage et al., 2007; Sage et al., 2009; Ciccarelli et al., 2009; Canu et al., 2011) and temporal WM (Sage et al., 2007; Sage et al., 2009). A few studies have also observed increased MD in several frontal and temporal WM regions (Sage et al., 2009; Agosta et al., 2007; Canu et al., 2011). Extra-motor WM microstructural damage may be independent of brain tissue loss (Canu et al., 2011). Using diffusion tensor tractography, decreased FA (Sato et al., 2010) and increased axial diffusivity (Agosta et al., 2010a) were demonstrated in the uncinate fasciculus in ALS patients. Performance in cognitive tasks assessing attention and executive functions have been correlated with DTI changes in the CC, CST and long association tract, including the cingulum, inferior longitudinal, inferior fronto-occipital, and uncinate fasciculi (Sarro et al., 2011). A whole brain DTI study with network analysis demonstrated a sub-network of impaired connectivity overlapping intracerebral motor connections, suggesting propagation of disease along structural connections (Verstraete et al., 2011).

Phenotyping

DTI has been used to examine differences across clinical phenotypes. Patients with bulbar-onset have among the most marked cerebral FA decreases generally (Ellis et al., 1999; Aoki

et al., 2005; van der Graaff et al., 2011). Voxel-based DTI studies of patients with PMA (van der Graaff et al., 2011) showed decreased FA in the WM underneath the right PMC (van der Graaff et al., 2011) and the CST (Sach et al., 2004), including those patients that later developed ALS (Sach et al., 2004), suggesting that DTI may also be a marker for early and clinically silent UMN involvement.

Those with PLS also have FA decreases within the CST and the body of the CC compared with healthy controls (Iwata et al., 2011; van der Graaff et al., 2011; Unrath et al., 2010). A DTI study directly comparing the two showed that PLS patients had lower FA in the body of the CC and in the WM adjacent to the right PMC, while ALS patients had reduced FA adjacent to the superior frontal gyrus (Ciccarelli et al., 2009). DTI tractography was used to reconstruct the CST and three regions of the CC (i.e., genu, body and splenium) in PLS and ALS patients. Both groups had reduced FA and increased MD of the CST and CC body compared with controls, but those with PLS showed the greatest change in FA and MD within the subcortical WM underlying the PMC (Iwata et al., 2011). In PLS, disease progression rate was associated with decreased FA in the WM adjacent to the PMC (Ciccarelli et al., 2009) and clinical measures of UMN dysfunction correlated with increased CST MD (Iwata et al., 2011). Translation of these findings into earlier diagnostic separation of PLS from UMN-predominant ALS would be valuable.

Finally, DTI has been used to quantify WM changes in patients with a consistently slowly progressive familial form of ALS, those homozygous for the recessive 'D90A' *SOD1* mutation, compared with sporadic ALS and healthy controls. Six such familial patients showed less extensive WM changes in motor and extra-motor pathways compared to sporadic ALS patients, despite similar levels of disability (Stanton et al., 2009). Using diffusion tensor tractography, CST FA was more reduced in the sporadic ALS patients despite similar levels of clinical UMN involvement (Blain et al., 2007). Both findings point to a distinct pattern of cerebral vulnerability possibly accounting for the difference in progression rate.

Sensitivity to longitudinal change

DTI has been used to track WM change over time in ALS though such studies are challenging as accumulated disability, particularly orthopnoea as a result of diaphragm weakness, may preclude MRI (Sage et al., 2007; van der Graaff et al., 2011; Blain et al., 2007; Agosta et al., 2009b; Mitsumoto et al., 2007). In serial DTI studies with an approximately eight month interval there was a significant progression of brain CST damage at a group

level compared with controls (most notably the right superior portion), which also correlated with worsening of disability (Sage et al., 2007; Zhang et al., 2011). Changes in DTI parameters have been reported over just six months in the CST, CC and several regions in the frontal and temporal lobes in both ALS and PMA patients (van der Graaff et al., 2011). Based upon the changes in FA rates in the right superior CST over a mean interval of 8 months, a sample size of 263 patients per therapeutic trial arm was estimated to be needed in order to detect a 25% treatment effect on FA at 80% power and an alpha level of 0.05 (Zhang et al., 2011), compared to 100 patients for the simpler (and cheaper) clinical measure of the revised ALS Functional Rating Scale (Miller et al., 2007). Whilst further such analyses are needed, and standardisation of parameters such as the number of diffusion gradient directions (Cosottini et al., 2010), it suggests that a single MRI measure is inadequate and multiple markers will be ultimately required.

FUNCTIONAL MRI

Functional MRI (fMRI) is unique in its ability to study cerebral activity non-invasively. The most common approach exploits differences in the paramagnetic properties of oxygenated and deoxygenated blood, namely blood-oxygenation-level-dependent (BOLD) MRI signal. BOLD-based analysis assumes that alteration in neuronal activity leads to a reduction in local blood oxygenation, in turn to an increase in demand and so cerebral blood flow. A change in the proportion of oxygenated blood forms the image contrast. Studies can be carried out carefully gated to active tasks during the scan, or studying background patterns of regional activity in the resting state (Table 2.3).

Active paradigms probing motor networks

ALS patients demonstrate increased brain activation as measured by fMRI in tasks of limb movements compared with healthy controls, in keeping with previous PET studies (Kew et al., 1993). Increased premotor, supplementary motor and cerebellar activity was observed during a finger flexion task (Konrad et al., 2002), in motor areas during a sequential finger tapping task (Han and Ma, 2006), and in a task involving random joystick movements (Stanton et al., 2007b). Furthermore, it was noted that activity spread to anterior regions of the premotor cortex during upper limb tasks (Konrad et al., 2002; Han and Ma, 2006; Lule et al., 2007b; Cosottini et al., 2012). Such changes might reflect compensatory cortical plasticity, in response to loss of pyramidal cells of the primary motor cortex (Schoenfeld

et al., 2005), or reduced local inhibitory (presumed interneuronal) function (Kew et al., 1993; Turner and Kiernan, 2012).

Spread of activation to encompass supplementary motor areas (Konrad et al., 2002; Han and Ma, 2006; Cosottini et al., 2012; Konrad et al., 2006), sensorimotor cortices (Han and Ma, 2006; Stanton et al., 2007b; Mohammadi et al., 2011) and temporoparietal associative sensory areas (Konrad et al., 2002; Stanton et al., 2007b; Cosottini et al., 2012; Schoenfeld et al., 2005; Konrad et al., 2006) has been observed, again previously noted using PET (Kew et al., 1993). Interestingly, activity in the contralateral sensorimotor cortex activity was increased the stronger the physical impairments were in patients (Mohammadi et al., 2011). Accordingly, in a task of maximal force handgrip there was a hypoactivity in sensorimotor cortex probably representing UMN loss and matching with cortical atrophy measured with VBM (Cosottini et al., 2012). Furthermore, inferior parietal and superior temporal gyrus activity was bilaterally increased in ALS patients during upper limb motor task performance (Stanton et al., 2007b). Within the sensorimotor cortices there was an alteration in somatotopy (Han and Ma, 2006; Stanton et al., 2007b). This anterior shift has been noted in stroke, this lending some support to the notion of a compensatory response to primary motor region neuronal loss (Weiller et al., 2006).

Activation in cortical areas ipsilateral to symptoms, including sensorimotor (Han and Ma, 2006; Stanton et al., 2007b) and primary motor cortices (Schoenfeld et al., 2005) has been noted, perhaps representing compensation in relation to disability (Schoenfeld et al., 2005). Involvement of cerebral regions involved in motor learning has been noted in ALS patients, including basal ganglia, cerebellum (Han and Ma, 2006; Konrad et al., 2006) and brainstem (Konrad et al., 2006). Basal ganglia dysfunction may reflect UMN pathology (this was specifically noted as a strong correlation in a PET study of microglial activation (Turner et al., 2004)), including extra-motor involvement, such as the anterior cingulate cortex during hand movements (Tessitore et al., 2006).

Decreased activity was seen for bulbar movements compared to limb movements, suggesting two different patterns of cortical activation changes corresponding to site of disease onset (Kollewe et al., 2011; Li et al., 2009a; Mohammadi et al., 2009b). Lack of compensatory capacity for bulbar movements compared to spinal movements might account for this. Imagined motor movements involve similar areas to those seen in physical movement. In ALS however, right hand movement was associated with a reduced BOLD response in the left anterior parietal, anterior cingulate, and medial pre-frontal cortices (Stanton et al., 2007a), and in the anterior cingulate cortex for movement imagery of both

Table 2.3 Functional MRI studies in ALS (all are 1.5T field strength unless shown otherwise)

Paradigm	Subjects/ Field strength	Main findings	Reference
Task-induced	11 ALS 13 HC	Increased anterior activation pattern during motor task	(Konrad et al., 2002)
	28 ALS 18 HC	Decreased regional activation during cognitive task	(Abrahams et al., 2004)
	6 ALS 6 HC	Extended ipsilateral activation area during motor task	(Schoenfeld et al., 2005)
	15 ALS 15 HC	Extended activation area during motor task	(Han and Ma, 2006)
	3T		
	10 ALS 10 HC	Extended activation area during motor task	(Konrad et al., 2006)
	16 ALS 13 HC	Decreased activation during motor task	(Tessitore et al., 2006)
	16 ALS 9 ND 17 HC	Extended activation area during motor task	(Stanton et al., 2007b)
	16 ALS 17 HC	Decreased regional activation during motor imagery	(Stanton et al., 2007a)
	13 ALS 14 HC	Extended regional activation area during motor task and extended and decreased regional activity during motor imagery task	(Lule et al., 2007b)
	13 ALS 15 HC	Extended activation during emotion processing task	(Lule et al., 2007a)
	20 ALS 20 HC	Decreased regional activity during bulbar movement task in patients with bulbar symptoms	(Mohammadi et al., 2009b)
	3T		
	10 ALS 10 HC	Extended activation in bulbar movement task in patients without bulbar symptoms, Decreased activation in bulbar movement task in patients with bulbar symptoms	(Li et al., 2009a)
	3T		
	9 ALS 10 HC	Decreased regional activity in right hemisphere during emotion processing task	(Palmieri et al., 2010)
14 ALS 18 HC	Decreased regional activity during sensory stimulation	(Lule et al., 2010)	
14 ALS 8 HC	Extended activation in cognitive task	(Goldstein et al., 2011)	

Table 2.3 continues on next page

Paradigm	Subjects/ Field strength	Main findings	Reference
Task-induced	20 ALS 20 HC 3T	Extended activation in limb motor task, Decreased activation in bulbar movement task in patients with bulbar symptom	(Kollewe et al., 2011)
	22 ALS 22 HC 3T	Extended activation in contralateral sensorimotor cortex in motor task, negative correlation between activation and disease progression	(Mohammadi et al., 2011)
	20 ALS 16 HC	Reduced activation in primary somatosensory and frontal dorsal areas and extended activation in premotor and fronto-parietal motor circuit during maximal force grip task matching with cortical atrophy (VBM)	(Cosottini et al., 2012)
Resting state	20 ALS 20 HC 3T	Decreased activation in sensorimotor and default mode network	(Mohammadi et al., 2009a)
	20 ALS 20 HC 3T	Decreased interhemispheric primary motor cortical connectivity	(Jelsone-Swain et al., 2010)
	12 ALS 12 HC 3T	Increased functional motor connectivity in faster progressing patients	(Verstraete et al., 2010)
	26 ALS 15 HC	Increased functional connectivity in (left) sensorimotor areas	(Agosta et al., 2011)
	25 ALS 15 HC 3T	Increased functional connectivity in motor, premotor, frontal areas positively correlated with rate of disease progression	(Douaud et al., 2011)

HC = healthy controls; VBM = voxel-based morphometry.

hands (Lule et al., 2007b). This differential pattern might reflect disruption of the normal networks associated with motor imagery.

In summary, motor task-based fMRI data in ALS demonstrate a widened recruitment of premotor and higher order cortical regions linked to motor processing. This might represent a futile attempt at compensation for progressive ALS-associated disability, or reflect a more primary dysfunction of local modulating interneuronal circuits.

Active paradigms probing extra-motor networks

The established clinical and pathological association of ALS with FTD is supported by fMRI studies. Reduced activation in the middle and inferior frontal gyri, anterior cingulate, parietal and temporal cortices is associated with reduced verbal fluency in ALS patients without frank dementia (Abrahams et al., 2004). An increased cerebral activation accompanying the performance of the Stroop effect and areas of decreased activation during the negative priming comparison suggests altered inhibitory processing in ALS for the cognitive processing pathway (Goldstein et al., 2011).

Processing of socio-emotional stimuli was noted to be altered in non-demented ALS patients studied over six months (Lule et al., 2007a). Reduced activity in right sided frontal areas during processing of aversive emotional stimuli support the assumption of an impaired emotional processing pathway in ALS (Palmieri et al., 2010). In a paradigm involving visual, auditory and somatosensory stimuli, patients demonstrated reduced activity in primary and secondary sensory areas and increased activity in higher associative areas. The higher the physical restrictions, the higher the activity in those areas (Lule et al., 2010). Overall, fMRI data present functional evidence for multi-system involvement of cognitive, emotional and sensory processing pathways in ALS.

Resting state networks

Analysis of resting-state fMRI (rs-fMRI) reveals the temporal correlation between the low-frequency spontaneous fluctuations in the resting whole-brain. These form functionally-distinct networks (Smith et al., 2009), and rs-fMRI has potential clinical value as a sensitive marker in several disease states (Greicius, 2008; van den Heuvel and Hulshoff Pol, 2010).

In ALS, initial rs-fMRI studies confirmed the intuitive expectation of a decrease in activity, seen in the somatosensory and default-mode resting state networks (Mohammadi et al., 2009a), supported by evidence of impaired interhemispheric functional connectivity between primary motor cortices (Jelsone-Swain et al., 2010). However, subsequent studies have identified regions of *increased* functional connectivity, including somatosensory areas (Agosta et al., 2011), with higher rates of functional connectivity generally in those with faster disease progression (Verstraete et al., 2010). In a study using a pre-defined 'ALS-specific' cortical network, increased functional connectivity was found over a large area spanning sensorimotor, premotor, prefrontal and thalamic regions, and significantly

overlapping the areas of structural change identified using DTI (Douaud et al., 2011). The observation that those with the highest rates of disease progression had the greatest functional connectivity lends support to a pathogenic loss of local inhibitory circuitry, rather than only compensatory recruitment (Turner and Kiernan, 2012).

2

Opportunities

The fusion of structural and functional information using MRI holds major promise for more sensitive biomarker panels in ALS. The combination of structural and resting-state functional connectivity shows the greatest potential yet to separate the full range of ALS phenotypes from healthy controls (Douaud et al., 2011). The sensitivity of fMRI measures to longitudinal change in ALS, and so their suitability as therapeutic trial outcome measures, is awaited.

MAGNETIC RESONANCE SPECTROSCOPY

Magnetic resonance spectroscopy (MRS) permits the measurement of tissue metabolites non-invasively. Though more than thirty metabolites can be distinguished in healthy brains by ¹H-MRS (Govindaraju et al., 2000), N-acetylaspartate (NAA), total-creatine (Cr) and total-choline (Cho) have been most studied due to their simple (singlet) spectral patterns and relatively high concentrations in the brain. NAA is localized primarily in neurons and so its concentration in the brain as measured by ¹H-MRS is directly related to neuronal density, metabolism and functional status. Cr, which consists of creatine and phosphocreatine, indicates the status of cellular energetics. Cho, which has combined contributions from the brain cell membrane components glycerophosphocholine and phosphocholine, and free choline, provides information on the membrane structural integrity, synthesis and degradation. Other less prominently observable brain metabolites but relevant to ALS, are the excitatory neurotransmitter glutamate (Glu, or Glx in combination with glutamine), and myo-inositol (m-Ins) localized within astrocytes and considered to be a glial maker.

MRS data acquisitions in the brain of patients with ALS have historically largely necessitated using either single voxel (Jones et al., 1995; Giroud et al., 1996; Han and Ma, 2010; Usman et al., 2011) or slice (Pioro et al., 1994; Rooney et al., 1998) data acquisition methods, rather than a whole brain analysis (Figure 2.4) (the original article contains a table [eTable 5] including MRS studies applied to ALS and related disorders). An individual metabolite

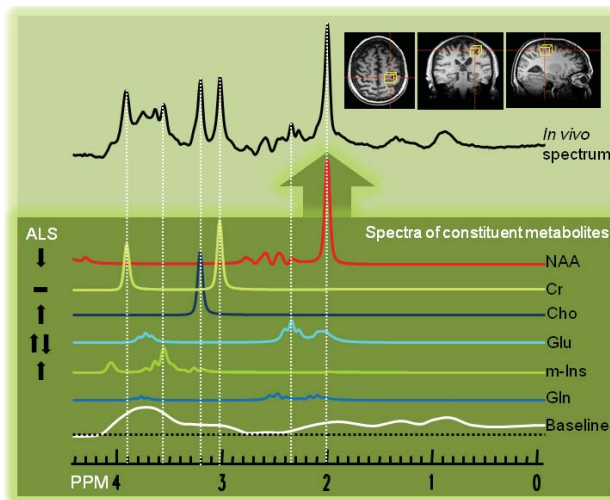


Figure 2.4 Proton MR spectrum changes in ALS

Proton MR spectrum acquired from a 64 year old male volunteer at 3T MRI scanner. The data for *in vivo* spectrum (top panel) was collected by localizing a voxel (yellow cube on the MRIs; 1 cm³ isotropic) at the precentral gyrus using a PRESS sequence with TR/TE of 2000/30 ms. Bottom: The fitted spectra from the metabolites that contributed to the *in vivo* spectrum (bottom panel) with the change in the concentration of these metabolites in patients

with ALS as compared to the values in control subjects indicated with arrows.

NAA = N-acetyl aspartate; Cr = total-creatine; Cho = total-choline; Glu = glutamate, m-Ins = myo-inositol; Gln = glutamine; baseline = signal contribution from macromolecules; PPM = parts per million.

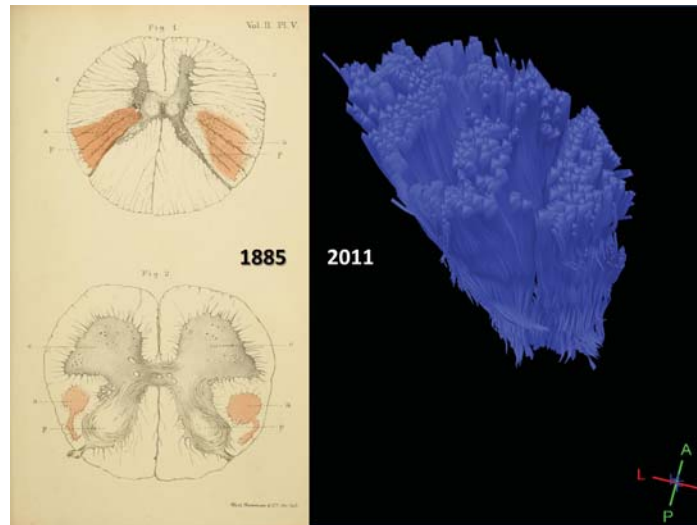


Figure 2.5 Pathology and neuroimaging

Lateral columns of the spinal cord (left panel, shaded) noted as damaged in the early *post mortem* studies of ALS carried out in the late 1800s by Jean-Martin Charcot. This can be contrasted with the vertical oblique view of the spinal cord showing longitudinal fibre tracts (right panel, A-anterior, P-posterior, L-left), in an image from an ALS patients acquired non-invasively using diffusion tensor imaging, and in which pathology can now be quantified *in vivo*.

(Left panel images from Charcot JM. Lectures on the Diseases of the Nervous System. [Sydenham Society, London, 1881])

is commonly reported either as a ratio to Cr, Cho or Cr+Cho or in institutional units. Reporting absolute concentrations requires additional measurements.

Motor findings

A pivotal study demonstrated decreased NAA:Cr in the PMC of ALS patients, in contrast to those with spinal muscular atrophy, when compared to healthy controls (Pioro et al., 1994). Studies have reported a variety of altered metabolite ratios in the PMC of patients with ALS including:

1. Decreased NAA (Mitsumoto et al., 2007; Gredal et al., 1997; Bradley et al., 1999; Pohl et al., 2001a; Sarchielli et al., 2001; Schuff et al., 2001; Block et al., 2002; Suhy et al., 2002)
2. Decreased NAA:Cr (Han and Ma, 2010; Pioro et al., 1994; Block et al., 2002; Suhy et al., 2002; Block et al., 1998; Abe et al., 2001; Rule et al., 2004; Yin et al., 2004; Kalra et al., 2006a; Kalra et al., 2006b; Charil et al., 2009; Lombardo et al., 2009; Pyra et al., 2010; Sivak et al., 2010)
3. Decreased NAA:(Cr+PCr) (Jones et al., 1995)
4. Decreased NAA:Cho (Jones et al., 1995; Giroud et al., 1996; Block et al., 2002; Suhy et al., 2002; Block et al., 1998; Rule et al., 2004; Kalra et al., 2006a; Pyra et al., 2010)
5. Decreased NAA:(Cr+Cho) (Rooney et al., 1998; Suhy et al., 2002; Rule et al., 2004)
6. Decreased Cr (Pohl et al., 2001a; Block et al., 2002)
7. Increased Cho (Schuff et al., 2001; Suhy et al., 2002; Bowen et al., 2000)
8. Increased Cho:Cr (Block et al., 2002; Block et al., 1998; Lombardo et al., 2009; Pyra et al., 2010)
9. Increased Cho:NAA (Suhy et al., 2002)
10. Increased m-Ins (Bowen et al., 2000)
11. Increased m-Ins:Cr (Block et al., 1998; Kalra et al., 2006a; Lombardo et al., 2009)
12. Increased Glu:Cr and Glx:Cr (Han and Ma, 2010)

Metabolite alterations in other discrete anatomical regions along the cranial CST have been reported in ALS patients, such as the PLIC (Han and Ma, 2010; Schuff et al., 2001), periventricular white matter (Yin et al., 2004), and corona radiata (Pyra et al., 2010).

Specific metabolite levels in the PMC of ALS patients have ranged from:

1. 8%–23% decrease for NAA (Schuff et al., 2001; Suhy et al., 2002)
2. 13%–20% increase for Cho (Schuff et al., 2001; Bowen et al., 2000)
3. 8%–32% decrease for NAA:Cr (Pioro et al., 1994; Suhy et al., 2002)
4. 11%–56% decrease for NAA:Cho (Giroud et al., 1996; Rule et al., 2004)

Reported correlations between the metabolite concentration changes in the PMC and clinical measures of UMN deficits (Mitsumoto et al., 2007; Rooney et al., 1998; Block et al., 2002; Bowen et al., 2000; Wang et al., 2006b), severity of disease (Abe et al., 2001; Wang et al., 2006b; Ellis et al., 1998), lateralization of clinical symptoms (Block et al., 2002) and disease progression (Pohl et al., 2001a; Pyra et al., 2010) suggest that MRS could be a useful tool to understand phenotype heterogeneity.

Metabolite changes have also been found in the brainstem of ALS patients (Bradley et al., 1999; Block et al., 2002; Cwik et al., 1998; Pioro et al., 1999; Hanstock et al., 2002). NAA:Cr in the brainstem was lower in patients with severe bulbar weakness or spasticity and near normal ratio in patients with predominantly LMN weakness (Cwik et al., 1998). A 55% higher level of Glu+glutamine (Glx) in the medulla of patients with ALS (Pioro et al., 1999) supports the wider concept of excitotoxicity in ALS (Rothstein, 2009).

Extra-motor findings

MRS studies have found decreased NAA:Cho in non-motor regions such as the thalamus and basal ganglia (Sharma et al., 2011), mid-cingulate cortex (Sudharshan et al., 2011), and the frontal and parietal lobes (Rule et al., 2004) of patients with ALS.

Sensitivity to longitudinal change and therapeutics

Longitudinal MRS studies have reported continued reduction in NAA:Cho (Pohl et al., 2001a; Block et al., 2002) and NAA (Suhy et al., 2002; Rule et al., 2004; Unrath et al., 2007) in the PMC of patients with ALS over follow up periods lasting up to 28 months (Block et al., 2002), with correlation between changes in PMC NAA:Cho and progression

rate ($r = 0.55$) (Pohl et al., 2001a) but no consistent pattern of longitudinal metabolite change overall.

MRS has been used to evaluate therapeutic effects on brain metabolites in ALS. An increase of 6% of NAA:Cr in the PMC of 11 patients after administration of Riluzole for three weeks was noted, whereas it decreased by 4% in a group of untreated patients (Kalra et al., 1998). However, there was no corresponding consistent symptomatic or functional improvement in the treatment group. A study of oral creatine therapy revealed increased creatine (8%) and reduced Glx (18%) in the frontal cortex 19 days after treatment initiation (Atassi et al., 2010).

For improved detection of UMN involvement in patients with ALS, the metrics of MRS and TMS (Pohl et al., 2001b; Kaufmann et al., 2004) or DTI (Wang et al., 2006b) were compared. MRS detected UMN involvement in 86% of the patients with definite UMN signs versus 77% by TMS (Kaufmann et al., 2004), but the results of individual methods taken together improved further sensitivity to detect UMN signs to 92%. NAA:Cr in the PMC and FA values in the PLIC in the 'affected' hemisphere in combination showed potential to predict disease duration (Wang et al., 2006b).

Limitations and opportunities

Though MRS is the only *in vivo* technique that provides CNS tissue chemistry information, disadvantages include low signal-to-noise ratio, poor spatial resolution (relative to DTI), and cumbersome non-standardised methods for acquiring, processing, analyzing and reporting data, which have all diminished its wider application. Nonetheless, NAA (in combination with other metabolites) has proved to be a sensitive and robust marker of neuronal loss in the PMC in ALS and the development of a comparatively high spatial resolution whole-brain MR spectroscopic imaging and automated processing software offers renewed potential as part of a multimodal biomarker panel. Very high field MRS (7T) improves the sensitivity and spectral resolution greatly, permitting the measurement of the inhibitory neurotransmitter GABA, with direct relevance to ALS pathogenesis (Turner and Kiernan, 2012).

SPINAL CORD MRI

The ‘dying-back’ theory of pathological spread in ALS suggests that early degeneration is more likely to be captured at the spinal anterior horn rather than brain (Dadon-Nachum et al., 2011). Multilevel spinal imaging supports this theory, with FA differences between ALS patients and healthy controls noted to be more significant in the more distal segments of the cord than proximally (Nair et al., 2010). *Post mortem* studies show maximum UMN and LMN loss within the spinal (or brainstem) level corresponding to the site of initial weakness, with spinal cord somatotopic anatomy postulated to be a key determinant of the progression of disability in ALS (Ravits and La Spada, 2009). Thus, there is value in developing spinal cord imaging.

High quality, quantitative spinal cord imaging is challenging. The small axial dimensions of the spinal cord mean that tissue segmentation is highly susceptible to partial volume effects. Physiological motion distortions secondary to breathing, swallowing, and cardiac pulsation; magnetic field inhomogeneities posterior to the vertebral bodies, and differences in coil requirements are being overcome by corrective methods such as cardiac and respiratory gating, spatial saturation pulses, and retrospective image correction models (Brooks et al., 2008; Figley and Stroman, 2009). Several spinal cord MRI studies have now been undertaken successfully in ALS (the original article contains a table [eTable 6] including all spinal cord MRI studies applied to ALS and related disorders).

Cord MRI signal change and segmental atrophy

High signal changes along the corticospinal tracts (CST) have been described in the spinal cord on T1, T2 - weighted, as well as on fluid attenuated inversion recovery (FLAIR) imaging (Terao et al., 1995; Waragai, 1997). The reported specificity and sensitivity of these findings to ALS vary greatly however (Sperfeld et al., 2005), making them unsuitable for biomarker purposes.

Whilst one study reported decreasing cross-sectional area on longitudinal spinal cord imaging (Agosta et al., 2009b), another reported no significant atrophy (Sperfeld et al., 2005). Quantifying spinal cord atrophy is challenging and different approaches have been used, including measuring spinal cord cross-sectional area, the anterior-posterior diameter of the spinal cord and 3D-modified driven equilibrium Fourier transform (Freund et al., 2010).

DTI in the cord

The power of *in vivo* neuronal tractography can now be applied to the spinal cord (Figure 2.5). Patients with ALS have been shown to have considerably lower average FA of the cervical cord than healthy controls with a very tight correlation to disability (Valsasina et al., 2007). Longitudinal decrease in cord average FA and an increase in cord MD was shown during a mean follow-up of 9 months (Agosta et al., 2009b).

MRS in the cord

Reduced NAA ratios in the cervical cord appear to correlate with reduced forced vital capacity in ALS in a single voxel MRS study (Carew et al., 2011b). A pivotal MRS study of pre-symptomatic carriers of pathogenic *SOD1* mutations identified reduced metabolite ratios in the cervical cord similar to affected ALS patients (Carew et al., 2011a), raising the potential for very early biomarkers in this group.

Animal studies

A range of high-field MRI techniques have been applied to rodent models of ALS (Evans et al., 2012), including study of the spinal cord using DTI (Underwood et al., 2011), MRS (Choi et al., 2009), Magnetic Resonance Microscopy (Wilson et al., 2004) and Pharmacologic MRI (phMRI) (Choi et al., 2010).

Opportunities

Spinal cord fMRI is a relatively novel technique in evolution and not yet applied to ALS. The potential of the technique has been convincingly demonstrated with both upper (Bouwman et al., 2008) and lower limb (Kornelsen and Stroman, 2004) motor tasks. Advanced DTI techniques such as high angular resolution diffusion imaging (HARDI) and Q-ball imaging (QBI) (Cohen-Adad et al., 2008) are ideally suited to spinal applications as they detect commissural, medio-lateral and dorso-ventral fibres. Very high-field spinal cord imaging at 7 Tesla provides greater signal-to-noise ratio and in-plane resolution (0.18mm) (Sigmund et al., 2012). Such developments promise to bring the full range of traditionally brain-based MRI techniques to ALS research.

FUTURE PERSPECTIVE

Novel techniques

Advances in image analysis offer the potential to extract 'hidden' potential biomarkers from routine clinical imaging (Ding et al., 2011), but novel MRI applications to ALS continue to emerge. Relaxometry is a technique relying on changes in the biophysical water environment or metal load (e.g. iron content) within a given tissue altering the relaxation rate of the proton magnetic moment. Voxel-based relaxometry (VBR) based on T2-weighted images, might offer greater sensitivity along the corticospinal tract (Minnerop et al., 2009). Abnormal relaxometry, interpreted as iron deposition along the CST, has also been reported in ALS patients (Langkammer et al., 2010). Magnetization transfer ratio (MTR) imaging uses a radio frequency pre-pulse to preferentially saturate immobile protons of macromolecules, which then transfer magnetization to mobile protons in free water, that are in turn used to detect changes in brain tissue structure. Modest signal change in magnetization transfer contrast have been noted in the CST of ALS patients (da Rocha et al., 1999; Kato et al., 1997; Tanabe et al., 1998) and also frontal regions (Cosottini et al., 2012), but the combination in both the CST and posterior CC was reported to be 100% specific for ALS (though < 40% sensitive) (Carrara et al., 2012). BOLD MRI is recognised to be an indirect measure of neuronal activity, influenced by a number of inter-related factors including cerebral blood flow (CBF). Using a novel MRI technique called arterial spin labelling (ASL), CBF can be non-invasively assessed, and changes observed in grey matter have been linked to disability in ALS patients (Rule et al., 2010). Finally, the development of novel PET ligands for *intracellular* targets (Skotland, 2012) such as TDP-43 for ALS, would mark a major biomarker advance.

A network approach

The human brain is a network in which specialized functional regions are interlinked by numerous white matter connections (Sporns, 2011). Network-based analysis is not restricted to a particular imaging modality and has been applied to rs-fMRI (van den Heuvel and Hulshoff Pol, 2010; Achard et al., 2006), DTI (Hagmann et al., 2007) and T1-based images (Chen et al., 2008). Such analyses suggests a small-world topology (Stam, 2004; van den Heuvel et al., 2008a) and highly connected brain hubs appear to have a strong tendency to be mutually interconnected, with a 'rich club' of topologically central

brain regions possibly having a greater impact on brain functioning (van den Heuvel and Sporns, 2011). Future network-based research in ALS might reveal (1) different stages of the disease, (2) subtypes for cognitive impairments and (3) a connectivity profile associated with a better or worse prognosis.

Pre-symptomatic study

The failure of many therapeutic trials may simply be a feature of diagnosis occurring long after the pathological process begins, past the point of salvage. A lack of knowledge of those at risk for ALS or pre-clinical indicators prevents any vision of earlier intervention or primary prevention. Individuals carrying monogenetic abnormalities associated with high risk for developing ALS can provide valuable clues to the earliest changes. Such studies have ethical challenges, and are confounded by issues of incomplete penetrance. Nonetheless, this strategy represents a major opportunity to advance the ultimate hope of translation to sporadic disease. DTI (Ng et al., 2008) and MRS (Carew et al., 2011a) have already demonstrated the ability to detect change in this group.

How will neuroimaging in ALS evolve?

ALS is characterised by variable involvement of LMN, UMN and extra-motor neuronal 'compartments'. MRI seems uniquely placed to capture all three non-invasively. Whilst group-level analysis reveals important pathogenic mechanisms, the 'giant leap' will be to translate these to the individual. This seems likely to require multiple MRI measures (Douaud et al., 2011), perhaps also in combination with biofluid or neurophysiological biomarkers. This in turn requires larger, clinically well-characterised datasets (including large 'control banks') subject to standardisation and harmonisation. This is only achievable through international collaboration, and a broad framework for this type of approach has been established (Turner et al., 2011a), with the expectation that advanced neuroimaging will become a routine part of ALS patient management.

EXECUTIVE SUMMARY

Radionuclide imaging

- Activation PET provided some of the earliest *in vivo* evidence for the now established concept of ALS a multi-system cerebral neurodegeneration, and SPECT for the concept of a continuum with FTD.
- Ligand PET studies in ALS have demonstrated potentially important pathogenic mechanisms including loss of inhibitory interneuronal regulation, neuroinflammation and involvement of serotonergic systems. The development of novel ligands with relevance to key pathways in ALS pathogenesis uncovered by cell biology would renew interest in this highly sensitive technique.

Voxel and surface-based MRI morphometry

- VBM currently lacks sensitivity as an independent biomarker, but may have a greater impact in the deep phenotyping of cognitive impairment in ALS. SBM appears to have greater sensitivity to atrophy in cortical motor areas and its diagnostic potential needs further exploration.

Diffusion tensor imaging

- DTI is highly sensitive to cerebral white matter pathology and has increasing potential in the spinal cord. In this regard it is currently unrivalled as a neuroimaging biomarker of UMN involvement in ALS, though its sensitivity to longitudinal change may be more limited.

Functional MRI

- rs-fMRI offers a unique opportunity to study ALS as a ‘system degeneration’, through its visualisation of inter-related cerebral networks. This may provide crucial insights when applied to pre-symptomatic ALS cases, with the ultimate hope of testing strategies for primary prevention.

Magnetic resonance spectroscopy

- With increasingly harmonised methodology and whole-brain approaches, MRS is poised to capitalise on potentially sensitive metabolite biomarkers in ALS.

A multimodal approach

- The future is likely to involve a multimodal approach including structural and functional neuroimaging biomarkers from brain and spinal cord to create a 'signature' applicable to the range of phenotypes, and which can provide quantifiable evidence of efficacy in future therapeutic trials.

PART I
SPREAD OF DISEASE



3

Symptom development in patients with motor neuron disease

Renée Walhout*

Esther Verstraete*

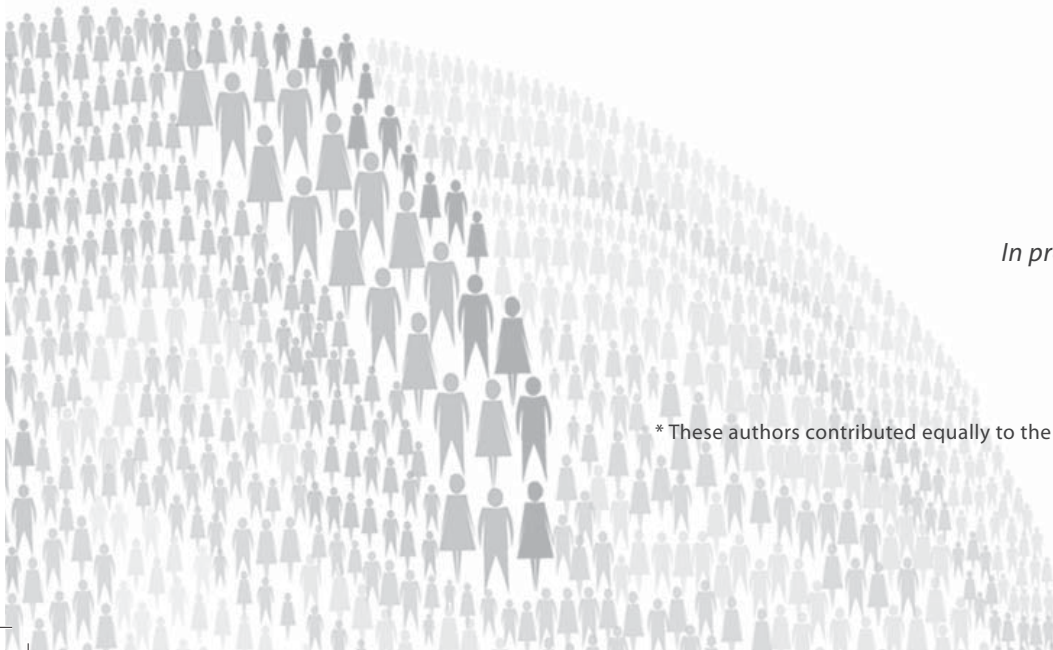
Martijn P. van den Heuvel

Jan H. Veldink

Leonard H. van den Berg

In preparation

* These authors contributed equally to the manuscript



ABSTRACT

Objectives: To investigate whether symptom development in motor neuron diseases (MND) is a random or organized process, in order to gain insight into the underlying mechanism of motor neuron degeneration.

Methods: Six hundred patients with amyotrophic lateral sclerosis (ALS), progressive muscular atrophy (PMA) and primary lateral sclerosis (PLS) were invited to complete a questionnaire concerning symptom development. A binomial test was used to examine whether distribution of symptoms from site of onset was random. Development of symptoms over time was evaluated by Kaplan Meier analysis.

Results: Four hundred seventy patients returned the questionnaire (ALS n = 254; PMA n = 100; PLS n = 116). ALS patients reported significantly more often symptoms in the contralateral limb following unilateral limb onset (arms: $p = 1.05 \cdot 10^{-8}$; legs $p < 2.86 \cdot 10^{-15}$). The same pattern was seen in patients with PMA (arms, $p = 6.74 \cdot 10^{-9}$; legs $p = 6.26 \cdot 10^{-6}$) and for PLS patients in the lower limbs ($p = 4.07 \cdot 10^{-14}$). With regard to the timing of symptom development in patients with limb onset, symptoms occurred consistently faster in the contralateral limb, followed by the other limbs and lastly by the bulbar region.

Conclusions: Symptom development in MND is an organized process, the preferred spread of symptoms from one limb to the contralateral limb being a uniform feature of both upper and lower motor neuron phenotypes. This nonrandom pattern of symptom development might suggest that neural connectivity guides spread of disease.

INTRODUCTION

Amyotrophic lateral sclerosis (ALS) is a neurodegenerative disease, characterized by degeneration of motor neurons in the cerebral cortex, brainstem and spinal cord, resulting in progressive muscle weakness. Mechanisms underlying the ongoing degeneration of motor neurons are still unknown. The question remains whether ALS is a multifocal disease with degeneration of independent vulnerable regions, or one focus of disease with subsequent spread throughout the nervous system (Eisen, 2009). Recently, it has been suggested that ALS spreads in a prion-like fashion with cell to cell transmission of misfolded, protein aggregates, leading to progressive loss of motor neurons (Polymenidou and Cleveland, 2011). If this is true, spread of disease is likely to be guided by neural connectivity, which might be reflected by the pattern of symptom development in patients.

It has been hypothesized that degeneration of lower motor neurons might differ from upper motor neuron degeneration, due to differences in somatotopic organization: lower motor neuron degeneration would preferentially spread at one level of the spinal cord, to the other side of the spinal segment, while degeneration of upper motor neurons would spread preferably along the cerebral cortex to adjacent, ipsilateral areas (Ravits and La Spada, 2009). Based on this concept of neurodegeneration, different patterns of symptom development would be expected in upper motor neuron degeneration compared to lower motor neuron degeneration. However, studies disentangling upper and lower motor neuron involvement in ALS are hampered by the fact that upper motor neuron signs can be masked by lower motor neuron dysfunction and an objective upper motor neuron marker is not available. While most of the studies thus far focused on symptoms in ALS (Fujimura-Kiyono et al., 2011; Korner et al., 2011; Gargiulo-Monachelli et al., 2012), patterns of symptom development in pure upper or lower MND – such as primary lateral sclerosis (PLS) and progressive muscular atrophy (PMA) – are relatively unexplored. We included these MND subtypes to examine whether development of symptoms differs in upper and lower motor neuron phenotypes.

In this study we investigated symptom development in a large cohort of patients with ALS, as well as PMA and PLS, looking for specific patterns of disease spread that might provide insight into the underlying mechanism of motor neuron degeneration.



METHODS

Patient selection

Patients were identified from a database of a prospective population-based study in the Netherlands (Huisman et al., 2011). This database contains information about patients with MND diagnosed in The Netherlands, including date and site of disease onset. From this database, we selected those patients with ALS, PMA and PLS who were still alive. At the time of diagnosis, patients were classified as having definite, probable or possible ALS using the revised El Escorial criteria (Brooks et al., 2000). In patients initially diagnosed with possible ALS, diagnosis was later confirmed by the progressive deterioration. Both sporadic and familial ALS cases were included. PMA was diagnosed in patients with a clinically isolated lower motor neuron disorder, while PLS was diagnosed in those patients presenting with an upper motor neuron phenotype without any lower motor neuron findings on examination or electromyography. Diseases, known to mimic MND (e.g. multifocal motor neuropathy, cervical spondylosis), were excluded by laboratory testing and neuroimaging.

Data collection

A questionnaire was designed to evaluate symptom development in patients with MND, consisting of a schematic representation of the body, including six anatomical sites (bulbar region, right/left arm, trunk, right/left leg) that may be involved in the disease course. Patients were asked to order these sites by number, according to the onset of symptoms. Symptoms were defined for the limbs and trunk as weakness, and for the bulbar region as difficulties with speech or swallowing. Weakness of the trunk was exemplified as difficulty to get up or walk upright. While the respiratory muscles are innervated by cervical, as well as thoracic segments of the spinal cord, symptoms of dyspnea were not particularly asked for as these would not differentiate between the cervical and thoracic region. If symptoms had started in multiple sites at the same time, patients were asked to assign the same number to those sites. In addition, for each site, patients were asked to report the date of symptom onset. Date of onset was defined as the time of the first symptom noticed by the patient. To investigate the spread of symptoms after onset in a particular site, we defined body sites relative to the site of onset as ipsilateral and contralateral. Contiguous spread was defined as spread of symptoms to adjacent sites (e.g. right arm to left arm), while non-contiguous spread was defined as spread to distant sites (e.g. bulbar to legs).

Standard protocol approvals, registrations, and patient consents

This study was approved by the medical ethics committee for research into humans of the University Medical Center Utrecht. Written informed consent was given by all patients participating in the study.

Statistical analysis

Calculations were performed using SPSS for Windows (version 15.0, SPSS, Chicago, IL) and R software package for statistical computing (www.R-project.org, R 2.11.1 GUI 1.34). The binomial test of proportions was used to examine whether development of symptoms from site of onset to any other site was random. Under the null hypothesis (independent foci), the site of onset and involvement of subsequent symptomatic sites should be independent and therefore, symptoms should be equally distributed to subsequent sites. The Bonferroni method was used to correct for multiple testing. A statistical threshold of $\alpha < 0.05$ was considered statistically significant. Corrected p-values are shown.

Kaplan Meier analysis was performed to evaluate the development of symptoms over time per site of onset. Using the reported dates of symptom onset, time to progression from the initial site of onset to any site could be calculated in months. If patients did not report a site as being symptomatic, the time of censoring (1 January 2011) was used to calculate the symptom-free period. The percentage of patients reporting symptoms in a specific site after one and two years was calculated and compared. For example, in case of bulbar onset, the percentage of patients reporting subsequent arm involvement was compared to the percentage having subsequent leg symptoms. If dates of symptom onset were not reported at all, the patient was excluded from analysis.

RESULTS

Between November and December 2010, the questionnaire was sent to 600 patients. Nineteen patients turned out to be deceased. Of the remaining 581 patients, 470 patients returned the questionnaire (response 81%). Baseline characteristics are listed in Table 3.1.

3



Table 3.1 Demographic and clinical characteristics of respondents per diagnosis (n = 470)

	ALS		PMA		PLS	
Diagnosis, n (%)	254	(54)	100	(21)	116	(25)
Gender, n (%)						
Male	163	(64)	76	(76)	71	(61)
Female	91	(36)	24	(24)	45	(39)
Age at diagnosis, median (range), y	59.5	(23–81)	63.0	(25–80)	58.0	(20–81)
Age at onset, median (range), y	58.0	(23–80)	59.0	(18–77)	53.0	(16–77)
Site of onset, n (%)						
Bulbar	59	(23.2)	0	(0.0)	17	(14.7)
Cervical	91	(35.8)	53	(53.0)	6	(5.2)
Thoracic	3	(1.2)	6	(6.0)	0	(0)
Lumbosacral	101	(39.8)	41	(41.0)	93	(80.2)
Disease duration, median (range), months	37	(7–378)	68	(11–451)	109	(20–462)
ALS type, n (%)						
Sporadic	240	(94)				
Familiar	14	(6)				
El Escorial score, n (%)						
Definite ALS	30	(12)				
Probable ALS	113	(45)				
Probable ALS lab supported	49	(19)				
Possible ALS	62	(24)				

ALS = amyotrophic lateral sclerosis; PMA = progressive muscular atrophy; PLS = primary lateral sclerosis.

Spread of symptoms from initial site of onset

In total, 370 out of 470 patients reported a focal site of onset (79%): 216 ALS patients, 70 PMA patients and 84 PLS patients. In these patients, the development of symptoms from site of onset to subsequent sites appeared not randomly distributed. Site of onset, preferred development of symptoms from site of onset and corresponding p-values are shown in Figure 3.1.

In ALS patients with arm onset, the contralateral arm was significantly more often the next symptomatic site, compared with other sites ($p = 1.05 \cdot 10^{-8}$). The same pattern was seen in ALS patients with leg onset, there was significantly more spread of symptoms to the contralateral leg ($p < 2.86 \cdot 10^{-15}$). In those patients reporting subsequent symptoms development in the contralateral leg, the arms (28/51 [54.9%], $p = 0.00488$) were more often the next symptomatic site compared to the bulbar region (4/51 [7.8%], $p = 1.073 \cdot 10^{-4}$).

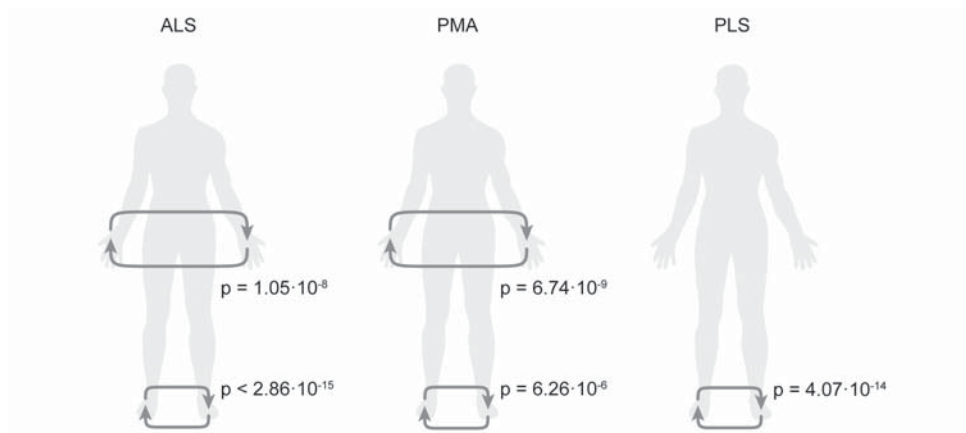


Figure 3.1 Spread of symptoms from site of onset to subsequent body regions

This figure shows the preferred spread of symptoms for each MND subtype (ALS, PMA and PLS). Green arrows indicate the distribution of symptoms from site of onset to sites that were significantly more often reported as being symptomatic. Shown p-values are corrected for multiple testing by Bonferroni. ALS = amyotrophic lateral sclerosis; PMA = progressive muscular atrophy; PLS = primary lateral sclerosis.

A similar pattern to what we found in patients with ALS was observed in PMA patients: in patients with symptom onset in the arms or legs, the contralateral limb was significantly more often reported as the subsequent symptomatic site, compared to other body regions (arms, $p = 6.74 \cdot 10^{-9}$; legs $p = 6.26 \cdot 10^{-6}$). As expected, patients diagnosed with PLS mostly presented with symptoms in the legs. Involvement of the contralateral leg was significantly more often reported compared to other regions ($p < 4.07 \cdot 10^{-14}$).

By subdividing the body into the four regions of the El Escorial criteria (bulbar, cervical, thoracic and lumbosacral) – instead of including right and left limbs as separate sites – involvement of body regions was further explored (Table 3.2). In ALS patients with bulbar onset, we found more subsequent cervical involvement compared to the more distant lumbosacral region (31/53 [58.5%], $p = 0.00242$). The same pattern was seen in ALS patients and PMA patients with a lumbosacral onset, the cervical region being more frequently reported as symptomatic than the bulbar region (ALS 49/89 [55.1%], $p = 4.05 \cdot 10^{-10}$; PMA 22/33 [66.7%], $p = 0.00108$).

With regard to the 100 patients reporting multifocal onset, 86 showed bilateral limb involvement: 60 patients lower limb onset and 26 upper limb onset. This pattern was similar for all MND subtypes.

Table 3.2 Spread of symptoms from region of onset

1st region → 2nd region	ALS			PMA			PLS		
	n	(%)	p-value	n	(%)	p-value	n	(%)	p-value
Bulbar onset	53			0			15		
→ cervical	31	(58.5)	0.00242 *				4	(26.7)	NS
→ thoracic	5	(9.4)	0.00122 #				2	(13.3)	NS
→ lumbosacral	17	(32.1)	NS				9	(60.0)	NS
Cervical onset	83			43			6		
→ bulbar	20	(24.1)	NS	4	(9.3)	0.00446 #	1	(16.7)	NS
→ thoracic	12	(14.5)	0.00188 #	12	(27.9)	NS	0	(0)	NS
→ lumbosacral	51	(61.4)	2.93·10 ⁻⁶ *	27	(62.8)	0.00109 *	5	(83.3)	NS
Lumbosacral onset	89			33			72		
→ bulbar	13	(14.6)	1.42·10 ⁻⁴ #	2	(6.0)	0.00291 #	16	(22.2)	NS
→ cervical	49	(55.1)	4.05·10 ⁻¹⁰ *	22	(66.7)	0.00108 *	34	(47.2)	NS
→ thoracic	27	(30.3)	NS	9	(27.3)	NS	22	(30.6)	NS

p-values corrected for multiple testing by the Bonferroni method. Regions with significantly more subsequent involvement are marked by an asterisk (*). Regions with significantly less subsequent involvement are marked by a hashtag (#).

ALS = amyotrophic lateral sclerosis; PMA = progressive muscular atrophy; PLS = primary lateral sclerosis; NS = not significant.

Finally, we looked more specifically into the clinical characteristics of ALS patients with a non-contiguous pattern of symptom development. In ALS patients with a bulbar onset, 16 out of 55 patients (29%) reported subsequent involvement of the legs. In addition, 7 out of 78 patients with leg onset (9%) reported subsequent involvement of the bulbar region. There were no significant differences in clinical characteristics (age at onset and diagnosis, survival) in patients with non-contiguous spread.

Symptom development over time

Reported dates on symptom development were available for 188 ALS patients, 61 PMA patients and 70 PMA patients (86% of patients with a focal onset). Involvement of body regions over time according to site of onset is illustrated with Kaplan Meier curves (Figure 3.2). The patient numbers of PLS patients with bulbar onset (n = 14) and arm onset (n = 4) were insufficient to produce meaningful curves, as was thoracic onset for all MND subtypes. The Kaplan Meier curves were used to compare involvement of specific sites after disease onset. Differences in frequency of involvement one and two years after disease onset are shown in Table 3.3.

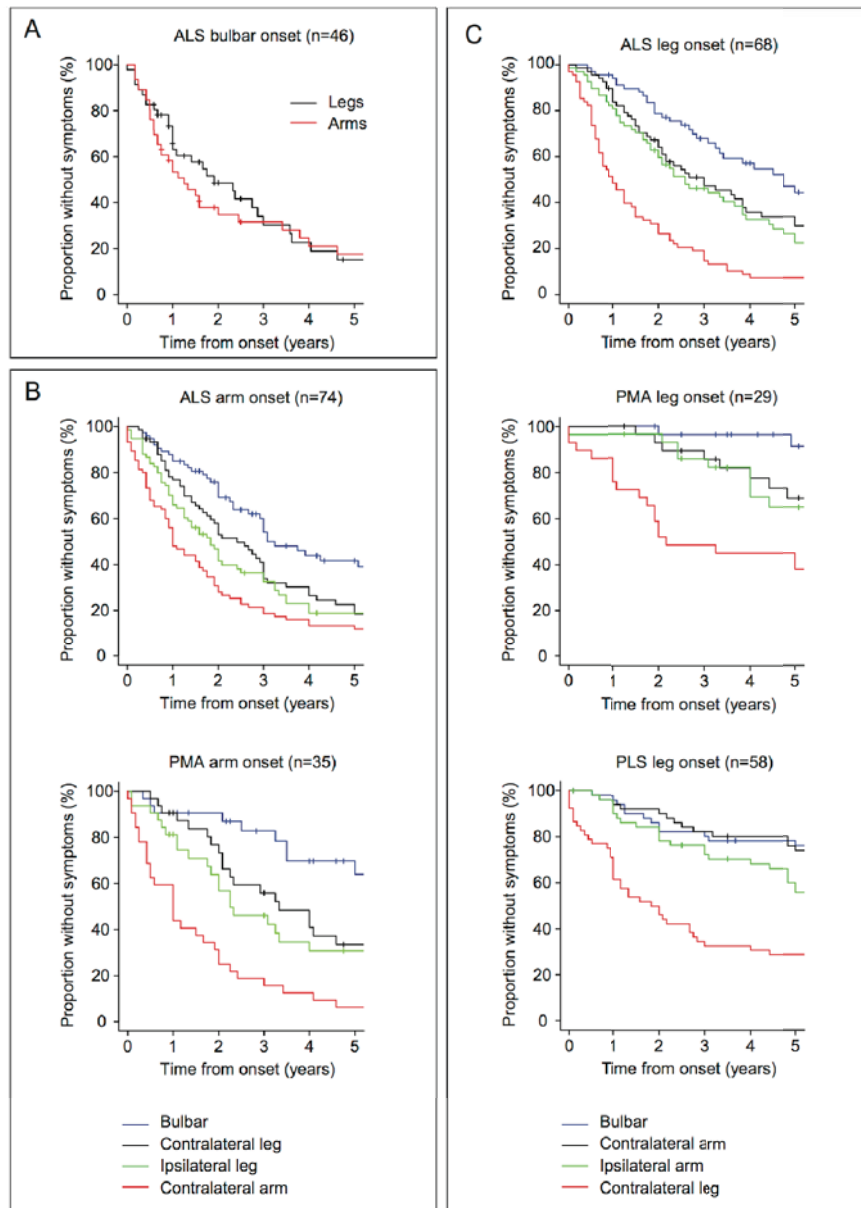


Figure 3.2 Symptom development over time in MND patients according to site of onset

Kaplan Meier curves showing involvement of sites over time according to site of onset in patients with MND. (A) Bulbar onset in ALS patients. There was no significant difference in subsequent development of arm symptoms compared to leg symptoms (B) Arm onset. Both in ALS and PMA patients, symptoms in the contralateral arm were reported faster compared to the legs and bulbar region. (C) Leg onset. In ALS patients, symptoms in the contralateral leg were reported significantly faster than involvement of the arms and bulbar region, respectively. A similar pattern was seen in patients with PMA and PLS.

Table 3.3 Symptom development in MND patients according to site of onset

Site of onset	1 year		2 years	
	Patients with symptoms (%)	Difference (%)	Patients with symptoms (%)	Difference (%)
A: Bulbar onset				
ALS (n = 46)				
Arms vs. legs	46.7 vs. 34.3	12.4	62.1 vs. 51.4	10.7
B: Arm onset				
ALS (n = 74)				
Bulbar vs contralateral arm	15.0 vs. 52.0	37.0 *	30.9 vs. 72.0	41.1 *
Bulbar vs. contralateral leg	15.0 vs. 23.2	8.2	30.9 vs. 47.0	16.1
Bulbar vs ipsilateral leg	15.0 vs. 34.1	19.1 *	30.9 vs. 58.5	27.6 *
Opposite arm vs contralateral leg	52.0 vs. 23.2	28.8 *	72.0 vs. 47.0	25.0 *
Opposite arm vs ipsilateral leg	52.0 vs. 34.1	17.9 *	72.0 vs. 58.5	13.5
Contralateral leg vs ipsilateral leg	23.2 vs. 34.1	10.9	47.0 vs. 58.5	11.5
PMA (n = 35)				
Bulbar vs. contralateral arm	9.4 vs. 56.3	46.9 *	9.4 vs. 75.0	65.6 *
Bulbar vs. contralateral leg	9.4 vs. 26.7	0.0	9.4 vs. 26.7	17.3
Bulbar vs. ipsilateral leg	9.4 vs. 18.8	9.4	9.4 vs. 43.3	33.9 *
Contralateral arm vs. contralateral leg	56.3 vs. 26.7	46.9 *	75.0 vs. 26.7	48.3 *
Contralateral arm vs. ipsilateral leg	56.3 vs. 18.8	37.5 *	75.0 vs. 43.3	31.7 *
Contralateral leg vs. ipsilateral leg	26.7 vs. 18.8	9.4	26.7 vs. 43.3	16.6
C: Leg onset				
ALS (n = 68)				
Bulbar vs contralateral leg	5.9 vs. 51.5	45.6 *	21.3 vs. 73.5	52.3 *
Bulbar vs. contralateral arm	5.9 vs. 16.3	10.4	21.3 vs. 35.9	14.6
Bulbar vs. ipsilateral arm	5.9 vs. 19.1	13.2 *	21.3 vs. 40.3	19.1 *
Opposite leg vs. contralateral arm	51.5 vs. 16.3	35.2 *	73.5 vs. 35.9	37.6 *
Opposite leg vs. ipsilateral arm	51.5 vs. 19.1	32.3 *	73.5 vs. 40.3	33.2 *
Contralateral arm vs. ipsilateral arm	16.3 vs. 19.1	2.9	35.9 vs. 40.3	4.4
PMA (n = 29)				
Bulbar vs. contralateral leg	0.0 vs. 24.1	24.1 *	3.7 vs. 48.3	44.6 *
Bulbar vs. contralateral arm	0.0 vs. 0.0	0.0	3.7 vs. 7.1	3.4
Bulbar vs. ipsilateral arm	0.0 vs. 3.4	3.4	3.7 vs. 3.4	0.3
Contralateral leg vs. contralateral arm	24.1 vs. 0.0	24.1 *	48.3 vs. 7.1	41.1 *
Contralateral leg vs. ipsilateral arm	24.1 vs. 3.4	20.7 *	48.3 vs. 3.4	44.8 *
Contralateral arm vs. ipsilateral arm	0.0 vs. 3.4	3.4	7.1 vs. 3.4	3.7

Table 3.3 continues on next page

Site of onset	1 year		2 years	
	Patients with symptoms (%)	Difference (%)	Patients with symptoms (%)	Difference (%)
PLS (n = 58)				
Bulbar vs. contralateral leg	3.9 vs. 38.5	34.5 *	17.6 vs. 53.8	36.1 *
Bulbar vs. contralateral arm	3.9 vs. 5.9	2.0	17.6 vs. 9.8	7.8
Bulbar vs. ipsilateral arm	3.9 vs. 9.8	5.9	17.6 vs. 21.6	3.9
Contralateral leg vs. contralateral arm	38.5 vs. 5.9	32.6 *	53.8 vs. 9.8	44.0 *
Contralateral leg vs. ipsilateral arm	38.5 vs. 9.8	28.7 *	53.8 vs. 21.6	32.3 *
Contralateral arm vs. ipsilateral arm	5.9 vs. 9.8	3.9	9.8 vs. 21.6	11.8

After one and two years from symptom onset, the percentage of symptoms per site according to site of onset was calculated. Subsequently, these percentages were compared to each other. Differences in symptom development are displayed. Significant differences between subsequent site involvement are marked by an asterisk (*).

Bulbar onset

For ALS patients who initially had bulbar symptoms (n = 46), the time to develop arm symptoms was compared with the time to develop leg symptoms (panel A). After one year, the percentage of ALS patients reporting arm symptoms was 46.7% (95% CI 29.8 to 59.6), while the percentage reporting leg symptoms was 34.3% (95% CI 18.5 to 47.1). After two years, the percentage of ALS patients having arm symptoms was 62.1% (95% CI 44.1 to 74.3), while the percentage having leg symptoms was 51.4% (95% CI 32.7 to 64.9). The difference in development of arm symptoms compared to leg symptoms was not significant.

Arm onset

Among ALS patients with arm onset (n = 74), additional involvement of the contralateral arm developed significantly faster, as compared to any other site (panel B). After one year, the percentage of patients reporting symptoms in the contralateral arm was 52.0% (95% CI 39.3 to 62.1); after two years, this percentage was 72.0% (95% CI 59.7 to 80.5). Following the contralateral arm, symptoms developed more rapidly in the ipsilateral leg and then the contralateral leg. The difference between ipsilateral and contralateral leg involvement was, however, not significant. Bulbar involvement was reported by 30.9% of the patients after two years.

In case of arm onset in patients with PMA (n = 35), development of symptoms also occurred significantly faster in the contralateral arm.



Leg onset

In ALS patients with leg onset ($n = 68$), symptoms in the contralateral leg occurred significantly faster than involvement of the arms and bulbar region, respectively (panel C). After one year, the percentage of ALS patients having symptoms in the contralateral leg was 51.5% (95% CI 38.0 to 62.0); after two years, this percentage was 73.5% (95% CI 60.7 to 82.2). Symptom development in the other body sites showed the same trend as in patients with arm onset, with no significant difference in involvement of the ipsilateral arm compared with the contralateral arm or bulbar region compared with the contralateral arm. Again, involvement of the bulbar region was relatively less frequent (21.3% after two years). For PMA patients ($n = 29$) and PLS patients ($n = 58$) with leg onset, the Kaplan Meier curves show a pattern similar to ALS patients, with early involvement of the contralateral leg compared to other sites.

DISCUSSION

In this study we investigated symptom development within the spectrum of motor neuron diseases, looking for patterns of disease spread. We demonstrated that disease progression in patients with MND is characterized by a nonrandom spread of symptoms from site of onset to subsequent body regions. The results of our study suggest that disease progression in MND is an organized process, with preferred and most rapid development of symptoms in the contralateral limb. Following limb onset, the bulbar region is relatively spared, being less frequently the next symptomatic site and showing late involvement. This organized development of symptoms to adjacent regions is similar throughout the spectrum of MND, being present in both upper and lower motor neuron phenotypes.

In 1991, Brooks was the first to suggest that symptoms develop most often in adjacent anatomic sites during disease progression, (Brooks, 1991; Brooks et al., 1991) which was confirmed by more recent neuropathological and clinical studies (Fujimura-Kiyono et al., 2011; Korner et al., 2011; Gargiulo-Monachelli et al., 2012; Ravits et al., 2007a). While several studies investigated symptom development in ALS at the level of upper and lower motor neuron involvement (Korner et al., 2011; Ravits et al., 2007b), studies on the natural disease course of pure upper or lower motor neuron diseases are, however, scarce. In a study on 25 PLS patients, symptoms usually began unilaterally in one leg, before developing in the contralateral leg and ascending to the arms and bulbar region (Zhai et al., 2003). PMA has previously been characterized by a diffuse symmetric weakness and severe

muscular atrophy usually starting in the distal limb regions (Norris et al., 1993; Visser et al., 2008; Van den Berg-Vos et al., 2009). Overall our findings are in line with other reports, however, we now included various MND phenotype, including a large cohort of PMA and PLS patients to gain insight into the mechanisms of upper and lower motor neuron degeneration underlying the clinical manifestations of MND.

This study shows that preferred distribution of symptoms from one limb to the contralateral limb is a uniform feature of MND, present in both upper and lower motor neuron phenotypes. For the lower motor neuron, this pattern of symptom development suggests that the disease process is likely to spread locally to the contralateral side of the spinal segment, before propagating to more distant regions of the spinal cord. For the upper motor neuron, if degeneration of the neurons most likely spreads to adjacent regions of the motor cortex, as hypothesized by Ravits et al. (Ravits and La Spada, 2009), we would have expected that symptoms would develop preferably in sites ipsilateral to the site of onset. However, our results in patients with PLS – as a pure upper motor neuron phenotype – show a pattern of symptom development to the contralateral side of the body instead. This pattern is in contrast with contiguous spread over the motor cortex, but rather suggests interhemispheric spread of disease potentially guided by the corpus callosum as the main interconnecting white matter tract between the left and right motor cortices (Figure 3.3). Involvement of this tract has been consistently reported in conventional MRI studies (Van Zandijcke and Casselman, 1995), diffusion tensor imaging (Sach et al., 2004; Senda et al., 2009; Sage et al., 2009; Filippini et al., 2010; Verstraete et al., 2010) and post mortem studies (Smith, 1960; Yamauchi et al., 1995) of ALS patients as well as PLS patients (Ciccarelli et al., 2009). Early dysfunction of callosal tracts was also shown by transcranial magnetic stimulation studies, even in the absence of clinical signs of upper motor neuron degeneration (Karandreas et al., 2007; Wittstock et al., 2007). Alternatively, rather than interhemispheric spread, the observed pattern in PLS could also be due to selective vulnerability of a subtype of motor neuron (e.g motor neurons involved in the control of lower limbs), resulting in bilateral involvement of corresponding regions in the motor cortex. Either way, the preferred symptom development to the contralateral side of the body appears to be irrespective of upper or lower motor neuron involvement.

Based on our current findings, we hypothesize that neural connectedness might facilitate spread to and from structurally and functionally related body regions. Spread of disease along neural connections is potentially a uniform feature in neurodegenerative diseases in which misfolded protein aggregates spread from neuron to neuron (Frost and Diamond,

3



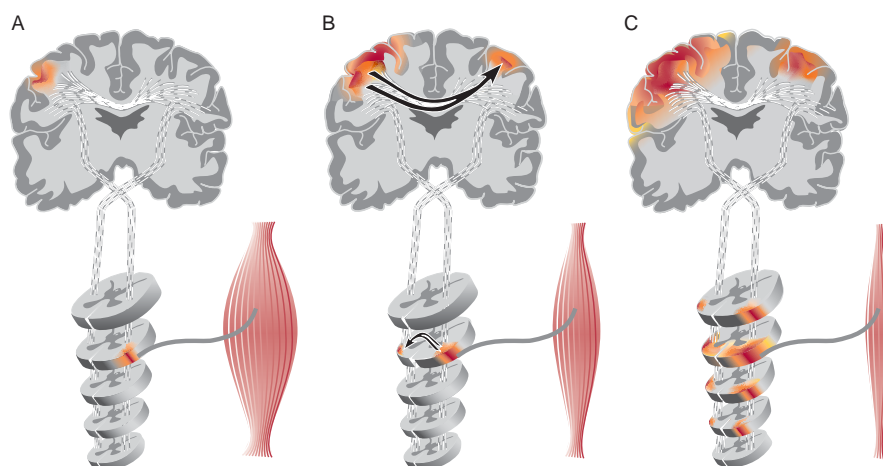


Figure 3.3 Schematic representation of upper and lower motor neuron degeneration, underlying symptom development in MND

(A) Motor neuron degeneration starts with a focal site of onset in the brain and spinal cord, leading to regional symptoms. (B) From this focal site of onset, spread of disease is guided by neuronal connectivity to highly connected regions of the neural network. For the upper motor neuron, this involves early interhemispheric spread via the corpus callosum; at the level of the spinal cord, disease spreads to the contralateral site of the spinal segment. The result is a pattern of symptom development with subsequent symptoms in the contralateral site, both in upper and lower MND. (C) Neurodegeneration continues to adjacent regions of the motor cortex and spinal cord, reflected by generalization and progression of muscle atrophy and weakness.

2010; Zhou et al., 2012). This type of spread is typically referred to as prion-like spread (Polymenidou and Cleveland, 2011; Kanouchi et al., 2012). Recently this hypothesis was supported by a neuroimaging study suggesting disease spread along the connections of the brain network (Verstraete et al., 2011). The hypothesis that disease spreads along neural connections, however, needs to be explored further.

Although our results suggest that there are certain patterns discernible in symptom development of MND, this study has a number of limitations. In this study, the diagnosis of PLS was based on pure upper motor neuron signs on initial evaluation. According to the diagnostic criteria stated by Gordon et al. (Gordon et al., 2006), these patients should have been followed up for four years, as some of them might develop lower motor neuron signs over time. The same argument holds for PMA patients, who may develop upper motor neuron signs later in their disease course. In addition, the retrospective design

of the study carries the risk of selection bias, as patients in whom the disease course is very progressive or in an advanced stage might have been excluded from the analysis. However, the demographics suggest that the responders were representative of the general population of MND patients. Another limitation is the use of questionnaires for assessing symptom development, which might have caused systematic errors due to recall bias. Frequency of thoracic symptoms was relatively low in all patient groups, this might be due to underreporting as it is more difficult to become aware of weakness in this region. Our results on symptom development in this region should therefore be interpreted with caution. On the other hand, because of the progressive nature of the disease and the impact on daily life, we assumed that patients are quite able to remember the order of the disease course. The most objective way of assessing lower motor neuron function would have been to use electromyography. However, this would be time-consuming and put a disproportionate burden on patients suffering from progressive disabilities. In addition, there is as yet no reliable quantitative marker for upper motor neuron involvement. Hence, using a questionnaire was a simple, yet efficient and patient friendly method to gain insight into the disease course of patients with MND.

In conclusion, we found a nonrandom pattern of symptom development in MND, with preferred spread of symptoms from a single site of onset toward highly connected anatomical regions in upper as well as lower motor neuron phenotypes. The results of our study might suggest that the ongoing motor neuron degeneration underlying symptom development is guided by structural connectedness of the neural network.

3



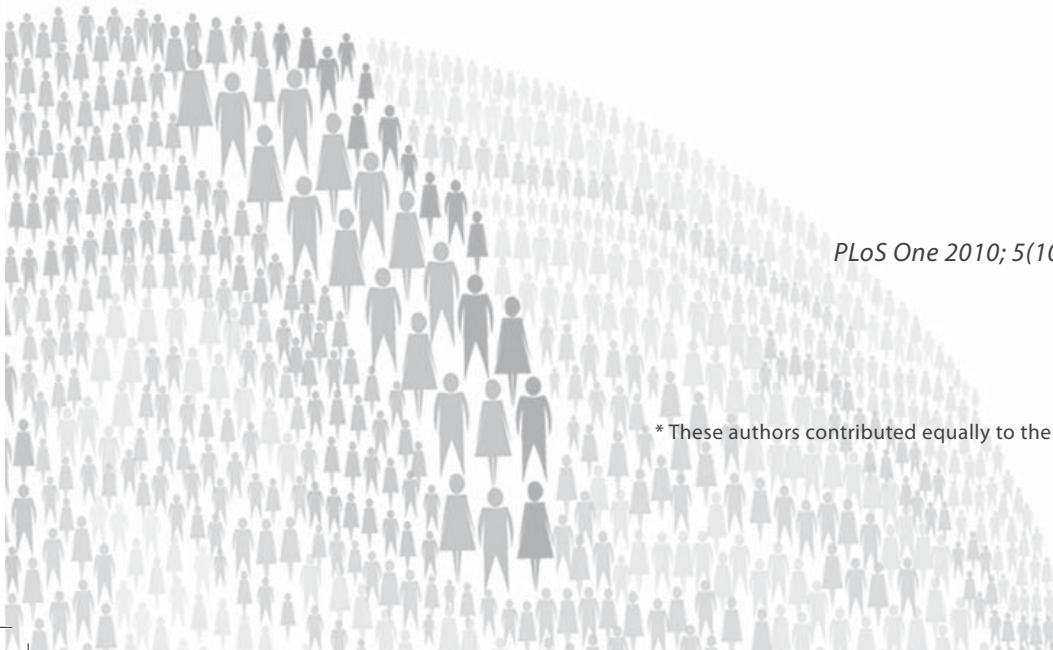
4

Motor network degeneration in ALS: a structural and functional connectivity study

Esther Verstraete*
Martijn P. van den Heuvel*
Jan H. Veldink
Niels Blanken
René C. Mandl
Hilleke E. Hulshoff Pol
Leonard H. van den Berg

PLoS One 2010; 5(10): e13664

* These authors contributed equally to the manuscript



ABSTRACT

Background: Amyotrophic lateral sclerosis (ALS) is a neurodegenerative disease characterised by motor neuron degeneration. How this disease affects the central motor network is largely unknown. Here, we combined for the first time structural and functional imaging measures on the motor network in patients with ALS and healthy controls.

Methods: Structural measures included whole brain cortical thickness and diffusion tensor imaging (DTI) of crucial motor tracts. These structural measures were combined with functional connectivity analysis of the motor network based on resting state fMRI.

Results: Focal cortical thinning was observed in the primary motor area in patients with ALS compared to controls and was found to correlate with disease progression. DTI revealed reduced FA values in the corpus callosum and in the rostral part of the corticospinal tract. Overall functional organisation of the motor network was unchanged in patients with ALS compared to healthy controls, however the level of functional connectedness significantly correlated with disease progression rate. Patients with increased connectedness appear to have a more progressive disease course.

Conclusions: We demonstrate structural motor network deterioration in ALS with preserved functional connectivity measures. The positive correlation between functional connectedness of the motor network and disease progression rate could suggest spread of disease along functional connections of the motor network.

INTRODUCTION

Amyotrophic lateral sclerosis (ALS) is a devastating disease characterised by degeneration of motor neurons in the brain and spinal cord leading to progressive muscle weakness. With a prevalence of approximately 6/100,000 it is considered a rare disease. The pathogenesis of ALS is heterogeneous with monogenetic causes in familial ALS and environmental and genetic risk factors in sporadic ALS (Kunst, 2004; Rothstein, 2009; Sreedharan et al., 2008). The natural history shows a large variability. With a median survival of three years it is intriguing that a minority of patients survive more than ten years. Currently we are unable to predict the disease course in the individual patient. Regardless a few clinical prognostic indicators it is largely unknown which factors determine the rate of clinical decline. We hypothesized that motor network characteristics could influence vulnerability to neurodegenerative effects.

Previous structural imaging studies on either gray or white matter in patients with ALS have revealed signs of upper motor neuron degeneration *in vivo* (Ellis et al., 2001; Chang et al., 2005a; Turner et al., 2007; Thivard et al., 2007; Sage et al., 2007; Ciccarelli et al., 2009; Senda et al., 2009; Graham et al., 2004; Sach et al., 2004). A limited number of functional imaging studies have reported altered functional neuronal activity of central motor regions (Tessitore et al., 2006; Schoenfeld et al., 2005; Stanton et al., 2007b; Mohammadi et al., 2009a). These neuroimaging studies have, however, focused on discrete measures and lack the network perspective in combination with clinical markers.

A neural network can be defined as a population of interconnected nodes that perform a specific physiological function, just as the motor network controls muscle tone and movement. The properties and integrity of cortical neural networks can be explored using structural or functional measures. We performed cortical thickness measures to assess the quality of the computational units (nodes) in the neural network (Figure 4.1a) and Diffusion Tensor Imaging (DTI) to explore the integrity of the interconnecting white matter tracts (structural connectivity) (Figure 4.1b). DTI is a technique that measures the water diffusion profile in brain tissue. This technique enables the reconstruction of white matter tracts and estimates its microstructural integrity, which is typically expressed as the fractional anisotropy (FA). As fibres degenerate, diffusion becomes less directional and the FA decreases (Kim et al., 2007). We studied the functional characteristics of the motor network by resting-state functional MRI (rs-fMRI). rs-fMRI is designed to detect inter-regional correlations in spontaneous neuronal activity as measured by blood

4



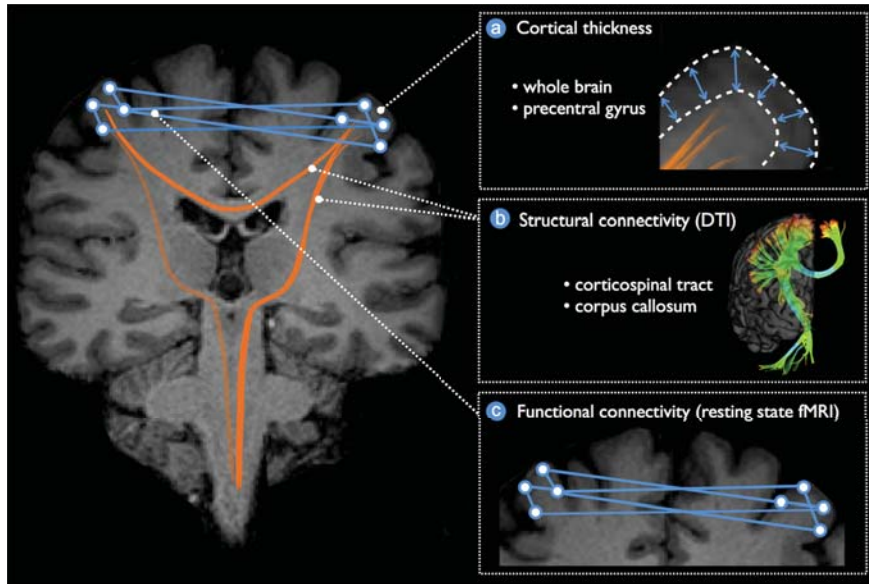


Figure 4.1 Schematic overview of the performed measures

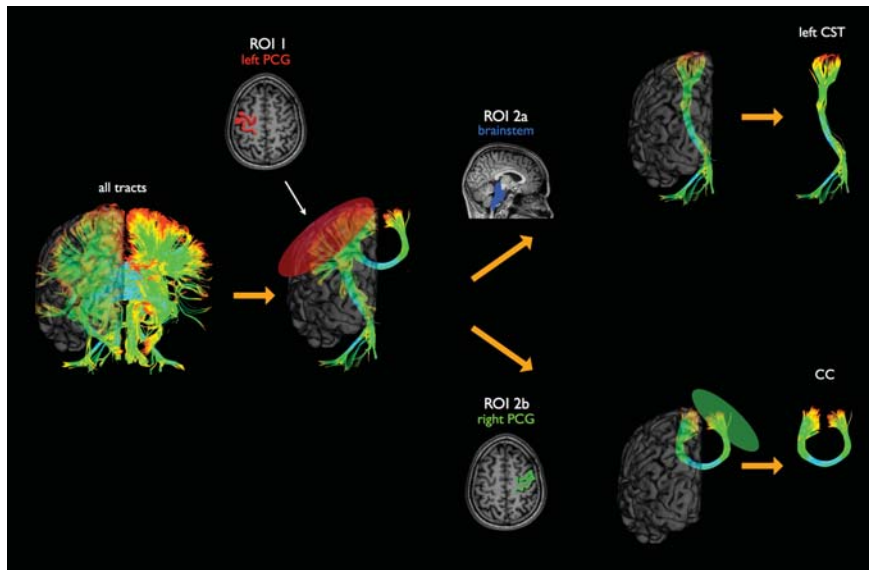


Figure 4.2 Selection of corticospinal tract (CST) and corpus callosum (CC) fibers

First, all fibres were tracked. Secondly, the left precentral gyrus was selected as region of interest (ROI 1) and the fibres touching this ROI were selected. Thirdly, the brainstem was selected as second ROI (ROI 2a). The left CST was defined by all fibres touching both ROI 1 and ROI 2a. Finally, a third ROI (ROI 2b) was defined as the right precentral gyrus. The CC was defined by all fibres touching both ROI 1 and ROI 2b. The tracts of the right CST were defined in a similar manner.

ROI = region of interest; PCG = precentral gyrus; CST = corticospinal tract; CC = corpus callosum.

oxygen level-dependent (BOLD) signal fluctuations over time. This phenomenon was first described in the motor system as a manifestation of functional connectivity (Biswal et al., 1995). Interestingly, recent studies have shown that functional connections in neuronal networks have a structural core of white matter (Wahl et al., 2007; Honey et al., 2009; van den Heuvel et al., 2009a; Van den Heuvel et al., 2008b). Combining these techniques in neurodegenerative diseases which typically affect a specific neural network, as ALS affects the motor network, has not been reported previously but is a promising future direction (Agosta et al., 2010c).

We hypothesized cortical atrophy to occur mainly in primary motor areas with conjoint loss of motor tract integrity. The degree of structural motor network degeneration was expected to affect the functional connectivity. Finally, both structural and/or functional motor network decline was hypothesized to correlate with the clinical status. Here, we examined the neurodegenerative effects in patients with ALS by investigating the structural and functional motor network characteristics and we explored their link with clinical markers.



MATERIALS AND METHODS

Participants

Twelve patients with ALS (mean age and standard deviation: 48.8 ± 10.6 years) and twelve age and sex-matched healthy controls (age: 49.6 ± 10.5) were included. Subject demographics and relevant clinical information are listed in Table 4.1. Patients were recruited from the ALS outpatient clinic of the University Medical Centre, Utrecht and

Table 4.1 Demographic and clinical features of the participants

	ALS	Controls
Sex (M/F)	10/2	10/2
Age (years)	48.8 (33–65)	49.6 (33–64)
Disease duration (months)	14.3 (7–30)	
Time after diagnosis (months)	5.2 (1–14)	
Site of onset (spinal/bulbar)	11/1	
EE-criteria (possible/probable/definite ALS)	3/8/1	
ALSFRS-R	39.5 (30–46)	
Progression rate	0.65 (0.13–1.38)	

M = male; F = female; EE = El Escorial; ALSFRS-R = revised ALS functional rating scale.

were diagnosed with probable lab-supported, probable or definite ALS according to the El Escorial criteria (Brooks et al., 2000). All patients were treated with riluzole. To minimize confounding by non-ALS-related alterations within the brain we excluded subjects older than 65 years of age and subjects with a history of brain injury, epilepsy, vascular risk factors, psychiatric illness and other systemic diseases. Clinical status of the patients was evaluated using the ALS Functional Rating Scale-Revised (ALSFRS-R) and disease progression rate was calculated ($48 - \text{ALSFRS-R-score}/\text{disease duration (months)}$). Additional clinical information is provided in the Supplemental Table S4.1.

All of the subjects gave their informed written consent, in line with the Declaration of Helsinki, and as approved by the local medical ethics committee for research into humans.

Image acquisition

All imaging data were acquired on a 3 Tesla Philips Achieva Medical Scanner. Imaging included the acquisition of an anatomical T1-weighted image, Diffusion Tensor Imaging (DTI) and resting-state functional MRI (rs-fMRI).

Cortical thickness: T1-weighted imaging

High-resolution T1-weighted imaging was performed for cortical thickness measurements and anatomical reference. Acquisition parameters: 3D FFE using parallel imaging; TR/TE = 10/4.6 ms, flip-angle 8 degrees, slice orientation: sagittal, 0.75 x 0.75 x 0.8 mm voxelsize, FOV = 160 x 240 x 240 mm, reconstruction matrix = 200 x 320 x 320 covering whole brain.

Structural connectivity: Diffusion Tensor Imaging

In the same scanning session, 2 DTI sets, each consisting of 30 diffusion-weighted and 5 diffusion-unweighted scans $B = 0$ scans ($b = 0 \text{ s/mm}^2$), were acquired to examine structural connectivity of the motor network. Acquisition parameters: DTI-MR using parallel imaging SENSE p-reduction 3; high angular gradient set of 30 different weighted directions (Jones, 2004; Jones et al., 1999), TR/TE = 7035/68 ms, voxel-size 2 x 2 x 2 mm, FOV = 120 x 120 x 150 mm, reconstruction matrix = 120 x 120 x 75 covering whole brain, $b = 0 \text{ s/mm}^2$ for the diffusion-unweighted scans and $b = 1000 \text{ s/mm}^2$ for the diffusion-weighted scans, second set with reversed k-space read-out (Van den Heuvel et al., 2008b; van den Heuvel et al., 2009b).

Functional connectivity: resting-state functional Magnetic Resonance Imaging

To examine the functional connections of the motor network, resting-state BOLD signals were recorded for a period of 8 min. Acquisition parameters: 3D PRESTOSENSE p/s-reduction 2/2, TR/TE = 22/32 ms using shifted echo, slice orientation: sagittal, flip-angle 10 degrees, dynamic scan time 0.5 sec, voxel-size 4 x 4 x 4 mm, FOV = 128 x 256 x 256 mm, reconstruction matrix = 40 x 64 x 64 (covering whole brain). A short volume acquisition was used to allow for proper sampling of information in the frequency domain up to 1 Hz, effectively minimising the contribution of respiratory and cardiac oscillations (0.3 and > 0.8 Hz, respectively), into the resting-state lower frequencies of interest (0.01–0.1 Hz) (Cordes et al., 2001).

**DATA ANALYSIS AND STATISTICS****Structural morphology of the motor network: cortical thickness**

Cortical thickness measures were performed using the validated and freely available Freesurfer software package (<http://surfer.nmr.mgh.harvard.edu/>). First, for each individual dataset (both ALS and healthy controls), the anatomical T1-weighted scan was placed into standard space and grey and white matter were segmented. Secondly, for each individual dataset, cortical thickness at every small region of the cortical surfaces was determined by computing the distance between the computed white matter and grey matter surface reconstructions (Fischl and Dale, 2000). Thirdly, a group average anatomical image and surface rendering were constructed by normalising all anatomical images to standard space using spherical normalisation. All individual datasets (both of patients with ALS and healthy controls) were normalised to the computed group average anatomical surface, allowing for group comparison between patients with ALS and group matched healthy controls at each small sliver of cortical surface (vertex), covering whole brain.

Whole brain cortical thinning between ALS patients and healthy participants was assessed using General Linear Model (GLM) by testing differences at all vertices. Furthermore, to examine specifically the hypothesised selective thinning of the precentral gyrus in ALS information of the automatic parcellation of the cortical surface (Desikan et al., 2006; Fischl et al., 2004) was used, parcellating each hemispheric cortical surface in 34 different regions, enabling the computation of an average cortical thickness of each of these region, separately for the two hemispheres. These 68 regions (each hemisphere covering 34 regions)

included the left and right precentral gyrus forming the key regions of the motor network. These primary motor regions were selected for further analysis. Group comparison of the cortical thickness in the precentral gyrus was analyzed using a General Linear Model (GLM) included in the used SPSS software package (<http://www.spss.com/software/statistics/>). Age and whole brain average cortical thickness were included as covariates to adjust for residual confounding despite global matching (Rogers et al., 2007; van der Schot et al., 2009). For singly testing the primary motor regions, a statistical threshold of $\alpha \leq 0.05$ was considered statistically significant. To examine the role of cortical thinning as a possible marker of disease, the level of cortical thickness of the clinically most affected precentral gyrus was correlated with clinical parameters using linear regression.

Structural connectivity of motor network: Diffusion Tensor Imaging

Preprocessing DTI

Diffusion Tensor Imaging (DTI) data was pre-processed with the diffusion toolbox of Andersson et al. (Andersson and Skare, 2002; Andersson et al., 2003) and in-house developed software (Van den Heuvel et al., 2008b; Mandl et al., 2008). First of all, each of the two acquired DTI sets, both consisting of 5 diffusion-unweighted scans ($b = 0$ s/mm²) and 30 diffusion-weighted images ($b = 1000$ s/mm²), was averaged, resulting in 2 average diffusion-unweighted images, one for each set. Secondly, possible susceptibility distortions which are often reported in single-shot EPI images (Andersson et al., 2003), were corrected by combining the information of the two DTI datasets. Possible distortions were estimated by computing a field distortion map based on the two averaged diffusion-unweighted $B = 0$ images, acquired with an opposite k-space read-out direction (Andersson et al., 2003). The resulting field map was applied to the two sets of 30 diffusion-weighted images, resulting in a single corrected set of 30 diffusion-weighted directions (Andersson et al., 2003). Finally, correction for eddy-currents and small head movements (linear distortions) was performed (Andersson and Skare, 2002).

Reconstruction of white matter tracts

To select the CST and corpus callosum tracts of interest fibre tracking was applied. A tensor was fitted to the diffusion profile of each voxel using a robust tensor fit method based on M-estimators (Chang et al., 2005b) and the principal eigenvector of the voxel-specific fitted tensor was selected as the main diffusion direction in that voxel (Mori et al., 2002). For each voxel-wise tensor, the fractional anisotropy (FA) was computed, indicating the level

of preferred diffusion within that white matter voxel. Next, using the principal diffusion direction of each voxel, the Fibre Assignment by Continuous Tracking (FACT) algorithm was used to reconstruct the total collection of white matter tracts of the brain (Mori et al., 2002), by starting 8 seeds in each voxel and following the principal diffusion direction from voxel to voxel, until either the fibre exceeded the brain, the fibre trajectory made a sudden change (an angle of > 45 degrees) or when the fractional anisotropy value reached below 0.2. This procedure resulted in the reconstruction of all white matter tracts in the brain. The resulting collection of fibres was then used as a starting point for the selection of the tracts of interest (van den Heuvel et al., 2009a; Van den Heuvel et al., 2008b; Mandl et al., 2010).

Selection of CST and corpus callosum tracts of interest

The tracts of interest in this study were the left and right CST and tracts of the body of the corpus callosum interconnecting left and right precentral gyrus. The left (or right) CST was defined as the fibres touching the left (or right) precentral gyrus and crossing the brainstem. The corpus callosum tracts were defined as the fibres touching both the left and right precentral gyrus. Selection of the tracts of interest was done using a 4-step procedure (van den Heuvel et al., 2009a). First, the total collection of all reconstructed tracts was selected. Second, to select the left CST, the left precentral gyrus was taken as a region of interest (ROI-1) and all fibres that touched this ROI were selected. Third, the brainstem was selected as a second ROI (ROI-2) and all fibres of the collection of tracts resulting from step 2 that touched ROI-2 were selected. Step 1–3 resulted in the tracts that touched the left precentral gyrus and crossed the brainstem, selecting the left CST. Finally, in step 4, the resulting individual fibres were normalized to the group anatomical image by using non-linear normalization parameters of the subject specific T1-weighted image to the standard group anatomical image and an average group fibre was constructed, to allow comparison between individual datasets (Mandl et al., 2010). Similarly, to select the right CST, ROI-1 was chosen as the right precentral gyrus. In addition, to select the corpus callosum tracts interconnecting left and right precentral gyrus, ROI-1 was selected as the left and ROI-2 was selected as the right precentral gyrus (Figure 4.2).

White matter integrity

To determine the level of integrity of whole brain white matter and, in particular, the selected CST and corpus callosum tracts of interest, the fractional anisotropy (FA) of each white matter voxel and tract were computed. FA reflects the preference of the diffusion profile in



a specific direction and ranges between 0 and 1, with 0 indicating no preferred direction of diffusion in a voxel and FA values towards 1 indicating an increasing preference of the water molecules to diffuse in a specific direction. Higher levels of FA represent a higher level of microstructural organisation and decreased values of FA in patients are marking a decrease in white matter integrity (Kim et al., 2007; Budde et al., 2007; Budde et al., 2008). For each individual reconstructed fibre tract, the FA profile along the tract was determined by flagging the fibre with the FA values of crossing voxels.

Group tract

To allow for a point-by-point comparison of the tracts between the group of ALS patients and healthy controls, for each of the tracts of interest (left and right CST and corpus callosum), an average group fibre was constructed by averaging the individual tracts of interest (Mandl et al., 2010). Each individual tract was then normalized to the average group tract, to allow for point-by-point comparison of the fiber tract integrity values across the group of patients and healthy controls. Hypothesized decrease of white matter integrity of the left and right CST and corpus callosum in ALS, were examined by comparison of the individual normalized tracts between patients and the matching healthy controls using multiple linear regression analysis. As a control condition the FA was measured along the visual tracts and the whole brain average FA was computed and compared between patients and controls.

Functional connectivity of the motor network: resting-state fMRI

To examine possible alterations in the functional communication in the motor network in ALS, resting-state fMRI was acquired (Biswal et al., 1995; Lowe et al., 2000). Functional connectivity is defined as the temporal coherence between neuronal signals of anatomically separated brain regions (Aertsen et al., 1989; Friston et al., 1993). Resting-state fMRI can be used to map functional connectivity by measuring interregional correlations in spontaneous neuronal synchronization reflected by coherency in low-frequency (< 0.1 Hz) blood oxygen level-dependent (BOLD) signal fluctuations (Biswal et al., 1995; Lowe et al., 2000; Cordes et al., 2000; Beckmann et al., 2005; Achard et al., 2006; Damoiseaux et al., 2006; van den Heuvel et al., 2008a). Especially regions of the primary motor network are known to show a high level of synchronisation between their spontaneous resting-state time-series, suggesting ongoing functional communication between motor regions (van den Heuvel et al., 2008a; Damoiseaux et al., 2008; Salvador et al., 2007).

Pre-processing resting-state fMRI

fMRI pre-processing was performed with the SPM5 software package (<http://www.fil.ion.ucl.ac.uk>). First, functional time-series were realigned to correct for possible small head movements. Next, functional time-series were co-registered with the T1-weighted image, for anatomical reference and ensuring overlap with the cortical parcellation maps, and thus allowing the selection of the fMRI voxels overlapping the left and right precentral gyrus. Next, the individual datasets were normalised to allow for spatial group comparison. Resting-state time-series were bandpass filtered to select the resting-state frequencies of interest (0.01–0.08Hz).

Functional network analysis

To examine the quality of the functional motor network, graph analysis was used, assessing the integrity of functional communication efficiency in the motor network (Stam and Reijneveld, 2007; Bullmore and Sporns, 2009). Representing a dynamic system as a network of regions and their interactions as connections allows for the examination of specific properties of the network. These properties include the level of connectedness or cliqueness of the nodes in the network, indicating how close nodes are connected to their direct neighbours (Stam and Reijneveld, 2007; Bullmore and Sporns, 2009; Reijneveld et al., 2007).

A graph $G = (V, E)$ is a mathematical description of a network, consisting of nodes V reflecting static points with connections E interconnecting the nodes of the network, illustrated in Figure 4.1c. From each individual resting-state dataset an individual functional motor network was defined consisting of all primary motor network voxels (van den Heuvel et al., 2009b; van den Heuvel et al., 2008a). The steps of this analysis can be described as follows. First, voxels overlapping the left and right precentral gyrus (as defined by the cortical parcellation maps) were selected as nodes. This resulted in a fine-grained representation of the motor network in approximately 500 nodes (mean 505; SD 49) for each individual dataset. Next, of all possible voxel-pairs within the motor network the level of functional connectivity was computed as a zero-lag correlation between the voxel-wise resting-state fMRI time-series. This resulted in a $N \times N$ connectivity matrix M , with N being the number of motor network nodes, with $M(i,j)$ reflecting the level of functional connectivity between voxel i and voxel j of the motor network with i and j in N . Matrix M was thresholded with a threshold T , setting all connections below this threshold to 0 and all supra-threshold connections to 1. We calculated the network characteristics at ranging



thresholds from $T = 0.3$ to $T = 0.5$ in steps of 0.05. This resulted in a binary connectivity matrix B , directly reflecting a connectivity graph G^{motor} , with nodes overlapping all regions of the motor network (i.e. voxels) and connections between voxels functionally connected regions of the motor network.

The level of connectivity in the motor network was examined by computing the total number of connections (k). k reflects the average number of connections of a node in the motor network, indicating on average how strong a node is connected to the other nodes of the network. To correct for differences in the number of nodes, k was normalized by the total number of possible connections that could occur in the network, resulting in an index between 0 and 1.

To examine the level of local clustering of the network as a measure of how strongly interconnected the individual motor network is, the clustering-coefficient C of each of the resulting networks was computed (Stam and Reijneveld, 2007; Bullmore and Sporns, 2009; Reijneveld et al., 2007; Rubinov and Sporns, 2010). The clustering coefficient C indicates the level of how close the nodes of the network are interconnected. It is represented by the ratio between the number of connections between the direct neighbours of a node and the total number of possible connections between these neighbours, reflecting the level of local connectedness of the network. The clustering-coefficient C_i of a single node i is defined as (Rubinov and Sporns, 2010):

$$C_i = \frac{\# \text{ edges in } G_i^{motor}}{\frac{1}{2} k_i(k_i-1)} \quad (1)$$

with G_i^{motor} the local sub-network of connected voxels of node i . The overall clustering-coefficient C was defined as the average over all nodes:

$$C = \frac{1}{N} \sum_{i \in G} C_i \quad (2)$$

C expresses the level of local connectedness of the network, reflecting how on average the direct neighbours of a node are interconnected themselves.

Typically C is compared to the clustering-coefficient (C^{random}) of a random organised network (G^{random}) with an identical number of nodes and connections as the motor network G^{motor} . The connections between the nodes do not, however, follow a specific organisation but are randomly distributed. The ratio between C and C^{random} results in the normalised

clustering-coefficient gamma. Gamma is typically > 1 for networks that are more ordered than random networks, reflecting the level of local efficient information processing within a network (Latora and Marchiori, 2001). For each of the evaluated motor networks (i.e., for all individual datasets) a collection of $h = 10$ random graphs were computed. G^{random} was computed as the average over all $C^{random}(h)$. To ensure that each $G^{random}(h)$ had the same number of nodes, connections and degree distribution as the original motor network, each $G^{random}(h)$ was computed by randomizing the connections of G by randomly swapping the connections in G until all connections were distributed keeping the connectivity distribution and similarity of the adjacency matrix intact (Sporns and Zwi, 2004). Graph randomization and the computation of C and gamma was performed with the Brain Connectivity Toolbox (Rubinov and Sporns, 2010) (<http://www.brain-connectivity-toolbox.net>). To correct for a possible effect of variation in the number of k on network organization, the interaction effect of k on gamma was regressed out of gamma using GLM. Finally, to examine the correlation with clinical parameters (within the ALS patients group), k and gamma were corrected for age.

In summary, functional connectivity analysis included examining the number of connections providing information on the total level of connectedness of the network, together with the normalised clustering-coefficient (gamma) providing information about the level of local connectedness and level of local information processing, given by the ratio between the number of connections with the direct neighbours of a node and the total number of possible connections between these neighbours.

Organisational functional connectivity characteristics (the number of connections and level of local connectedness gamma) were compared between ALS patients and healthy controls using GLM statistics, controlling for possible effects of age.

Integration of structural, functional and clinical data

The relation between structural and functional measures was explored. The average FA value of the corpus callosum was compared with the number of functional interhemispheric connections using linear correlation. Finally, the main structural and functional measures were compared with the clinical parameters (ALSFRS-R and progression rate) in a similar manner.



RESULTS

Cortical thickness

Whole vertex-wise brain comparisons revealed cortical thinning in the precentral gyrus in patients with ALS compared to healthy controls as illustrated in Figure 4.3 (left and right precentral gyrus: $p < 0.0001$ and $p < 0.001$, respectively). Focussing on the precentral gyrus, most pronounced thinning in ALS was found bilaterally in the two subareas overlapping the central motor representations of the hand and leg. Interestingly, thinning of the primary motor regions was found to be specific, as no other cortical regions showed any changes in cortical thickness ($p < 0.01$). Indeed, post-hoc analysis of whole brain average cortical thickness revealed that ALS patients showed no differences in whole brain average cortical thickness (mean 2.28 mm; SD 0.090 mm) compared to controls (mean 2.27 mm; SD 0.045 mm; $p = 0.81$). Furthermore, focussing on the primary motor network, the average cortical thickness of the precentral gyrus as a more broadly defined anatomical region was significantly reduced in patients with ALS compared to healthy controls (ALS mean 2.59 mm; SD 0.120 versus controls mean 2.68 mm; SD 0.087; $p = 0.04$) (Figure 4.4a).

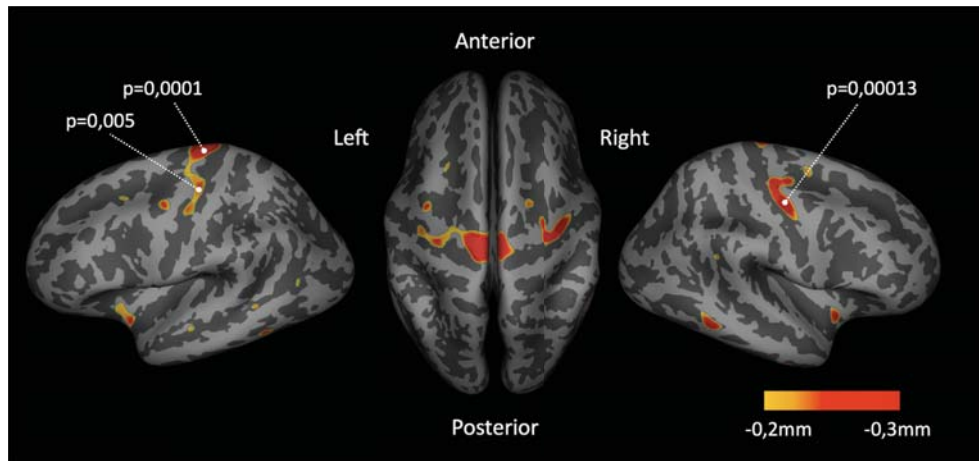


Figure 4.3 Whole brain cortical thickness

Whole brain cortical thickness measurements in patients with ALS compared to healthy controls. Cortical areas with (uncorrected) p-values < 0.01 are marked. The threshold for this illustration was set at 0.2mm cortical thickness reduction in ALS.

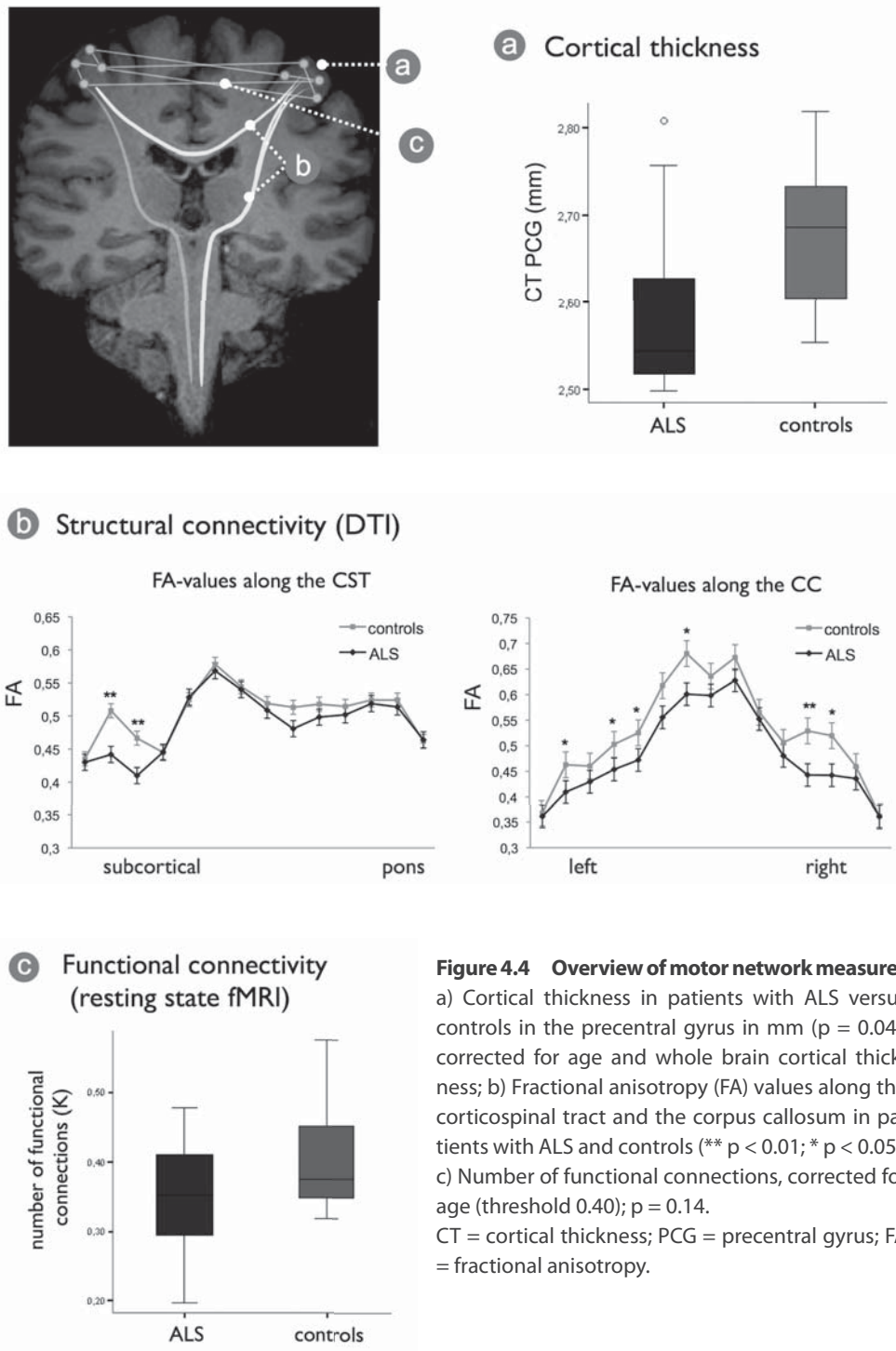


Figure 4.4 Overview of motor network measures
 a) Cortical thickness in patients with ALS versus controls in the precentral gyrus in mm ($p = 0.04$), corrected for age and whole brain cortical thickness; b) Fractional anisotropy (FA) values along the corticospinal tract and the corpus callosum in patients with ALS and controls (** $p < 0.01$; * $p < 0.05$); c) Number of functional connections, corrected for age (threshold 0.40); $p = 0.14$.
 CT = cortical thickness; PCG = precentral gyrus; FA = fractional anisotropy.

Structural connectivity

FA values in the corpus callosum and the CST were found significantly reduced ($p < 0.05$) in ALS patients compared to controls (Figure 4.4b). The FA reduction was more dispersed in the corpus callosum compared to the CST. Tract-based results, analysing the trajectory of FA along the CST tracts, showed that the reduction in FA becomes less pronounced as the tract descends from the cortex to the brainstem corresponding to more loss of integrity in the rostral part compared to the caudal part of the CST (Figure 4.4b). The FA along the visual tracts as a negative control condition was found to be unchanged in patients with ALS (0.583) compared to healthy controls (0.576) ($p = 0.07$). The whole brain average FA was 0.453 in patients and 0.458 in controls ($p = 0.48$).

Functional connectivity

Functionally, a reduced number of functional connections between the right and left motor cortex was found in ALS. This reduction was not statistically significant ($p = 0.14$; threshold 0.4), indicating relative sparing of functional connectivity (Figure 4.4c). Indeed, the overall normalised clustering coefficient gamma, as a measure of local connectedness and local efficiency of the network was unchanged, indicating comparable local functional motor network organisation in patients in comparison to healthy controls. However, focussing on the patient group, gamma values did significantly correlate with disease progression rate in patients with ALS, i.e. stronger interconnected motor networks show a more progressive disease course (Figure 4.5c).

No association between the structural and functional properties of the motor network was found by correlating the microstructural integrity of the corpus callosum fibres with the number of functional connections. Figure 4.5 shows the correlation of the motor network measures with clinical markers. Both the average cortical thickness of the precentral gyrus and the level of functional organisation show a significant correlation with progression rate (Figure 4.5a and 4.5c respectively).

DISCUSSION

The present study demonstrates a decline of structural integrity with preserved functional organisation of the motor network in ALS. Firstly, cortical thickness was significantly reduced in the precentral gyrus, known as the primary motor area, in patients with

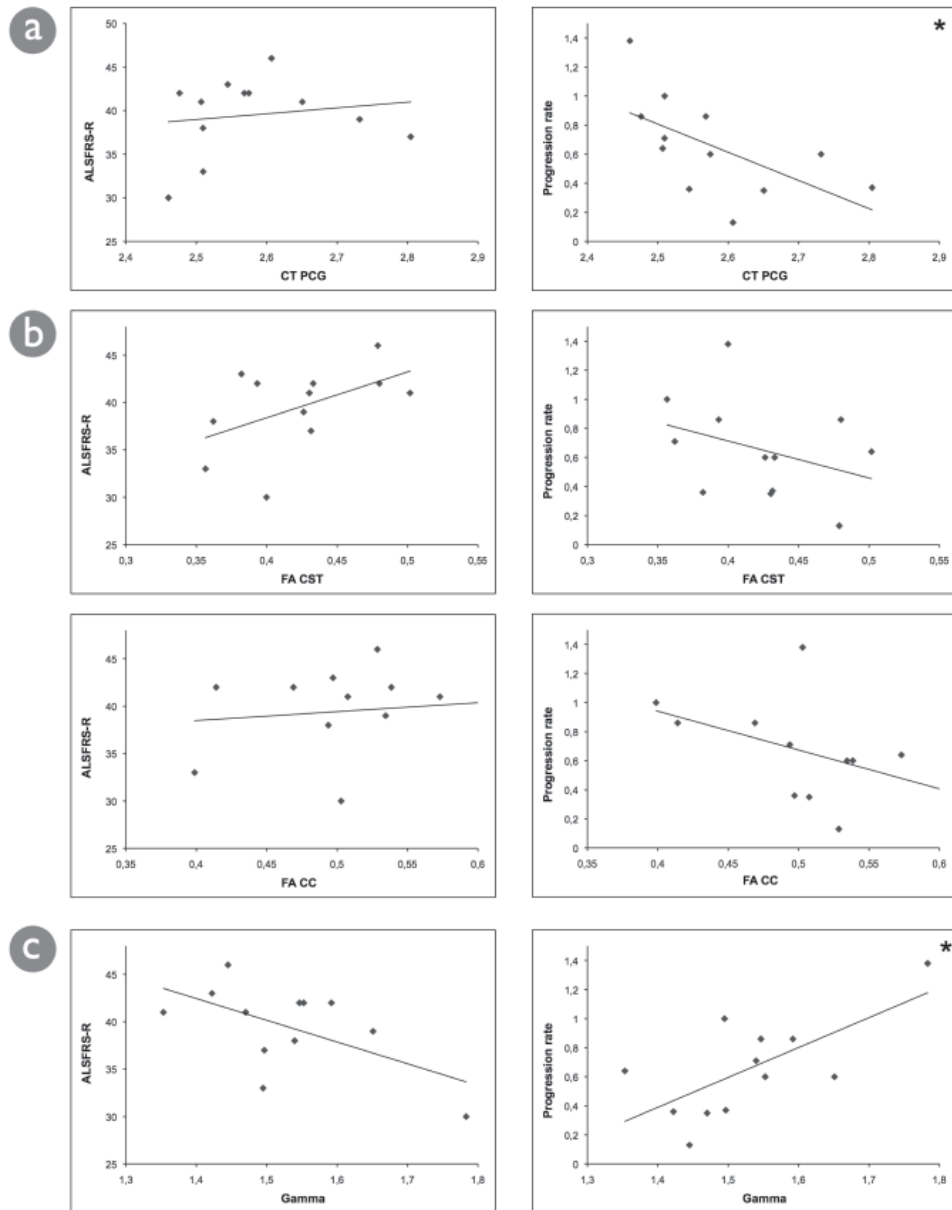


Figure 4.5 Correlation of imaging parameters with clinical measures

Correlation of ALSFRS-R score and progression rate with; a) cortical thickness in the precentral gyrus (CT PCG) of the clinically most affected side. Cortical thickness is corrected for average whole brain cortical thickness and age; b) FA in the – rostral part of the – corticospinal tract (CST) and FA in the corpus callosum (CC); c) Gamma – or local connectedness – corrected for the number of functional connections and age (threshold 0.30). * $p < 0.05$.

ALSFRS-R = ALS Functional Rating Scale Revisited; FA = fractional anisotropy; CST = corticospinal tract; CC = corpus callosum.

ALS. Secondly, a significant reduction in microstructural organisation was found in the corticospinal tracts (CST) as the major efferent motor conduits to the spinal cord. This involved mainly the rostral part of CST. Furthermore, the corpus callosum, interconnecting the motor network was found affected as a whole. Thirdly, exploring the functional connectivity of the motor network in ALS, we found the functional organisation to be intact, however the local connectedness was found related with disease progression. This might suggest that strong functional connectivity allows for rapid spread of disease.

We observed bilateral cortical thinning of the precentral gyrus in ALS. Interestingly, these effects were most pronounced in two subregions overlapping the somatotopic representation of the hand and leg. These findings are supported by pathological studies which have demonstrated these specific regions to be the areas of the motor cortex with maximal clustering of cortical motor neurons (Betz cells) (Rivara et al., 2003), of which degeneration is considered to be a pathological hallmark of ALS (Kiernan and Hudson, 1991). Indeed, taking the precentral gyrus as a whole, the average cortical thickness in this region was found significantly reduced in patients compared to controls. The cortical thickness in the precentral gyrus was shown related to disease progression rate, which could suggest increased vulnerability to degenerative effects. Previous studies on gray matter in ALS have shown more widespread atrophy in frontal and temporal regions as well (Chang et al., 2005a; Thivard et al., 2007; Agosta et al., 2007; Grossman et al., 2008). These studies were exclusively performed using voxel based morphometry, a technique which is known to have an increased signal to noise ratio and is relatively insensitive to cortical atrophy localised in the brain sulci (Hutton et al., 2009). In other neurodegenerative diseases clinical syndromes were shown to be associated with a specific pattern of cortical thinning which evolves during disease progression marking the clinical relevance of this measure (Bakkour et al., 2009; Rohrer et al., 2009; Rosas et al., 2008). As such, cortical thinning patterns could assist in the differentiation between distinct neurodegenerative diseases or identification of subtypes.

With regard to the structural connectivity of the motor network, it was primarily the rostral part of the CST that was found affected. This finding may suggest that the decrease in axonal integrity originates from the cell body, which is in accordance with the observed cortical thinning. These results are supported by the previous observation that cortical hyperexcitability precedes the development of clinical symptoms in pre-symptomatic carriers of a SOD1 mutation (Vucic et al., 2008), thereby suggesting that the early abnormalities in ALS occur within the corticomotorneurons, with anterograde

excitotoxicity (often referred to as ‘dying forward’). This aspect of degeneration has been the subject of ongoing debate (Vucic et al., 2008; Eisen, 2009) and longitudinal assessments will need to show whether these effects spread caudally during the course of the disease. In addition, our results showed a severe reduction of white matter integrity in corpus callosum tracts interconnecting the affected left and right cortical regions of the primary motor network. Indeed, callosal dysfunction has been found to be an early phenomenon in ALS (Wittstock et al., 2007) and structural involvement of the corpus callosum has been reported in combination with functional impairment (Bartels et al., 2008). Recently, it has been suggested that the corpus callosum plays an important role in the spread of ALS (Eisen, 2009), supporting our functional and structural findings.

Assessment of the functional connectivity showed that patients with a stronger connectedness of the motor network had a faster progression of disease, indicating a potential role for the functional organisation of the motor network in disease progression. Little is known about how ALS affects the overall functional properties of the motor network. A recent study has suggested reduced connectivity in the default-mode network in ALS, a network linked to high-order cognitive processes and similar to our results no significant overall reduction in inter-hemispheric functional connectivity of the primary motor cortex was reported (Mohammadi et al., 2009a). As the overall organisation of the motor network was preserved in ALS compared to controls, these results suggest that motor network connectedness may not be implicated in the aetiology of ALS but is involved in the spread of the disease along the structurally and functionally linked primary motor regions (Eisen, 2009). In other neurodegenerative diseases like Alzheimer’s disease this hypothesis is supported by the observation that pathological tau-protein spreads *in vivo* from one brain region to functionally connected spatially distinct regions (Clavaguera et al., 2009). In addition, imaging studies have found cortical degeneration in clinical subtypes of dementia occur in distinct functional neural networks (Seeley et al., 2009). The actual mode of transmission and the applicability of this finding to other neurodegenerative diseases remain, however, subjects for further research. Since, in our study, functional connectivity was found to be of potential prognostic importance it could become a target for therapeutic intervention. Interestingly riluzole, the only drug which delays disease progression in ALS is known to increase intra-cortical inhibition and therefore reduce functional connectivity (Kahkonen and Ilmoniemi, 2004). An alternative explanation for our findings is that increased local connectedness in patients with a faster disease progression is due to loss of cortical inhibitory interneurons. This effect has been reported



previously in studies on excitability of the motor cortex (Vucic et al., 2008; Vucic et al., 2009). However, in that case one would expect the average local connectedness to be increased in ALS compared to controls, which is not. Our data did not show a correlation between the functional and structural connectivity in the corpus callosum. This is in accordance with our opposing results regarding structural and functional connectivity, as well as, previous studies exploring this correlation (Lowe et al., 2008; Morgan et al., 2009).

A possible limitation of our study is the limited sample size and the absence of longitudinal MRI measures. However, ALS is a rare disease with patients often losing ambulation shortly after diagnosis making it difficult to do this type of research in large cohorts of patients. In addition, the objective of the present study was to apply multiple imaging techniques to a relatively homogeneous group of patients to explore the central motor network characteristics in relation to clinical markers. Previous studies have too been able to pick up significant functional effects in similar small sample sizes (Zhou et al., 2010). However, future studies should further clarify the relevance of neural network characteristics regarding vulnerability to neurodegenerative effects. Secondly, using tractography, it may be difficult to differentiate FA changes in the corpus callosum from changes in the rostral part of the CST, as both tracts originate from the same cortical region and cross each other at the level of the corona radiata. This phenomenon of ‘crossing fibres’ is a general technical limitation in the DTI field and the differences found in this region can be interpreted in multiple ways, either the corpus callosum degeneration alone is responsible for these effects, or the CST degeneration or both. Thirdly, little is known about the reproducibility of resting-state fMRI data. However networks with a strong structural connectivity show more reliable functional connectivity across scanning sessions (Honey et al., 2009).

Our findings reporting on cortical thickness, white matter integrity and functional connectivity, strongly suggest a decline of structural motor network integrity in ALS. Functional connectivity was relatively preserved but was found to be related to disease progression, supporting the hypothesis that neurodegeneration in ALS spreads along functional connections.

SUPPLEMENTAL INFORMATION

Table S4.1 Clinical characteristics of the patients with ALS

Age (years)	Male/ female	Site of onset	Side of onset	Time to diagnosis (months)	Disease duration (months)	ALSFRS-R	Disease progression rate	El Escorial category	Predominant UMN/LMN
36	Male	Cervical	Left	5	10	42	0.60	Probable lab supported	LMN
40	Male	Cervical	Left	12	15	46	0.13	Probable lab supported	LMN
53	Male	Cervical	Right	6	7	42	0.86	Probable	LMN
47	Female	Bulbar	Left	9	15	33	1.00	Probable	UMN
62	Male	Cervical	Right	12	15	38	0.67	Definite	UMN
33	Male	Cervical	Left	6	20	41	0.35	Probable	LMN
46	Male	Lumbosacral	left	27	30	37	0.37	Probable	LMN
44	Male	Cervical	Right	6	7	42	0.86	Probable	UMN
52	Male	Lumbosacral	Left	7	11	41	0.63	Probable lab supported	LMN
44	Female	Cervical	Left	11	13	30	1.38	Probable	LMN
65	Male	Lumbosacral	Right	3	15	39	0.60	Probable	LMN
64	Male	Cervical	Left	6	14	43	0.36	Probable	LMN

ALSFRS-R = revised ALS functional rating scale; Probable lab supported = Probable laboratory supported; UMN = upper motor neuron; LMN = lower motor neuron.



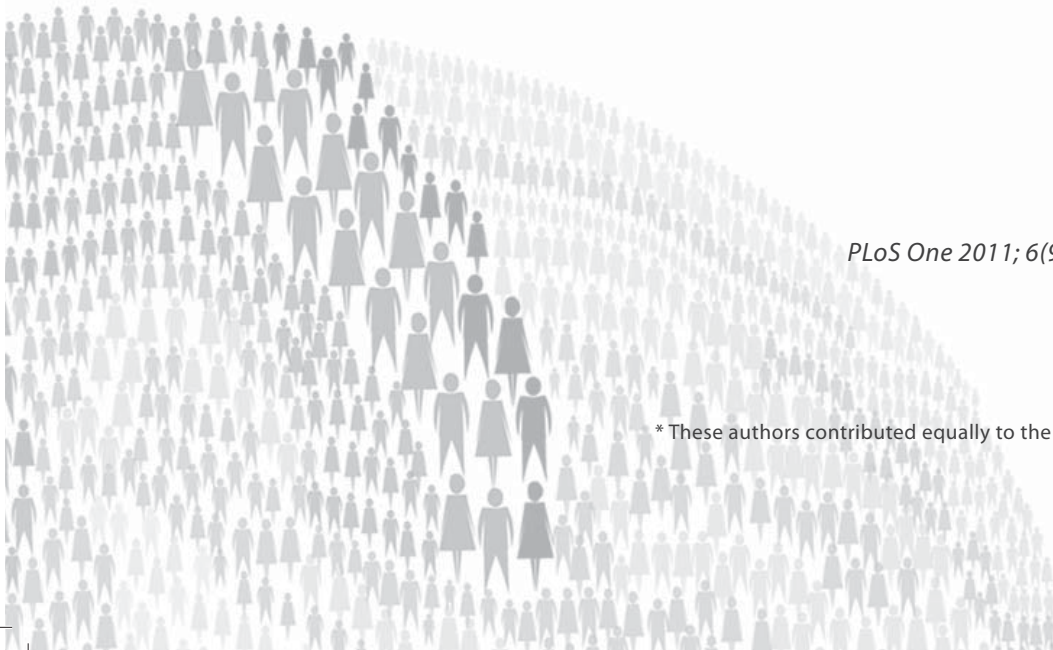
5

Impaired structural motor connectome in ALS

Esther Verstraete
Jan H. Veldink
Rene C.W. Mandl
Leonard H. van den Berg*
Martijn P. van den Heuvel*

PLoS One 2011; 6(9): e24239

* These authors contributed equally to the manuscript



ABSTRACT

Amyotrophic lateral sclerosis (ALS) is a severe neurodegenerative disease selectively affecting upper and lower motor neurons. Patients with ALS suffer from progressive paralysis and eventually die on average after three years. The underlying neurobiology of upper motor neuron degeneration and its effects on the complex network of the brain are, however, largely unknown. Here, we examined the effects of ALS on the structural brain network topology in 35 patients with ALS and 19 healthy controls. Using diffusion tensor imaging (DTI), the brain network was reconstructed for each individual participant. The connectivity of this reconstructed brain network was compared between patients and controls using complexity theory without *a priori* selected – regions of interest. Patients with ALS showed an impaired sub-network of regions with reduced white matter connectivity ($p = 0.0108$, permutation testing). This impaired sub-network was strongly centered around primary motor regions (bilateral precentral gyrus and right paracentral lobule), including secondary motor regions (bilateral caudal middle frontal gyrus and pallidum) as well as high-order hub regions (right posterior cingulate and precuneus). In addition, we found a significant reduction in overall efficiency ($p = 0.0095$) and clustering ($p = 0.0415$). From our findings, we conclude that upper motor neuron degeneration in ALS affects both primary motor connections as well as secondary motor connections, together composing an impaired sub-network. The degenerative process in ALS was found to be widespread, but interlinked and targeted to the motor connectome.

INTRODUCTION

Amyotrophic lateral sclerosis (ALS) is a fatal neurodegenerative disease, characterized by selective loss of lower motor neurons in the spinal cord and upper motor neurons in the brain. Patients suffer from progressive paralysis and eventually die from respiratory failure. Besides motor symptoms, a subset of patients develop cognitive disturbances or even frontotemporal dementia (FTD), indicating ALS can involve extra-motor brain regions. The peak incidence of this devastating disease lies between 50 and 75 years of age and the average time of survival is about 3 years after onset of symptoms (Logroscino et al., 2008).

The effects of upper motor neuron degeneration on the brain are largely unknown. Enhancing the insight in these degenerative effects of ALS is essential towards better treatment. Conventional magnetic resonance imaging (MRI) of the brain does not show characteristic changes indicating upper motor neuron loss in ALS (Ngai et al., 2007). Computational MRI analysis techniques have shown to be more promising in demonstrating the degenerative effects of ALS (Turner et al., 2009; Verstraete et al., 2010; Filippini et al., 2010). Previous DTI studies have mainly been focused on the corticospinal tract, the white matter ‘highway’ connecting the upper and lower motor neurons, showing reduced white matter integrity in ALS (Roccatagliata et al., 2009; Iwata et al., 2008; Nelles et al., 2008; Sage et al., 2007; Wong et al., 2007). In addition, recent studies have consistently demonstrated involvement of the corpus callosum, being the primary intracerebral motor connection (Verstraete et al., 2010; Filippini et al., 2010). However, the involvement of other intracerebral structural connections has only been partly explored. A small number of DTI studies have included analysis of fractional anisotropy (FA) data in a voxelwise manner showing widespread degenerative effects (Sage et al., 2009; Senda et al., 2011). It is unknown, however, whether these widespread effects occur independently or linked to each other.

Brain regions are interconnected as a network, thereby strongly influencing each other (Bullmore and Sporns, 2009; van den Heuvel et al., 2009a). A mathematical framework to examine the topology of complex network systems has been adopted to study the organization of these connections (Sporns and Zwi, 2004; Reijneveld et al., 2007; Kaiser, 2011). Modern neuroimaging techniques, e.g. DTI, permit reconstruction of white matter tracts of the human brain (Basser et al., 2000). Studies using complexity theory – like graph theory – demonstrated that the organization of the brain network or connectome plays a crucial part in healthy brain functioning (van den Heuvel et al., 2009b; Li et al., 2009b; Bassett et al., 2009).



As the brain is a complex system of interacting regions, local degeneration of upper motor neurons in ALS may have a widespread effect on the brain network. Here, by combining DTI and graph theory, we examined the integrity of the structural brain network in patients with ALS to provide further insight in whether the degenerative effects of ALS occur independently or as a connected system.

METHODS

Ethics statement

The medical ethics committee for research in humans of the University Medical Center Utrecht, the Netherlands has approved this research. Informed written consent was obtained from all participants. All clinical investigation has been conducted according to the principles expressed in the Declaration of Helsinki.

Participants

Thirty-five patients with ALS (mean age 50.8; SD 13.0 years; 28 males and 7 females) and 19 age-matched healthy control subjects participated in this study (mean age 53.1; SD 10.5 years; 14 males and 5 females). Patients diagnosed with ALS according to the El Escorial criteria were recruited from the ALS outpatient clinic of the University Medical Center, Utrecht. The clinical characteristics are listed in Table 5.1. No patients fulfilled the clinical criteria of FTD (Neary et al., 1998). Subjects with a history of brain injury, epilepsy, psychiatric illness and other neurodegenerative diseases were excluded, resulting in the group of participants described. Clinical status of the patients was evaluated using the ALS Functional Rating Scale-Revised (ALSFRS-R). The ALSFRS-R is a validated rating instrument for monitoring the progression of disability in patients with ALS (Cedarbaum et al., 1999). Disease progression rate was calculated, defined as the average decline in ALSFRS-R-score since disease onset $((48 - \text{ALSFRS-R-score})/\text{disease duration in months})$.

MRI acquisition

All participants underwent a 35-minute scanning session, in which Diffusion Tensor Imaging (DTI) – for reconstructing the white matter tracts of the brain network – and T1 images – for anatomical reference – were acquired and manually checked. MRI scans were made on

Table 5.1 Demographic and clinical characteristics of all study participants

	Healthy controls (n = 19) Mean ± SD (range)	ALS patients (n = 35) Mean ± SD (range)
Age (years)	53.1 ± 10.5 (33–67)	50.8 ± 13.0 (26–78) ^a
Sex (male/female)	14 / 5	28 / 7 ^b
Site of onset (n)		Bulbar 5 (14%) Cervical 18 (51%) Lumbosacral 12 (35%)
Side of onset (n)		Left 19 (54%) Right 9 (26%) Symmetrical 7 (20%)
Disease duration (months)		17.7 ± 18.0 (3–59)
ALSFRS-R		40.1 ± 4.3 (30–47)
Progression rate		0.6 ± 0.5 (0.1–2.0)

SD = standard deviation; ALSFRS-R = revised ALS functional rating scale. ^a comparison of age between the groups, did not result show any significant differences (t-test statistics, $p = 0.49$); ^b the proportion males and females is not significantly different in patients versus controls (Fisher's exact test, $p = 0.42$).

a 3 Tesla Philips Achieva Clinical scanner at the University Medical Center Utrecht using a sixteen channel SENSE receiver head-coil. Within each scanning session, first, 2 DTI sets, each consisting of 30 weighted diffusion scans and 5 unweighted $B = 0$ scans, were acquired (DTI-MR using parallel imaging SENSE p-reduction 3; high angular gradient set of 30 different weighted directions (Verstraete et al., 2010; van den Heuvel et al., 2009a; Jones et al., 1999; van den Heuvel et al., 2010), $TR/TE = 7035/68$ ms, $2 \times 2 \times 2$ mm, 75 slices, $b = 1000$ m/s, second set with reversed k-space read-out). Directly after the acquisition of the DTI scans, an anatomical T1-weighted image was acquired (3D FFE using parallel imaging; $TR/TE 10/4.6$ ms; FOV 240×240 mm, 200 slices, 0.75 mm isotropic voxelsize).

Image preprocessing

DTI preprocessing and fiber tracking

The DTI preprocessing and reconstruction of the white matter pathways included the following steps. First, the 5 $B = 0$ images of each of the two DTI sets were averaged, improving the signal to noise ratio of the $B = 0$ images. Next, susceptibility distortions were corrected



by computing a field distortion map using the two average unweighted $B = 0$ images, based on the fact that they were acquired with an opposite k-space read-out direction (Andersson et al., 2003). The resulting field map was then applied to the two $B = 0$ images and the two sets of 30 weighted images (Andersson et al., 2003), resulting in a single set of 30 weighted directions which were realigned with a corrected $B = 0$ image (Andersson and Skare, 2002). Third, eddy-current distortions, often observed in acquisition of single-shot EPI images, were corrected (Andersson and Skare, 2002). Fourth, for each voxel, the diffusion profile was fitted a tensor using a robust tensor fit method based on M -estimators (Chang et al., 2005b). The principal eigenvector of the eigenvalue decomposition of the fitted tensor was computed, marking the preferred diffusion direction in each voxel. For each voxel the FA was computed (Beaulieu and Allen, 1994a; Basser and Pierpaoli, 1996), with high FA values indicating a preferred, diffusion direction of the water molecules. Next, in the final (fifth) step, for each individual DTI dataset, white matter tracts of the brain were reconstructed, often referred to as *fibers* or *tracts*, using the *Fiber Assignment by Continuous Tracking* (FACT) (Mori et al., 1999; Mori and van Zijl, 2002; Mori et al., 2002). Tracking parameters were set as follows: from each white voxel in the brain mask, a single seed was started, following the main diffusion direction of each voxel, traveling from voxel to voxel, reconstructing the white matter fiber step-by-step. Fiber tracking was stopped when the fiber trace reached a voxel with a FA value lower than 0.1, when the trajectory of the traced fiber exceeded the brain mask or when the streamline made a turn of more than 45 degrees. Only streamlines with a length that exceeded 30 mm were considered for further analysis. Furthermore, to indicate the integrity of a reconstructed fiber tract, each point of the fiber tract was colored with the FA values of the voxels along the 3D path of the fiber (van den Heuvel et al., 2009a; Mandl et al., 2008; Mandl et al., 2010; Van den Heuvel et al., 2008b).

T1 preprocessing and brain region parcellation

Cortical and sub-cortical brain regions were selected by parcellating the cerebrum into distinct, anatomically separated brain regions on the basis of the T1-weighted image, using the well-validated Freesurfer suite (V4.5, <http://surfer.nmr.mgh.harvard.edu/>). In short, this included the automatic segmentation of grey and white matter tissue, followed by parcellation of the segmented grey matter mask into distinct brain regions, based on a normalized template, parcellating the brain into a number of brain regions, including left and right caudate nucleus, globus pallidum, nucleus accumbens, thalamus, amygdala, hippocampus and 70 cortical brain regions. In total, 82 distinct brain regions were parcellated (Fischl et al., 1999; Fischl et al., 2004).

Construction of structural brain networks

Using the collection of all reconstructed DTI fiber tracts and the collection of parcellated brain regions, for each individual dataset a structural brain network was constructed, using a validated network framework (Bullmore and Sporns, 2009; van den Heuvel et al., 2009b; Hagmann et al., 2007). This procedure included the following steps, illustrated one-by-one in Figure 5.1. A graph $G = (V, E)$ is a mathematical description of a network, consisting of a collection of nodes V and a collection of connections E , that interconnect the nodes of

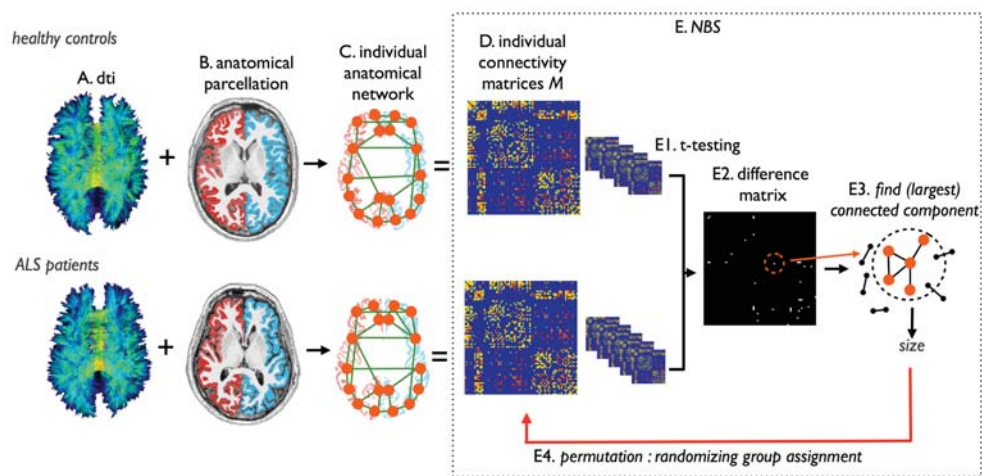


Figure 5.1 Overview of the network selection procedure and the Network Based Statistics (NBS)

(a) Using the DTI data, white matter tracts of the brain were reconstructed. (b) Cortical and sub-cortical brain regions were selected by automatic parcellation of the cerebrum. (c) An individual brain network was defined, consisting of nodes (i.e. the parcellated brain regions) and connections between nodes i and j that were connected by a white matter pathway. (d) Repeating this for each region i and j in the collection of parcellated brain regions, resulted in a (weighted) connectivity matrix M . Connections were weighted by their FA value, as determined from the DTI measurement. Next, using Network Based Statistics (NBS), the connectivity matrices of ALS patients and controls were compared. (e1) First, each connection between region i and j was tested between patients and controls using t-statistics. (e2) This resulted in a binary difference matrix, with 1s for those connections that showed a (absolute) t-value between controls and patients higher than a set T-threshold T , and 0 otherwise. Third, the sizes of the (largest) connected components in the difference matrix was computed, revealing sub-networks of regions showing affected connectivity in patients. Fourth, permutation testing was used to define a distribution of (largest) component size that could occur under the null-hypothesis (i.e. no difference between patient and controls). 5000 permutations, permuting group assignment, were computed. Finally, the original observed component size (i.e. difference between patients and controls) was given a p-value based on the computed null-distribution, by defining the percentage of the null-distribution that exceeded the size of the observed impaired network in patients.



the network. Within this framework, the brain network can be expressed as a collection of nodes, reflecting the different anatomical regions and a collection of connections between the nodes, representing the white matter tracts interconnecting cortical and sub-cortical regions. Two nodes i and j of the network (i.e. brain region i and region j) were defined as being connected when there was a reconstructed white matter tract in the collection of DTI fibers that interconnected region i and region j . This selection covered the following specific steps. First, for each individual dataset, the brain regions (i.e. nodes of the G) were defined as the individually segmented brain regions. Next, the existence of connections between the nodes (i.e. anatomical brain regions) was computed: for each pair of regions in the individual specific parcellation map it was determined whether the two regions were connected by a white matter pathway (van den Heuvel et al., 2009a; Van den Heuvel et al., 2008b). When the fiber selection procedure did not reveal any fibers between region i and j , no connection was included in G . This procedure was repeated for all regions i and j in the parcellation map. Furthermore, for each connection in G , the strength S of the connection was taken as its average FA (believed to reflect the level of microstructural organization of the tract). Repeating this procedure for all combinations of regions i and j in the network resulted in a sparsely weighted connectivity matrix M , with weighted connections between those brain regions that are structurally connected and zeros otherwise. Next, to correct for possible individual differences in overall connectivity strength, the connectivity matrix M was scaled to the maximum FA value within M (van den Heuvel et al., 2010). As a result, each individual matrix M expressed the connectivity structure of the brain network, with the cells of M representing the connections and their values representing the connectivity efficacy between brain regions. Please note that, related to the noise of the DTI signal, it is known that streamline tractography may result in the construction of some incorrect streamlines, possibly leading to the inclusion of false positives. However, as a falsely constructed streamline is likely to only occur in a single subject or in a small subgroup across the total group of subjects – otherwise it is more likely to represent a true (i.e. true positive) existing white matter pathway – false positives were controlled for by taking into consideration only those connections that were present in 2/3 of both the patients and controls. Hereby minimizing the effect of incorrect streamlines on the analysis.

Overall topology of the brain network

Overall topology of the structural brain networks – in both patients and healthy controls – were examined by computing the overall connectivity strength S (sum of the connectivity

matrix), the average shortest path length L (as a measure of global connectivity), the average clustering coefficient C (as a measure of local connectivity in the network). Typically C and L values are normalized to the clustering-coefficient and path length of a collection of random graphs to examine how the graph metrics C and L relate to the properties of a randomly organized network. To this end, C and L were compared to the metrics of 100 random graphs with equal degree and degree distribution as the examined brain networks (Rubinov and Sporns, 2010). Furthermore, providing insight in the distribution of connectivity, the average connectivity distribution – i.e. a histogram of how many times a certain level of node-specific strength S occurs in the network – of the brain networks of patients and controls was computed. Possible differences in S , C , L , normalized C and/or normalized L between the two groups were examined using permutation testing (5000 permutations) (van den Heuvel et al., 2010).



Statistical testing for impaired networks

Next, using the individual brain networks (i.e. matrices M) of patients and controls, it was examined whether patients with ALS showed impaired structural connections (i.e. reduced connectivity strength of specific node-to-node connections), compared to the brain networks of the healthy controls. Network Based Statistic (NBS), as proposed by Zalesky et al. (Zalesky et al., 2010), was used to identify impaired sub-network(s) in patients in comparison to healthy controls. The rationale behind NBS expands the notion of Statistical Parameter Mapping, marking that impaired connections that form a network (i.e. together make up a connected component in the network) have a higher probability of indicating true abnormality, than single connections (i.e. not forming a connected component), hence providing control for the high number of tests performed (i.e. good control for type I error in the problem of multiple comparison). A detailed description of the NBS methodology is given by Zalesky et al. (Zalesky et al., 2010). The performed NBS analysis consisted of the following steps. First, for each connection in the brain network the mean difference in connectivity strength between the group of patients and the group of controls was tested using a two-sample t-test (leaving out zeros). Within the NBS framework, differences in connectivity strength between the group of patients and the group of controls with a t-value larger than a set threshold T were marked by 1 in a difference matrix D , and 0 otherwise. Within the NBS procedure, the choice of T-threshold is rather arbitrary (Zalesky et al., 2010). However, in this context it is worth mentioning that type I error is always ensured with NBS, irrespectively of the choice of T-threshold as illustrated by simulations performed

in the original NBS paper of Zalesky and colleagues (Zalesky et al., 2010). However, type II error (false negative rate) may be impacted by the choice of T-threshold. Therefore, two analyses were performed: (1) using a two-sided T-threshold reflecting a p-value of 0.0075 (Zalesky et al., 2010); (2) using a more exploratory one-sided threshold matching a p-value of $1/N$, with N the number of nodes in the network. From the resulting matrix D the size of the largest interconnected component was computed, marking the size of the cluster of affected connections in the group of patients related to the group of controls. Thirdly, permutation analysis was used to create a distribution (i.e. null-distribution) of component size that can occur under the null-hypothesis. For each of the permutations, (1) subjects (patients and controls) were randomly assigned to two random groups (of similar size as the original patient and control groups); (2) the difference matrix D between these two groups was computed; (3) matrix D was thresholded; (4) the size of the largest component (i.e. the number of nodes and connections involved) was computed. In the present study, 5000 permutations were performed to create a null-distribution. Fourthly, given the obtained null-distribution, a corrected p-value of the components observed in the original difference matrix D between the patients and controls was computed as the percentage of the null-distribution that had a higher value than the observed component size (Zalesky et al., 2010).

Examining the topology of impaired sub-network(s)

The observed impaired structural network(s), expressing reduced connectivity strength in patients compared to controls, was taken for further analyses on topology (van den Heuvel et al., 2010; Rubinov and Sporns, 2010; Zalesky et al., 2010). For all individual subjects (both patients and controls) a sub-network was formed out of the connections of the reported NBS network(s), by extracting the connectivity values out of the individual connectivity matrices M . Next, for each of the individual sub-network(s) the level of connectivity strength S was computed, expressing how strong the nodes of the impaired network(s) were interconnected, together with the level of efficiency E , expressing the level of efficiency of how each region was connected to other regions in the network. In addition, to S and E , the level of local clustering (expressed by the clustering-coefficient C) was computed, providing information on possible changes in the level of local efficiency or local cliqueness of the affected sub-network (Rubinov and Sporns, 2010). Furthermore, to examine the role of each of the nodes in the impaired sub-network(s), the node-specific connectivity strength S_i and the node-specific efficiency Eff_i were computed. The connection

strength S_i of each node i expresses how strong a node is connected to the other nodes of the network and was computed by summing up the weights of all its connections. The level of efficiency Eff_i of node i was defined as the sum of the inverse distances between node i and all other nodes j in the network, indicating how efficient information from node i can be shared with the other nodes of the network (Rubinov and Sporns, 2010).

Linking graph organizational measures to clinical scores

A possible association between the topology of the impaired network(s) – revealed by the NBS procedure – and clinical scores was explored. ALSFRS-R and disease progression rate was examined against S_i and Eff_i metrics of the impaired network(s) using linear regression.



RESULTS

Overall network topology

Table 5.2 summarizes the global graph metrics of the brain networks of ALS patients and healthy controls, supporting the results of recent studies, indicating a high level of local clustering and a short overall path length (van den Heuvel et al., 2010; Hagmann et al., 2008). The average connectivity distribution of patients and controls is given in Supplemental

Table 5.2 Global graph metrics

Table summarizes the global values of connectivity strength S , shortest path length L , normalized path length, and normalized clustering coefficient C (normalized to 100 random graphs).

Graph metrics	FA weighted brain network	
	Healthy controls Mean \pm SD	ALS patients Mean \pm SD
Connectivity strength S (sum of M)	840 \pm 75.8	843 \pm 72.8
Shortest path length L	3.04 \pm 0.18	3.04 \pm 0.14
Clustering coefficient C	0.37 \pm 0.02	0.36 \pm 0.02
Normalized characteristic path length	1.11 \pm 0.014	1.08 \pm 0.017
Normalized clustering-coefficient	2.2 \pm 0.16	2.1 \pm 0.17

FA = fractional anisotropy; SD = standard deviation.

Figure S5.1. As expected, no differences were found in any of the overall graph metrics in ALS (permutation testing, 5000 permutations), suggesting an intact organization of the global brain network in patients.

Impaired sub-network

The NBS revealed a single impaired sub-network, consisting of 9 nodes and 10 (bidirectional) connections, of reduced connectivity in patients with ALS (NBSa; $p = 0.0108$, permutation testing). This impaired network overlapped with the left and right precentral gyrus, left pallidum, left hippocampus, left and right caudal middle frontal gyrus, right paracentral gyrus, right posterior cingulate and right precuneus (Figure 5.2a and 5.4). Interestingly, although a whole brain analysis was performed without any a priori selection of motor regions, the regions of this impaired network strongly overlap with regions that are known to play a key role in motor movement and control. To further examine this overlap an additional analysis was performed (see below).

Furthermore, using a NBS-threshold matching a p-value of $1/N$, a more extended network was found, including frontal and temporal regions as shown in Figure 5.2b (NBSb; $p = 0.0084$, permutation testing). Similar to the more conservative selected network, the sub-network overlapped with the primary motor regions (bilateral precentral gyrus and paracentral lobule), supplemental motor regions (bilateral caudal middle frontal gyrus, superior frontal gyrus and pallidum), but also with a number of other frontal cortical regions (right rostral middle frontal gyrus and right pars triangularis), temporal cortical

Figure 5.3 Overlap between motor network and impaired NBS network

(a) Direct cortical connections of the primary motor network. The direct connections of the left and right precentral gyri in the group of healthy controls are shown. Figure illustrates (per region) the percentage of healthy control subjects that showed a direct structural white matter connection to the left or right precentral gyrus. The primary motor network was selected as those regions that were connected to the primary motor regions in the majority of healthy controls ($> 75\%$). (b) Figure shows the overlap (right column) between the exploratory NBS network (left column, NBSb network, Figure 5.2b) and the regions of the healthy motor network (middle column, showing regions of Figure 5.3a). The impaired NBS network was found to strongly overlap the motor network ($p < 0.0001$, Fisher's exact test). Right = Right; Left = Left.

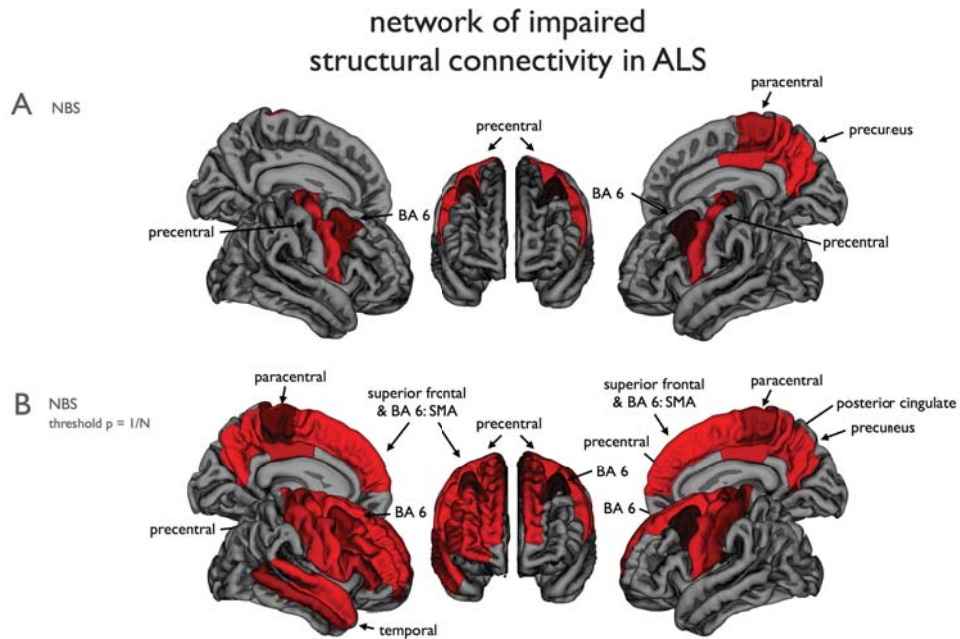
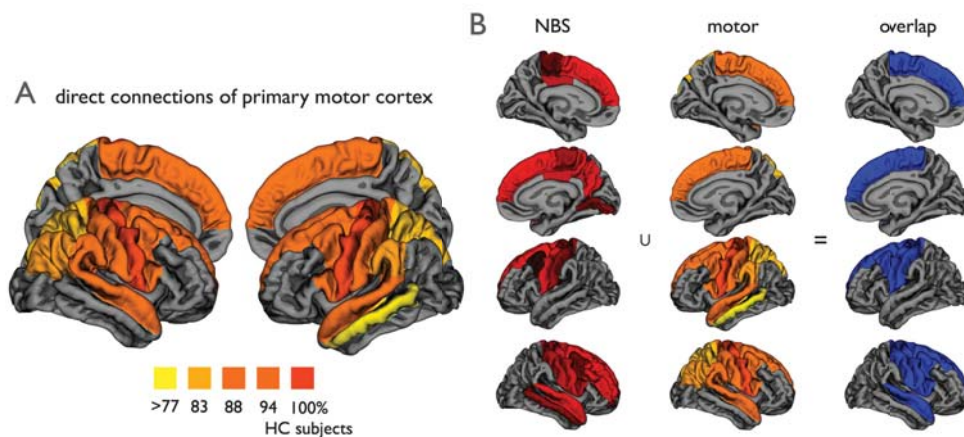


Figure 5.2 Cortical brain regions with impaired structural connectivity in ALS

(a) The NBS procedure revealed a sub-network of brain regions showing significantly reduced structural connectivity in ALS patients, compared to the healthy controls. Figure shows the set of involved parcellated cortical regions ($p = 0.0075$, see materials and methods). (b) Using an NBS threshold of $p = 1/N$ (N being the number of nodes of the network), a similar but more extended network was revealed. This model-free approach revealed a sub-network consistent with known motor regions, including precentral and paracentral gyri (primary motor), caudal middle frontal and superior frontal gyri (supplemental motor areas, BA6). The subcortical structures found with the NBS procedure were not included in this figure. Right = Right; Left = Left.



regions (right middle and superior temporal gyrus), parietal cortical regions (bilateral postcentral gyrus, posterior cingulate and precuneus) and the bilateral hippocampus and right amygdala. The involved cortical regions are shown in Figure 5.2b. [A post-hoc analysis including age as a covariate in the NBS analysis revealed no fundamental changes in the significance and/or topology of the observed NBS network (Figure 5.2)].

Overlap with the motor network

To further examine this consistency between the impaired network and the motor network, we determined the overlap between the regions that form the motor network and the observed impaired sub-network in patients with ALS. The overlap was statistically assessed using Fisher's exact test. First, the healthy motor network was determined by selecting the (direct) connections of the left and right precentral gyrus – as primary motor regions – with other brain regions in the group of healthy controls. The connectivity matrix M of the group of healthy controls was used to extract the direct connections of the left and right precentral gyrus. Figure 5.3a illustrates the regions that together form the (direct) motor network, i.e. those regions that show a direct connection with the left and right primary motor regions in the majority of the group of healthy subjects. Comparing this motor network to the found impaired sub-network in ALS patients, the NBSa network (Figure 5.2a) showed large overlap with the motor network. The regions found with the NBSa procedure were 89% motor regions and non-NBSa regions were 66% non-motor regions (Fisher's exact test: $p = 0.0025$). Furthermore, the overlap with the extended NBSb network (Figure 5.2b) was found to be significant as well ($p < 0.0001$); 76% of the NBSb regions were motor regions and 75% of the non-NBSb regions were non-motor (the overlap is illustrated in Figure 5.3b). Exact numbers of overlapping regions are given in Table 5.3.

Topology of the impaired NBS network

Examining the topology of this impaired network (NBSa, Figure 5.2a) revealed a significantly reduced level of network efficiency E ($p = 0.0095$, t-test, $df = 52$), as well as a reduced level of overall clustering C ($p = 0.0415$, t-test, $df = 52$). Also overall connectivity density S was found to be reduced in patients, but this effect did not reach the set statistical threshold ($p = 0.062$). Examination of the node-specific organizational measures, revealed a significant lower efficiency Eff_i of the left precentral ($q < 0.05$, $q = \text{FDR corrected } p\text{-value}$), left caudal middle frontal gyrus ($q < 0.05$), right paracentral ($q < 0.05$), right precuneus

Table 5.3 Overlap between the impaired sub-network in ALS and the motor network

The overlap of included regions is depicted for both NBS thresholds (see methods). The resulting p-value of the Fisher's exact test is included.

(Figure 5.3a)	NBSa	Non NBSa
Motor	8	25
Non-motor	1	48
p = 0.0025		
(Figure 5.3b)	NBSb	Non NBSb
Motor	19	14
Non-motor	6	43
p < 0.0001		

NBS = network based statistics.

and posterior cingulate cortex ($q < 0.05$). The left precentral gyrus ($p = 0.042$, $df = 52$) and right paracentral lobule ($p = 0.0150$) also showed a reduced level of connectivity strength S_i , but these effects did not survive FDR correction.

ALSFRS or progression rate scores were not significantly correlated with network topology measures.

DISCUSSION

The main finding of this study is a reduced efficiency of a widespread motor connectivity network in ALS. Patients revealed a significantly impaired structural network overlapping bilateral primary motor regions (precentral gyrus and paracentral lobule, Brodmann area (BA) 4), bilateral supplementary motor regions (caudal middle frontal gyrus, BA 6), parts of the left basal ganglia (pallidum) and right posterior cingulate and precuneus (Figure 5.2). Specifically examining the structural topology of the NBS network using graph analysis, revealed a significant decrease in efficiency E of this community of regions, most pronounced in left and right primary and supplemental motor regions (Figure 5.4). These results suggest that ALS not only affects primary motor connections, but also the capacity of primary motor regions to connect and communicate to supplemental motor regions. In addition, motor connections to the precuneus and posterior cingulate regions, strong connected regions or hubs of the brain network (van den Heuvel et al., 2010; Hagmann



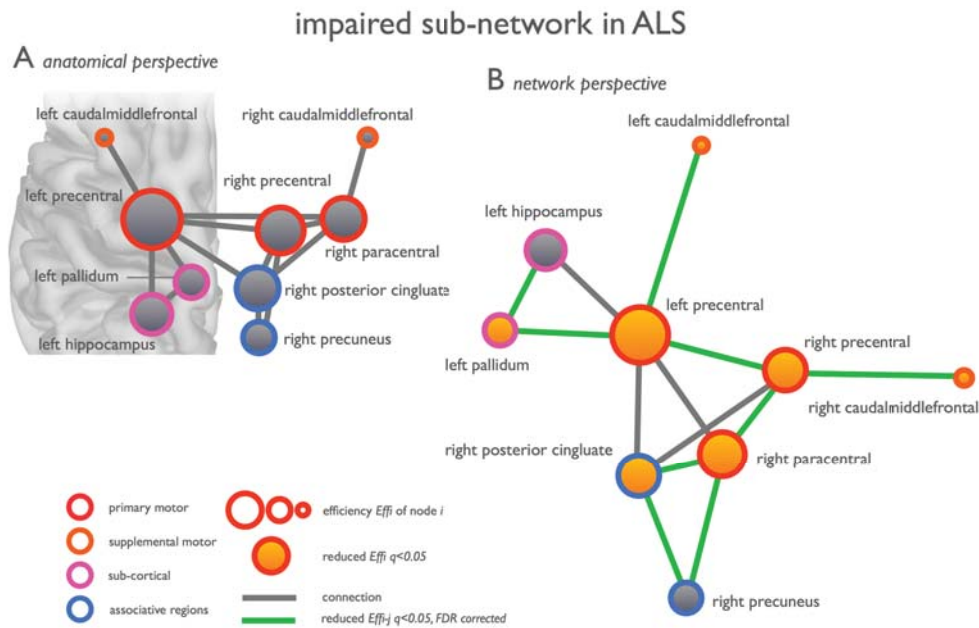


Figure 5.4 Network of impaired structural connectivity in ALS

(a) The nodes and interconnections of the NBS network (NBSa network, Figure 5.2a) as viewed from an anatomical perspective. (b) The NBS network from a network perspective (optimizing free Kamada-Kawai energy, constructed with pajek <http://vlado.fmf.uni-lj.si/pub/networks/pajek/>). Nodes and connections showing significantly reduced efficiency in patients are highlighted.

et al., 2008), were found to be affected in ALS. Hub regions are known to play a central role in the communication between remote brain regions (Van den Heuvel et al., 2008b; Greicius et al., 2008). Taken together, our findings suggest that not only the primary motor network is affected, which tends to be the current opinion on ALS (Verstraete et al., 2010; Filippini et al., 2010), but that ALS may have a much more global effect on connectivity and communication efficiency of the human connectome.

As shown in Figure 5.3b, the impaired sub-network in patients strongly overlapped with the motor network as we found in healthy controls. Based on the central role of the primary motor regions in the NBS network (see Figure 5.4b), it is tempting to speculate about the idea that the disease starts in the precentral gyrus and progresses along the structural connections of the primary motor regions towards secondary motor regions. Our current study did not, however, show direct correlations of network impairment with severity

or progression rate of the disease. Alternatively, brain plasticity could have potentially attributed to the reduced motor connectivity. Longitudinal and combined structural and functional MRI studies are needed to validate our hypothesis of disease progression along functional and structural connections of the motor network from primary motor regions towards secondary motor regions. Measurements of functional connectivity were not included in this study, but previous data have suggested that functional connectedness of the motor network is correlated with a faster disease progression (Verstraete et al., 2010).

Our finding, of degenerative effects in extra-motor regions in ALS, is in line with previous imaging studies on ALS. A number of grey and white matter voxel-based morphometry (VBM) studies (Senda et al., 2011; Thivard et al., 2007; Agosta et al., 2007; Kassubek et al., 2005) as well as DTI studies (Sage et al., 2007; Sage et al., 2009; van der Graaff et al., 2011; Agosta et al., 2010a; Senda et al., 2009) have reported extra-motor degenerative effects in ALS. These studies mostly resulted in an enumeration of found affected brain regions. Interpretation of this type of findings, however, is difficult and often limited to linking the function of the found regions to the clinical features in ALS. In contrast, the graph analytical network approach applied in this study provides the opportunity to examine ALS as a network disease, focusing on how the disease affects the white matter connectivity structure between brain regions. Our study may now provide a new insight into ALS, showing that the affected extra-motor regions are highly connected to the precentral gyri (primary motor regions) as the center of the degenerative process. The notion of a more widespread effect on brain connectivity, is supported by recent findings of impaired functional connectivity in patients (Jelsone-Swain et al., 2010; Mohammadi et al., 2009a). A study on resting-state fMRI data of patients with ALS showed a reduced level of functional communication in the so-called 'default-mode network', a clustered network overlapping medial inferior and lateral superior frontal, precuneus and inferior parietal and superior temporal brain regions (Mohammadi et al., 2009a). This reduced default mode connectivity is in accordance with our findings of impaired structural connectedness of the motor network to the precuneus and posterior cingulate regions, key regions of this 'default-mode network' (van den Heuvel et al., 2009a; Greicius et al., 2008).

Recent studies have reported an association between structural and functional connections in the brain network, confirming that anatomical connectivity – to some extent – bounds and shapes functional communication and connectivity between brain regions (van den Heuvel et al., 2009a; Van den Heuvel et al., 2008b; Hagmann et al., 2008; Honey et al., 2007;



Honey et al., 2009). Most importantly, a recent study showed that apparent local structural effects, for example focal damage to a primary motor node, can have widespread effects on whole brain functional network communication (Alstott et al., 2009). As such, our findings of impaired structural efficiency in ALS may suggest strong functional implications for efficient information processing and integration in the motor network. Indeed, reduced levels of global efficiency and affected functional connectivity of the brain network have been reported in neurological and psychiatric brain disorders, like Alzheimer's disease (Stam et al., 2009; Chen et al., 2011), Parkinson (Wu et al., 2009; van Eimeren et al., 2009) and schizophrenia (van den Heuvel et al., 2010; Liu et al., 2008), diseases known to affect cognitive processing. Higher levels of global brain network efficiency (and especially of frontal and temporal brain regions) are known to play a key role in cognitive functioning (van den Heuvel et al., 2009b; Li et al., 2009b; Achard and Bullmore, 2007). Our current results, together with recent studies examining whole-brain functional connectivity in ALS, show that ALS may affect more than simply the regions and topology of the motor network and that this underlying reduction of brain efficiency may be related to (subtle) cognitive dysfunction, observed in quite a large number of patients (Ringholz et al., 2005; Raaphorst et al., 2010; Gordon et al., 2010). This calls for future studies including ALS patients with FTD and quantitative neuropsychological testing. Examining this sub-population in a similar graph analytical approach may provide further information on whether brain network efficiency metrics are related to an increased probability of FTD development in ALS.

A potential weakness of our study is the disproportionate number of control subjects compared to patients, as well as the lack of longitudinal measures. The study was, however, set up to examine potential effects of disability and disease progression on motor network connectivity, and therefore to include a large group of patients. The total group included less disabled patients (ALSFRS-R > 40), as well as patients with major disabilities (ALSFRS-R < 40). Much to our disappointment, no effects were found to correlate with either the functional impairments, disease duration or disease progression rate. In addition, turning to the methodological aspects of this study, although DTI is an established method for investigating white matter integrity, the biological substrate of FA changes is still not completely understood. Fractional anisotropy is widely used as a measure of white matter integrity, it is influenced by multiple factors, complicating a direct interpretation of the results. Well-known influences are crossing fibers, fiber re-organisation, increased membrane permeability, destruction of intracellular compartments and glial alterations

(Acosta-Cabronero et al., 2010; Beaulieu, 2002). Second, in this study, connectivity between brain regions was taken as the average FA along a tract (van den Heuvel et al., 2010), rather than the number of streamlines interconnecting a pair of regions (Hagmann et al., 2008; Zalesky et al., 2011). The latter measure has been argued to be more sensitive when the impairment of a tract is relatively local, a streamline is in that case likely to terminate at the point of impairment, resulting in a reduced streamline count. This in contrast to using FA as a measure of connectivity, when local impairment may then be attenuated as the remaining part of the fiber streamline is not affected. However, this argument only holds when the impairment is severe, bringing the FA value along a point of the fiber below the stopping threshold of the tracking procedure (in this study 0.1). Based on previous DTI studies in ALS, such a severe impairment in microstructural integrity is unlikely to occur. FA alterations along the corticospinal and corpus callosal tracts – being the most extensively affected white matter tracts in ALS – appear to be rather modest (approximately 10%), despite profound motor disability among studied patients (Verstraete et al., 2010; Filippini et al., 2010; van der Graaff et al., 2011; Agosta et al., 2009b). As a result this will likely not have a strong effect on the tracing procedure; the FA value along the tracts in patients will still exceed the stopping criteria of ~ 0.1 , resulting in normal reconstructed tracts. Indeed, no differences were found in overall number of streamlines – overall and in corticospinal and corpus callosal tracts – in this study and in previous studies of our group (Verstraete et al., 2010). Furthermore, as expected, performing a post-hoc analysis in which the NBS analysis was performed on the number of streamlines instead of FA (i.e. connectivity matrices were constructed from the (scaled) number of streamlines that could be found between region i and j in the network) did not reveal a subnetwork of affected regions related to ALS. These post-hoc results support our overall conclusion, suggesting that most fiber tracts are still present in patients with ALS, but that their microstructural organization is altered due to disease.

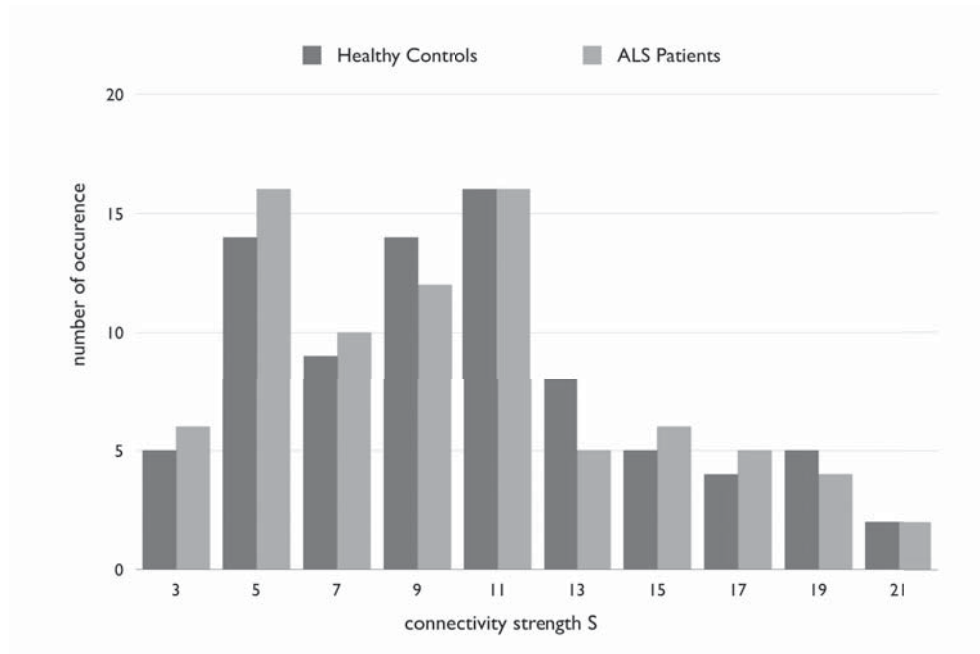
Third, in this study, streamline fiber tracking was used to reconstruct the connections of the brain network. The used deterministic fiber tracking algorithm (FACT) is based on having sufficient directional information at each point along the tract. When however the directional information at some point along a fiber stream is not univocal – for example due to ‘crossing fibers’ – ambiguous information on the diffusion direction may lead to low FA values, which could prematurely terminate a fiber streamline. As a result, some fiber pathways may be only partly reconstructed, leading to a reduced streamline count or some key fiber pathways may be missed at all. Alternative methods have been suggested, including



tracing methods based on shortest paths (Zalesky, 2008) and probabilistic fiber tracking (Behrens et al., 2003). In addition to false negatives, due to noise in the DTI data, streamline tractography may sometimes lead to false positives, meaning the construction of incorrect streamlines, which in turn may result in an incorrect connection between region i and j in the connectivity matrix M . To control for the effect of false positives in the analysis, a group threshold of $2/3$ was applied, stating that only connections that were present in more than 66% of both the group of patients and the group of controls were considered for analysis (see for a full description the Methods section). A useful alternative method to control for false positives, might be to include an initial streamline-threshold at the individual level, stating that only a connection between region i and j is said to be present when it consists out of more than a certain number of streamlines. Performing such an additional analysis, including a streamline threshold of 10 (i.e. taking only connections into consideration that included ≥ 10 streamlines, identical NBS procedure, 5000 permutations) revealed a similar affected sub-network ($p < 0.0030$, NBS), covering the same regions as presented in Figure 5.2a. These additional analyses suggest that the effect of false positives to our presented results (Figure 5.2 and 5.3) is minimal. Fourth, brain networks were examined on a macroscopic scale at a relative low spatial resolution, representing the brain as a graph of 82 segmented brain regions (i.e. nodes). Recent studies have, however, suggested the use a more high-resolution approach (going up to more than a 1000 smaller regions) (Hagmann et al., 2007; Zalesky et al., 2010; van den Heuvel et al., 2008a). ‘Graph resolution’ has been reported to have an effect on the topological properties of brain networks (Zalesky et al., 2010; Fornito et al., 2010; van den Heuvel and Hulshoff Pol, 2010).

Based on our present findings, we conclude that besides primary motor regions – as the center of the degenerative process in ALS – the motor connectome as a whole is affected in ALS including secondary motor connections. The widespread effects on the brain network were found to result from an interconnected degenerative process, suggesting that focal damage in primary motor regions in ALS may ultimately manifest in connectivity disturbances elsewhere in the brain.

SUPPLEMENTAL INFORMATION



Supplemental Figure S5.1 Average connectivity distribution of the group of patients with ALS and the group of healthy controls

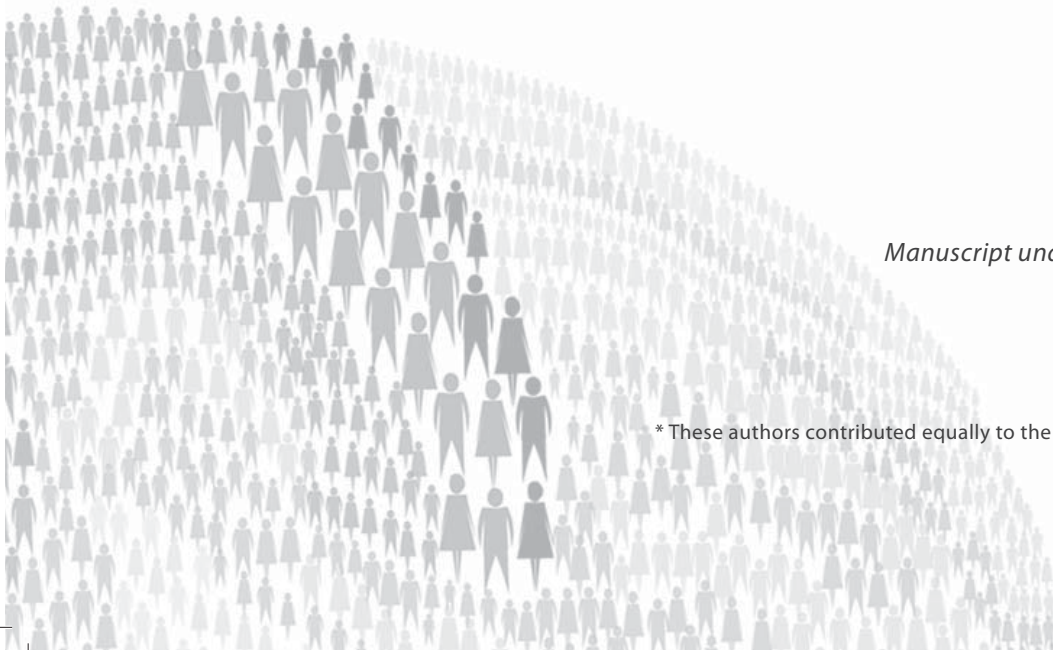
6

Structural brain network imaging shows progressive disconnection of the motor system in ALS

Esther Verstraete
Jan H. Veldink
Leonard H. van den Berg*
Martijn P. van den Heuvel*

Manuscript under review

* These authors contributed equally to the manuscript



ABSTRACT

Amyotrophic lateral sclerosis (ALS) is a severe neurodegenerative disease, which primarily targets the motor system. The structural integrity of the motor network and the way it is embedded in the overall brain network is essential for motor functioning. We studied the longitudinal effects of ALS on the brain network using diffusion tensor imaging and questioned whether over time an increasing number of connections become involved or whether there is progressive impairment of a limited number of connections. The brain network was reconstructed based on 'whole brain' diffusion tensor imaging data. We examined: 1) network integrity in 25 patients with ALS at baseline (T = 1) and at a more advanced stage of the disease (T = 2; interval 5.5 months) compared to a group of healthy controls, and 2) progressive brain network impairment comparing patients at two time-points in a paired-analysis. These analyses demonstrated an expanding sub-network of affected brain connections over time with a central role for the primary motor regions (p-values T = 1 0.003; T = 2 0.001). Loss of structural connectivity mainly propagated to frontal and parietal brain regions at T = 2 compared to T = 1. No progressive impairment of the initially affected (motor) connections could be detected. The main finding of this study is a progressive loss of network structure in patients with ALS. In contrast to the theory of ALS solely affecting a fixed set of primary motor connections, our findings show that the network of impaired connectivity is expanding over time. These results are in support of disease spread along structural brain connections.

INTRODUCTION

Amyotrophic Lateral Sclerosis (ALS) is a severe neurodegenerative disease progressively affecting both upper motor neurons in the motor cortex and lower motor neurons in the brainstem and spinal cord, with a median survival time of as little as 3 years after onset of symptoms (del Aguila et al., 2003; Hardiman et al., 2011). Progressive motor neuron loss results in declining motor function involving more and more body regions and increasing functional impairment over time. Based on clinical observations, it has been hypothesized that ALS is a focal process spreading contiguously through the nervous system (Ravits et al., 2007; Ravits and La Spada, 2009). *In vivo* insight into the pattern of disease spread within the brain – and the motor system in particular – is crucial as it could provide new therapeutic targets.

Recent imaging studies in ALS have revealed neurodegenerative effects in specific white matter motor tracts, showing consistent involvement of bilateral corticospinal tracts and corpus callosum (Grosskreutz et al., 2008; Nair et al., 2010; Filippini et al., 2010; Verstraete et al., 2010; Agosta et al., 2010a). However, the degree of corticospinal tract integrity correlates poorly with clinical markers and progression over time has not been consistently demonstrated (Senda et al., 2011; van der Graaff et al., 2011; Mitsumoto et al., 2007; Blain et al., 2007). These observations cast doubt on whether progressive degeneration of these main motor tracts is the leading cause of deteriorating motor functions in ALS.

The brain should be regarded as an integrative complex system, rather than a set of independently operating regions (Sporns, 2006; Stam and Reijneveld, 2007; van den Heuvel and Hulshoff Pol, 2010). In this context, the structural integrity of the motor network and the way it is embedded in the overall brain network is essential for normal motor functioning. It is, therefore, highly plausible that dysfunction of the motor network underlies ALS, but the extent and evolution of dysfunction has not yet been elucidated (Verstraete et al., 2011; Rose et al., 2012). Using diffusion tensor imaging (DTI) in a longitudinal setting, we investigated how disease progression in ALS is reflected in the reconstructed structural brain network and questioned whether, over time, an increasing number of connections become involved or whether the same initially involved (motor) connections become progressively impaired.

6



MATERIALS AND METHODS

Subjects

Twenty-five patients with sporadic ALS (23 males; mean age/SD: 57.3/12.0 years) and 19 healthy controls (14 males; mean age/SD: 52.8/10.6 years) participated in this longitudinal study (see Table 6.1 for full demographics and clinical characteristics) (Verstraete et al., 2011). Patients, recruited from the outpatient clinic for motor neuron diseases of the University Medical Center Utrecht and Radboud University Medical Center, Nijmegen (The Netherlands), were diagnosed with ALS according to the El Escorial criteria. Subjects did not have a history of brain injury, epilepsy, psychiatric illness or neurodegenerative diseases other than ALS. Clinical status of the patients was evaluated using the revised ALS Functional Rating Scale (ALSFRS-R). Rate of disease progression was defined as the average decline in ALSFRS-R score per month since onset of symptoms. After an average interval of 5.5 months, patients were examined again. Clinical status and follow-up times are provided in Supplemental Table S6.1.

The Ethical Committee for research in humans of the University Medical Center Utrecht approved study protocols. All subjects provided informed written consent according to the Declaration of Helsinki.

Table 6.1 Subject demographics and clinical characteristics

	Healthy control subjects (n = 19) Mean ± SD (range)	ALS patients (n = 25) Mean ± SD (range)
Age (years)	52.8 ± 10.6 (33–70)	57.3 ± 12.0 (38–74)
Male / Female	14 / 5	23 / 2
Site of onset (n (%))		Bulbar 2 (8%) Upper limbs 15 (60%) Lower limbs 8 (32%)
Diagnostic category (n (%))		Possible 2 (8%) Probable-lab-supported 9 (36%) Probable 12 (48%) Definite 2 (8%)
Time to diagnosis (months)		10.6 ± 11.2 (2–55)

SD = standard deviation.

Image acquisition

During each of the two sessions, participants underwent a 35-minute scan using a 3 Tesla Philips Achieva Clinical scanner at the University Medical Center Utrecht with a SENSE receiver head-coil. High resolution DTI was performed to reconstruct the white matter tracts of the brain network. Within each scanning session, 2 DTI sets, each consisting of 30 weighted diffusion scans and 5 unweighted B0 scans, were acquired (DTI-MR using parallel imaging SENSE p-reduction 3; high angular gradient set of 30 different weighted directions, TR/TE = 7035/68 ms, 2 x 2 x 2 mm, 75 slices, b = 1000 s/mm², second set with reversed k-space read-out). Then, directly after the acquisition of the DTI scans, an anatomical T1 weighted image (3D FFE using parallel imaging; TR/TE 10ms/4.6ms; FOV 240 x 240 mm, 200 slices, 0.75 mm isotropic voxel size) was obtained for anatomical reference.



Image preprocessing

DTI preprocessing

DTI preprocessing included the following steps (van den Heuvel and Sporns, 2011). First of all, susceptibility distortions, often reported in single-shot EPI DTI images, were corrected for by computing a field distortion map based on the two B = 0 images, which were acquired with an opposite k-space direction. This map was then applied to the 2 sets of 30 weighted images (Andersson et al., 2003), resulting in a single set of 30 corrected weighted directions. Secondly, images were realigned with the corrected B = 0 image, correcting for small head movements and eddy-current distortions (Andersson and Skare, 2002). Thirdly, the diffusion profile within each voxel was fitted a tensor (based on robust tensor fit method) (Chang et al., 2005b) and the preferred diffusion direction was determined as the principal eigenvector of the eigenvalue decomposition of the fitted tensor. To provide information on the microstructural organization of white matter, for each voxel the fractional anisotropy (FA) was computed, a measure often used as a marker for white matter integrity (Beaulieu and Allen, 1994b; Basser and Pierpaoli, 1996). Fourthly, streamline tractography was applied to reconstruct white matter tracts (Mori et al., 1999; Mori and van Zijl, 2002). Within each voxel, a single streamline was initiated, which then followed the main diffusion direction from voxel to voxel, reconstructing a white matter fiber. A streamline was terminated when the fiber track reached a voxel with an FA value lower than 0.1 (indicating low levels of preferred diffusion), when the streamline made an angle of more than 45 degrees, or when the trajectory of the traced fiber exceeded the brain

mask. To assess the integrity of a streamline, each reconstructed fiber tract was assigned the FA values of the voxels crossed (Mandl et al., 2008; Van den Heuvel et al., 2008b; van den Heuvel et al., 2009a).

T1 preprocessing

T1 images were realigned with the B = 0 images to obtain spatial overlap between the anatomical and DTI images. T1 images were used to select cortical and sub-cortical regions, resulting from parcellating the brain into distinct regions, using the well-validated Freesurfer suite (V4.5, <http://surfer.nmr.mgh.harvard.edu/>). This analysis included the automatic segmentation of grey and white matter tissue, followed by a parcellation of the segmented grey matter mask into 68 distinct cortical regions (34 within each hemisphere), 14 sub-cortical regions (bilateral thalamus, hippocampus, amygdala, accumbens, caudate, pallidum and putamen) and the brainstem.

Reconstruction of structural brain networks

A graph is a mathematical description of a network, consisting of a collection of nodes and a collection of connections. The nodes were selected as the 83 segmented regions; the connections were taken as the white matter pathways that interlink the regions. For each dataset (both patients and healthy controls), and for each time-point (i.e. longitudinal measurement) an individual brain network was reconstructed (Verstraete et al., 2011; van den Heuvel and Sporns, 2011). This procedure included the following steps. First of all,

Figure 6.2 Overview of longitudinal connectome imaging methods

Cortical and sub-cortical brain regions were selected by automatic parcellation of the cerebrum. Using the DTI data, white matter tracts of the brain were reconstructed. An individual brain network was defined consisting of nodes (i.e. the parcellated brain regions) and white matter connections between the nodes resulting in a (FA-weighted) connectivity matrix M . Next, using Network Based Statistics (NBS), the connectivity matrices of ALS patients at T = 1 and T = 2 were compared with healthy controls (Analysis 1). Using t-statistics each connection was tested resulting in a binary difference matrix ($D1$); connections with a statistical difference larger than a set threshold of $\alpha < 0.01$ were set to 1, and otherwise to zero. The size of the (largest) connected component in the difference matrix was computed, revealing a sub-network of affected connectivity in patients. Permutation testing was used to define the p-value of this component based on the computed null-distribution of (largest) connected component sizes as can occur under the null-hypothesis (no difference between patients and controls). An identical analysis was performed comparing brain connectivity at T = 1 and T = 2 in patients (Analysis 2).

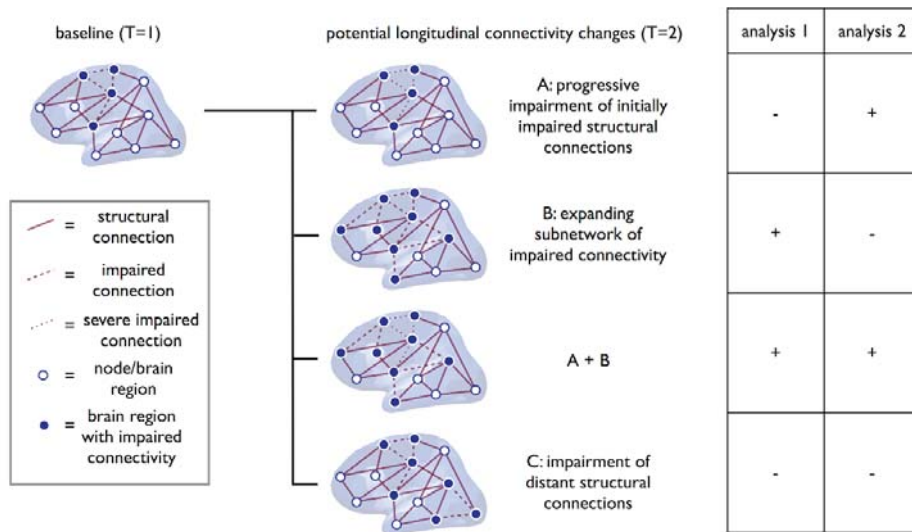
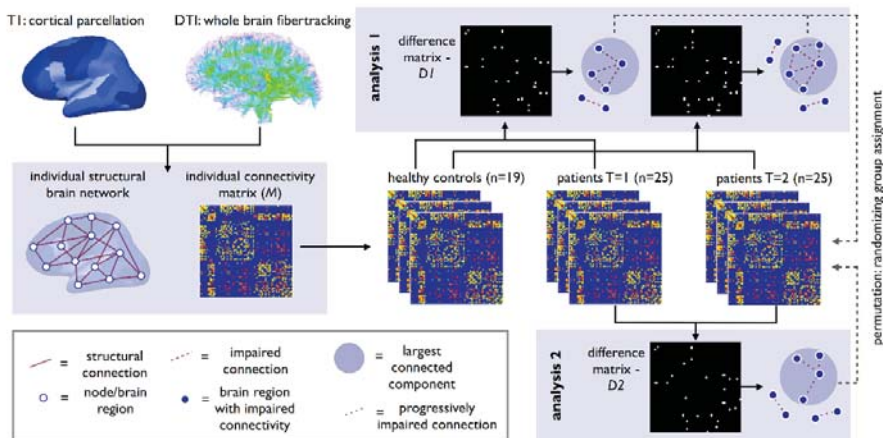


Figure 6.1 Potential longitudinal connectivity changes in ALS

This figure shows four potential scenarios for longitudinal neurodegeneration in ALS and the hypothesized results of the two types of analyses. (A) Progressive impairment within a subnetwork of initially impaired structural connections and regions will be detected by Analysis 2. Analysis 1 will not detect this type of progressive degeneration. (B) If the degenerative changes over time show spatial spread within the brain, this will be detected by Analysis 1 as this will result in an expanding subnetwork of impaired connections. (A+B) The third scenario is a combination of both progressive impairment of initially impaired structural connections, as well as expansion of the impaired connectivity (i.e. scenario A and B combined). In this scenario, both analyses show positive results. (C) The fourth scenario is longitudinal degeneration involving distant structural connections to the initially impaired subnetwork or multifocal degeneration. As the NBS analysis is designed to detect changes within a network, both Analysis 1 and 2 will show negative results when distant structural connections become impaired over time.



from the total collection of reconstructed streamlines, those that touched both region i and region j were selected. Secondly, from the resulting fiber streamlines, the average FA values were computed as the average of all points and all included streamlines. This value was incorporated into cell $c(i,j)$ in connectivity matrix M . If no tracts were found between regions i and j , the value of zero was assigned to matrix M , reflecting the non-existence of a direct tract between regions i and j in the brain network. This procedure was repeated for all regions in the total collection of regions (V), resulting in a connected, undirected, weighted graph G .

Statistical analyses

To examine the status of the brain's network during different stages of disease, Network Based Statistics (NBS) was used (Verstraete et al., 2011; Zalesky et al., 2010). NBS is based on the idea of Statistical Parameter Mapping, extending the notion that changes in connections that occur together – by forming a connected component – are more likely to indicate true network abnormality than effects that occur in relative isolation (i.e. solitary connections). Two types of analyses were performed: 1) examining the status of the brain network during different stages of disease compared to healthy controls, and 2) studying the effect of disease progression on the brain networks of patients (= within subject effect). These two analyses detect different types of longitudinal connectivity changes. We hypothesized four different scenarios: 1) progressive degeneration within the initially impaired structural connections (Figure 6.1, scenario A) will be detected by the paired analysis (only positive results with Analysis 2); 2) degenerative changes over time show spatial spread (Figure 6.1, scenario B), this will be detected by Analysis 1 as these changes will result in an expanding subnetwork of impaired connections and leave negative results with Analysis 2; 3) both progressive impairment of initially impaired structural connections, as well as expansion of the impaired connectivity (positive results on both Analysis 1 and Analysis 2; Figure 6.1, scenario A+B). 4) longitudinal degeneration involving brain regions distant to the initially impaired subnetwork or multifocal degeneration (negative results on both Analysis 1 and Analysis 2, Figure 6.1, scenario C). The NBS analysis is designed to detect changes within a network and therefore both Analysis 1 and 2 will be negative when structural connections distant to the initial degenerative process become impaired over time. Finally, if no longitudinal changes occur, both analyses will turn out negative as well. The two types of analyses included the following steps.

Analysis 1

To assess the longitudinal changes in the brain network, the connectivity profiles of the 25 patients at baseline ($T = 1$) and at a more advanced stage of the disease ($T = 2$) were compared to the reconstructed brain networks of healthy controls using NBS (Figure 6.2). DTI data of the group of 19 healthy controls was used to obtain a good stable estimate of normal brain connectivity. First of all, for each time-point, a difference matrix, $D1$, between controls and the brain networks of patients was created by two-sample t-testing across the two groups (controls vs. patients) for all entries (i.e. connections) in M . Secondly, effects showing a statistical difference larger than a set threshold of $\alpha < 0.01$ were set to 1, and otherwise to zero. Thirdly, from the resulting difference matrix, $D1$, the size(s) of the largest component(s) of connections that formed an interconnected sub-cluster of nodes was computed. Fourthly, permutation testing, randomly mixing group assignment, was performed to obtain a null-distribution of component size, independent of group status (10000 permutations) (Figure 6.2). The component(s) of reduced connectivity observed between patients and controls was assigned a p-value (corrected for multiple comparisons) based on the proportion of the null-distribution that showed a larger component size than the observed sub-network of impaired connectivity. The NBS procedure is known to show good control over type-I errors and to correct properly for multiple testing (Zalesky et al., 2010).

Analysis 2

The individual connectivity matrices (M) of the patients, one for each time point, were compared to detect possible progressive changes in connectivity strength of connections between regions i and j over time (Figure 6.2). First of all, a progressive difference matrix, $D2$, was created by performing a paired sample t-test for each of the cells in M . Differences showing a statistical difference of $\alpha < 0.01$ were marked by 1 in $D2$ and otherwise zero. Secondly, from the resulting matrix, $D2$, the largest connected component was extracted, forming the sub-network of progressively involved structural brain connections. Thirdly, following the same procedure as in Analysis 1, a null-distribution of component sizes that could occur by chance, rather than related to time effects, was created using permutation (Figure 6.2). For this procedure, each measurement was randomly assigned to one of two pseudo time-points, effectively randomizing $T = 1$ and $T = 2$ time-points across subjects. A null-distribution of component size that could occur under the null hypothesis was established by performing 10,000 permutations. Fourthly, given the computed null-distribution, the size of component(s) observed in the original longitudinal difference



matrix, $D2$ (reflecting longitudinal changes in connectivity strength in ALS) were assigned a p-value representing the proportion of the null-distribution that showed a larger component size than the size of the observed sub-network (Zalesky et al., 2010).

Network integrity and clinical characteristics

To study the relation between clinical markers (ALSFRS-R and progression rate) and network integrity, we correlated the cumulative FA of all the structural connections included in the NBS network with clinical markers using Pearson's correlation testing.

RESULTS

Analysis 1: structural brain networks in patients at two time-points compared to healthy controls

Using 'whole-brain' DTI data we reconstructed the structural brain networks of patients (at different time points) and healthy controls. Network impairment at baseline ($T = 1$) was assessed and compared with the affected sub-network at a more advanced stage of the disease ($T = 2$). The methods applied are schematically displayed in Figure 6.2.

Figure 6.3 shows the sub-network of affected connectivity in ALS (as compared to the brain networks of healthy controls) at the two measured time points $T = 1$ and $T = 2$. The affected network (NBS-corrected $p = 0.003$, 10,000 permutations) at $T = 1$ consisted of 18 regions and 19 affected connections. The following regions were included: cortical motor (precentral gyrus and paracentral lobule left and right), subcortical (thalamic nucleus right; pallidum left; hippocampus left; caudate right), frontal (caudal middle frontal left and right; superior frontal left), parietal (precuneus left and right; posterior cingulate gyrus right; inferior parietal left; postcentral left), temporal (supramarginal left) and the brainstem.

The affected network at $T = 2$ (after on average 5.5 months) revealed a more extensive network of 38 affected structural connections and 33 regions (NBS-corrected $p = 0.001$, 10,000 permutations). The impaired sub-network at $T = 2$ consisted of the following regions: cortical motor (precentral gyrus and paracentral lobule left and right), subcortical (thalamic nuclei and pallidum left and right; putamen right; caudate nucleus left), frontal (superior frontal gyrus, caudal middle frontal, rostral middle frontal and parstriangularis left and right; parsorbitalis right; parsopercularis right), parietal (superior parietal and

postcentral left and right; precuneus right; posterior cingulate right; inferior parietal left), temporal (supramarginal left; middle temporal right; superior temporal right; temporal pole right), insula right and the brainstem.

The cortical regions included in the affected network at T = 1 and T = 2 are displayed in Figure 6.4. Comparing the regions involved in the network at T = 2 with those involved

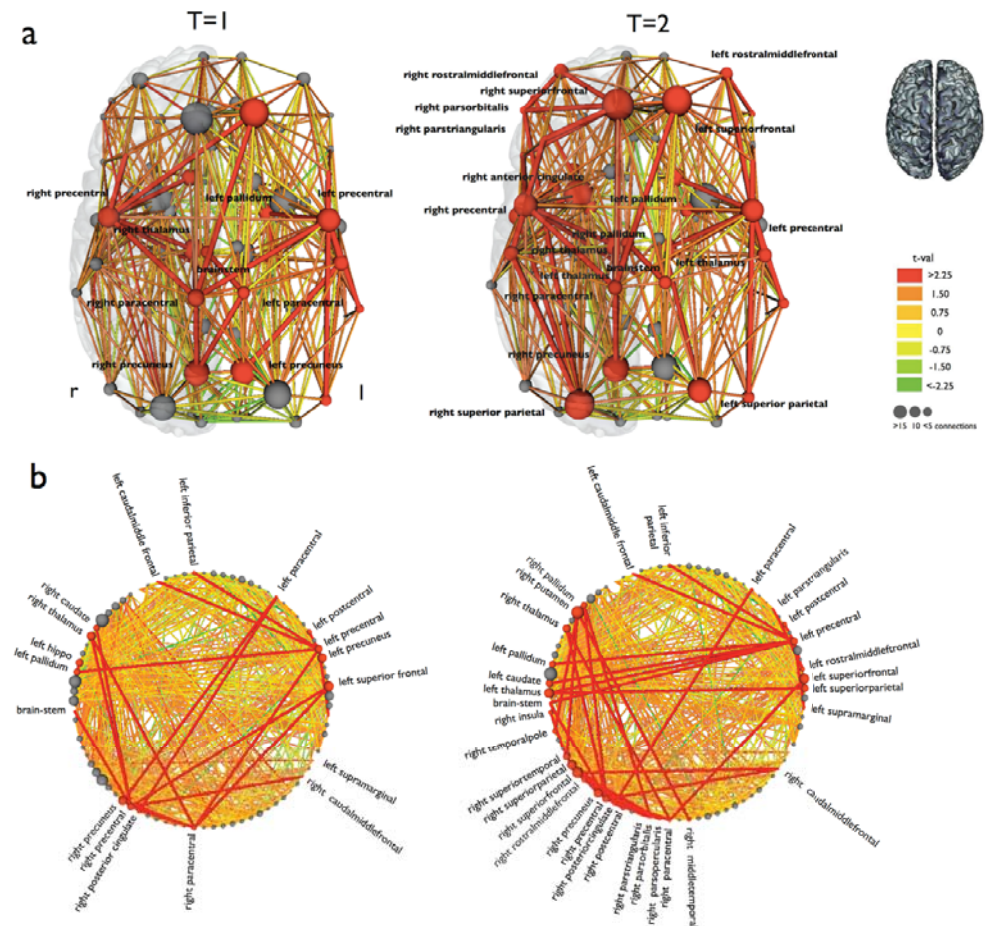


Figure 6.3 The reconstructed brain network and the affected structural connections in ALS at two time points

(A) The affected connections and interconnecting nodes are displayed comparing patients at T = 1 and T = 2 with the group of healthy controls. The size of the nodes is determined by their degree (number of structural connections). Nodes and connections were colored red if they were part of the affected sub-network. The affected sub-network at T = 2 included more structural connections, extending mainly to frontal and parietal brain regions. (B) This figure shows all regions arranged on a ring. The red colored nodes and connections are part of the affected sub-network, showing an increasing number of affected connections and regions at T = 2 compared to T = 1.

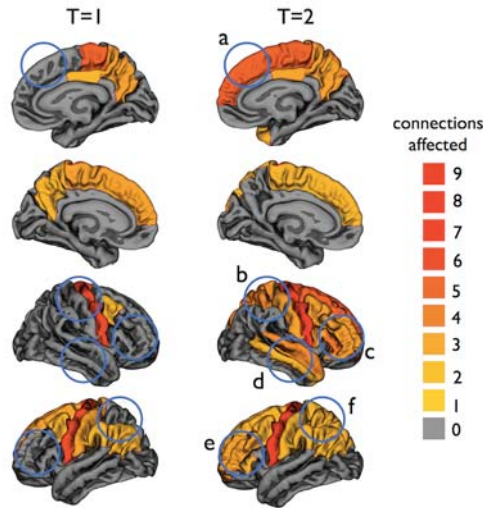


Figure 6.4 Cortical regions included in the affected sub-network at T = 1 and T = 2

The regions are colored based on the number of affected connections. The blue circles indicate the newly affected cortical regions at T = 2 compared to T = 1 (a: superior frontal right; b: postcentral and superior parietal right; c: rostral middle frontal, pars orbitalis, pars triangularis and pars opercularis right; d: temporal pole, superior and middle temporal right, insula right [not visible]; e: rostral middle frontal and pars triangularis left and f: superior parietal left).

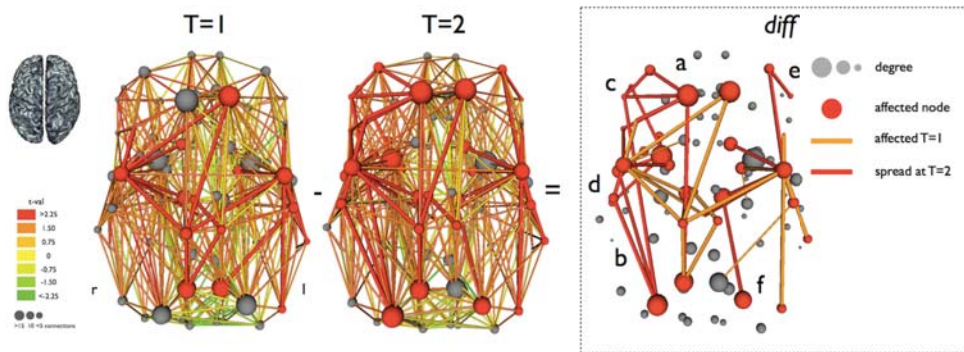


Figure 6.5 Longitudinal reduction of structural connectivity in ALS

The differences are shown (*diff*, third panel of figure) between the affected sub-networks at T = 1 and T = 2. Connections affected at T = 1 (and T = 2) are colored orange and newly affected connections at T = 2 are colored red. The newly involved cortical regions are indicated (a: superior frontal right; b: postcentral and superior parietal right; c: rostral middle frontal, pars orbitalis, pars triangularis and pars opercularis right; d: temporal pole, superior and middle temporal right, insula right; e: rostral middle frontal and pars triangularis left and f: superior parietal left). This figure marks the spatial spread of disease, resulting in progressive motor network disintegration.

at $T = 1$, reveals that it is mainly the connections with frontal and parietal brain regions which are newly affected as disease progresses, indicating spatial spread of disease along motor-related structural connections of the brain's network (Figure 6.5).

Analysis 2: longitudinal structural brain network changes in patients with ALS

To study the progressiveness of degenerative effects *within* structural connections, we compared the brain networks of the group of 25 patients at $T = 1$ and $T = 2$ using paired-NBS (Figure 6.2). This analysis did not reveal a sub-network of progressively affected connections and regions, indicating that the initially affected motor network – as measured by whole brain diffusion tensor imaging – is not progressively affected in ALS. A post-hoc analysis studying the individual structural connections, which had a significantly lower FA at $T = 2$ compared to $T = 1$ in the paired-NBS analysis, showed that the majority (67%) of these connections was linked to the impaired network found at $T = 1$ (Analysis 1). This suggests progressive disconnection following the brain network structure.

No significant correlation was found between the integrity of the NBS network (at both $T = 1$ and $T = 2$) and clinical markers.

DISCUSSION

The main finding of this study is a progressive loss of network structure in patients with ALS. Previous studies have suggested reduced motor network integrity in patients with ALS (Verstraete et al., 2011; Rose et al., 2012). Our findings now show that the network of impaired connectivity is expanding over time, involving more and more connections and regions (as shown by Analysis 1), rather than progressively affecting a fixed set of impaired connections (as shown by Analysis 2; Figure 6.1). Therefore, these results suggest spread of disease following the connectivity architecture of the brain network.

The observation of progressive brain network impairment in ALS puts previous findings in a new perspective. Longitudinal DTI studies using a voxel-wise comparison in a similar number of patients demonstrated widespread FA reduction over time (Senda et al., 2011; van der Graaff et al., 2011) as well as progressive loss of global FA (Sage et al., 2007). These widespread effects may be part of an expanding network of affected white matter connections, resulting in disintegration of the motor network as is illustrated by scenario

6



B in Figure 6.1. Previous longitudinal imaging studies in ALS, examining specific white matter tracts, revealed no progressive degeneration of corticospinal tracts, the primary efferent motor fiber pathways from the motor cortex to the spinal cord (Mitsumoto et al., 2007; Blain et al., 2007; Agosta et al., 2009b). This supports our findings that the limited number of initially involved white matter tracts are not progressively affected (Analysis 2). Summarizing, the degenerative effects observed in the corticospinal tracts appear to be an early sign of the degenerative process in ALS. However, our data suggest that clinical deterioration over time might result from progressive disconnection of the motor system as a whole.

Clinical milestones are currently the leading modality to assess the stage of disease (Roche et al., 2012), however, clinical characteristics in ALS are largely dependent on lower motor neuron functioning. An independent assessment of the upper motor neuron or motor network in the brain is seemingly impossible by means of clinical examination but might extend our insight and understanding on ALS. Examining the integrity of the brain network over time revealed an increasing number of affected white matter tracts, besides direct motor connections involving indirect motor connections. It is tempting to speculate about possible different stages of disease based on motor network connectivity. For other neurodegenerative diseases which stay confined to the brain, staging systems have been established based on the extent of pathology in *post mortem* studies like the well-known 'Braak'-stages in Alzheimer's disease (Braak et al., 1993). From *post mortem* studies in ALS we have learned that the neuropathological changes are inconsistent with clinical observations (Ince et al., 1998; Piao et al., 2003). Therefore, the lack of correlation between imaging findings and clinical parameters in this study is not surprising. The observation of an expanding subnetwork of impaired connectivity might, however, be a first step to independent assessment of the brain network integrity *in vivo*. Promising future directions might be the identification of endophenotypes and studying network impairment over time, ultimately this would result in a marker of disease enabling rapid drug screening in clinical trials (Turner et al., 2012). Concluding, we stress out the importance of future studies examining the brain network structure – and the motor network in particular – a larger groups of patients, to assess the different 'brain connectivity stadia' in ALS as disease progresses.

Disease spread in ALS has is a topic of interest for some time now. Clinical observations have given rise to the hypothesis that there might be a focal onset with subsequent spread to other body regions (Ravits et al., 2007b; Ravits and La Spada, 2009). In support of this

hypothesis, we now provide *in vivo*, imaging-based evidence for spatial spread of disease following the architecture of the brain network, which may be in line with “prion-like” spread as recently suggested by molecular studies (Polymenidou and Cleveland, 2011; Guo et al., 2011; Munch et al., 2011). Characteristic of prion diseases is the trans-synaptic transport of pathological prion protein (Frost and Diamond, 2010). The central pathological mechanism involves aggregates of misfolded proteins causing their native counterparts to adopt the same pathogenic conformation (Polymenidou and Cleveland, 2011). Our imaging-findings – suggesting propagation of disease along structural brain connections – are in support of this potential pathological mechanism. A similar mechanism has been proposed for other neurodegenerative diseases involving protein aggregates, including Alzheimer’s (Eisele et al., 2010; Jucker and Walker, 2011) and Parkinson’s disease (Winner et al., 2011). Recent imaging studies in subtypes of dementia have shown that neurodegenerative diseases target specific neural networks (Seeley et al., 2009), and brain regions with high functional and structural connectedness to “epicenters” for disease (i.e. primarily affected regions) have a greater disease-related vulnerability (Zhou et al., 2012; Raj et al., 2012). It is notable that the brain regions, included in the impaired subnetwork we found, show great overlap with the activation patterns observed with functional MRI during motor tasks (Poujois et al., 2012). The view that ALS potentially has a focal onset with subsequent spread along brain connections might open the way to the development of local treatment strategies in an early disease stage or of disease-modifying agents to target trans-synaptic spread.

We did not include elaborate neuropsychological testing to assess possible cognitive decline, however, none of the patients in our study actually fulfilled the clinical criteria of frontotemporal dementia (Neary et al., 1998). In future studies, it would be of great interest to examine a possible link between ALS-related cognitive impairment and the extent of brain network impairment, as suggested by reports on a direct link between brain connectivity and cognitive performance (Bassett et al., 2010; van den Heuvel et al., 2009b). Also, analysis of specific differences in the extent or spread of degeneration in (presymptomatic) carriers of the intronic repeat expansion in C9orf72, compared to other patients with ALS and their cognitive profile, would be of great value (DeJesus-Hernandez et al., 2011).

DTI measurement of structural brain network integrity is influenced by multiple factors including crossing fibers, fiber re-organisation, increased membrane permeability, destruction of intracellular compartments and glial alterations (Acosta-Cabronero et al.,



2010). This limits the direct comparison of lower fraction anisotropy and structural brain network integrity. Second, the examined structural brain network comprised 83 segmented brain regions. Future work examining connectome abnormalities in ALS using a higher resolution of the brain's network may result in a more finely grained representation of the motor connections. Third, following the procedures of previous longitudinal studies in ALS (Senda et al., 2011; van der Graaff et al., 2011), we did not perform routine longitudinal measures in healthy controls, as aging effects in this short time period are unlikely. In order to provide insight into possible scanner effects, a subset ($n = 7$) was evaluated after an average of 7 months, performing an analysis identical to that used in the group of patients. No significant network changes were found in controls. For the future it is important to reproduce our findings in a larger cohort of longitudinally assessed patients with ALS, as will be facilitated by currently emerging international collaboration (Turner et al., 2011a).

The observations in the present study, which examines longitudinal spread of ALS within the nervous system, suggest progressive loss of motor network connectivity, consisting of spatial spread along the architecture of the brain's network. The idea that ALS is a progressive disease of the brain network, potentially with a focal onset in primary motor regions, is important in helping to understand the progressive nature of the disorder and providing new leads for the future development of therapeutic targets.

SUPPLEMENTAL INFORMATION

Supplemental Table S6.1 Clinical scores at the time of scanning

Patients: Gender (M/F) – Age	T = 1: First scanning session					T = 2: Second scanning session					
	Disease duration (months)	Symptoms			Disease duration (months)	ALSFRS-R	Symptoms			ALSFRS-R	Progression rate
		B	UL	LL			B	UL	LL		
1: M 40y	16	47	no	yes	no	20	46	no	yes	no	0.1
2: M 50y	23	42	no	no	yes	26	42	no	no	yes	0.2
3: M 39y	17	46	no	yes	no	27	35	no	yes	yes*	0.5
4: M 53y	3	42	no	yes	yes	11	31	no	yes	yes	1.5
5: M 46y	6	45	yes	yes	no	9	44	yes	yes	no	0.4
6: M 38y	27	44	no	yes	no	33	42	no	yes	no	0.2
7: M 46y	31	37	no	yes	yes	35	35	no	yes	yes	0.4
8: M 45y	13	33	yes	yes	yes	16	32	yes	yes	yes	1.0
9: M 44y	8	42	yes	yes	yes	11	37	yes	yes	yes	1.0
10: M 74y	12	41	yes	yes	yes	19	28	yes	yes	yes	1.1
11: M 70y	9	42	yes	yes	no	14	33	yes	yes	yes*	1.1
12: M 65y	15	39	yes	yes	yes	19	37	yes	yes	yes	0.6
13: M 64y	17	43	no	yes	yes	22	43	no	yes	yes	0.2
14: M 65y	7	38	yes	yes	yes	10	33	yes	yes	yes	1.5
15: M 69y	4	42	yes	yes	no	10	34	yes	yes	yes*	1.4
16: M 64y	7	39	yes	yes	yes	13	35	yes	yes	yes	1.0

Supplemental Table S6.1 continues on next page



Supplemental Table S6.1 Continued

Patients: Gender (M/F) – Age	T = 1: First scanning session					T = 2: Second scanning session								
	Disease duration (months)	Symptoms			Disease duration (months)	ALSFRS-R	B	Symptoms		ALSFRS-R	B	Symptoms		Progression rate
		UL	LL	LL				UL	LL			UL	LL	
17: F 74y	59	42	no	yes	yes	68	39	no	yes	yes	0.1			
18: M 63y	25	42	no	no	yes	31	43	no	no	yes	0.2			
19: M 52y	10	46	no	no	yes	19	36	yes*	yes*	yes	0.6			
20: M 69y	9	42	no	yes	no	14	33	yes*	yes	no	1.1			
21: M 42y	21	48	no	yes	no	33	46	no	yes	no	0.1			
22: M 61y	6	45	no	yes	no	11	41	no	yes	no	0.6			
23: M 65y	11	31	no	yes	yes	15	25	no	yes	yes	1.5			
24: F 63y	15	38	yes	yes	yes	19	34	yes	yes	yes	0.7			
25: M 71y	16	32	yes	yes	yes	20	32	yes	yes	yes	0.8			
Mean	15.5	41.1				21.0	36.6				0.7			
SD (range)	11.7 (3–59)	4.4 (31–48)				12.6 (9–68)	5.6 (25–46)				0.5 (0.1–1.5)			

M = male; F = female; y = years; ALSFRS-R = revised ALS functional rating scale; B = bulbar; UL = upper limb; LL = lower limb; Progression rate = (48 – ALSFRS-R) / disease duration (months); SD = standard deviation; * new symptomatic regions.

PART II
BIOMARKERS



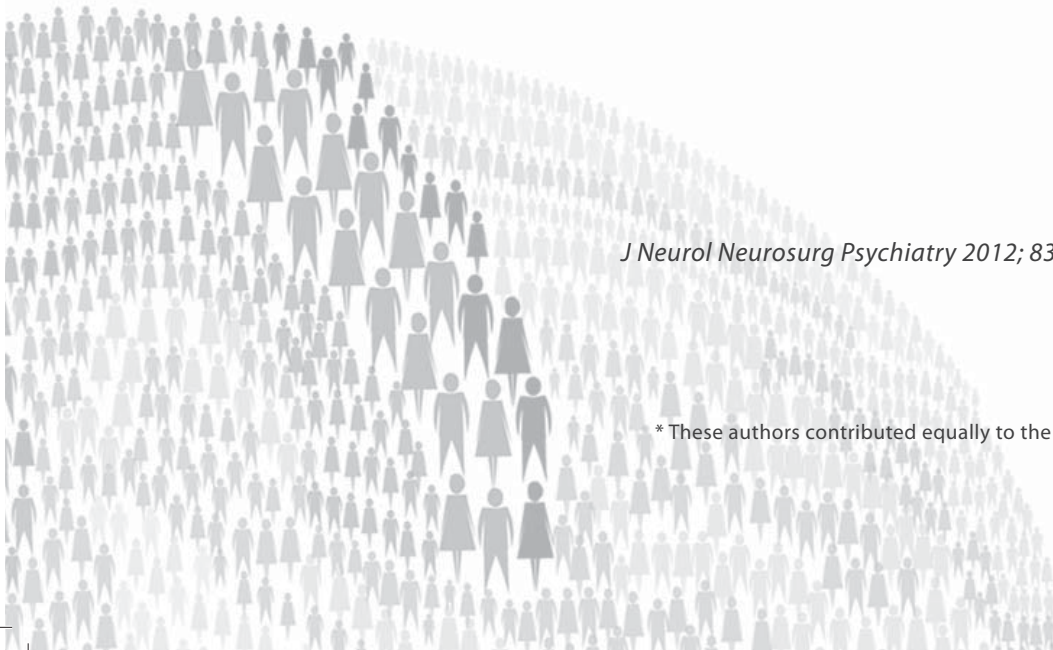
7

Structural MRI reveals cortical thinning in ALS

Esther Verstraete
Jan H. Veldink
Jeroen Hendrikse
H. Jurgen Schelhaas
Martijn P. van den Heuvel*
Leonard H. van den Berg*

J Neurol Neurosurg Psychiatry 2012; 83(4): 383-8

* These authors contributed equally to the manuscript



ABSTRACT

Objectives: Amyotrophic lateral sclerosis (ALS) is a fatal disease characterised by combined upper and lower motor neuron degeneration. An early and accurate diagnosis is important for patient care and might facilitate the search for a more effective therapy. MRI was used to study the whole cortical mantle applying an unbiased surface-based approach to identify a marker of upper motor neuron involvement in ALS.

Methods: Surface-based cortical morphology analyses were performed on structural, 3T MRI data of 45 patients with ALS and 25 matched healthy controls in a case-control study design. These analyses consisted of measuring cortical thickness, surface area and volume. The effects of disease progression were examined by correlating cortical measures with progression rate and by longitudinal measures in 20 patients.

Results: Cortical morphology analyses revealed specific thinning in the precentral gyrus, considered the primary motor cortex, in patients with ALS compared with controls ($p = 6.3 \times 10^{-8}$). Surface area was reduced in the right inferior parietal region ($p = 0.049$) and volume – the product of cortical thickness and surface area – was reduced in the right precentral gyrus ($p = 0.031$). From these findings, it appears that cortical thickness is superior in detecting the degenerative effects of ALS. Relative cortical thinning in temporal regions was related to faster clinical progression (right inferior temporal gyrus: $p = 3.3 \times 10^{-4}$).

Conclusions: Cortical thinning of the primary motor cortex might be a diagnostic marker for upper motor neuron degeneration in ALS. Relative thinning in temporal regions was associated with a rapidly progressive disease course.

INTRODUCTION

Amyotrophic lateral sclerosis (ALS) is a fatal neurodegenerative disease characterized by the loss of motor neurons in the cortex, brainstem, and spinal cord leading to progressive muscle weakness. There is as yet no definitive diagnostic test available for ALS. Diagnosis is mainly on clinical grounds based on internationally recognized El Escorial criteria after excluding ALS mimics using laboratory testing and imaging (Brooks et al., 2000). During the early stages, or in atypical presentations, both false positive and false negative diagnoses are common. The average time from onset of symptoms to a confirmed ALS diagnosis can be as long as 12 to 18 months, which is about one-third of the expected survival time (Chio et al., 2011a; Kiernan et al., 2011). An early and accurate diagnosis in patients with ALS is important for patient care as it shortens the phase of diagnostic uncertainty and enables early initiation of multidisciplinary care and treatment with riluzole. In addition it facilitates the search for an effective drug, allowing more patients to become eligible for inclusion into clinical trials at an earlier phase of the disease course (Cudkowicz et al., 2010; Schrooten et al., 2011).

The El Escorial diagnostic criteria use a combination of upper motor neuron and lower motor neuron signs to establish levels of diagnostic certainty. These criteria have, however, been criticized for their low sensitivity in the early stages of disease, even in patients in whom there is a strong clinical suspicion for ALS (Schrooten et al., 2011; Carvalho and Swash, 2009). Lower motor neuron loss can be assessed by electromyographic examination to improve diagnostic certainty. A similar, objective marker for upper motor neuron involvement would facilitate the diagnosis of ALS. This holds in particular for patients with clinically uncertain upper motor neuron features such as asymmetric reflexes or reflexes in wasted muscle groups, or pure lower motor neuron syndromes that may evolve into clinical ALS at later stages (Visser et al., 2007; Van den Berg-Vos et al., 2009; Wijesekera et al., 2009). Such a marker for loss of upper motor neurons is not yet available in routine clinical practice.

In ALS, MRI of the brain and spinal cord is mostly used in the diagnostic process in order to exclude ALS mimic syndromes. In some ALS patients, high signal intensity is evident along the corticospinal tract on T2-weighted, FLAIR, and proton density MR images, but these signs are non-specific for ALS (Turner et al., 2009). Computational MRI techniques have shown to be more successful in demonstrating and quantifying the degenerative effects of ALS. Techniques mostly applied include voxel-based morphometry (VBM) to quantify



grey matter volume (Ellis et al., 2001; Abrahams et al., 2005; Chang et al., 2005a; Kassubek et al., 2005; Grosskreutz et al., 2006; Agosta et al., 2007; Mezzapesa et al., 2007; Thivard et al., 2007; Grossman et al., 2008; Agosta et al., 2009a; Minnerop et al., 2009; Filippini et al., 2010; Senda et al., 2011), and diffusion tensor imaging (DTI) to assess the integrity of white matter connections (Turner et al., 2009; Thivard et al., 2007; Filippini et al., 2010; Senda et al., 2011; Agosta et al., 2010a). Currently the neuroimaging field in ALS is moving to an advanced level, from confirming differences at a group level to a marker for assessing the upper motor neuron in the individual patient (Turner et al., 2011a).

In the present study we examined the potential of cortical morphology MRI measures as objective markers for upper motor neuron involvement in a large cohort of patients with ALS compared to controls using a surface-based approach. This method allows for disentangling effects on whole brain cortical thickness, surface area and volume. In addition, the cortical effects of disease progression were studied, possibly allowing for identification of endophenotypes with enhanced vulnerability to the neurodegenerative effects of ALS.

METHODS

Participants

A total of 45 consecutive patients with ALS, and 25 age and gender frequency-matched healthy controls were enrolled in the study. Subject demographics and clinical information are listed in Table 7.1. All subjects gave their informed written consent, in line with the Declaration of Helsinki, and the study was approved by the medical ethics committee for research into humans of the University Medical Center Utrecht. MRI scans were performed within 6 months after diagnosis in 32 ALS patients (71%), recruited from the outpatient clinic for motor neuron diseases of the University Medical Centre, Utrecht and Radboud University Medical Centre, Nijmegen (The Netherlands) from January 2009 to December 2010. All patients were diagnosed according to the revised El Escorial criteria (possible, probable laboratory-supported, probable, or definite ALS) (Brooks et al., 2000). Subjects with a history of brain injury, epilepsy, psychiatric illness, and other neurodegenerative diseases were excluded. Clinical status of the patients was evaluated using the revised ALS Functional Rating Scale (ALSFRS-R) and disease progression rate was assessed ($48 - \text{ALSFRS-R-score} / \text{disease duration (months)}$). Since bulbar involvement has been found to correlate with more extensive cortical involvement, we calculated the bulbar score based

Table 7.1 Demographic and clinical features of the participants

	Controls	ALS
Male, % (n/N)	80 (20/25)	80 (36/45)
Age, mean (SD)	55.1 (10.5)	54.6 (13.3)
Duration of disease, months, mean (SD)		17.2 (13.3)
Type of onset, % (n/N)		
Bulbar		15.6 (7/45)
Cervical		53.3 (24/45)
Lumbosacral		31.1 (14/45)
El Escorial diagnostic category, % (n/N)		
Possible		17.8 (8/45)
Probable-lab-supported		26.7 (12/45)
Probable		37.8 (17/45)
Definite		17.8 (8/45)
Time since diagnosis, % (n/N)		
0–6 months		71.1 (32/45)
6–12 months		17.8 (8/45)
> 12 months		11.1 (5/45)
ALSFRS-R, mean (SD)		40.6 (4.2)
Progression rate, mean (SD)		0.62 (0.49)

ALSFRS-R = ALS functional rating scale revised; Progression rate = $48 - \text{ALSFRS-R} / \text{disease duration (months)}$.

on the ALSFRS-R (assessing speech, salivation and swallowing). Furthermore, to examine possible longitudinal effects, patients were invited for a follow-up MRI. In total 20 patients underwent follow-up scanning sessions after 3 to 10 months.

Data acquisition

To examine the neuroanatomical profile in ALS, structural imaging data sets were acquired on high-field 3 Tesla Philips Achieve Medical Scanner. A high-resolution T1-weighted image was acquired for surface-based morphology. Acquisition parameters are: 3D FFE using parallel imaging; TR/TE = 10/4.6 ms, flip-angle 8 degrees, slice orientation: sagittal, 0.75 x 0.75 x 0.8 mm voxelsize, FOV = 160x240x240 mm, reconstruction matrix = 200 x 320 x 320 covering whole brain (Verstraete et al., 2010).



Data analysis

Surface-based cortical morphology measures were performed using the well-validated and freely available FreeSurfer software package version 4.5.0 (<http://surfer.nmr.mgh.harvard.edu/>). In short, firstly, for each individual T1-weighted scan, segmentation of grey and white matter was followed by three-dimensional reconstruction of the grey matter surface, the cortical mantle. Secondly, cortical thickness at every small region of the cortical mantle (vertex) was determined by computing the distance between the white matter and grey matter surface reconstructions (Fischl and Dale, 2000). Thirdly, a group average anatomical image and surface rendering was constructed by spherical normalization of the surface renderings to standard space. All individual datasets (both for patients with ALS and healthy controls) were then normalized to the computed group average anatomical surface, allowing for group comparison between patients with ALS and matched, healthy controls at each small fragment of cortical surface, which is called ‘vertex-wise comparison’ between patients and controls.

In addition to vertex-wise comparison, we performed a ‘region-wise comparison’ between patients and controls. Regional changes in cortical morphology were examined for each of the 70 anatomical cortical regions in the brain measuring cortical volume (expressing the volume of a brain region in cubic mm), thickness (expressing the average thickness of a brain region in mm), and surface area (expressing the surface area of a brain region in squared mm). The anatomical cortical regions were defined by means of an automatic parcellation of the cortical surface (Desikan et al., 2006; Fischl et al., 2004).

Statistical analysis

Whole brain vertex-wise analysis of cortical thickness was performed using a General Linear Model (GLM) examining differences between patients and controls including age as a covariate. The resulting significance levels per vertex were plotted on a group-averaged brain template. Statistical maps for patients versus controls (ALS – controls) were thresholded at 2, meaning vertices with $p < 0.01$ (uncorrected) were highlighted, marking the cortical areas with significant changes.

Region-wise group comparison of cortical morphology (cortical volume, thickness, and surface area) was performed using GLM included in the R software package for statistical computing (www.R-project.org, R 2.11.1 GUI 1.34). Cortical morphology measures for each region were evaluated separately to detect region-specific differences

between patients and controls taking age and whole brain average cortical thickness or surface area (for volume and surface area) as covariates (Rogers et al., 2007). Regions with a p-value of 0.05 or lower were taken as significant. To control for multiple testing, each p-value was tested according to the Benjamini & Hochberg false discovery rate (FDR). Regions with an FDR corrected p-value equal to or below 0.05 were considered to be 'whole brain significant'.

In order to examine the relation between the average cortical thickness in the 70 anatomical regions and disease progression rate, we used a GLM including whole brain average cortical thickness as a covariate. Longitudinal effects were examined using a random effects model for repeated measurements, to account for intersubject and intrasubject variation. The model was designed to identify the brain regions attributing to the ALSFRS-R-score, including disease duration and whole brain average cortical thickness as covariates.



RESULTS

Whole brain cortical imaging

The unbiased whole brain vertex-wise comparison of cortical thickness between ALS patients and controls showed significant thinning of the precentral gyrus, the primary motor region, in patients (Figure 7.1). Region-wise analyses in which the 70 anatomical regions of the brain were compared for cortical morphology measures between patients and controls, cortical thickness also showed whole brain significant cortical thinning in the left and right precentral gyrus (left $p = 4.5 \times 10^{-5}$; right $p = 7.8 \times 10^{-4}$) (Figure 7.2A). Cortical surface area did not reveal any whole brain significant effects of ALS, in particular, no effects were found in the cortical motor regions and the pattern of differences between patients and controls was not symmetrically distributed (Figure 7.2B; right inferior parietal $p = 0.049$). Regional cortical volume (Figure 7.2C) is the product of surface area (Figure 7.2B) and average cortical thickness of a given region (Figure 7.2A). Based on our findings, these two variables (thickness and surface area) are independent of each other, as also supported by previous studies on cortical morphology (Winkler et al., 2010; Eyer et al., 2011). Effects found with cortical volume are, therefore, diluted effects, caused either by changes in cortical thickness or surface area. This is illustrated by our finding of reduced cortical volume in the right precentral gyrus ($p = 0.031$) which was, in contrast with thickness, not whole brain significant (Figure 7.2).

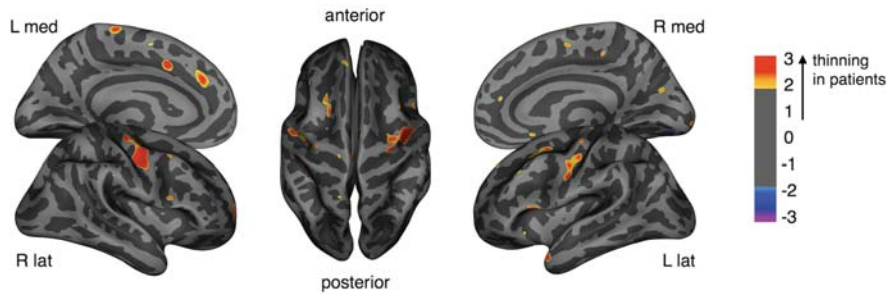


Figure 7.1 Cortical thickness in patients with ALS compared with healthy controls
 Differences in cortical thickness between patients and controls were projected onto an average brain template in a vertex-wise analysis. Areas showing cortical thinning in patients with ALS ($p < 0.01$) are colored yellow/red. The precentral gyrus demonstrates cortical thinning on both sides.

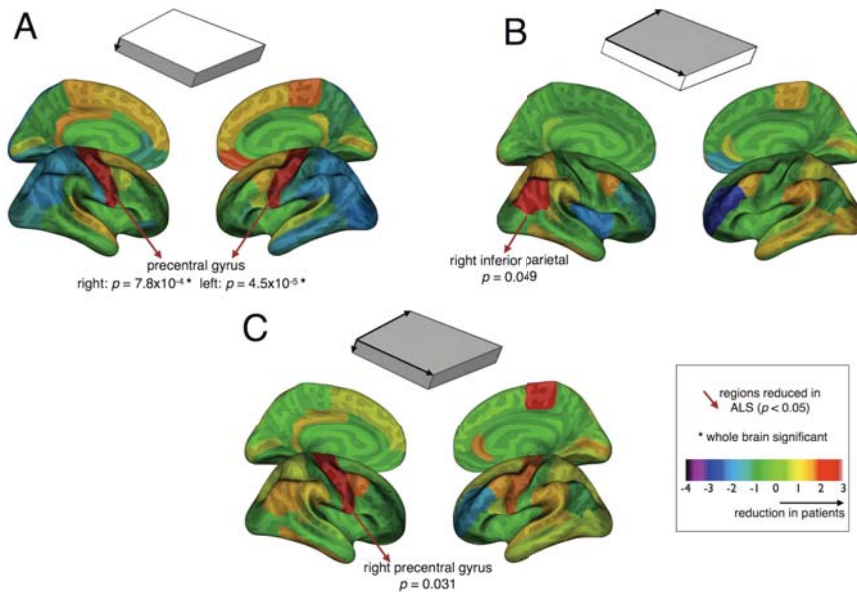


Figure 7.2 Cortical morphology
 Cortical morphology measures (cortical thickness, surface area, and cortical volume) are compared between patients and controls in a region-wise analysis. The t-values per region are plotted on an average brain template. The yellow/red regions show a reduction in patients compared to controls and the blue/purple regions an increase. The regions showing a significant reduction ($p < 0.05$) are indicated as well as the regions reaching whole brain significance. **(A) Cortical thickness** shows significant thinning of the precentral gyrus bilaterally, whole brain significant. **(B) Surface area** comparison between patients and controls shows a different pattern of effects compared to cortical thickness. Only the inferior parietal region (on the right) showed a reduced surface area. **(C) Cortical volume** – as a product of cortical thickness and surface area – shows a reduced volume in the right precentral gyrus. This effect appears to be driven by the cortical thinning found in this region. Cortical thickness and surface area are independent modalities, together composing cortical volume.

Cortical thickness and clinical characteristics

We further explored the individual average cortical thickness in the precentral gyrus (left and right) – corrected for age and whole brain average cortical thickness – in relation to clinical characteristics. As shown in Figure 7.3A these measures largely distinguished patients with ALS from healthy controls ($p = 6.3 \times 10^{-8}$). An explorative receiver operating characteristic curve showed an optimal cutoff value of 2.42 mm average cortical thickness in the precentral gyrus, corresponding to a specificity of 82% and a sensitivity of 84% (Figure 7.3A). It is important to note that this proposed diagnostic accuracy should be

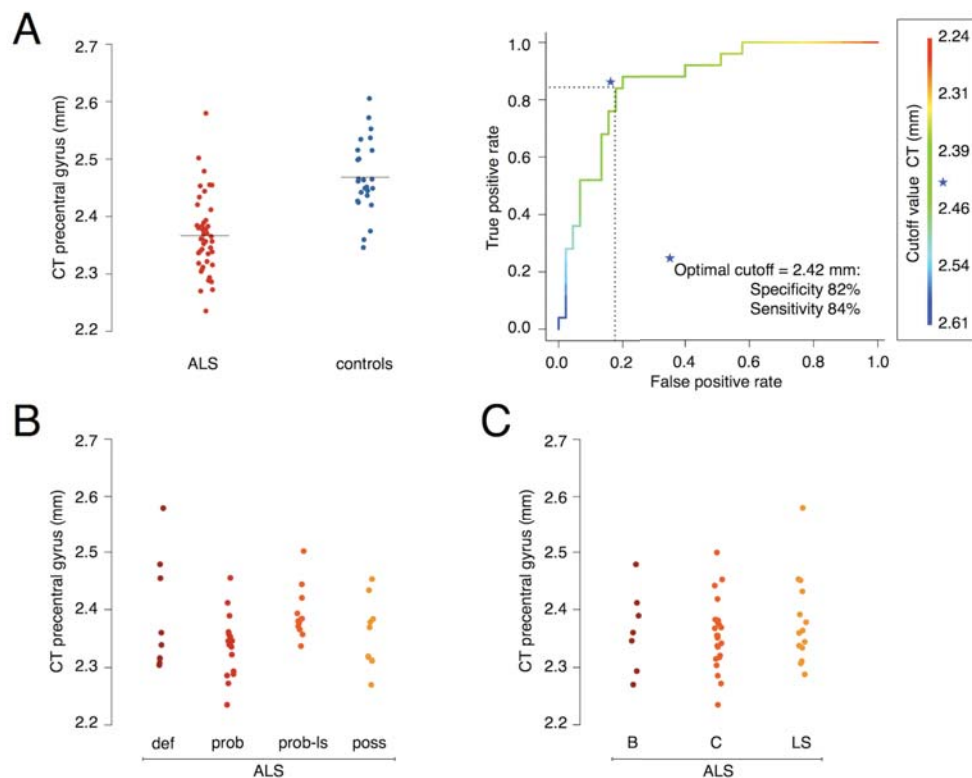


Figure 7.3 Cortical thickness and clinical characteristics

The average of left and right cortical thickness in the precentral gyrus was plotted for each individual participant. **(A)** The patients with ALS (red) demonstrated significant cortical thinning in the precentral gyrus compared to the healthy control subjects (blue) ($p = 6.3 \times 10^{-8}$). **(B)** Comparing the different diagnostic categories, the cortical thinning in the precentral gyrus was consistent in all categories. **(C)** The site of onset was found unrelated to the cortical thickness in the precentral gyrus as well. CT = cortical thickness; def = definite ALS; prob = probable ALS; prob-ls = probable laboratory supported ALS; poss = possible ALS; B = bulbar onset; C = cervical onset; LS = lumbosacral onset.

validated in a (neuromuscular) disease control group; as such these findings are, to a certain extent, over inflated. No significant relation was found for the thickness in the precentral gyrus with diagnostic El Escorial category, ALSFRS-R score, disease duration, site of onset, number of regions showing upper motor neuron signs clinically or bulbar score (Figure 7.3B).

In addition, we examined in a post-hoc analysis the effect of bulbar score on cortical thickness in extra-motor regions, using a GLM. Several temporal regions were found to show cortical thinning related to bulbar involvement: left and right parahippocampal (left $p = 0.046$; right $p = 0.034$), right insula ($p = 0.0027$), right temporal pole ($p = 0.0090$), left entorhinal ($p = 0.022$), left superior temporal ($p = 0.049$), none of these regions were whole brain significant.

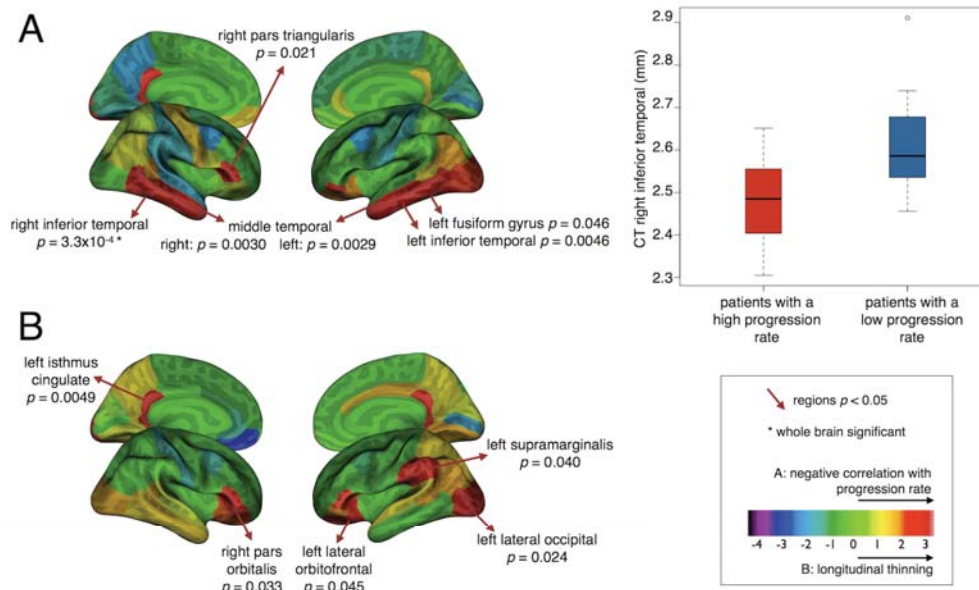


Figure 7.4 Cortical thickness and disease progression

(A) All anatomical regions were analyzed for their relation with disease progression rate. The cortical thickness in the middle and inferior temporal gyrus showed an inverse relation with progression rate. The right inferior temporal gyrus demonstrated whole brain significance, further illustrated by a box plot comparing the cortical thickness in this region between patients with a high disease progression rate (> 0.5 ; $n = 22$) and patients with a low disease progression rate (< 0.5 ; $n = 23$). **(B)** The longitudinal analysis revealed parietal and frontal regions related to the clinical decline in ALS. Despite the nearly symmetrical pattern of effects, none of the regions reached whole brain significance. CT = cortical thickness; progression rate = $48 - \text{ALSFRS-R} / \text{disease duration}$.

Cortical thickness and disease progression

Regional cortical thickness measures were analyzed for their relation with disease progression rate. Bilateral temporal regions (inferior and middle temporal gyrus) showed a significantly negative correlation between cortical thickness and progression rate, indicating that temporal thinning is associated with a faster disease progression (right inferior temporal gyrus $p = 3.3 \times 10^{-4}$; whole brain significant) (Figure 7.4A). Besides temporal regions, a single frontal region, being the right pars triangularis, was found to be associated with disease progression rate ($p = 0.021$) (Figure 7.4A).

Longitudinal analysis was performed in a subset of 20 patients who were able and willing to undergo a follow-up MRI scanning session. The ALSFRS-R-score in these patients had significantly declined during the follow-up (ALSFRS-R-score 41.5 at the first versus 36.8 at the second MRI; $p = 0.002$). Longitudinal cortical thinning was found in the following regions: isthmus cingulate left ($p = 0.0049$), lateral occipital left ($p = 0.024$), pars orbitalis right ($p = 0.033$), supramarginalis left ($p = 0.040$) and lateral orbitofrontal left ($p = 0.045$). None of these regions reached whole brain significance, but the pattern of effects (Figure 7.4B) approached a symmetrical involvement of frontal and parietal regions.



DISCUSSION

The main finding of this unbiased whole brain cortical imaging study was the significant cortical thinning in the precentral gyrus in ALS which was demonstrated using vertex-wise and region-wise approaches. The precentral gyrus is considered the primary motor region and therefore this finding appears to be a radiological correlate of upper motor neuron signs observed clinically in patients with ALS. Another important finding of this study is that patients with ALS, showing relative cortical thinning in temporal regions, were found to have a more progressive disease course.

The strong – and specific – cortical thinning of the precentral gyrus suggests focal degeneration of primary motor areas in ALS. Up till now, studies on grey matter changes have mainly focused on measuring grey matter density as a proxy of cortical volume using voxel based morphometry (VBM) (Ellis et al., 2001; Abrahams et al., 2005; Chang et al., 2005a; Kassubek et al., 2005; Grosskreutz et al., 2006; Agosta et al., 2007; Mezzapesa et al., 2007; Thivard et al., 2007; Grossman et al., 2008; Agosta et al., 2009a; Minnerop et al., 2009; Filippini et al., 2010; Senda et al., 2011). A previous study performed cortical thickness

measures in ALS using a region of interest approach including the precentral, postcentral and lateral occipital cortex (Roccatagliata et al., 2008). This study reported significant cortical thinning in the precentral gyrus in 14 patients with ALS compared with 12 controls. No significant cortical thinning was found in the control regions, which supports our findings. This study simultaneously performed diffusion tensor imaging measures on the corticospinal tract which also showed degenerative changes. As ALS is a motor neuron disease, it is striking that the primary motor areas have not been consistently reported in VBM studies. Divergent results could be due to true neurostructural heterogeneity in ALS, clinical variety in the studied patients, and methodological differences. The present study may have some advantages over previous reports. Firstly, in most grey matter studies magnetic field strength was 1.5T, rather than 3T. Secondly, the sample sizes were limited to a maximum of 26 patients with ALS. Thirdly, volumetric measures with VBM were found to have a lower signal to noise ratio and were relatively insensitive to cortical atrophy localized in brain sulci compared with cortical thickness measures (Hutton et al., 2009). Fourthly, degeneration in the primary motor areas appears to affect primarily thickness and therefore effects on the three-dimensional measure volume can get weakened. These differences could explain the current cortical imaging study showing strong and specific grey matter effects.

Longitudinal measures of cortical thickness, unexpectedly, did not show further cortical thinning of primary motor areas. This could be due to insufficient follow-up time or structural loss was mostly completed by the time of diagnosis. The latter phenomenon has been observed in other neurodegenerative diseases such as Parkinson's disease where 70% to 80% of striatal dopamine neurons are lost before symptoms occur (Wu et al., 2011). Recently, a cortical thickness study in Alzheimer's disease showed cortical thinning was present before the clinical manifestations as we suggest here for ALS (Becker et al., 2011; Dickerson et al., 2011). Cortical thickness measurements in ALS might, therefore, have the potential to be a marker for upper motor neuron involvement in the diagnostic phase and possibly the preclinical phase. Similar to electromyographic examination revealing (subclinical) lower motor neuron involvement, it would be of interest to study the reliability of cortical thickness as a diagnostic upper motor neuron marker including ALS mimics. Previous neurophysiological studies have revealed cortical hyperexcitability preceding clinical symptoms, suggesting ALS might have its origin in the brain (Vucic et al., 2008). Our findings are in support of this 'dying forward' hypothesis in which corticomotoneurons induce anterograde excitotoxic motoneuron degeneration (Eisen and Weber, 2001). An

alternative hypothesis for cortical thinning present before the time of diagnosis could be that a thinner motor cortex is a risk factor for developing ALS. The risk factor hypothesis poses a number of questions for future research, including the genetic background and environmental influences on the morphology of the motor cortex. A previous study on risk factors for Alzheimer's disease demonstrated the apolipoprotein E allele to be associated with the thickness of the entorhinal cortex in children and adolescents (Shaw et al., 2007). This striking relation between genetics and imaging measures demonstrates the feasibility and relevance of this type of research.

No relation was found between our main outcome measure – cortical thinning in the precentral gyrus – and clinical characteristics. This poor consistency between clinical observations and imaging or neurophysiological upper motor neuron markers is known from pathological studies. For example, patients suffering from motor neuron disease without upper motor neuron involvement clinically, can still show degenerative effects in the brain apart from the spinal cord typical of ALS (Ince et al., 2003). As clinical assessment lacks objectivity and can be masked by lower motor neuron signs, an objective upper motor neuron measure would contribute to the diagnostic process. This could explain the observed cortical thinning in patients with (just) possible ALS and the lack of correlation with the El Escorial criteria. In addition, the lack of progressive cortical thinning with advancing disease is in support of the idea that cortical thinning might be present before the time of diagnosis. Another important clinical feature is the presence of bulbar symptoms, which has been associated with more extensive cortical involvement, observed in both pathological studies (Piao et al., 2003) and neuropsychological assessments (Abrahams et al., 1997). We found bilateral temporal thinning (ie parahippocampal) to be related to the presence of bulbar symptoms. This finding corresponds with previous pathological studies in which temporal lesions and/or inclusions have been observed in relation with bulbar region involvement (Piao et al., 2003). As such, our findings appear to be in agreement with *post mortem* studies in ALS.

Cortical thinning in temporal regions was also found to be associated with a rapidly progressive disease course. From epidemiological studies, co-occurrence of frontotemporal dementia and even executive dysfunction is an unfavourable prognostic factor supporting our finding (Elamin et al., 2011). None of our subjects had noticeable cognitive impairment, but in the absence of formal neuropsychological testing it is unclear whether the relative temporal thinning was accompanied by (subclinical) cognitive impairments. Alternatively, this structural heterogeneity with apparent clinical implications could suggest an



endophenotype of ALS demonstrating enhanced vulnerability to neurodegeneration. The symmetrical involvement of neighbouring temporal regions increases the reliability of these findings. Relative cortical thinning in temporal regions might be considered a stratifier for randomizing patients in clinical trials.

Longitudinal analysis did not reveal – whole brain significant – cortical thinning in regions over time. Nevertheless, the pattern of effects (Figure 7.4B) does show a nearly symmetrical involvement of parietal and frontal regions which are part of the default mode network (isthmus cingulate, pars orbitalis, supramarginalis and lateral orbitofrontal) (Greicius et al., 2003). This network is believed to integrate cognitive and emotional processing and has previously been demonstrated to be involved in ALS (Mohammadi et al., 2009). Although speculative, these data could support involvement of the default mode network in the disease course of ALS.

The lack of cognitive testing is a potential weakness. In addition, we did not include patients with ‘mimic disorders’, which we need to differentiate from ALS in clinical practice. However, it is not expected for the most common ALS mimics (cervical myeloradiculopathy, multifocal motor neuropathy) to show significant cortical thinning in primary motor regions. Future research should focus on the external validity of cortical thickness measures for ALS in a study following the STARD statement (<http://www.stard-statement.org/>). The recent international collaboration in the ALS neuroimaging research field could facilitate such steps towards a diagnostic marker (Turner et al., 2011a).

We conclude from whole brain cortical morphology analysis, that cortical thickness of primary motor regions (precentral gyrus) may be a potent marker for central motor neuron degeneration in ALS. Progression of disease does not introduce further cortical degeneration of the motor cortex, although relative cortical thinning in temporal regions was found to be associated with a rapidly progressive disease course.

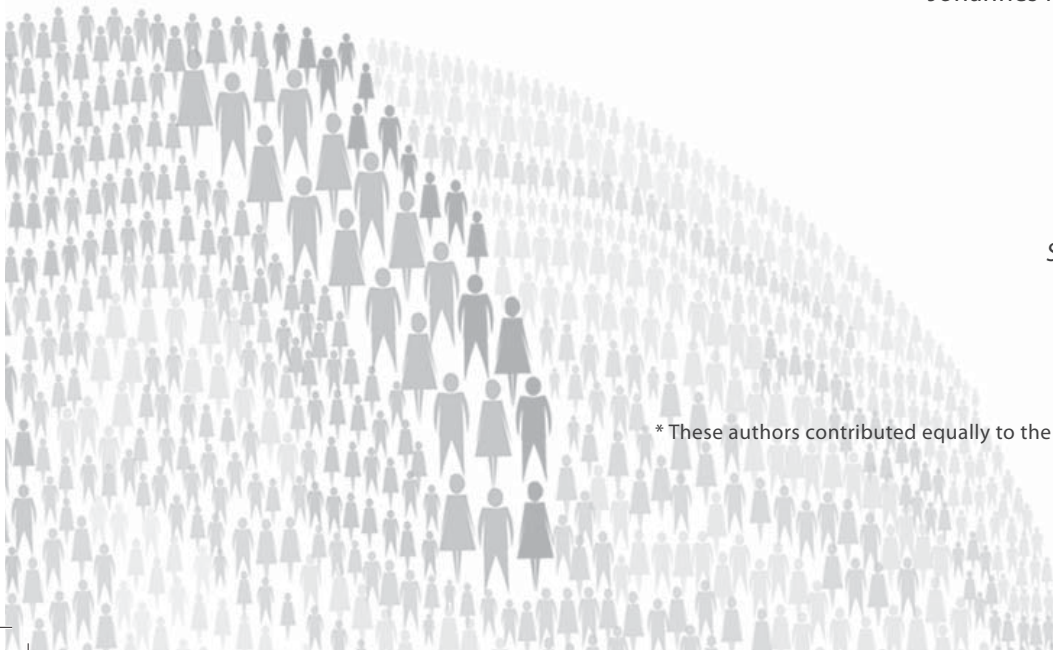
8

Multimodal tract-based analysis in ALS patients at 7T

Daniël Polders*
Esther Verstraete*
René C.W. Mandl
Martijn P. van den Heuvel
Jan H. Veldink
Peter Luijten
Leonard H. van den Berg
Johannes Hoogduin

Submitted

* These authors contributed equally to the manuscript



ABSTRACT

Objective: To explore the value of additional MR contrasts in elucidating the decrease in fractional anisotropy (FA) as has been observed in the corticospinal tracts (CST) of patients with amyotrophic lateral sclerosis (ALS).

Methods: Eleven patients and nine healthy control subjects were scanned at 3T and 7T MRI. Whole brain and tract specific comparison was performed of both diffusion weighted (3T), quantitative T_1 (qT_1), magnetization transfer ratio (MTR) and amide proton transfer weighted (APT_w) imaging (7T).

Results: Whole-brain comparison using histogram analyses showed no significant differences between patients and controls. Measures along the CST showed a significantly reduced FA together with a significantly increased diffusivity perpendicular to the tract direction in patients as compared to controls. In addition, patients showed a small but significant increase in MTR values within the right CST. No significant changes were observed in qT_1 and APT_w values.

Conclusions: Our findings, based on a multimodal approach, revealed that the decrease in FA is most likely caused by an increased diffusivity perpendicular to the CST. This finding, together with the increase in MTR might indicate that an increase of free liquid spins rather than demyelination is the primary cause of observed FA decrease in the CST in patients with ALS.

INTRODUCTION

The upper motor neurons in the brain and the lower motor neurons in the brainstem or spinal cord are connected through the corticospinal tract (CST), the great white matter 'highway' of the motor system. This tract has consistently been found to show degenerative effects in patients with amyotrophic lateral sclerosis (ALS), both in *post mortem* and in imaging studies (Smith, 1960; Turner et al., 2012). Most notably, diffusion tensor imaging (DTI) measures have demonstrated reduced fractional anisotropy (FA) in the CST (Filippini et al., 2010; Agosta et al., 2010a; Verstraete et al., 2010).

The central assumption is that FA reflects white matter integrity, as intact axonal and myelin boundaries will restrict diffusion perpendicular to the white matter fibers and thus increase FA, while loss of white matter integrity will reduce diffusion restriction and thus lower FA (Beaulieu, 2002). However, besides white matter integrity, DTI measures are influenced by multiple factors including: crossing fibers, fiber re-organization, increased membrane permeability, destruction of intracellular compartments, and glial alterations (Beaulieu, 2002; Acosta-Cabronero et al., 2010). Which of these factors are the cause of reduced FA in the CST in ALS, might be elucidated by application of additional magnetic resonance imaging (MRI) contrasts.

Other MRI contrasts which might increase our insight into the degenerative changes within the CST in patients with ALS include quantitative T_1 mapping (qT_1 mapping), magnetization transfer contrast (MTC; expressed using the magnetization transfer ratio, MTR) and chemical exchange saturation transfer (CEST). It has been shown that the image intensities found in qT_1 mapping can be used as a marker for the degree of myelination in disease and during brain development (Glasser and Van Essen, 2011; Paus et al., 2001; Barkovich, 2005). MTR reflects the exchange between water bound to macromolecules and the unbound water fraction. Correlations of MTR with neuronal integrity or the degree of myelination have been shown (Henkelman et al., 2001). For example, patients with multiple sclerosis have been reported to show a global decrease in MTR (Moll et al., 2011). CEST is a relatively new imaging modality, a particular type of magnetization transfer experiment focused on measuring exchange of protons between specific solutes and free water. CEST can be used to study endogenous exchanging protons, such as amide protons resonating at +3.5 ppm from water, resulting in amide proton transfer weighted imaging, APTw imaging (Dula et al., 2011). Amide protons are abundantly present in protein backbones and peptides, and APTw imaging is expected to reflect physiological changes in this specific



proton pool in case of disease. It has been suggested that APTw imaging may be sensitive for myelination (Dula et al., 2011; Mougín et al., 2010), and it would be of interest to see if APT measurements can contribute to the further understanding of ALS pathology.

In this study we investigated whether measures of qT_1 , MTR and APTw imaging, applied at ultra-high field (7 Tesla), might help to disentangle which factors contribute to the FA reduction in the CST of patients with ALS and provide more detailed *in vivo* tissue characterization.

METHODS

Subjects

Eleven patients with ALS (mean age 55.5 years; range 35–71; 8 males and 3 females) and nine age and gender matched healthy controls (mean age 54.2 years; range 36–67; 7 males and 2 females) were included in this study. Patients, diagnosed according to the El Escorial criteria, were recruited from the ALS outpatient clinic of the University Medical Center Utrecht, excluding subjects with a history of brain injury, epilepsy, psychiatric illness and other neurodegenerative diseases. Demographic and clinical characteristics are provided in Table 8.1, including the functional impairment as measured using the ALSFRS-R and the subscores for bulbar (B score, items 1, 2 and 3), upper limb (UL score, items 4 and 5) and lower limb (LL score, items 8 and 9) functioning. The local Medical Ethics Committee for Research in Humans approved this study and written informed consent was obtained from all subjects, in concordance with the Declaration of Helsinki.

MRI hardware

DTI data was acquired on a 3T whole body MR scanner (Philips Medical Systems, Best, The Netherlands). The body coil and 8 channel head coil (Nova Medical Inc., Burlington, MA, USA) were used for signal transmission and reception respectively.

Quantitative T_1 , MTR, and APTw imaging measurements were performed at a 7T whole body MR scanner (Philips Medical Systems, Cleveland, USA). A quadrature birdcage transmit head coil (Nova Medical Inc., Burlington, MA, USA) was used in combination with a receive-only coil (Nova Medical Inc., Burlington, MA, USA). A B_0 mapping sequence was included, covering the brain volume. This was then used to optimize the shim settings up to the third order.

Table 8.1 Demographic and clinical characteristics of the patients

	Gender	Age (years)	Site of onset	Time to diagnosis (months)	Disease duration (months)	EE	ALSFRS-R	PR	B score	UL score	LL score
1	F	65	LL	11	15	prob	39	0.6	11	6	3
2	M	51	LL	22	33	prob	41	0.2	12	8	3
3	M	47	UL	2	16	poss	40	0.5	11	3	7
4	M	35	UL	9	45	prob	31	0.4	11	3	2
5	M	39	UL	2	42	poss	38	0.2	12	3	6
6	M	58	LL	11	25	prob-LS	44	0.2	12	8	5
7	M	63	LL	12	25	prob	42	0.2	12	7	3
8	F	61	UL	12	18	def	38	0.6	9	5	7
9	F	60	UL	11	21	prob	46	0.1	12	6	8
10	M	61	UL	10	15	prob	40	0.5	12	6	5
11	M	71	UL	3	17	prob-LS	31	1.0	12	2	4
		55.5 (11.2)		9.5 (5.8)	24.7 (10.8)		39.1 (4.7)	0.4 (0.3)			

F = female; M = male; B = bulbar; UL = upper limbs; LL = lower limbs; EE = El Escorial category; poss = possible; prob-LS = probable laboratory supported; prob = probable; def = definite; ALSFRS-R = revised ALS functional rating scale; PR = progression rate (48 – ALSFRS-R / disease duration).
 At the bottom row of the table mean values and standard deviations (between brackets) are provided.



DTI and fiber tracking

DTI measurements were acquired using methods described earlier (Verstraete et al., 2010; Verstraete et al., 2011). Calculation of the DTI parameters was performed using the ExploreDTI toolbox (Polders et al., 2011). After brain extraction, DTI volumes were corrected for residual eddy current and motion artifacts by aligning the diffusion weighted images to the $b = 0$ s/m² image using 3D affine registration and reorientation of the B-matrix (Leemans and Jones, 2009). Tensor values were estimated using the RESTORE algorithm (Chang et al., 2005b). Finally, DTI-based parameter volumes were transformed to MNI-space. We further investigate the effects in FA by looking at the changes in longitudinal diffusivity (D_{long}) and transversal diffusivity (D_{trans}).

Fiber streamlines were selected by placing seed regions of interest (ROIs) in both the left or right motor tract at the level of the pons. Fiber tracking was then performed by deterministic streamline fiber tractography (Basser et al., 2000) from 125 seed points distributed homogeneously over each voxel in the seed ROI. The following settings for streamline reconstruction were applied: minimal FA = 0.2, maximal angle = 20°, streamline step size = 1 mm, minimal/maximal fiber length = 40/500 mm. Additional selection criteria were placed as an inclusion-ROI at the level of the primary motor cortex to select those streamlines that connected both the pons level and cortical level ROIs. Two exclusion-ROIs were placed to prevent inter-hemispheric crossover and connections to the cerebellum (Figure 8.1).

T₁ mapping

A multi-slice T₁ mapping sequence was acquired (Ordidge et al., 1990; Clare and Jezzard, 2001). In this T₁ mapping approach, after an inversion pulse, all slices in the volume are acquired successively using slice-selective 90° excitations and EPI read-outs. During the following repetitions, the slice ordering is shifted, so all slices are acquired at different inversion times. A slice-shift of 2 slices was applied, so that in 23 repetitions, all 46 slices were sampled at 23 different time points after inversion, allowing for robust and precise estimation of the longitudinal relaxation time.

A single-shot EPI sequence forms the basis of the T₁ mapping method. The acquired and reconstructed matrix covered a field of view (FOV) of 224 x 224 mm. The 46 slices had a thickness of 1.5 mm with a 0.5 mm slice-gap, covering 91.5 mm. The phase encoding direction was set to be anterior-posterior, with the fat-shift direction towards the anterior. The sequence was accelerated using a SENSE acceleration factor of 3.6 in the phase encoding

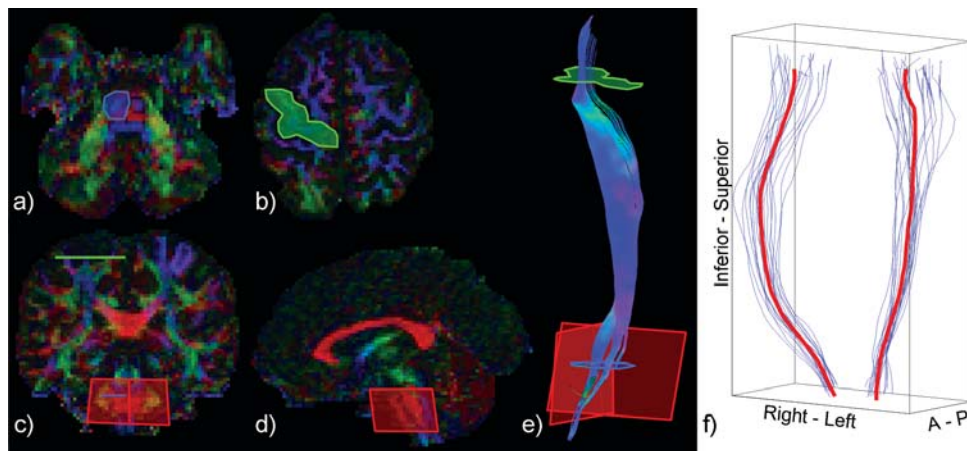


Figure 8.1 CST selection procedure

This figure shows the location of the regions of interest (ROIs) for the selection of the CST fiber bundles. (a) At the level of the pons a seed region (bleu encircled) was placed on an axial slice, the fiber direction was indicated by color. From this ROI the fiber tracking was initiated. (b) Another ROI (green) was placed directly on the primary motor cortex (precentral gyrus) selecting all fibers both crossing the pons and the motor cortex. (c) To exclude fibers connecting the cerebellum, an ROI (red) was placed in the coronal plane, deselecting all fibers crossing this ROI. (d) A second, excluding ROI (red) was placed in the sagittal plane to deselect fibers connecting the other hemisphere. (e) This procedure resulted in a number of fibers, together forming a reconstruction of the CST. (f) For each subject an average fiber curve (blue) was calculated, resulting in two group-average curves for the left and right CST (red).

direction, a half-scan factor of 0.609, resulting in an EPI factor of 65. Fat suppression was accomplished by spectral inversion of the fat signal (SPIR) before each slice excitation. TR and TE were 10 s and 8.3 ms, respectively. Inversion was achieved by a non-selective adiabatic inversion. Inversion times for odd slices ranged from 20 ms to 5,036 ms, and even slices from 134 to 5,150 ms. The total scan duration for this sequence was 4 minutes and 10 seconds.

The longitudinal relaxation time T_1 is a central MR parameter that reflects the capability of the spin-lattice to relax longitudinal magnetization back to equilibrium. In normal tissue, the speed of relaxation is directly dependent on the amount and nature of interactions of the bulk water with the surrounding lattice. In free water such as CSF (around 4,500 ms at 7T), T_1 is long, and in structured tissue such as myelinated white matter, T_1 is short (around 1,100 ms at 7T). By quantitatively determining the longitudinal relaxation time, as



opposed to weighting an image with an unknown amount of T_1 effect, we can discriminate small changes in T_1 , and thus identify small changes due to pathology (Deoni, 2010). To calculate the T_1 on a voxel-by-voxel basis, the signal intensity after inversion of the magnetization can be sampled at different time points. This is called the inversion curve, and in this paper, it was modeled by the following expression:

$$I(t) = I_0 \cdot \left(1 - 2 \cdot e^{(-t/T_1)} + e^{(-TR/T_1)} \right)$$

Where $I(t)$ is the measured signal intensity at inversion time t , I_0 is the fitted voxel intensity at the fully relaxed state, T_1 is the longitudinal relaxation time, and TR is the repetition time of the sequence. The difference between the data and this expression was minimized using a Levenberg-Marquardt optimization within the following parameter space: T_1 : [0 – 10,000] ms, I_0 : [0 – 10 x I_{highest}], where I_{highest} is the highest signal intensity of the sampled curve.

MTR and APTw imaging

MTR and APTw imaging were conducted using the pulsed steady state method as previously described (Jones et al., 2012). One unsaturated and 17 saturated volumes with different saturation frequencies ranging from -4.03 ppm to +4.03 ppm were acquired using a segmented 3-D EPI readout scheme. Each volume was acquired in ~190 repetitions. Saturation was accomplished by short off resonance saturation pulses before each excitation pulse, building up a steady state while acquiring the outer regions of k-space. The saturation pulse had a duration of 50 ms at 1.8 μ T nominal B1 amplitude. Excitation was achieved using an 18.5° binomial pulse for water only excitation. The scan was accelerated using a SENSE acceleration factor of 2.5 in the phase encoding direction (AP), leading to an EPI factor of 15. The acquired resolution (2.00 x 2.13 x 2.00 mm) was reconstructed to 2 mm³ isotropic and covered an FOV of 224 x 224 x 100 mm³.

Magnetization transfer ratio (MTR)

Magnetization transfer imaging is a technique that probes the macro-molecular environment of bulk water protons by assessing the amount of magnetization transfer from the bound water to the bulk water pool. This is done in a saturation transfer experiment, where the amount of signal reduction directly reflects the amount of bound water molecules (and therefore macromolecular content). To compare the amount of magnetization transfer between subjects, the saturation effect is expressed in the MTR, which quantifies the

amount of signal suppression due to magnetization transfer. The amount of magnetization transfer contrast is directly dependent on the amount of myelination of the tissue, with areas that are strongly myelinated showing large MTR values such as the corpus callosum, while deep white matter, sub-cortical white matter u-fibers and grey matter areas displaying decreasing MTR values (Tofts et al., 2003).

Because the off-resonance frequency is relatively close to the water resonance, it is expected that direct water saturation has a significant effect on the total observed saturation. To correct for this, we fit and remove a Lorentzian lineshape from the measured saturation curves as follows.

In our experiments, the saturated volumes were normalized to the unsaturated volume, and corrected for residual B_0 offsets and direct water saturation by fitting the middle offset frequencies (i.e.: ± 150 , ± 75 , and 0 Hz) to describe a Lorentz lineshape:

$$L(A, w, f_{sat}) = 1 - A \left(\frac{(w)^2}{(w)^2 + 4(f_0 - f_{sat})^2} \right)$$

Where A is the fitted amplitude of the Lorentz peak, w is the fitted line width at half minimum, f_0 is the fitted peak center which corresponds to the water resonance frequency for that voxel, and f_{sat} is the off resonance frequency of the saturation pulse. The signal intensities at the frequencies of interest were then found by spline interpolation of the acquired data. For each voxel, the MTR at a given saturation frequency f_{sat} was calculated as follows:

$$MTR(f_{sat}) = 1 - \frac{S_{sat}(f_{sat})}{S_0} - L(f_{sat})$$

Where $S(f_{sat})$ is the signal intensity with a saturation pulse at ~ 1200 Hz off resonance, normalized to the unsaturated image S_0 , and $L(f_{sat})$ is the fitted Lorentz peak height for that frequency.

Amide proton transfer weighted (APT_w) imaging

Another, more specific, mechanism for measuring magnetization exchange is by sensitizing for chemical exchange using a method called CEST. This method has gained much traction in the last few years, because it offers a fundamental insight in the chemical nature of the tissue, probing the concentration and exchange rates of endogenous amide protons (van Zijl and Yadav, 2011). CEST measurements are performed by repeating MT measurement



with varying off-set frequencies of the saturation pulse. This results in a sampling of the Z-spectra, which is roughly symmetric around the water resonance, except for those frequencies where the exchanging protons resonate. By means of asymmetry analysis, i.e. taking the difference between saturated image at the resonance frequency of interest and its opposite counterpart frequency, chemical transfer effects can be distinguished from the conventional MT effects. In this work, we focus on the exchanging amide protons, which resonate at +3.5 ppm from the water resonance, and the resulting images are called APTw images. For many applications amide protons are of interest, due to their increased natural abundance in pathology and appropriate exchange rates for saturation experiments (Zhou et al., 2003). In our experiments, APTw volumes were calculated by calculating the difference in MTR at +3.5 ppm and -3.5 ppm as follows:

$$APT_w = MTR_{asymmetry} (\pm 3.5 \text{ ppm}) = MTR (+ 3.5 \text{ ppm}) - MTR (- 3.5 \text{ ppm})$$

Quantitative comparison

For quantitative comparison, qT_1 , MTR, and APTw volumes were registered to each subjects' FA map by rigid body registration using a normalized mutual information cost function and tri-linear interpolation. For the MTR based volumes, the 4.03 ppm saturated image was used in the registration procedure and the resulting transformation matrix was used for all following parameter maps.

Averaged normalized histograms were compared to evaluate the MR contrasts between patients and controls on a whole brain level. The histograms were calculated over all voxels in the brain volume, excluding those that were obviously affected by signal voids due to air-tissue boundaries, such as near the nasal cavities and ear-canals, as observed in EPI based methods. Included in these histograms were grey matter and the ventricles, so a contribution of cerebrospinal fluid (CSF) is to be expected. After normalizing to their total count, the average histograms for patients and controls were calculated and plotted with the accompanying standard deviations.

The goal of the tract-based analysis was to compare quantitative MRI measures along the CST, while allowing for inter-subject variation of each 3D trajectory. Following the method described in (Mandl et al., 2010), each subject's reconstructed CST (consisting of a collection of ~150 streamline trajectories) was averaged to a single curve. The values of the different MRI contrasts of interest of the voxels crossed by the fiber trajectories were

mapped to the nearest corresponding point on the curve. As a result, each subject's curve reflects the averaged values along that curve. Similarly, the group average curves were calculated by taking the average curve over all subjects. The resulting two averaged curves correspond to the group-average left and right CST. We report the median values (\pm interquartile ranges) for each MR contrast (FA, D_{long} , D_{trans} , qT_1 , MT, and APTw) along the CST.

Statistical analysis

The entire brain volumes were compared between patients and controls by testing for difference between the mean values for each subject, using a two-tailed t-test. The multiple measures along the left and right CST sections were compared, for each modality, between patients and controls using a repeated measurements analysis by a linear mixed-effects model with maximum likelihood estimation (ML), including group assignment (patient or healthy control) as a factor and gender as a covariate. Additionally, for each separate point along the group-averaged tract, the measures in patients and controls were compared using a Mann–Whitney–Wilcoxon or Rank test. The effect size was calculated by calculating the difference between the medians. For all analyses, a statistical threshold of $p \leq 0.05$ was considered statistically significant.



RESULTS

Whole brain histogram analysis

At the whole brain level, based on histogram analysis, none of the MR contrasts revealed any significant differences between patients and controls. Figure 8.2 shows the whole brain histograms for each MR contrast, with an example slice of a single subject. A difference in the MTR peak locations for patients (0.19) and controls (0.15) can be observed. However, the whole brain average MT values did not show significant differences between patients and controls.

Corticospinal tract measures

We report the values of several MR contrasts measured along the fiber tractography streamlines of the CST. Because the coverage of the DTI volume is larger than that of the other contrasts, we focus here on the region of the CST where all acquired volumes

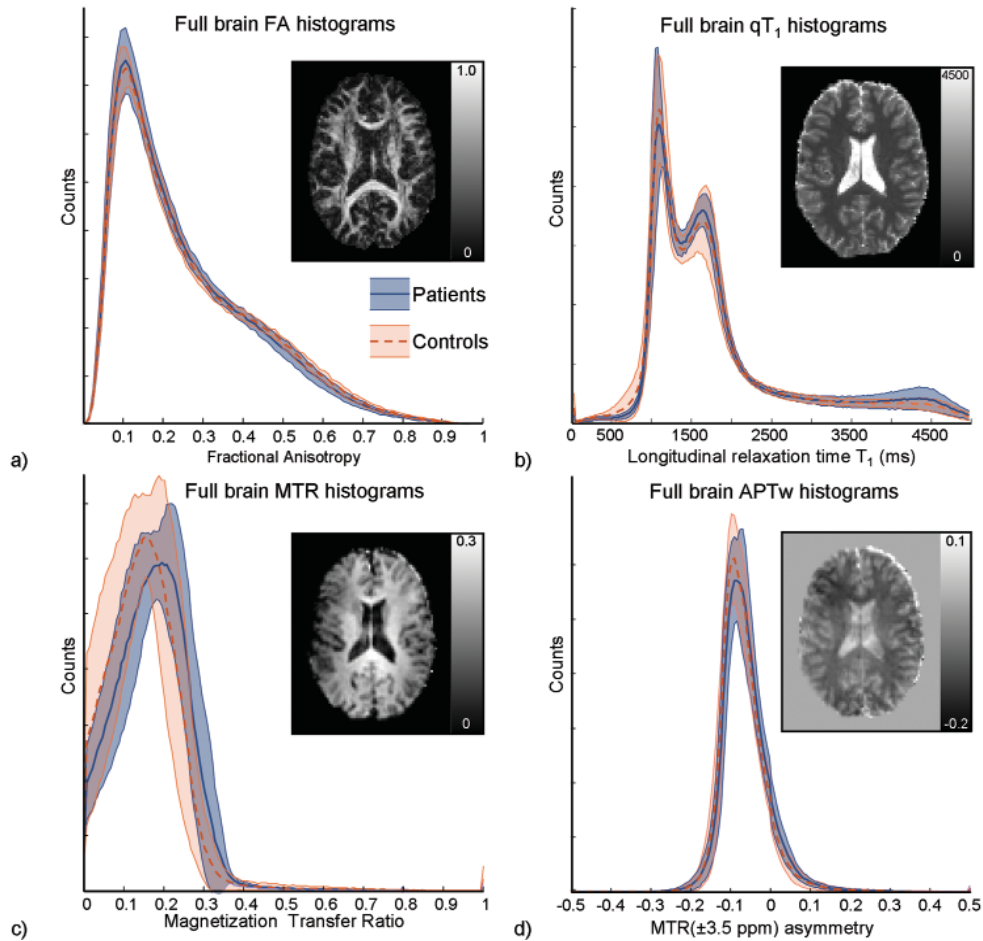


Figure 8.2 Average whole brain histograms for FA, qT_1 , MTR, and APTw imaging

Blue and pink indicate the mean with standard deviations for patients and controls respectively. Each histogram includes an example slice of a single subject. No significant differences were found in these whole brain analyses.

overlapped. In the presented results, we show the median values over the left and right group averaged CST each consisting of 41 points, spanning roughly 8 cm in the feet-head direction.

The tract specific measures along the CST revealed, a significantly reduced FA in patients compared to controls along the right CST ($p = 0.01$) and a trend-like reduced FA along the left CST ($p = 0.09$). Figure 8.3a shows the FA measures for patients and controls along the tract, significantly reduced FA was found both in the subcortical region (right) and

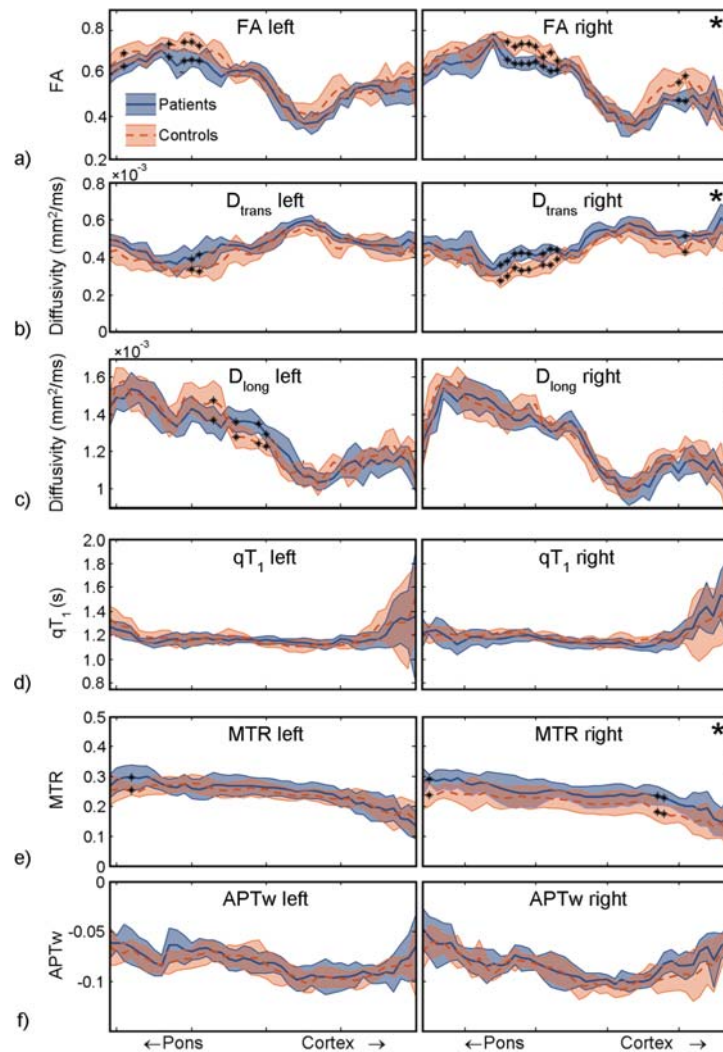


Figure 8.3 Quantitative MR measures along the CST

MR measures along the tract were sampled every 2 mm and the group results for patients (blue) and controls (red) were plotted for the left and right motor tracts. The median values and inter-quartile ranges are shown. Measurements along the tract highlighted with a * showed significant differences (Mann–Whitney–Wilcoxon test, $p < 0.05$, two tailed). The plots marked with a * in the upper right corner showed significant differences over the complete CST section. (a) FA values were significantly lower in patients compared to controls along the right CST, however, also the left CST shows a subtrajectory with significantly reduced FA measures. (b) D_{trans} showed significantly increased in patients compared to controls along the right CST similar to the changes in FA. (c) D_{long} showed no consistent differences between patients and controls. (d) qT_1 showed no significant differences between patients and controls. The measures in the cortical grey matter (right side of the plot) showed more variation compared to the white matter trajectory as was expected. (e) MTR, showed a significant increase along the right CST in with patients compared to controls. (f) APTw imaging, showed no significant changes between patients and controls.

more caudally (posterior limb of the internal capsule, left and right). Diffusivity transverse to the largest direction of diffusion, D_{trans} shows a significant increase along the right CST ($p = 0.04$). The measures over the left CST are not significantly different in patients compared to controls ($p = 0.15$), similar to the FA results (Figure 8.3b). Longitudinal diffusivity, D_{long} , measures are not significantly different along the CST (left $p = 0.37$; right $p = 0.46$), indicating that the change in FA originates from an increased D_{trans} in the patient group (Figure 8.3c).

No significant changes in qT_1 (Figure 8.3d) values were found (left $p = 0.58$; right $p = 0.34$). The MTR measures (Figure 8.3e) demonstrated a significant increase in patients compared to controls along the right CST ($p = 0.05$), again the changes in the left CST were not significant ($p = 0.24$). APTw scores along the averaged fiber bundles, showed no significant changes between patients and controls (left $p = 0.50$; right $p = 0.21$) (Figure 8.3f).

We did not find a significant correlation using Pearson's correlation testing between imaging measures (averaged along the CST) and clinical markers (ALSFRS-R, progression rate [48 - ALSFRS-R / disease duration] and disease duration).

DISCUSSION

In this study, quantitative MR parameters were compared between ALS patients and age-matched healthy controls, both in a 'whole brain' analysis, as well as, specifically along the CST. We found a significant decrease in FA along the right CST, consistent with previous studies (Filippini et al., 2010; Verstraete et al., 2010; van der Graaff et al., 2011). Increased diffusivity perpendicular to the CST (D_{trans}) was found underlying the decrease in FA. Additionally, exploratory data, acquired on ultra-high field MRI, showed a significant increase in MTR in the right CST in the patient group. The other MRI contrasts, qT_1 and APTw imaging, did not reveal significant changes.

We observed a reduced FA both subcortical as well as in the posterior limb of the capsula interna, which is consistent with previous findings (Verstraete et al., 2010; van der Graaff et al., 2011). To gain more insight in the underlying changes in the brain tissue causing reduced FA in the CST, other diffusion-based parameters were assessed. Decomposing the FA values into the longitudinal and transverse diffusivities (parallel and perpendicular) to the CST direction revealed a significantly increased D_{trans} and no significant changes in D_{long} in patients compared to controls. An increase in the observed D_{trans} indicates a loss of diffusion restriction perpendicular to the main direction of diffusion. Diffusivity

changes were asymmetrical with predominant changes within the right CST, which has been repeatedly observed in ALS (Cosottini et al., 2012; Agosta et al., 2007; Kassubek et al., 2005). It has been suggested that the right hemisphere is more vulnerable to the neurodegenerative process (Chen and Ma, 2010).

MTR is considered an indicator for the capacity of water bound to macromolecules in (nervous) tissue to exchange magnetization with unbound water molecules (Mougin et al., 2010). In white matter tissue, MTR is mainly determined by the myelin content and, to a lesser extent, the number of axons or gliosis (Stanisz et al., 1999). Demyelination has been demonstrated to cause a reduced MTR, however, in this study we found a significant increase of MTR in the right CST. This finding is different from what we expected and from what has been previously reported (Kato et al., 1997; Tanabe et al., 1998), therefore we need to interpret these data cautiously. As illustrated by Figure 8.3c the data shows largely overlapping variation and the effect size is small. In addition, there is relatively little experience with MTR data on ultra-high field, and it has been suggested that MTR in white matter is more variable at 7T compared to 3T (Mougin et al., 2010). However, since MTR is sensitive for the magnetization transfer between macromolecular and liquid protons, an increase of the liquid fraction in tissue has the potential to increase MTR (Henkelman et al., 2001). This hypothesis is supported by the finding of increased transverse diffusion, which might also be caused by an increased liquid fraction. Another potential cause of increased MTR in ALS might be the accumulation of pathological protein aggregates (macromolecules) – as is well known to occur in ALS. The correspondence of predominant changes in the right CST for diffusivity characteristics and MTR measures increases the credibility of our findings. The combination of decreased FA and increased MTR in the CST of patients is remarkable since in general a decreased FA (e.g. due to demyelination) is related to a decreased MTR. Therefore, we further assessed the relationship between FA and MTR – in a post-hoc analysis – by assessing the correlation between these two parameters within individual subjects. This analysis confirmed a positive correlation between these two modalities, indicating that at a group level it is unlikely that demyelination is the primary cause of reduced FA in patients. Summarizing, an increased tissue liquid fraction, potentially in combination with protein accumulation, might have caused an overall increase of MTR values in patients (da Rocha et al., 2012). These effects apparently outweigh some degree of demyelination, which is supported by findings in *post mortem* studies in ALS (Iwanaga et al., 1997; Ikeda et al., 2002). Based on these data, pathological changes which lead to an increase in the liquid fraction such as proliferation



of glial cells and extracellular matrix expansion (Hughes, 1982; Philips and Robberecht, 2011; Ince et al., 2011) are more likely to be the primary cause of reduced FA within the CST of patients with ALS.

CEST and quantitative T_1 imaging measurements did not show significant differences between patients and controls along the CST. APTw imaging – a variant of CEST – at high field has been suggested as a noninvasive biomarker of white matter pathology, potentially providing complementary information to other MRI methods in current clinical use (van Zijl and Yadav, 2011). Grey matter is known to show lower APTw contrast compared to white matter, potentially due to fewer membrane-associated (extracellular, cytosolic, and transmembrane) proteins such as those found in myelin (Dula et al., 2011). However, for ALS, APTw imaging has not shown the same sensitivity for white matter pathology as FA. More research on the effects of brain tissue pathology and the APTw contrasts is needed to further elucidate its dynamics in health and disease. No changes in T_1 contrast were found, which is contrary to previously published results showing that T_1 weighted imaging with MTC enhancement allowed for the visualization of CST lesions (da Rocha et al., 2004; Carrara et al., 2012). T_1 contrast has also shown to be related to the degree of myelination and the amount of bulk water (Fatouros and Marmarou, 1999). For example, lesions in MS showed shortened T_1 values indicating plaque formation while global histogram analysis indicated elongated T_1 values, pointing at diffuse demyelination (Neema et al., 2007; Vrenken et al., 2006). To rule out effects in qT_1 that might have been missed in the tract specific analysis due to misregistration of the qT_1 parameter maps to their corresponding FA volumes, the whole brain volumes were compared using a post-hoc VBM analysis to highlight significant differences (data not shown). This additional analysis did not yield any significant results. Together with our results in MTR, the lack of effects in APTw and qT_1 imaging might lend further support that demyelination is not the main cause of FA decrease found in the CST of ALS patients (Philips and Robberecht, 2011; Ince et al., 2011).

Given the exploratory nature of this study, there are limitations to which these results need to be interpreted. First, the sample size of patients and controls employed in this study is small and the variation of the measurements between subjects is relatively large, hampering the detection of subtle differences. Second, the modeling of MTR based methods, especially the calculation of APTw images is still a very active field of research, and it is expected that future developments will improve both the sensitivity and reproducibility of this new method and that more factors influencing or contributing to this MR contrast will be elucidated.

To conclude, we explored multiple MR contrasts at ultra-high field in relation to FA reduction in the CST of patients with ALS. MR contrasts were selected based on their sensitivity to neuronal loss and/or demyelination of white matter. A reduced FA in the CST of patients with ALS was confirmed, and further showed to originate from an increase in D_{trans} . In addition, we found an increase in MTR in the right CST, which makes demyelination as cause of reduced FA less likely. Increased magnetization transfer due to more free liquid spins is in accordance with the observed changes in diffusivity, particularly an increase in D_{trans} . The other contrasts, qT_1 and APTw imaging, did not reveal any significant changes in ALS. Future studies are needed to validate our findings in larger groups of patients and further advances in both MR technology and neuroscience are needed to increase insights into the dynamics of these MR contrasts in health and disease.

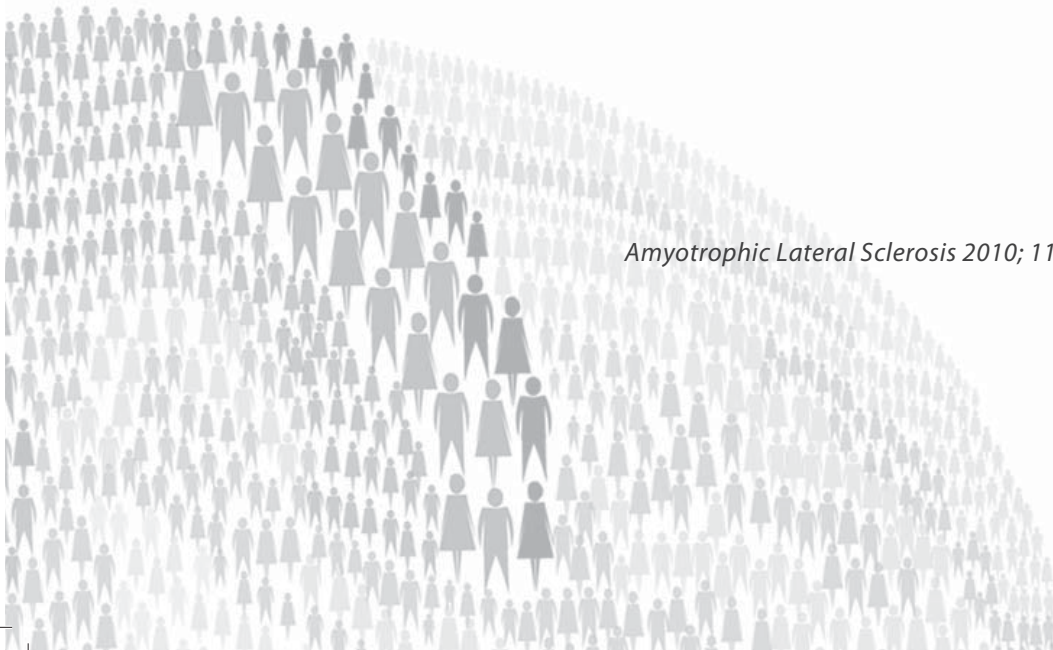


9

No evidence of microbleeds in ALS patients at 7 Tesla MRI

Esther Verstraete
Geert-Jan Biessels
Martijn P. van den Heuvel
Fredy Visser
Peter R. Luijten
Leonard H. van den Berg

Amyotrophic Lateral Sclerosis 2010; 11(6): 555-7



ABSTRACT

There have been several reports about disruption of the blood-spinal cord barrier and blood-brain barrier in SOD1 mutant mice. Pathologically microbleeds and hemosiderine deposits were found. We investigated patients with ALS for the occurrence of cerebral microbleeds with 7 Tesla MRI. Twelve patients with ALS and twelve age and sex matched healthy controls were studied. We performed T2*-weighted imaging which enables whole-brain *in vivo* detection of cerebral microbleeds and hemosiderin deposits in humans. No microbleeds were found in patients with ALS.

INTRODUCTION

The pathogenesis of motor neuron degeneration in ALS is largely unknown. There have been several reports about disruption of the blood-spinal cord barrier (BSCB) and blood-brain barrier (BBB) in SOD1 mutant mice, a disease model for ALS (Garbuzova-Davis et al., 2007; Zhong et al., 2008; Nicaise et al., 2009). These mice were reported to have a reduction of tight junction proteins, causing microbleeds and release of neurotoxic haemoglobin-derived products, with consecutive reduction in microcirculation. In a later phase inflammatory changes occur, but these are apparently not the cause of BSCB or BBB disruption (Zhong et al., 2008). However, in patients with ALS the occurrence of microbleeds has not been explicitly reported, as conventional neuroimaging techniques are not sensitive enough to detect these kind of small microbleeds.

Ultra-high field neuroimaging techniques now enable whole-brain *in vivo* detection of cerebral microbleeds and hemosiderin deposits in humans with increased sensitivity compared to low field neuroimaging. Using 7 Tesla MR these microbleeds can be depicted as areas of signal loss on a T2*-weighted image (Greenberg et al., 2009). Here we report on a study examining the the presence of cerebral microbleeds with T2*-weighted imaging on 7 Tesla MR.

MATERIAL AND METHODS

Twelve patients with ALS (mean age and standard deviation: 48.8 ± 10.6 years) and 12 age- and sexmatched healthy controls (age: 49.6 ± 10.5 years) participated in this study. Patients were recruited from the ALS outpatient clinic of the University Medical Center Utrecht, The Netherlands and were diagnosed with probable laboratory-supported (three patients), probable (eight patients) or definite (one patient) ALS according to the El Escorial criteria. Since the microbleeds were reported as an early phenomenon in the ALS mice we predominantly included patients who were only recently diagnosed. Nine of the 12 patients were examined within six months after diagnosis. The average disease duration was 14.3 months (four within one year after onset of weakness; six between 12 and 18 months; and two longer than 18 months after onset). To minimize age and non-ALS related small vessel changes we selected patients younger than 65 years of age. Subjects with a history of brain injury, epilepsy, vascular risk factors, psychiatric illness and other systemic diseases that affect brain function were excluded. Clinical status was evaluated with the revised ALS Functional Rating Scale (ALSFRS-R). All subjects gave written consent as approved by



the medical ethics committee for research in humans of the University Medical Center Utrecht, The Netherlands.

Whole brain T2*-weighted imaging was obtained using a volume transmit and 16-channel receive head coil on a 7T MRI scanner (Philips Healthcare). The T2*-weighted imaging sequence parameters were: TR 20 ms; echo time 1 (TE1) 2,4 ms; TE2 15 ms; flip angle 20; reconstructed voxel size 0.35 x 0.35 x 0.30 mm. The acquisition time was 8.58 min. To obtain optimal arterial inflow images with threedimensional flow compensation at TE1, the echo was sampled at partial Fourier. This did not allow for phase reconstruction for both echoes even though TE2 was sampled at full Fourier. After post-processing 12 to 20 minimal intensity projections (MIP) slabs were generated.

Cerebral microbleeds were identified as hypointensities on MIP slabs of T2*-weighted scans at the acquired echo times (Figure 9.1) (Greenberg et al., 2009). Signals from vessel flow voids, mineralization of the basal ganglia, or cranial sinuses were excluded. For each subject the MIP slabs were assessed by two blinded investigators (EV and GJB).

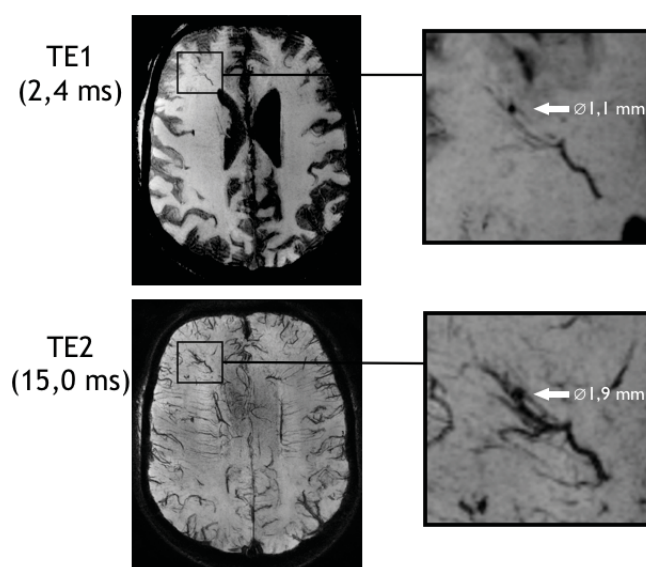


Figure 9.1 Hypointensity suggestive for cerebral microbleed

Minimal intensity projection of T2*-weighted scans at TE1 (2,4 ms) and TE2 (15 ms), showing a microbleed in the right frontal lobe as observed in one of the healthy controls. The hypointensity shows typical enlargement at TE2 compared to TE1.

RESULTS

The ALS patients had an average ALSFRS-R score of 39.5 (range 30–46). No microbleeds were detected in any of the ALS patients. Two healthy individuals were found to have a solitary microbleed marking the potential of finding microbleeds with 7T T2*-weighted imaging.

DISCUSSION

The presence of cerebral microbleeds as an indicator of BBB dysfunction was studied in a cohort of predominantly recently diagnosed and young ALS patients. In contrast with the findings in ALS mice, no microbleeds or hemosiderin deposits were detected in our group of sporadic ALS patients using sensitive high-field 7T T2*-weighted imaging.

The mice were studied in a preclinical stage and the patients in a clinical manifest stage, but with the absence of cerebral microbleeds in our study this methodological difference, however, is irrelevant since microbleeds remain detectable for years after they have occurred (Greenberg et al., 2009).

Cerebral microbleeds have been reported in association with small vessel brain disease e.g. hypertension (Greenberg et al., 2009; Won Seo et al., 2007), but also in neurodegenerative diseases, especially Alzheimer's disease (Staekenborg et al., 2009; Kirsch et al., 2009). In this context they have been suggested as a source for the increased brain iron noted in these patients (Johnstone and Milward, 2010). Increasing age seems to be an important factor in developing microbleeds as was also observed in our cohort since the two individuals with a microbleed were both older than sixty years of age (Greenberg et al., 2009).

We selected the more prevalent sporadic ALS patients and not the subgroup of patients with an SOD1 mutation. It is possible that the observed microbleeds in the mouse model are specific for ALS due to SOD1 pathology. In our study using sensitive high-field 7T MR scans, we did not find evidence for microbleeds in patients with sporadic ALS.



10

TDP-43 plasma levels are higher in ALS

Esther Verstraete*

H. Bea Kuiperij*

Marka M. van Blitterswijk

Jan H. Veldink

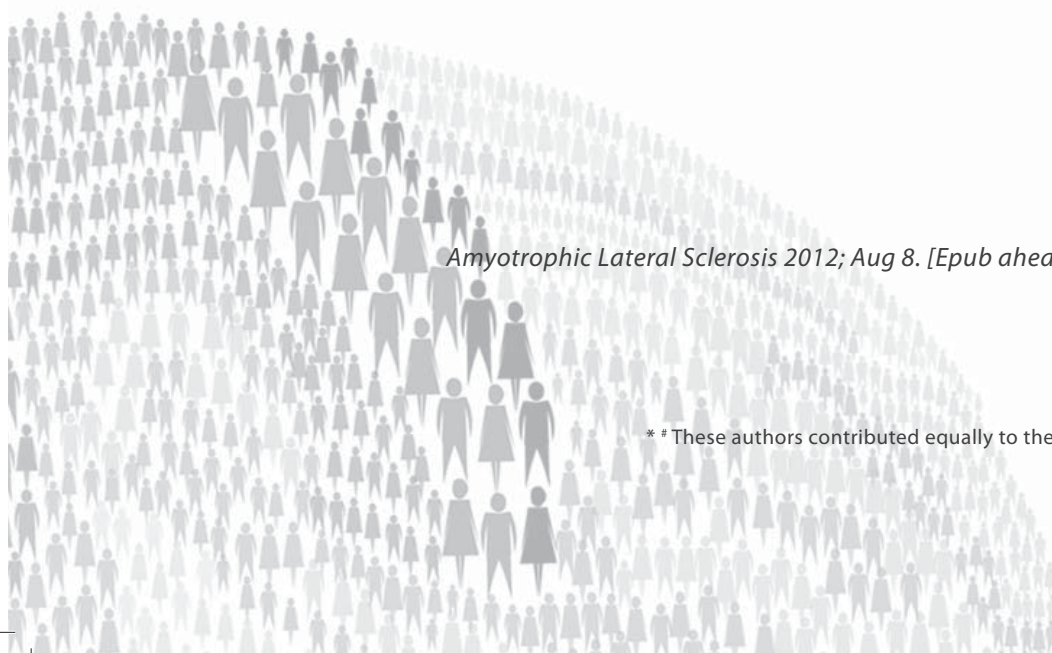
H. Jurgen Schelhaas

Leonard H. van den Berg#

Marcel M. Verbeek#

Amyotrophic Lateral Sclerosis 2012; Aug 8. [Epub ahead of print]

* # These authors contributed equally to the manuscript



ABSTRACT

Our objective was to investigate TDP-43 plasma levels in patients with amyotrophic lateral sclerosis (ALS). TDP-43 has been identified as a major component of protein inclusions in the brain of patients with ALS; mutations in the corresponding gene (*TARDBP*) have also been identified. Although increased TDP-43 levels have been reported in the cerebrospinal fluid, plasma levels have not yet been assessed in patients with ALS. TDP-43 levels were quantified by sandwich ELISA in plasma of 219 patients and 100 controls. In addition, we sequenced exon 6 of *TARDBP*, and performed longitudinal TDP-43 plasma measurements in a subset of patients. Results showed that TDP-43 plasma levels were significantly increased in patients with ALS ($p = 0.023$) and we found a positive correlation with age in patients and controls. Longitudinal measurements of TDP-43 plasma levels showed an increase in only one patient, with stable levels in five others. Three *TARDBP* variations were identified in the ALS group (1.7%), but the association with TDP-43 plasma levels was ambiguous. In conclusion, our data indicate that TDP-43 plasma levels may have potential as a marker for ALS. A genotype-phenotype relationship could not, however, be established in this cohort.

INTRODUCTION

Amyotrophic lateral sclerosis (ALS) is a neurodegenerative disease characterized by loss of motor neurons from the brain and spinal cord. Patients suffer from progressive muscle weakness, eventually leading to respiratory failure and death, on average within three to five years (Hardiman et al., 2011). A subset of patients with ALS develops frontotemporal dementia (FTD) and vice versa, as such, they seem to be part of the same clinical and pathological spectrum (Ringholz et al., 2005; Lillo et al., 2010).

A characteristic feature of degenerating motor neurons in ALS is the presence of cytoplasmic inclusions positive for ubiquitin. In 2006, the RNA-processing protein TAR DNA-binding protein 43 (TDP-43) was discovered to be the major component of these protein inclusions (Neumann et al., 2006) and, therefore, characteristic for the sporadic cases and most of the familial cases of ALS. Proteins found in the minority of patients with TDP-43 negative inclusions are superoxide dismutase 1 (SOD1) and fused in sarcoma (FUS) (Mackenzie et al., 2010). The mechanisms leading to TDP-43 accumulation and neurodegeneration have not yet been elucidated. Mutations in the TDP-43-gene, *TARDBP*, have been identified in a subset of patients with ALS and cerebral TDP-43 accumulation (Kabashi et al., 2008; Sreedharan et al., 2008). These mutations account for 4% of all familial and 0-2% of sporadic ALS cases (Kabashi et al., 2008; Daoud et al., 2009; Ticozzi et al., 2011). Most mutations have been detected in exon 6 of *TARDBP* and affect the C-terminal region of TDP-43, which has been suggested to affect normal protein-protein interactions (Kabashi et al., 2008). TDP-43-positive protein inclusions have been detected in most cases of tau-negative FTD, providing the pathological substrate for the clinical overlap between ALS and FTD (Mackenzie et al., 2010).

In patients with FTD, TDP-43 protein levels have been assessed in plasma by means of ELISA, showing increased levels in 46% of the patients with clinical FTD compared to 8% of the control subjects (Foulds et al., 2008). Pathological studies have, however, been unable to correlate these plasma levels of TDP-43 with either the presence or the amount of TDP-43 protein in brain tissue (Foulds et al., 2009). The significance of increased TDP-43 in plasma needs to be elucidated.

A biochemical marker for the diagnosis and prognosis of ALS is currently lacking, but is urgently needed to reduce diagnostic delay and to optimize patient care. The TDP-43 protein, as a key player in ALS pathogenesis, is an obvious candidate marker.

10



We hypothesized that a subset of ALS patients would show increased TDP-43 plasma levels, analogous to the findings in FTD patients. TDP-43 plasma levels were measured using ELISA and cross-sectionally compared between patients with ALS and control subjects. In addition, longitudinal measures were performed in a subset of patients. As mutations in *TARDBP* can cause ALS, we also screened ALS patients and control subjects for mutations in *TARDBP* and examined the association with plasma levels of TDP-43.

MATERIALS AND METHODS

Subjects

Plasma samples of 219 patients with ALS were studied and compared with 100 age- and gender-matched healthy control samples. All subjects gave written informed consent, in line with the Declaration of Helsinki, as approved by the Medical Ethics Committee for Research in Humans of the University Medical Centre Utrecht, The Netherlands. Patients were recruited from a national referral centre for motor neuron disease, the University Medical Centre Utrecht, and diagnosed with possible, probable or definite ALS according to El Escorial criteria (Brooks et al., 2000). The demographic and key clinical features of the participants are outlined in Table 10.1; none of the patients fulfilled the clinical criteria for FTD (Neary et al., 1998).

Plasma was separated from whole-blood samples (10 ml blood with EDTA acting as anti-coagulant) by routine methods, and stored at -80 °C until the assay.

Table 10.1 Demographic and clinical characteristics of the patients and healthy subjects

	Healthy control subjects (n = 100) Mean ± SD (range)	ALS patients (n = 219) Mean ± SD (range)
Age (years)	61.2 ± 10.4 (28–84)	62.6 ± 12.3 (24–89)
Male / Female	62 / 38	140 / 79
Site of onset (n)		
Bulbar		68 (32%)
Spinal		151 (68%)
Time to diagnosis (months)		12.0 ± 12.9 (2–131)
Disease duration (months)*		13.3 ± 17.4 (1–173)

* At time of sampling.

Recombinant TDP-43 protein

The full open reading frame of human TDP-43 was obtained by PCR using an IMAGE clone as template and subcloned into the pET-46-EK/LIC system (Novagen, EMD chemicals, Darmstadt, Germany), introducing an N-terminal polyhistidine tag. The protein was expressed in *E. coli* BL21 (DE3) pLysS (Novagen), and purified using Ni-NTA agarose (Qiagen, Venlo, The Netherlands) according to the manufacturer's instructions. The protein concentration was determined by BCA protein assay (Pierce, Thermo Scientific, Rockford, Illinois, USA) and the purified protein (estimated purity > 90%) was used as a standard in the ELISA.

TDP-43 ELISA

The ELISA for TDP-43 was performed essentially as described previously (Foulds et al., 2008; Kasai et al., 2009). In brief, a mouse monoclonal antibody directed against TDP-43 (clone 2E2-D3, Abnova, Taipei City, Taiwan) was coated overnight at 4 °C in 0.1 M NaHCO₃ buffer pH 9.6, followed by blocking with 1% bovine serum albumin (BSA) in phosphate buffer solution (PBS) for 1 h at room temperature. Plasma and standard samples were incubated for 2 h at 37 °C, followed by incubation with a rabbit polyclonal antibody directed against TDP-43 (Proteintech Group, Manchester, UK) for 1 h at 37 °C. A goat anti-mouse horseradish peroxidase conjugated secondary antibody (Jackson ImmunoResearch Laboratories, Suffolk, UK) was incubated for 1 h at 37 °C, followed by detection of luminescence using SuperSignal ELISA Femto maximum sensitivity substrate (Pierce, Thermo Scientific) and a Lumistar Optima instrument (BMG Labtech, Ortenberg, Germany).

Sequencing exon 6 of TARDBP

A subset of ALS patients and control subjects available for sequencing (175 and 83 cases, respectively) were screened for mutations in exon 6 of *TARDBP* (Kabashi et al., 2008; Sreedharan et al., 2008). Primers have been described previously (Sreedharan et al., 2008). We used BigDye Terminator 3.1 sequencing kit (Applied Biosystems, Foster City, California, USA) and a DNA Analyzer 3730XL for sequencing. Data analysis was performed with PolyPhred and identified mutations were confirmed on genomic DNA (Nickerson et al., 1997). PMut was used to predict the impact of these mutations on the structure and function of TDP-43 (<http://mmb2.pcb.ub.es:8080/PMut/>).

10



Statistical analysis

All data were analysed using the R software package for statistical computing (<http://www.R-project.org>, R Version 2.12-0 GUI 1.35); TDP-43 plasma levels were tested for normality with the Kolmogorov-Smirnov test. As the data were skewed, normality requirements were not met and log-transformation was performed. Subsequently, normality was reached and the difference between patients and healthy control subjects was assessed using a linear model, including covariates: age, gender and disease duration (at the time of sampling).

RESULTS

TDP-43 concentration in plasma

TDP-43 levels were significantly increased in patients with ALS as compared to healthy control subjects ($p = 0.023$) (Figure 10.1). In 28% of ALS patients, the absolute TDP-43 concentration was above the detection limit ($0.31 \mu\text{g/l}$; defined as two standard deviations

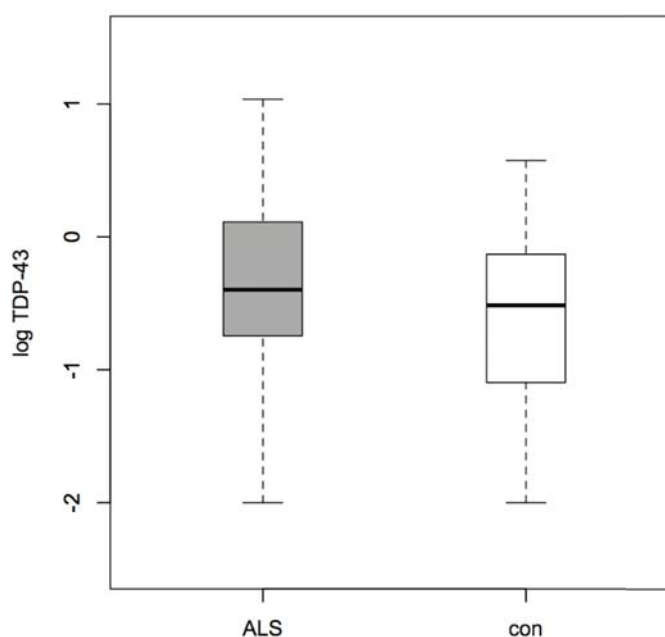


Figure 10.1 TDP-43 plasma levels in patients with ALS and healthy control subjects

TDP-43 protein levels were determined using ELISA in plasma of ALS patients and healthy controls (con). This box plot shows the log-transformed data indicating the median, quartiles, maximum, and minimum. TDP-43 plasma levels are significantly increased in patients with ALS compared to controls.

above the mean background signal) versus 21% of the control subjects. It is important to note that whereas the highest absolute measure in control subjects was 3.76 µg/l it was up to 10.85 µg/l in ALS patients. Specifically examining the subgroup of patients with measures above the highest of controls (n = 8) did not reveal a distinct clinical profile compared to the total group of patients (Table 10.2). Survival analysis using a Cox regression model including high TDP-43 levels as a factor, besides other prognostic factors (age, site of onset and time to diagnosis) did not reveal a significant contribution of increased TDP-43 plasma levels (different cut-off values were explored). The distribution of measurements as shown in Figure 10.2 draws attention to a subgroup of relatively young patients with high TDP-43 plasma levels (encircled in graph), high measures in young patients might have more specificity for disease.

A linear model examining TDP-43 levels and age at sampling showed a significant positive correlation (p = 0.029; Figure 10.2), but no relation was found with other clinical variables such as gender (p = 0.86), disease duration (p = 0.53) and survival (p = 0.55; data not shown). If both disease status (as factor) and age at sampling were included in a linear model, the result was statistically significant (F-statistic; p = 0.008). Interaction between age at sampling and disease status was not significant.

10



Longitudinal measures

Samples, collected longitudinally at two to eight time points, were available from six patients. In five patients, the TDP-43 plasma levels were relatively consistent in time.

Table 10.2 Subgroup of patients with high TDP-43 measures

	ALS; normal TDP-43 levels (n = 211) Mean ± SD (range)	ALS; high TDP-43 levels (n = 8) Mean ± SD (range)	p-values
Age (years)	62.9 ± 12.1 (27–89)	55.6 ± 16.5 (24–72)	0.26
Male / Female	135/76	5/3	0.60
Site of onset (n)			
Bulbar	66 (31%)	2 (25%)	
Spinal	145 (69%)	6 (75%)	0.52
Time to diagnosis (months)	12.1 ± 13.1 (2–131)	9.6 ± 5.6 (2–21)	0.56
Disease duration (months)*	13.4 ± 17.7 (1–173)	11.0 ± 6.5 (2–21)	0.37

* At time of sampling.

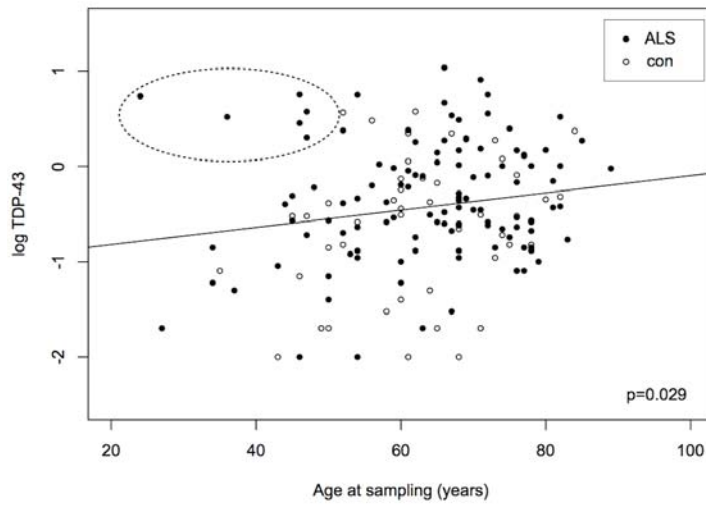


Figure 10.2 Correlation between TDP-43 plasma levels and age

The log-transformed TDP-43 plasma levels were plotted against the age at sampling in patients with ALS and control subjects (con). It is noticeable that a small number of relatively young patients have increased TDP-43 levels (encircled in plot).

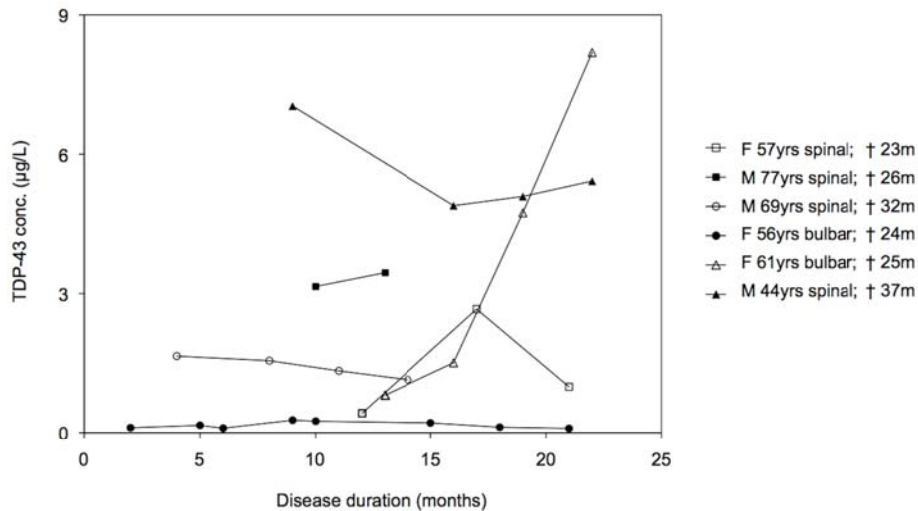


Figure 10.3 Longitudinal TDP-43 plasma measurements

In six patients we performed two to eight longitudinal measurements. This graph displays the TDP-43 plasma levels measured at different time points during the disease course. All patients were deceased at the time of analysing the data. The survival is indicated per subject in the legend. In five out of six patients these measurements are relatively stable over time; one patient (F 61 bulbar) had a rising plasma TDP-43 level.

Legend (gender (F = female; M = male); age at onset (years); site of onset (spinal/bulbar); survival (months)); TDP-43 conc. = TDP-43 plasma concentrations.

However, in one patient, four consecutive measurements showed a marked increase over time (Figure 10.3). This particular subject was a 61 years old female patient with a bulbar onset who died a few months after the last measurement. Other subjects who died during a similar follow up did not show an increase in TDP-43 level. There was one other subject with bulbar onset, but in this case, TDP-43 plasma levels were not detectable.

TDP-43 genotyping

In the patient group, we found three subjects (1.7%) with a *TARDBP* variation. In two of these, it was a non-synonymous variation in exon 6 of *TARDBP*, and, based on the PMut analysis, most probably pathogenic. One patient probably had a silent variation. The clinical characteristics of patients with *TARDBP* variants are presented in Table 10.3. The two patients with a pathogenic variation had a measurable TDP-43 concentration in plasma: 0.47 and 1.01 µg/l, respectively.

10



Table 10.3 Clinical characteristics of patients with *TARDBP* variants

PMut was used to predict the impact of the identified variants on the function of TDP-43. The p.G295C and p.N352S variants were predicted to be pathogenic.

Variant	PMut	Group	Gender	Age at onset	Site of onset	Survival (months)	TDP-43 plasma level (µg/L)
p.A315A	Silent	SALS	M	54	Cervical	> 48*	0.00
p.G295C	Pathogenic	FALS	F	80	Bulbar	43	1.01
p.N352S	Pathogenic	SALS	M	53	Cervical	180	0.47

M = male; F = female; SALS = sporadic ALS.

* Alive at the time of data-analysis.

DISCUSSION

In this study, we investigated whether the TDP-43 plasma level is a suitable biomarker for ALS, especially since nearly all ALS patients, apart from those with *FUS* or *SOD1* mutations, exhibit TDP-43 protein inclusions as a pathological entity in the brain. We showed that plasma TDP-43 levels were significantly increased in patients with ALS, compared to healthy control subjects. Furthermore, TDP-43 plasma levels correlated positively with age. In addition, we identified *TARDBP* variants in three ALS patients, but these could not be associated with TDP-43 protein levels in plasma due to the small number. In longitudinally

performed measurements, the levels appeared to be consistent over time with the exception of one subject who showed a marked increase with disease progression.

With the development of disease-modifying therapies, an *in vivo* assessment of the type and extent of neuropathological changes in the brain (e.g. by means of a blood test) is of increasing importance and would facilitate diagnosis and drug discovery. Our finding of significantly increased TDP-43 levels in plasma might be related to TDP-43 accumulation in the brain and is supported by a positive relationship with age. Previous studies have found raised plasma TDP-43 levels in FTD patients (Foulds et al., 2008) as well as in patients with inclusion body myositis (IBM), an important mimic of ALS (Kuiperij et al., 2010). FTD patients had detectable TDP-43 levels in 46% of cases, which is a higher number than in our study (28% of ALS patients) (Foulds et al., 2008). This could be due to minor technical differences in assay performance, more extensive protein accumulation in the brains of patients with FTD compared to ALS or differences in the pathogenesis yet unidentified. A study in patients with FTD that focused on the correlation between TDP-43 plasma levels and neuropathological changes could not, confirm a positive correlation (Foulds et al., 2009). As similar studies in ALS are currently lacking, the pathological correlate of elevated TDP-43 in plasma of patients with ALS remains to be established.

Previous studies in ALS have shown increased TDP-43 levels in cerebrospinal fluid (CSF) (Kasai et al., 2009; Steinacker et al., 2008; Noto et al., 2011). One of these studies suggests that patients with a short disease duration (of up to 10 months) have higher CSF levels of TDP-43 (Kasai et al., 2009) compared to those with longer disease duration. Another study suggested a relationship between increased TDP-43 levels and longer survival (Noto et al., 2011). In the present study we could not confirm a relationship between plasma TDP-43 and disease duration or survival. We did, however, observe an association of plasma TDP-43 with age.

Longitudinal measurements performed in a small subset of patients revealed stable levels over time in all but one patient. This particular subject did not have any specific characteristics compared to the other patients. The increase in TDP-43 protein levels was not a sign of impending death, since other patients also died within a similar follow-up period and did not show increasing plasma TDP-43 levels. The stable plasma levels found in the other five patients argues against TDP-43 in plasma as a biomarker of the total TDP-43 load in the central nervous system and is rather suggestive for increased TDP-43 as a risk factor for ALS. Nevertheless, this finding stresses the importance of including longitudinal analyses on a larger scale in future (international) studies.

Mutational analysis of *TARDBP* revealed three variants (1.7%), most probably pathogenic in two. This percentage is in accordance with previous studies on *TARDBP* gene mutations in sporadic ALS patients (Kabashi et al., 2008; Sreedharan et al., 2008; Daoud et al., 2009; Ticozzi et al., 2011). The numbers in this cohort are too small to establish a genotype-phenotype relationship as reported in studies on progranulin. Mutations in the progranulin gene (*GRN*) cause FTD and were found to be related to plasma levels of progranulin protein (Ghidoni et al., 2008).

We conclude from the present study that patients with ALS, as a group, have significantly raised plasma levels of TDP-43 compared to healthy controls, and that this finding could possibly be related to the cerebral accumulation of this protein. We could not assess a potential correlation between TDP-43 plasma levels and the three *TARDBP* variants due to the small numbers. Future studies should include pathological assessments to study a potential correlation between TDP-43 plasma levels and cerebral protein accumulation, as well as quantification of the pathological, phosphorylated form of TDP-43 in plasma. Finally, the specificity of TDP-43 levels for ALS as opposed to clinical mimics (Hardiman et al., 2011), e.g. cervical stenosis or multifocal motor neuropathy, needs to be established.

10



PART III
CLINICAL TRIALS

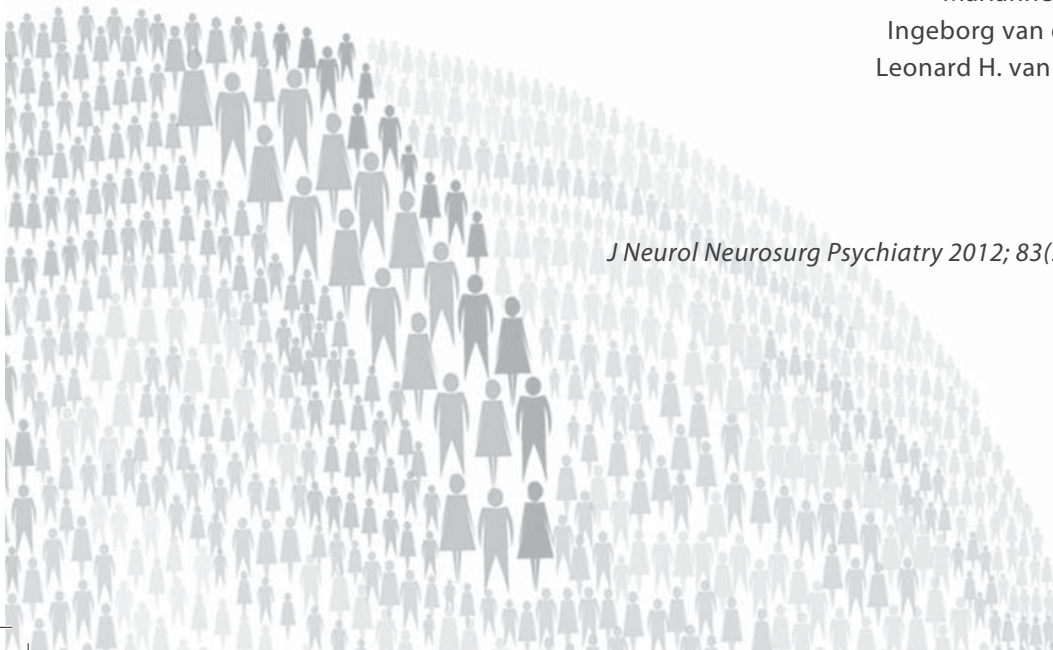


11

Lithium lacks effect on survival in ALS: a phase IIb randomized sequential trial

Esther Verstraete
Jan H. Veldink
Mark H.B. Huisman
Tim Draak
Esther V. Uijtendaal
Anneke J. van der Kooi
H. Jurgen Schelhaas
Marianne de Visser
Ingeborg van der Tweel
Leonard H. van den Berg

J Neurol Neurosurg Psychiatry 2012; 83(5): 557-64



ABSTRACT

Objectives: To determine the safety and efficacy of lithium for the treatment of amyotrophic lateral sclerosis (ALS) in a randomized, placebo-controlled, double-blind, sequential trial.

Methods: Between November 2008 and June 2011, 133 patients were randomized to receive lithium carbonate (target blood level 0.4–0.8 mEq/L) or placebo as add-on treatment with riluzole. Primary endpoint was survival, defined as death, tracheostomal ventilation, or noninvasive ventilation more than 16 hours/day. Secondary outcome measures consisted of the revised ALS Functional Rating Scale and forced vital capacity. Analysis was by intention to treat and according to a sequential trial design.

Results: A total of 61 patients reached a primary endpoint, 33 of 66 in the lithium group and 28 of 67 patients in the placebo group. Lithium did not significantly affect survival (cumulative survival probability of 0.73 in the lithium group [95% confidence interval (CI) 0.63–0.86] versus 0.75 in the placebo group [95% CI 0.65–0.87] at 12 months and 0.62 in the lithium group [95% CI 0.50–0.76] versus 0.67 in the placebo group [95% CI 0.56–0.81] at 16 months). Secondary outcome measures did not differ between treatment groups. No major safety concerns were encountered.

Conclusions: This trial, designed to detect a modest effect of lithium, did not demonstrate any beneficial effect on either survival or functional decline in patients with ALS.

INTRODUCTION

Amyotrophic lateral sclerosis (ALS) is a devastating neurodegenerative disorder characterized by progressive weakness. ALS is caused by loss of motor neurons in the spinal cord, brainstem, and motor cortex, and can occur at any time in adulthood. Median survival is 3 years after symptom onset and is modestly prolonged by riluzole. A more effective treatment is urgently needed.

Protein aggregates or ubiquitin-positive inclusions, containing proteins that are mutated in small subsets of ALS patients, have been recognized as the pathological hallmark of ALS. As the removal of misfolded or damaged proteins is critical for optimal cell functioning, impairment of protein turnover may play an important role in the pathogenesis of ALS and other neurodegenerative disorders (Deng et al., 2011; Neumann et al., 2006; Deng et al., 2010).

Lithium is well known for its mood-stabilizing effects in bipolar disorders, but is being increasingly recognized as a neuroprotective agent (Chuang et al., 2002; Bian et al., 2007; Rametti et al., 2008). An important pathway in exerting this neuroprotective effect is the promotion of protein clearance or autophagy (Sarkar and Rubinsztein, 2006). In an ALS SOD1 mouse model of ALS lithium showed reduced alpha-synuclein, ubiquitin and SOD1 aggregates in motor neurons, and besides its effects on protein clearance, lithium was found to increase the number of mitochondria and suppressed reactive astrogliosis (Fornai et al., 2008).

These promising results from preclinical studies led to the testing of lithium in patients, putting it forward as a disease-modifying agent for ALS. In a relatively small pilot study of 44 patients, 16 of whom received lithium at a dose leading to plasma levels ranging from 0.4 to 0.8 mEq/liter, a significant effect on survival was found at 12 and 15 months of follow-up along with a slowing of disease progression (Fornai et al., 2008). Subsequently, a trial designed to detect a large effect as found in the pilot study (40% decrease in the rate of functional decline), had to be stopped for futility at the first interim analysis at 6 months (Aggarwal et al., 2010). A more modest effect of lithium or an effect occurring after prolonged treatment could not be ruled out (Verstraete et al., 2010). Besides, no effect could be detected in trials comparing a low (subtherapeutic) and therapeutic dose of lithium (Chio et al., 2010), comparing the effect of lithium treated patients with historical controls (Miller et al., 2011), or using self-reported patient data (Wicks et al., 2011). However, a placebo-controlled randomized trial designed to detect an effect on survival was still considered necessary as has been repeatedly pointed out (Armon, 2010; Saute et al., 2010) (for a survey of previous studies, see Supplemental Table 11.1).

11



The progressive and fatal nature of ALS increases the importance of minimizing the burden for patients of participating in clinical trials. In addition, treatment of patients should not be delayed if a novel therapy is effective, but if treatment is ineffective, unnecessary continuation of a trial should be avoided. The sequential trial design requires, on average, fewer patients than traditional trial designs of equal power and permits discontinuation of a study as soon as enough evidence for a treatment effect or lack thereof is obtained (Groeneveld et al., 2003; Groeneveld et al., 2004; Groeneveld et al., 2007; Schoenfeld and Cudkowicz, 2008; Piepers et al., 2009; Whitehead, 1997).

The objective of this study was to examine the effect of lithium compared to placebo as an add-on treatment together with riluzole on survival in ALS, performing a randomized, clinical trial with sequential analysis.

METHODS

Study design

This was a sequential, randomized (stratified and balanced [1:1] randomization), double-blind, placebo-controlled, parallel-group trial conducted in The Netherlands (three sites) (Phase IIb trial). This trial was performed according to the Medical Research Involving Human Subjects Act (WMO) and the International Conference on Harmonization Good Clinical Practice (GCP) guidelines.

Patients

Patients were eligible if they were diagnosed as having clinically probable laboratory-supported, probable, or definite ALS according to the World Federation of Neurology El Escorial criteria (Brooks et al., 2000). Other inclusion criteria were: use of riluzole (50mg, twice daily); onset of symptoms at least 6 months and no longer than 36 months prior to inclusion; a forced vital capacity (FVC) of at least 70% of the predicted value based on gender, height, and age (in sitting position); age between 18 and 85 years; and written informed consent. Patients were excluded if they met any of the following criteria: tracheostomal ventilation of any type, noninvasive ventilation for more than 16 hours/day, or supplemental oxygen during the last 3 months prior to inclusion; any medical condition or intoxication known to have an association with motor neuron dysfunction, which might confound or obscure the diagnosis of ALS; presence of any concomitant

life-threatening disease or any disease or impairment likely to interfere with functional assessment; contra-indications for lithium therapy (e.g. confirmed renal insufficiency or cardiac arrhythmias); and other medication interacting with lithium with a significant risk of complications (e.g. verapamil). All patients gave written informed consent, and the ethics committees of the participating institutions approved the study.

Study settings

This study took place at the national referral centers for patients with motor neuron disease in The Netherlands (Netherlands ALS Center, a collaboration of the Departments of Neurology of the University Medical Center Utrecht, Academic Medical Center Amsterdam, and Radboud University Medical Center Nijmegen), from November 2008 to June 2011. An electronic case report form (eCRF) was used for optimal and timely communication between patients and investigators as well as across centers.

An external trial monitor was engaged to protect the rights and well-being of trial participants, to verify the accuracy of the reported trial data, and to guarantee that the conduct of the trial was in compliance with the currently approved protocol/amendments, with GCP guidelines, and with the applicable regulatory requirements. Internal audits with 'Source Data Verification' were performed to provide this additional level of security.



Intervention

Patients were assessed for eligibility at the screening visit, including blood tests (leucocytes, sodium, potassium, calcium, creatinin, glucose, and TSH), urine tests (albumin, sediment analysis, and specific gravity), body weight, and electrocardiography (ECG; in patients over 60 years of age). After confirmation of eligibility, patients were randomly assigned to receive either lithium carbonate once daily PO (lithium carbonate 400mg PCH, Haarlem, The Netherlands) at target concentration 0.4-0.8 mEq/L or identical placebo tablets (manufacturing pharmacy: 'Apotheek Haagse Ziekenhuizen', The Hague, The Netherlands). Both lithium carbonate and placebo tablets were packed in identically labeled containers by 'Apotheek Haagse Ziekenhuizen'. The manufacturing pharmacy was not involved in the study design, nor did they provide material support. Trial medication was handed out to the patients or sent by courier by the pharmacy of the UMC Utrecht.

Patients were instructed to commence with one tablet in the evening and a first control of lithium concentration took place after one week. To minimize the burden for patients, the

patients were bled at the general practitioner's surgery or local laboratory in return for an allowance (samples were obtained approximately 12 hours after the last dose). The samples were sent by mail to a central laboratory (at the UMC Utrecht) where blood concentrations were measured and the result was filled in the eCRF. For reasons of safety monitoring, patients filled out a questionnaire in the eCRF to report on possible side effects: polydipsia, polyuria, vomiting, diarrhea, fatigue, weight gain, tremor, concentration and/or memory problems, movement disturbances, skin changes, miscellaneous. An unblinded investigator (JHV) received an instant notification per email to make dose adjustments. Then, patients and the involved local investigator received an email about the new dosage and about the timing of the next blood control. As soon as the lithium concentrations were within the target range (0.4–0.8 mEq/L) the control frequency was lowered to a minimum of once every three months. Patients who received placebo were given simulated dose modifications identical to the lithium group.

Outcomes

The primary outcome measure with respect to efficacy in ALS was survival, defined as the time from inclusion to death, tracheostomal ventilation, or noninvasive ventilation for more than 16 hours/day. Caregivers and/or patients were instructed to report endpoints immediately. We chose survival as primary outcome measure as a relevant and sensitive means of determining a potential disease modifying effect (Lacomblez et al., 1996a).

The rate of decline in daily functioning, measured by the validated Revised ALS Functional Rating Scale (ALSFRS-R) and FVC were used as secondary outcome measures (Traynor et al., 2004). Unintended effects of the intervention were assessed by registration of all (serious) adverse events.

Secondary outcome measures were assessed during the visits every three months. In addition, body weight was assessed and blood samples were taken to measure lithium concentration, thyroid function (thyroid stimulating hormone), kidney function (creatinine), electrolytes (sodium, potassium), liver enzymes (aminotransferase concentrations, alkaline phosphatase, γ -glutamic transpeptidase), and leucocytes (at the first two visits). Patients who were not able to visit the hospital because of disease progression were called by telephone to document (serious) adverse events and ALSFRS-R. Serious adverse events as defined in the GCP guidelines were documented in the eCRF from which an automatic notification email was generated to the coordinating investigator.

The ethics committee was notified within two weeks about serious adverse events judged to be related to therapy and received a safety report of all adverse events (SAEs and AEs) twice a year. As of January 1st, 2010, the ethics committee was notified electronically about all serious adverse reactions and events within 15 days and in case of a lethal or life-threatening SAE, within 7 days.

Sample size

The trial was designed to detect a 15% increase in cumulative survival percentage in the lithium group, similar to the effect of riluzole (Lacomblez et al., 1996b). Assuming a cumulative survival percentage in the placebo group of 60% after 16 months and 75% in the lithium group (i.e. a hazard ratio of 0.56 of lithium compared to placebo), with a one-sided α level of 0.05 and a power ($1-\beta$) of 90%, on average 173 patients with 56 endpoints (90th percentile = 283 patients) would be required if the null hypothesis were true (i.e. no difference between placebo and lithium), and on average 191 patients with 62 endpoints (90th percentile = 311 patients) if the alternative hypothesis were true (treatment with lithium is superior to placebo).

This sample size calculation was based on the sequential trial design, which allows the study to be halted as soon as the cumulative data show efficacy of the studied drug or a lack thereof (Whitehead, 1997). This implies that the total number of patients to be included cannot be estimated beforehand but is determined by the course of the trial. For comparison, the total fixed sample size for a classic phase IIb RCT, based on the same expected difference in survival of 15% with a one-sided α of 0.05 and a power of 0.90, would be at least 338 patients with approximately 110 endpoints.

Interim analyses and stopping guidelines

A sequential design for an RCT allows a series of interim analyses on the emerging data to be conducted and specifies the circumstances that determine when the trial will stop or continue at each analysis. Sequential monitoring of the emerging survival data was conducted by an independent biostatistician (IvdT). Based on the 15% difference in cumulative survival, the one-sided type I error of 0.05 and a power of 90%, monitoring boundaries were specified. These boundaries are determined so that the probability of falsely declaring an ineffective treatment as effective remains controlled at 5% and the probability of incorrectly declaring an effective treatment to be ineffective remains



controlled at 10%, wherever the boundaries are crossed. These monitoring boundaries are straight lines, based on an idealized version of continuous monitoring (see Figure 11.1 for illustration). The analysis is not truly continuous but is performed on each new set of cumulative data, based on the occurrence of one or several new clinical endpoints. This (discrete) approximation of a truly continuous analysis is graphically depicted by the jagged inner lines below the upper and above the lower limit (the so-called ‘Christmas tree correction’) (Whitehead, 1997). A statistic Z is defined to measure the treatment effect as the difference between the observed number of events in the control group and the expected number under the assumption of treatment equivalence. A positive Z value indicates that the treatment is superior; a negative value indicates that the treatment is equal or inferior to placebo. Each new clinical endpoint or group of clinical endpoints leads to a new value for Z . The cumulative amount of information (concerning events) is expressed in the statistic V . For a sequential survival analysis, V is approximately equal to a quarter of the number of events observed. When the test statistic based on the cumulative data crosses the upper boundary, the null hypothesis of indifference is rejected. When the lower boundary is crossed, the null hypothesis is accepted (Figure 11.1). The effect size of lithium relative to placebo in terms of the hazard ratio (HR) was specified at 16 months to be able to calculate the monitoring boundaries and to determine the average number of patients required, thus assuming a constant proportional hazard ratio independent of follow-up time. It is nevertheless possible to continue monitoring patients after 16 months of follow-up. Data on patients, reaching an endpoint after 16-months, can therefore be included in the sequential survival analysis.

In addition to the efficacy analysis a safety analysis was performed comparing the proportion of patients who had a serious adverse event in the lithium group to those in the placebo group. Safety was also monitored sequentially (Whitehead, 1997; MPS Research Unit, 2000). The safety boundary is determined by the hypothesized SAE rates for the lithium and placebo group as well as the risk of false alarm. An SAE rate of 0.25 was expected in the placebo group; an SAE rate of 0.40 or more in the lithium group was considered undesirable. The type I error α was set at 0.10 (one-sided) as a warning when lithium would be unsafe. An independent data and safety monitoring board (DSMB) was installed, composed of people acquainted with either lithium, clinical trials and/or ALS (e.g. clinical pharmacologist, psychiatrist, nephrologist, trial neurologist and a biostatistician). The DSMB periodically reviewed the efficacy and safety data.

Randomization and blinding

Stratified randomization to receive lithium or placebo was performed manually by one of the investigators not involved in the care of trial patients (JHV). To ensure a balanced number of patients receiving lithium and placebo in the strata the minimization method as described by Pocock (Pocock and Simon, 1975) was applied stratified to the following prognostic factors: age (< 45; > 45 and < 65; or > 65 years), site of symptom onset (bulbar or spinal), FVC (< 85% or > 85%), and location (University Medical Center Utrecht, Academic Medical Center Amsterdam, or Radboud University Medical Center Nijmegen). The patient was assigned a unique medication code corresponding to either placebo or lithium. As such, unblinding of a single participant would not result in unblinding of the whole group. Besides the randomizing investigator, only the pharmacy and the biostatistician had access to the randomization sheet until the end of the trial. As each of the containers with trial medication was provided with a unique medication code, additional dispenses of trial medication to the same patient had a different code, but (obviously) corresponded to the same treatment arm.

Patients were assessed for eligibility at the screening visit. After confirmation of eligibility, the local investigator asked the randomizing investigator by email (including study number of the patient and the essential information for minimization) to randomize the patient. The medication code assigned to the patient was filled on the eCRF.

Statistical methods

The sequential design and analysis has been described above (*Interim analyses and stopping guidelines*). Sequential analysis was stratified for the factors described (*Randomization and blinding*). For descriptive reasons, Kaplan–Meier survival curves were estimated. The estimate for the HR has to be adjusted for the fact that the data are analyzed sequentially. PEST 4 software was used for the sequential analysis (Groeneveld et al., 2003; MPS Research Unit, 2000).

To estimate the difference in rate of decline in functional status and respiratory function, measured by the ALSFRS-R and FVC, we fitted the longitudinal data by maximum likelihood estimation using linear mixed-effects models, including time as a continuous variable and treatment group as a factor, adjusting for gender and the stratification factors as categorical variables (age, FVC, site of onset and center). A possible overall non-linear decline of the ALSFRS-R and FVC could be accounted for by also running the model with

11



time as a categorical variable (visit number), because slopes between visit numbers are compared between treatment groups. In addition, we explored additional models with time entered as an exponential continuous variable (powers 2, 4 and the square root). SAEs were monitored as described (*Interim analyses and stopping guidelines*). All adverse events were categorized per organ system and specific event and compared between groups using Fisher's exact tests. All results were analyzed on an intention-to-treat basis.

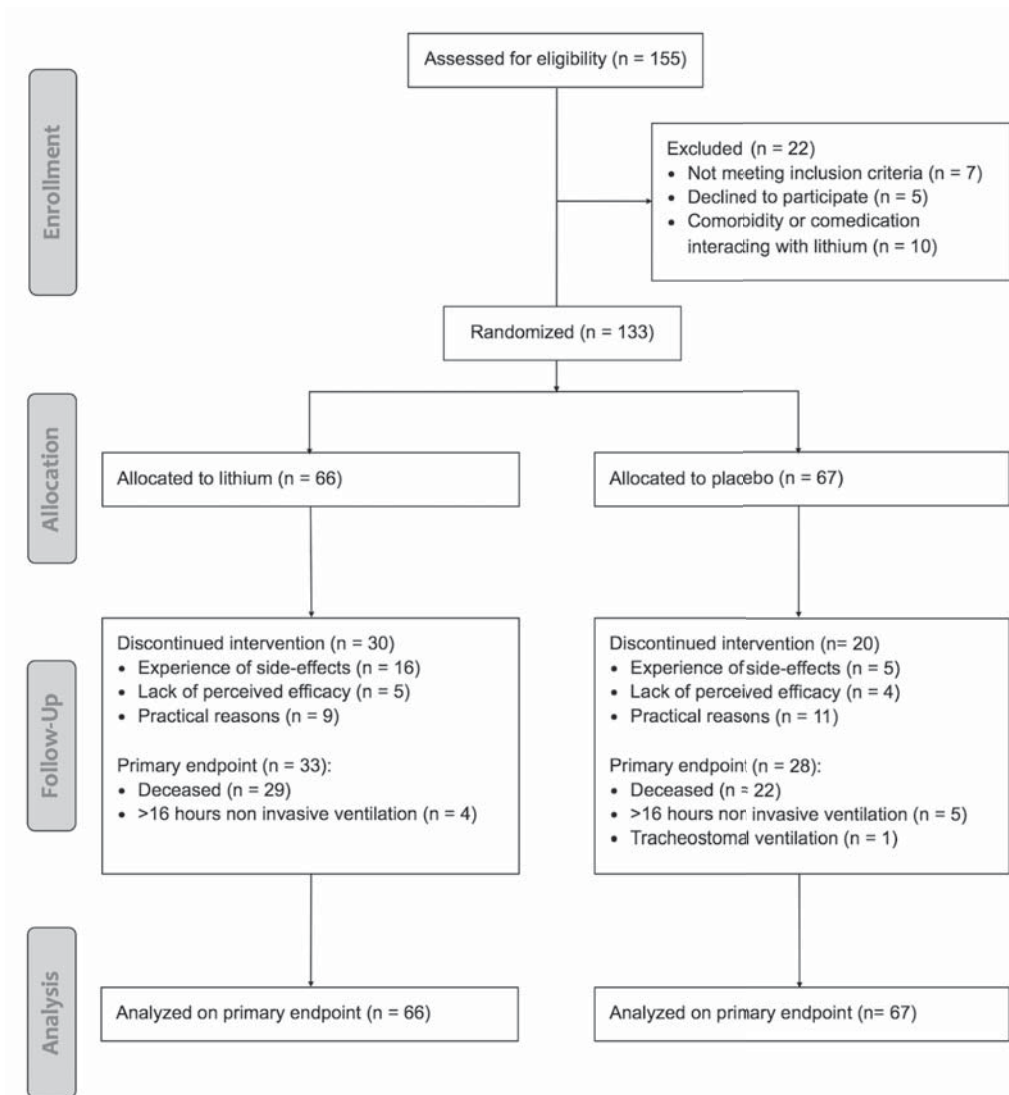
RESULTS

Patients

From November 2008 until June 2011, 155 patients were considered for enrollment. Twenty-two patients did not fulfill the inclusion criteria (Figure 11.1). After screening, 133 patients were randomly assigned to receive lithium (n = 66) or placebo (n = 67). Baseline characteristics of the participants are shown in Table 11.1. Thirty patients (45%) from the lithium group and 20 patients (30%) from the placebo group discontinued trial medication after on average 10 months of treatment. Significantly more patients in the lithium group discontinued trial medication due to experience of one or more side-effects ($p = 0.009$; fatigue or a general feeling of discomfort [lithium group: n = 5; placebo group: n = 1], tremor [lithium group: n = 5], psychological complaints [lithium group: n = 3; placebo group: n = 2], polyuria/nocturia [lithium group: n = 3; placebo group: n = 1], nausea [lithium group: n = 3], skin changes [lithium group: n = 1; placebo group: n = 2], elevated liver enzymes [lithium group: n = 1], and restless legs [lithium group: n = 1], headache [placebo group: n = 1] and palpitations [placebo group: n = 1]) (Figure 11.1). All randomized patients were included in the final analysis on the primary outcome. One participant was lost to follow-up for the secondary outcome measures shortly after randomization (no post-randomization measures were obtained); therefore this patient was not included in these analyses. The median follow-up was 16 months for the lithium group (n = 66) and 15 months for the placebo group (n = 67) (inter-quartile range 2–31 months for both groups).

Primary outcome measure: Survival

After 61 patients had reached a primary endpoint (lithium group: n = 33; placebo group: n = 28), the sample path of (Z, V) values (the X symbols in Figure 11.2) crossed the lower



11



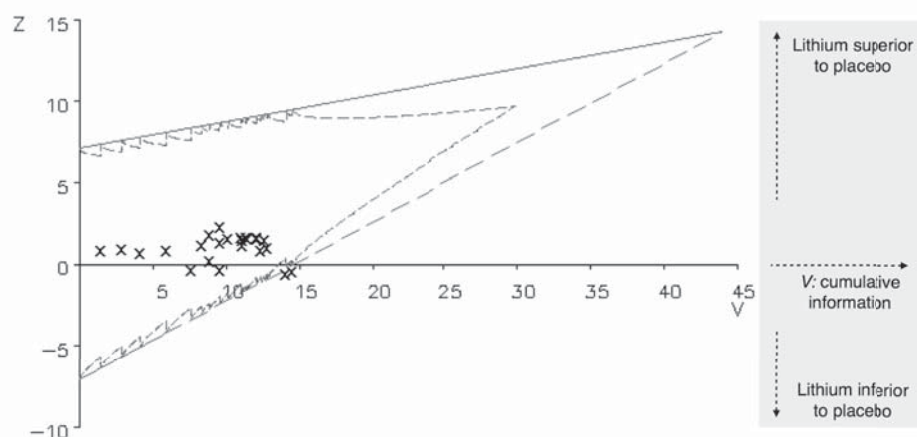
Figure 11.1 Flow diagram

boundary indicating that the null hypothesis of no difference between the two treatment arms could not be rejected ($p = 0.91$; Figure 11.2). The cumulative survival probability at 12 months was 0.73 in the lithium group (standard error [SE] 0.06; 95% CI 0.63–0.86) versus 0.75 (SE 0.06; 95% CI 0.65–0.87) in the placebo group, and at 16 months 0.62 in the lithium group (SE 0.06; 95% CI 0.50–0.76) versus 0.67 (SE 0.06; 95% CI 0.56–0.81) in the placebo group (Figure 11.3). The adjusted HR was 1.03 for lithium compared to

Table 11.1 Baseline characteristics of the study participants

	Lithium (n = 66)	Placebo (n = 67)
Male gender, n (%)	37 (56)	43 (64)
Median age in yrs (IQ range)	59.5 (52.3–66.8)	59 (51.0–66.5)
Limb onset, n (%)	47 (71)	48 (72)
Median ALSFRS-R score (IQ range)	42 (40–44)	41 (37–43)
Forced vital capacity, n (%)		
< 85%	18 (27)	20 (30)
≥ 85%	48 (73)	47 (70)
Location, n (%)		
Utrecht	31 (47)	34 (51)
Amsterdam	19 (29)	17 (25)
Nijmegen	16 (24)	16 (24)
Median time from symptom onset to inclusion in months (IQ range)	12 (9–18)	14 (10–21)

IQ range = inter-quartile range.

**Figure 11.2 Sequential survival analysis**

On the horizontal axis, the amount of information V increases as time passes and events accumulate. On the vertical axis, Z reflects the effect of lithium relative to placebo. When the sample path depicted by the X symbols crosses the upper (inner) boundary, the null hypothesis (i.e. no treatment effect) is rejected: the effect size is significant. When the test statistic crosses the lower (inner) boundary, it becomes highly improbable that the upper boundary of the triangle will also be crossed, and the null hypothesis of indifference cannot be rejected. Crossing of the first part of the lower boundary indicates a negative effect of lithium on survival. The inner margins of the triangle are the true boundaries to be crossed (the so-called 'Christmas tree correction'), whereas the straight lines that form the upper and lower (dashed) boundary are the hypothetical boundaries to be crossed if the analysis were truly sequential.

placebo with 90% confidence interval (0.66–1.63). Of the 61 patients who reached the primary endpoint, 51 patients died, 9 patients were on noninvasive ventilation for more than 16 hours/day, and in 1 patient, tracheostomal ventilation was initiated (Figure 11.1).

A post-hoc on-treatment analysis (patients on lithium for less than 3 months were considered as placebo, $n = 9$) using a log-rank test, was similar to the findings in the intention to treat analysis ($p = 0.50$).

Secondary outcome measures: Daily functioning and vital capacity

Figure 11.4 shows the decline of the mean ALSFRS-R and FVC for both treatment groups during the course of the trial. Linear mixed-effects modeling – adjusted for gender and stratification factors – showed that the interaction between treatment group and time was not statistically significant for ALSFRS-R ($p = 0.74$) and FVC ($p = 0.22$). Similar results were obtained by including time as a categorical variable (visit number) or time as an exponential continuous variable in the model, accounting for a possible overall nonlinear decline in the ALSFRS-R and FVC.

11

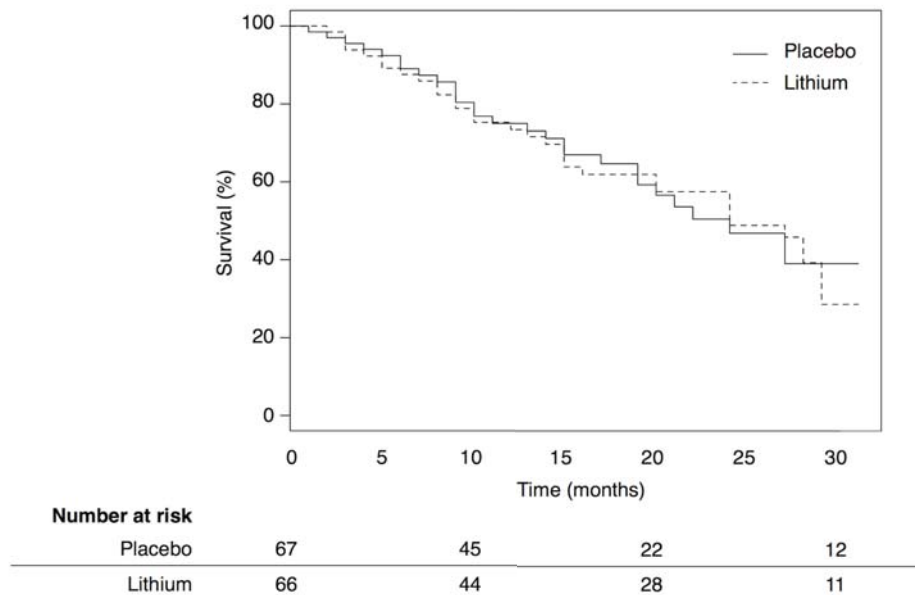


Figure 11.3 Kaplan–Meier survival curve

This figure shows the cumulative survival for the patients treated with lithium (dashed line) compared with the placebo group (solid line).

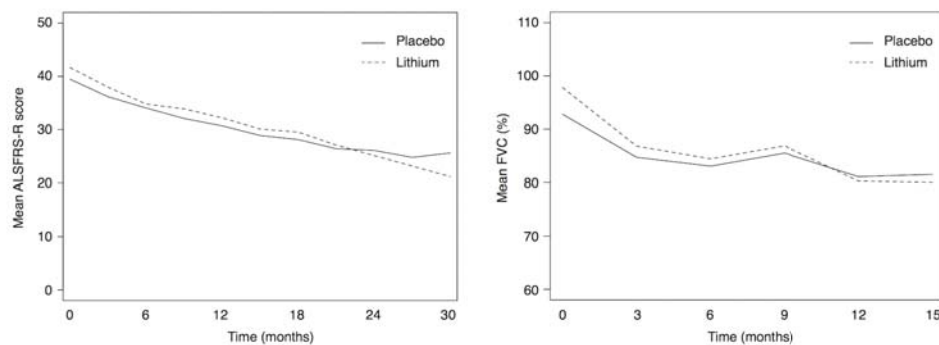


Figure 11.4 Secondary outcome measures

The level of daily functioning measured by the Revised Amyotrophic Lateral Sclerosis Functional Rating Scale (ALSFRS-R) and the forced vital capacity (FVC) for the lithium group (dashed line) compared to the placebo group (solid line). The decline over time does not differ significantly between treatment groups. As FVC measures could not be obtained in advanced stages of the disease, follow-up time is shorter compared to ALSFRS-R measures. It is important to note that the number of patients included in these analyses is declining over time as patients are sequentially included and die during the course of their disease (numbers at risk are given in Figure 11.3).

Lithium blood concentrations

Target blood concentrations (0.4–0.8 mEq/L) were established in 73% of patients on lithium. In addition, 87% of the measures were between 0.3 and 1.0 mEq/L. In a few patients consistent dose-dependent side-effects resulted in sub-target blood concentrations.

Adverse events

In the placebo group 35 of 67 patients and in the lithium group 39 of 66 patients experienced one or more serious adverse events (SAEs), which was not significantly different in the sequential safety monitoring as shown in Figure 11.5. Comparison of specific SAEs neither showed relevant differences (Table 11.2). One patient was unblinded after a toxic lithium concentration (1.9 mEq/L) was measured. This patient suffered from a rapid progression of bulbar weakness resulting in severe weight loss and dehydration. Study medication was discontinued but despite treatment with infusion of fluids and gastric tube placement she died shortly after this episode due to progressive respiratory failure. Another 6 SAEs in five patients were reported as possibly being related to the study medication by the (blinded) site investigators (chest pain/palpitations: $n = 3$; restlessness/confusion: $n = 2$; dehydration: $n = 1$). Three of these five patients received lithium.

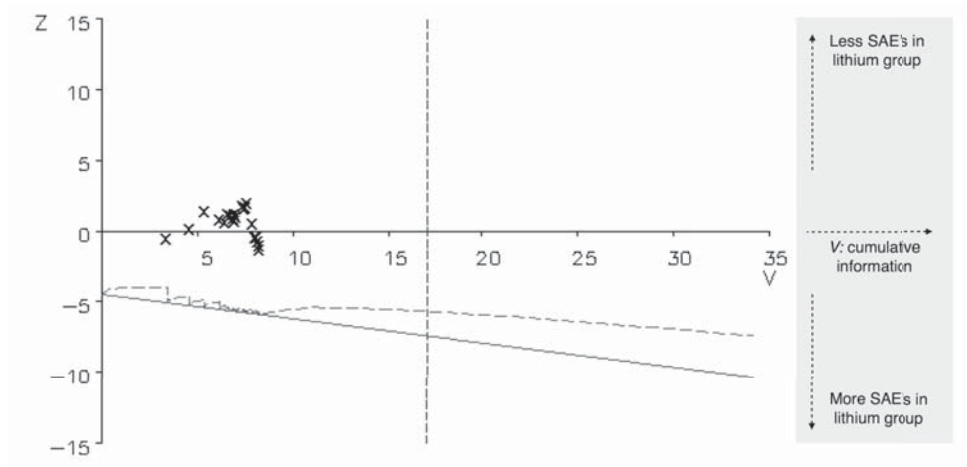


Figure 11.5 Sequential safety monitoring

On the horizontal axis, the amount of information V increases as time passes and SAEs accumulate. On the vertical axis, Z reflects the effect of lithium relative to placebo. If the sample path depicted by the X symbols were to cross the lower boundary, there would possibly be a safety problem for lithium. The inner boundary is the true boundary to be crossed (the so-called 'Christmas tree correction'), whereas the straight line that forms the lower boundary is the hypothetical boundary to be crossed if the analysis were truly sequential. The vertical boundary indicates the V -value corresponding to a sample size of 311.



Comparison of the classified adverse events – as reported by either investigators or patients – showed several events occurring in significantly more patients on lithium treatment: nausea (lithium group: $n = 17$; placebo group: $n = 6$; $p = 0.011$), vomiting (lithium group: $n = 12$; placebo group: $n = 2$; $p = 0.0043$), and polydipsia (lithium group: $n = 37$; placebo group: $n = 23$; $p = 0.014$). In Supplemental Table 11.2 the AEs are listed per organ system.

DISCUSSION

This study showed that lithium in combination with riluzole does not improve survival in patients with ALS. Lack of efficacy was established after the lower boundary of the sequential analysis was crossed, ruling out a modest beneficial effect of lithium defined as 15% increase in cumulative survival percentage. Secondary outcome measures supported the equivalence of lithium and placebo based on disease progression as measured by ALSFRS-R and vital capacity. Safety analyses did not reveal major safety issues, however,

Table 11.2 Overview of serious adverse events

	Lithium	Placebo
Gastrointestinal		
Gastric tube placement	29	23
Other	0	5
Respiratory		
Respiratory insufficiency	13	13
Pneumonia	2	7
Pulmonary embolism	2	1
Other	2	4
Cardiac complaints	1	1
Dehydration	2	0
Injury	1	1
Elective surgery	1	2
Agitation/delirium	0	1
Severe disease progression	1	0
Hospital admission due to neuropathic pain	0	1
Ischemic stroke	1	0
Septic arthritis	1	0
Allergic reaction to antibiotics	1	0

Data are numbers of patients with a certain event.

discontinuation of trial medication due to adverse effects occurred significantly more often in patients taking lithium compared to placebo.

Following the first pilot study (Fornai et al., 2008), preclinical studies with lithium could not consistently replicate the initial findings (Pizzasegola et al., 2009; Feng et al., 2008). In addition, a web-based observational study and five controlled clinical studies were initiated. It is noteworthy that the clinical trials with lithium published thus far have not solely focused on studying the efficacy of lithium but at the same time explored new trial designs (Aggarwal et al., 2010; Chio et al., 2010; Miller et al., 2011; Wicks et al., 2011) (see Supplemental Table 11.1). The only placebo-controlled trial thus far has efficiently ruled out a large and early effect of lithium (Aggarwal et al., 2010). However, we now report on a placebo-controlled trial ruling out a modest or delayed effect of lithium on cumulative survival using a sequential trial design (Groeneveld et al., 2007). This design

saved ‘time and patients’ as due to the sequential analysis the trial was stopped as soon as there was enough evidence for a lack of treatment effect. In addition, inefficacy of lithium for the treatment of ALS was demonstrated despite the inclusion of fewer patients than the calculated sample size had it been a fixed size trial design.

Defective cellular protein clearance (or autophagy) is increasingly recognized as an important mechanism of neurodegeneration in ALS (Deng et al., 2011; Neumann et al., 2006; Deng et al., 2010). These insights draw attention to candidate drugs promoting protein clearance such as lithium. A well-conducted randomized, clinical trial which provides a definite answer regarding the efficacy of lithium is mandatory. The current trial does not lend support for a beneficial effect of lithium on survival in ALS.

An important aim of this study was to assess the safety of lithium for the treatment of patients with ALS. The use of online questionnaires assessing potential side-effects yielded a large volume of safety data. Indeed, well-known side effects of lithium – e.g. nausea and polydipsia – occurred more frequently in the verum treated group. In line with a previous report, significantly more patients in the lithium group experienced these (and other) side effects which led to discontinuation of trial medication (Chio et al., 2010). Fortunately, we did not find any significant differences regarding the occurrence of SAEs. We, therefore, conclude that despite the known inconvenient side-effects, lithium can safely be given to patients with ALS.

The population participating in trials has been observed to be different from the incident cohort of patients with ALS. These differences are partly due to the in- and exclusion criteria as adopted in clinical trials and partly to the type of patients choosing to participate (Chio et al., 2011b). However, as most patients in this sequential trial were included shortly after diagnosis the clinical characteristics approached the incident cohort. This is best reflected by 29% bulbar onset patients participating which is close to the 30% bulbar onset based on epidemiological data (Huisman et al., 2011). A second limitation is the lack of different dosages since it may be hypothesized that the dosage used was not sufficient to induce effects. We examined the same dosage used in the initial pilot study, as this was found to be effective. A previous report comparing subtherapeutic (0.2–0.4 mEq/L) to therapeutic lithium treatment, found no dose-dependent effect (Chio et al., 2010). None of the previous studies on lithium in ALS have included higher dosages. As for the narrow therapeutic range of lithium and therefore the increased risk of toxicity, we refrained from including a higher dosage group out of concern about the safety of our patients. Third, the dropout rate for lithium trials tends to be higher compared to trials with other compounds in ALS,



which might have obscured the observed effects. We, therefore, performed an on-treatment analysis confirming lack of efficacy similar to the findings in the intention-to-treat analysis. Finally, it is noteworthy that little is known about potential interactions between lithium and riluzole. However, the limited evidence available suggests a potentiating rather than a detrimental effect of riluzole on the neuroprotective properties of lithium (Caldero et al., 2010).

In conclusion, this randomized, sequential, placebo-controlled trial demonstrated inefficacy of lithium for the treatment of ALS based on cumulative survival in a substantial cohort of patients. The use of a sequential trial design precludes unnecessary delay if the study drug is effective as well as undesirable continuation of an ineffective or even harmful treatment. The current results provide physicians with the evidence needed to adequately advise their patients with ALS on the use of lithium.

SUPPLEMENTAL INFORMATION

Supplemental Table 11.1 Overview of previous studies with lithium for the treatment of ALS

Author (year)	Patients (n)	Comparison with placebo	Follow-up (months)	Primary end-point	Efficacy	Safety
Fomai et al. (2008)	44	No (open label, no lithium; n = 28)	15	Survival	Prolonged survival in lithium group (p ≤ 0.05)	No issues reported
Aggarwal et al. (2010)	84	Yes (n = 44)	6	> 6 points decline in ALSFRS-R or death	No significant difference (p = 0.78)	No major concerns (more falls and back pain in lithium group; p < 0.05)
Chio et al. (2010)	171	No (subtherapeutic lithium 0.2-0.4 mEq/L; n = 84)	18	Survival or severe loss of autonomy	No significant difference (p = 0.94)	More discontinuations in therapeutic lithium group due to AEs/SAEs
Wicks et al. (2011)	596	No (open label, no lithium; n = 447)	12	ALSFRS-R, rate of decline	No significant difference (p = 0.22)	Not assessed
Miller et al. (2011)	107	No (historical controls; n = 249)	13	ALSFRS-R, rate of decline	Faster decline in lithium group (p = 0.04)	More SAEs than expected (based on historical data)
Verstraete et al. (2011)	133	Yes (placebo; n = 67)	31	Survival	No significant difference (p = 0.91)	No major concerns (more nausea, vomiting and thirst in lithium group; p < 0.05)

11



Supplemental Table 11.2 Overview of adverse events

Adverse events – classified per organ system – as occurred in the lithium and placebo group. Given are the number of unique events excluding multiple reports of a certain event in one subject. Between brackets are the number of patients in which these events occurred. Statistics by using a Fisher's exact test is performed on the number of patients. As such, gastrointestinal and genitourinary events occurred significantly more frequent in the lithium group ($p < 0.05$).

	Lithium	Placebo
Neurological	117 (58)	100 (54)
Psychiatric	6 (5)	4 (4)
Respiratory	15 (14)	29 (22)
Cardiac	5 (5)	4 (4)
Venous/lymphatic	7 (7)	1 (1)
Gastrointestinal	68 (42) *	48 (32)
Ear, nose, throat	7 (7)	6 (6)
Musculoskeletal	17 (12)	14 (13)
Endocrine	2 (2)	5 (4)
Dermatologic	33 (29)	25 (18)
Genitourinary	86 (48) *	57 (41)
Injury	13 (12)	8 (8)
Abnormal lab result	5 (5)	1 (1)
Other	91 (56)	89 (58)

Data are number of adverse events (occurring in n patients).

* Significantly more frequent ($p < 0.05$; Fisher's exact test).

12

Would riluzole be efficacious in the new ALS trial design?

Esther Verstraete
Jan H. Veldink
Leonard H. van den Berg

Lancet Neurol 2010; 9: 949-50



ABSTRACT (Aggarwal et al. Lancet Neurol. 2010)

Background: In a pilot study, lithium treatment slowed progression of amyotrophic lateral sclerosis (ALS). We aimed to confirm or disprove these findings by assessing the safety and efficacy of lithium in combination with riluzole in patients with ALS.

Methods: We did a double-blind, placebo-controlled trial with a time-to-event design. Between January and June, 2009, patients with ALS who were taking a stable dose of riluzole for at least 30 days were randomly assigned (1:1) by a centralised computer to receive either lithium or placebo. Patients, caregivers, investigators, and all site study staff with the exception of site pharmacists were masked to treatment assignment. The primary endpoint was the time to an event, defined as a decrease of at least six points on the revised ALS functional rating scale score or death. Interim analyses were planned for when 84 patients had been allocated treatment, 6 months later or after 55 events, and after 100 events. Analysis was by intention to treat. The stopping boundary for futility at the first interim analysis was a p value of at least 0.68. We used a log-rank test to compare the distributions of the time to an event between the lithium and placebo groups. This trial is registered with ClinicalTrials.gov, NCT00818389.

Findings: At the first interim analysis, 22 of 40 patients in the lithium group had an event compared with 20 of 44 patients in the placebo group (log rank $p = 0.51$). The hazard ratio of reaching the primary endpoint was 1.13 (95% CI 0.61–2.07). The study was stopped at the first interim analysis because criterion for futility was met ($p = 0.78$). The difference in mean decline in the ALS functional rating scale score between the lithium group and the placebo group was 0.15 (95% CI –0.43 to 0.73, $p = 0.61$). There were no major safety concerns. Falls ($p = 0.04$) and back pain ($p = 0.05$) were more common in the lithium group than in the placebo group.

Interpretation: We found no evidence that lithium in combination with riluzole slows progression of ALS more than riluzole alone. The time-to-event endpoint and use of prespecified interim analyses enabled a clear result to be obtained rapidly. This design should be considered for future trials testing the therapeutic efficacy of drugs that are easily accessible to people with ALS.

Comment on Aggarwal et al. Safety and efficacy of lithium in combination with riluzole for treatment of amyotrophic lateral sclerosis: a randomised, double-blind, placebo-controlled trial. [Lancet Neurol. 2010]

Aggarwal and colleagues report the results of a double-blind, placebo-controlled trial of lithium in patients with amyotrophic lateral sclerosis (ALS) (Aggarwal et al., 2010). Only one drug – riluzole – has proved effective in extending the lifespan of patients with ALS, and it does so by only 3–6 months (Bensimon et al., 1994; Lacomblez et al., 1996a). After the publication of a pilot study from Italy (Fornai et al., 2008), which showed a favourable effect of lithium in a transgenic mouse model of ALS and in an open-label study in 44 patients, Aggarwal and colleagues undertook their larger trial in Canada and the USA. This trial was designed to detect an effect of similar size to that in the pilot study, in which a 40% decrease in the rate of neurological decline was reported. Criteria for early stopping in the study by Aggarwal and colleagues were defined on the basis of this effect size and, indeed, the first interim analysis met the criterion for futility and the trial was stopped. This design has more advantages than the classic trial design, especially in the possibility for increased speed of drug screening, however, we have a few concerns.

First, we are concerned about the short treatment duration. The effect of riluzole was demonstrated in two placebo-controlled studies: the first included 155 patients with 21 months' follow-up (Bensimon et al., 1994), and the second was a dose-ranging study in 959 patients with 18 months' follow-up (Lacomblez et al., 1996a). In the study by Aggarwal and colleagues, on average, patients were on lithium or placebo for only 5.4 months, and 9 weeks were needed to reach therapeutic lithium serum concentrations. Of the 40 patients in the lithium group, six did not reach therapeutic drug concentrations, and only 27 patients were receiving lithium up to the final analysis. Could a treatment effect be expected in patients with ALS after such short exposure to the study drug? Second, the mean age of patients in the lithium group was higher than that in the placebo group (58.3 years vs 55.5 years). Because age is the most important prognostic factor for disease progression, this difference could have obscured a potential favourable effect of lithium. Randomisation according to the minimisation method could have prevented this drawback (Piepers et al., 2009). Third, we would like to emphasise the relevance of detecting small or moderate therapeutic effects, provided there are no safety concerns. A drug with a small therapeutic effect, such as riluzole, could be included in future combination treatments that have greater effects and could be important for the understanding of disease mechanisms (Kriz et al.,



2003). A more moderate (and realistic) effect of lithium cannot be ruled out in this trial design. Pilot studies often find large effect sizes, which after careful follow-up seem to be much smaller, albeit true (Ioannidis, 2008). We therefore propose that stopping rules in futility or sequential trial designs should be based on effect size in the range of the effect of riluzole (Piepers et al., 2009).

Futility or sequential trial designs for ALS are a promising alternative to a classic trial design in which sample size is fixed, because they allow stopping of a study as soon as a treatment effect can be significantly demonstrated or denied. However, realistic and more moderate stopping rules should be applied, and we believe a double-blind, placebo-controlled trial is still needed to show or exclude a more moderate effect of lithium in ALS.

13

General discussion



JUST IMAGINE...

2030

Every newborn is genetically screened for the risk of developing a number of diseases during lifetime, including ALS. This screening program has followed the heel prick and is based on the same principles. About 2.5% of the population turns out to be at risk for ALS, but only about 10% of this subpopulation will actually develop clinical symptoms and it is not known at what age the disease will manifest. Fortunately, there is an effective and non-invasive screening method available, advanced MRI-imaging of the brain, to evaluate the cortical surface in order to detect (focal) abnormalities (**chapter 7**). People at risk are screened starting at 18 years of age. If a focal, cortical abnormality or disease focus is found, this is usually an asymptomatic focus which is too small to cause symptoms, but which has the potential to spread throughout the brain and lead to progressive neurodegeneration. Which clinical phenotype will develop, bulbar or spinal onset, depends on the location of the disease focus. The organisation or architecture of the individual brain network has a role in the spread of disease e.g. the connectedness of a brain region will largely determine which brain region(s) will be involved next (**chapters 5 and 6**) and how fast other regions will become affected (**chapter 4**). However, before the disease develops and spreads further, the disease focus is irradiated, thereby impeding the development of clinical symptoms.

The ability to screen for ALS at an early stage – as, for example, is common for many years in breast cancer – and subsequently give focal treatment, has led to a significantly reduced mortality rate due to ALS. In addition, for the patients who still develop ALS, either because they were not at risk and therefore not included in the screening programme, or because they presented with a disseminated disease, survival has improved due to new disease-modifying drugs (e.g. by slowing disease spread). New potential treatments are effectively tested in worldwide trials facilitated by online data acquisition and using the sequential trial design (**chapters 11 and 12**).

We are still far from the scenario described above and the future will always be different from what we imagine it to be. However, a (dream) scenario like this greatly motivated us to perform the studies. Time will tell if any of our findings turn out to be of relevance for future patients with ALS.

Spread of disease

In this thesis we report on a number of observations, which support our hypothesis that spread of disease in ALS is guided by the brain's network structure (**chapters 3, 4, 5 and 6**).

Site of onset

The frequency of the initially affected body in ALS is almost evenly distributed over the bulbar, cervical and lumbosacral regions (**chapter 3**). The thoracic region is seldom the region of symptom onset (1.2% according to our data). This relative sparing of the thoracic region suggests that the chance of a triggering pathogenic event occurring is not similar for any level of the motor network, as has been suggested previously (Ravits and La Spada, 2009). Another indication that the site of onset is not random, is the observation that onset of symptoms in the limbs is preferentially distally located (Kanouchi et al., 2012). For the upper limbs this distal preference can even be further specified as being located in the muscles of the thenar complex (abductor pollicis brevis and first dorsal interosseous muscles), which are more frequently involved compared with the hypothenar muscle (abductor digiti minimi) (Eisen and Kuwabara, 2012). Both observations have been consistently reported, but not completely understood. Given the cortical representation of the motor system (Homunculus, see Figure 13.1), it is noticeable that the thoracic region corresponds with a very small region on the motor cortex and that the representation of the hypothenar muscle is less prominent compared to the thenar complex. The consistency between the frequency distribution in body region of onset and the size of its cortical representation might suggest that the disease focus has its onset in the upper motor neuron segment. Since the upper motor neuron segment connects monosynaptically with the lower motor neuron, spread to the corresponding spinal segment might occur very quickly. This type of spread is referred to as anterograde degeneration ('dying forward') (Eisen and Weber, 2001), opposing the retrograde degeneration ('dying back') hypothesis in which the triggering pathogenic event occurs in the lower motor neuron or even the neuromuscular junction (Chou and Norris, 1993).

Besides correspondence with cortical representation there are other indications that the site of onset is not random. For example, it has been shown that there is concordance between the site of onset and limb dominance (Turner et al., 2011). One possible explanation might be that excessive use increases the chance of triggering a pathogenic event (Veldink et al., 2005). In addition, it is well known that older age is associated with predominantly bulbar onset ALS (Chio et al., 2011). As older people tend to be less physically active, one might

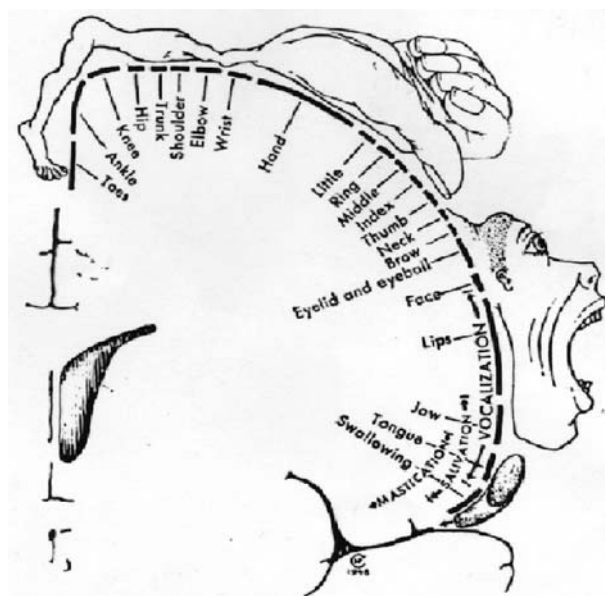


Figure 13.1 Representation of the different body regions on the motor cortex

This figure shows the Homunculus, representing the cortical area involved in motor control of the different body regions. Larger areas are devoted to body regions characterized by fine or complex movements and smaller areas to body regions characterized by gross movements involving few muscles. Hand, face, intraoral and, to some extent, foot muscles are particularly well represented (Penfield and Rasmussen, 1968).

question whether this change in activity has a role in the shift towards disease onset in the bulbar region.

Spread within the motor system

During the past few years, there has been a growing interest in disease spread in ALS. It has been suggested that motor neuron disease has a focal onset with contiguous spread throughout the motor system and that the fundamental molecular mechanisms might be uniform despite the apparently heterogeneous clinical course (Ravits and La Spada, 2009). We assessed symptom development – and thus indirectly spread of disease – in different MND phenotypes including ALS, as well as the pure upper and lower motor neuron syndromes: primary lateral sclerosis (PLS) and progressive muscular atrophy (PMA). Using self-reported data on symptom development, it was shown that there was a preferred spread to the opposite limb in all MND phenotypes (**chapter 3**). We concluded from our findings that there might be a role for neural connectivity in the spread of disease.

For the upper motor neuron this implies a role for inter-hemispheric spread through the corpus callosum, which has been shown to be both structurally (Smith, 1960; Filippini et al., 2010) and functionally impaired in ALS (Wittstock et al., 2007).

In **chapter 4**, we studied the structural and functional characteristics of the primary motor system using MRI data. This study confirmed reduced structural integrity of the corpus callosum; however, the functional connectivity between the right and left primary motor cortices was relatively preserved. Interestingly, we observed a positive correlation between functional connectivity and the rate of disease progression. This contradictory finding might support the corpus callosum as being an intermediate in the spread of disease in ALS. Our observation of increased functional connectedness in relation to disease progression was replicated in a larger study on structural and functional connectivity in ALS (Douaud et al., 2011).

One of the crucial questions in disease spread is why some patients have onset of symptoms in, for example, the right arm and subsequently develop symptoms in the left leg ('skipping pattern'). This observation appears to be in conflict with our hypothesis of disease spread guided by neural connectivity. However, it is important to note that the connectivity between upper motor neurons involved in controlling these 'distant' limbs is not zero, but less strong compared to the connectivity between opposite limbs. The chance of spread is, therefore, much smaller which is consistent with our observation that this type of distribution occurs less frequently.

Several studies have investigated survival or disease progression in relation to the site of onset. It is noticeable that patients with a lower limb onset have a markedly longer survival compared to patients with a bulbar onset of symptoms (Chio et al., 2011). Potential reasons given for this difference are that patients with bulbar weakness develop swallowing or respiratory difficulties much earlier in the disease process (Chio et al., 2009). In addition, bulbar onset patients are generally older, and age is a very strong predictor of survival. However, the observation that the spread of symptoms to other body regions is faster in bulbar onset compared to lower limb onset patients (**chapter 3**) suggests that a more rapid disease spread is another determinant for poorer survival rate (Fujimura-Kiyono et al., 2011). Little data is available on the connectivity of subregions within the primary motor cortex. It has, however, been shown that the precentral gyrus – in which the bulbar and cervical regions are represented – has a higher connectedness with the rest of the brain compared to the paracentral lobule, in which the lumbosacral region is represented (van den Heuvel and Sporns, 2011). We propose that increased neural connectivity of the site (or focus) of onset might facilitate spread and therefore be associated with a poorer prognosis.

Extra-motor involvement in ALS

ALS primarily targets the motor system, however, it is estimated that half of the patients have cognitive deficits, in addition to their motor symptoms (Raaphorst et al., 2010). This observation suggests there is a subset of patients in whom the disease spreads beyond the primary motor regions at such a level that it causes clinical symptoms. As the motor system is embedded in the brain network it might be expected that a disease like ALS, directly or indirectly, also affects other brain regions.

We examined how ALS affects the brain network by reconstructing the structural connections of the brain using diffusion tensor imaging (DTI) and comparing brain network integrity between patients and controls (**chapter 5**). A subnetwork of impaired connectivity was found, extending from the primary motor regions to other frontal, parietal and temporal regions. In order to further examine the extent to which these regions were linked to the primary motor regions (bilateral precentral gyrus), we mapped the motor connectivity in healthy controls and assessed the overlap between these regions and the regions of the impaired subnetwork in ALS. This analysis showed that regions connected with primary motor regions have a higher chance of being part of the impaired subnetwork in ALS, which might further support the notion that there is preferred spread of disease to regions strongly connected to the motor system. It is important to note that none of the studied patients had clinically overt cognitive deficits, however, formal neuropsychological testing was not performed in this cohort. In future research, when moving from group-wise analysis to a more individualized assessment, it is of great importance to relate brain network impairment to clinical or cognitive profiles.

Approaches similar to ours were used to study other neurodegenerative diseases. Specifically Alzheimer's disease and other dementia subtypes (including FTD) received considerable attention in early 2012 after two studies from two independent research groups found indications for transneuronal spread of disease (Raj et al., 2012; Zhou et al., 2012). It was shown that brain regions with a high connectivity to 'epicenters' of disease (i.e. regions with maximal atrophy) had an increased disease-related vulnerability. Since the underlying molecular mechanism – a TDP-43 proteinopathy – is in many cases identical in FTD and ALS, these results support our findings and might imply that universal mechanisms of spread are involved in different neurodegenerative diseases.

To further test our hypothesis of network-spread in ALS, we longitudinally assessed the structural brain network (**chapter 6**). This study revealed an expanding network of impaired

connectivity, showing both direct and indirect motor connections became involved over time. The initially impaired connections did not show progressive impairment. Converging results were revealed in our longitudinal cortical thickness assessment (**chapter 7**) as frontal and parietal regions (e.g. orbitofrontal and isthmus cingulate) showed cortical thinning over time without progressive involvement of primary motor regions. These findings on disease progression in ALS argue against shared or selective vulnerability hypotheses but provide additional support for disease spread guided by the architecture of the brain network.

Prion-like spread?

These imaging-based observations necessitate further research to improve our understanding of the underlying cellular and molecular mechanisms of disease spread. Unfortunately imaging data on the human brain network cannot directly inform us on cellular pathogenesis models. However, there is growing evidence suggesting that prion-like mechanisms might be involved in neurodegenerative diseases (Frost and Diamond, 2010; Jucker and Walker, 2011; Winner et al., 2011) which is in line with the observed network-spread of disease in ALS. The concept of prion-like spread is based on the ability of toxic, misfolded, nonprion protein species to let neighbouring, native counterparts adopt the same pathogenic configuration and subsequently move from neuron to neuron by transsynaptic transmission (Polymenidou and Cleveland, 2011; Guo et al., 2011; Munch et al., 2011). The natural occurrence of a certain protein in subpopulations of neurons might contribute to the vulnerability to disease. Different proteinopathies can cause ALS (e.g. TDP-43 and SOD1). It is known that familial ALS due to a mutation in the *SOD1* gene has a lower motor neuron dominant phenotype and is more resistant to cognitive involvement compared to ALS characterised by TDP-43 aggregates (Wicks et al., 2009; Ringholz et al., 2005). This observation might illustrate that indeed the vulnerability pattern is different depending on the underlying proteinopathy (Rohrer et al., 2011). We, therefore, suggest that neurodegenerative diseases, and specifically ALS, have a focal onset of disease with subsequent spread depending on the brain network architecture, as well as, the underlying proteinopathy.

Future directions

- Assessing the connectivity of subregions within the motor cortex might elucidate to what extent connectivity of the region of onset contributes to disease progression.

- To study the variable patterns of loss of connectivity in different genotypic ALS groups (gene-brain network interaction).
- Individual assessment of brain network impairment might enable staging of brain involvement in ALS.
- Cognitive deficits in patients with ALS should be assessed and linked to the extent or type of brain network involvement.
- Unraveling the molecular mechanisms involved in disease spread.

Biomarkers

The main finding from the biomarker studies we performed in ALS came from an imaging study measuring whole brain cortical thickness in 45 patients with ALS compared to a group of healthy controls (**chapter 7**). We found convincing cortical thinning in the bilateral precentral gyrus (primary motor regions) in ALS, suggesting this measure might be a marker for upper motor neuron involvement. In addition to the cross-sectional comparison between patients and controls, we investigated whether there was a relation with clinical markers and assessed how this measure changed over time. In contrast to what is generally considered to be a good biomarker, we did not find a correlation with clinical markers or progressive changes over time (Bowser et al., 2011). This does not, however, necessarily mean this measure is less informative about the disease, an aspect we will expand on in the following paragraphs.

Relevance of clinical correlation

A perfect correlation with a clinical measure means a biomarker has no additional value. Biomarkers should be complimentary to clinical assessment, just as electrophysiological investigation in ALS can reveal subclinical lower motor neuron involvement (Schrooten et al., 2011). Currently there is no measure for subclinical upper motor neuron involvement, which – from *post mortem* studies – is known to be common in ALS/PMA (Ince et al., 2003; Geser et al., 2011). The core clinical marker for ALS is the (revised) ALS functional rating scale (ALSFRS-R), which provides a fair indication of a patients' disabilities; however, patients with no upper motor neuron involvement at all can have a low ALSFRS-R score and vice versa. It does not seem rational to expect clinical (upper motor neuron) scores to correlate with imaging measures, which to some extent reflect the integrity of the upper motor neuron. But then how can we validate potential imaging markers in ALS? This is an important question for future neuroimaging studies.

Several options might be considered in order to validate imaging findings:

1. Clinical follow-up of patients (e.g. to observe if PMA patients with upper motor neuron involvement based on imaging measures develop upper motor neuron symptoms clinically during the course of disease or to see if patients with extra-motor involvement develop cognitive symptoms);
2. *Post mortem* examinations (e.g. correspondence of imaging findings with neuropathological findings).

A validated and objective upper motor neuron marker would improve diagnosis of ALS and truly enable differentiation between PMA and ALS, which might, for example, be relevant for the inclusion of patients in clinical trials.

Biomarkers and disease onset

Our cortical thickness study did not show progressive thinning of cortical motor regions over time, which led to the new hypothesis that the disease process might have started before the onset of clinical symptoms. Preclinical onset of neurodegeneration has been shown in Parkinson's (Wu et al., 2011) and Alzheimer's disease (Querbes et al., 2009; Dickerson et al., 2011). The human motor system also has a reserve capacity, which might allow ALS-related neurodegeneration to remain unnoticed until a relatively advanced stage. There have been studies on asymptomatic carriers of the SOD1-mutation in ALS suggesting degenerative changes are present before clinical onset (Ng et al., 2008). It would be of interest to see if asymptomatic carriers of familial ALS develop cortical thinning before symptoms occur.

Other biomarkers

In this thesis we report on other potential markers for which we used ultra-high field 7T MRI and newly developed acquisition sequences in two studies (**chapter 8 and 9**), as well as ELISA measurements of TDP-43 in plasma samples (**chapter 10**).

We aimed to disentangle which factors contribute to the fractional anisotropy reduction in the corticospinal tracts of patients with ALS using different MRI contrasts (**chapter 8**). This multimodal approach did not reveal any significant changes in contrast other than the known diffusivity changes. As the additional contrasts are sensitive to demyelination, we concluded that it is unlikely that demyelination is a primary cause of the reduced fractional anisotropy in ALS. Another 7T MRI study assessed the presence of microbleeds in sporadic ALS cases (**chapter 9**). Microbleeds were reported to be present in nervous

tissue of *SOD1*-mutant mice. Despite the highly sensitive acquisition sequence, we did not find indications for the presence of microbleeds in the patient group studied.

Our measures of TDP-43 protein in plasma revealed significantly raised levels in patients compared to healthy controls (**chapter 10**). This finding could be related to the cerebral accumulation of this protein. Future studies should aim to validate our findings and compare measurements in patients with those in ALS mimics.

Future directions

- Assessments of cortical thickness in subtypes of ALS (PLS, PMA, ALS/FTD), ALS mimics and asymptomatic carriers of familial ALS.
- Validation of cortical thickness as a marker for upper motor neuron involvement in ALS through (international) collaboration.
- Further efforts should be made to obtain longitudinal data, ideally both repeated imaging measures combined with clinical assessments (or only clinical follow-up in order to validate imaging findings).
- *Post mortem* examination of patients who participated in the MRI study to validate imaging findings (e.g. cortical thickness).

Clinical trials

We performed a randomised, placebo-controlled, double-blind, sequential trial studying the efficacy and safety of lithium in patients with ALS (**chapter 11**). Unfortunately our results did not support a beneficial effect of lithium on survival, nor disease progression. This trial has revealed the true effects of lithium, which are important for patients and physicians. However, much more was learned from the experience with lithium as a candidate drug for the treatment of ALS.

Importance of collaboration

During the course of our study, a number of publications appeared on other trials reporting lack of efficacy of lithium in ALS (see supplementary Table 11.1). These trials were all – in some way – different from the classical trial design in ALS, which is a placebo-controlled, randomised trial with survival as primary endpoint. Therefore, a definitive answer was still lacking, marking the relevance of continuing with our study. However, for patients with ALS the motivation to participate in a trial with lithium had,

ceased due to the negative reports; in particular potential safety concerns hampered the inclusion of new participants and was a reason for others to stop taking trial medication.

In the future, when there is a new candidate drug for ALS, there should be worldwide collaboration between ALS researchers in order to obtain a definitive answer concerning efficacy within a limited time period. As it is hardly feasible to reach complete harmonisation of study protocols or to obtain funding in a large number of countries and centres, we propose a prospective, sequential meta-analysis might be the optimal future trial design. Sequential analysis allows the trial to be halted as soon as efficacy or inefficacy of the candidate drug is shown, precluding unnecessary delay if the study drug is effective, or undesirable continuation of an ineffective or even harmful treatment (Groeneveld et al., 2007).

Future directions

- Candidate drugs in ALS should be studied by performing an international, prospective, sequential meta-analysis.
- Ideally, groups from several countries should perform combined clinical trials to avoid duplication and publication of underpowered trials.

Imagination

“The role of the imagination is to create new meanings and to discover connections that, even if obvious, seem to escape detection. Imagination begins with intuition, not intellect.” Paul Rand.

When interpreting results from scientific experiments, the ability of the human mind to form a mental image of what might be happening is crucial. Our research tools help to unlock bits and pieces of information that would otherwise have remained hidden to our perception; however, without imagination, research tools are useless.

In this thesis, we have challenged our imagination interpreting the ‘traces of disease’ we found. Let’s just hope some of our mental images will become reality...

Key findings

- Neuroimaging holds the promise for the future to become a routine part of the diagnostic workup in ALS.
- Symptom development in MND is not a random process, but there is symptoms spread preferably to the opposite limb.
- Our data support a role for connectivity within the motor network in both how fast and to which site the disease process spreads in ALS.
- ALS primarily targets the motor network and subsequently spreads to other brain regions guided by the structure of the brain network.
- Cortical thinning in the motor regions of the brain (precentral gyrus) is an important candidate marker for upper motor neuron involvement in MND.
- Lithium has no beneficial effect on survival, nor disease progression in patients with ALS.

References



REFERENCES

- Abe K, Takanashi M, Watanabe Y, et al. (2001) Decrease in N-acetylaspartate/creatine ratio in the motor area and the frontal lobe in amyotrophic lateral sclerosis. *Neuroradiology* 43:537-41.
- Abe O, Yamada H, Masutani Y, et al. (2004) Amyotrophic lateral sclerosis: diffusion tensor tractography and voxel-based analysis. *NMR Biomed.* 17:411-6.
- Abrahams S, Goldstein LH, Al-Chalabi A, et al. (1997) Relation between cognitive dysfunction and pseudobulbar palsy in amyotrophic lateral sclerosis. *J. Neurol. Neurosurg. Psychiatry* 62:464-72.
- Abrahams S, Goldstein LH, Simmons A, et al. (2004) Word retrieval in amyotrophic lateral sclerosis: a functional magnetic resonance imaging study. *Brain* 127:1507-17.
- Abrahams S, Goldstein LH, Suckling J, et al. (2005) Frontotemporal white matter changes in amyotrophic lateral sclerosis. *J. Neurol.* 252:321-31.
- Achard S, Bullmore E. (2007) Efficiency and cost of economical brain functional networks. *PLoS Comput. Biol.* 3:e17.
- Achard S, Salvador R, Whitcher B, Suckling J, Bullmore E. (2006) A resilient, low-frequency, small-world human brain functional network with highly connected association cortical hubs. *J. Neurosci.* 26:63-72.
- Acosta-Cabronero J, Williams GB, Pengas G, Nestor PJ. (2010) Absolute diffusivities define the landscape of white matter degeneration in Alzheimer's disease. *Brain* 133:529-39.
- Aertsen AM, Gerstein GL, Habib MK, Palm G. (1989) Dynamics of neuronal firing correlation: modulation of "effective connectivity". *J. Neurophysiol.* 61:900-17.
- Aggarwal SP, Zinman L, Simpson E, et al. (2010) Safety and efficacy of lithium in combination with riluzole for treatment of amyotrophic lateral sclerosis: a randomised, double-blind, placebo-controlled trial. *Lancet Neurol.* 9:481-8.
- Agosta F, Pagani E, Rocca MA, et al. (2007) Voxel-based morphometry study of brain volumetry and diffusivity in amyotrophic lateral sclerosis patients with mild disability. *Hum. Brain Mapp.* 28:1430-8.
- Agosta F, Gorno-Tempini ML, Pagani E, et al. (2009a) Longitudinal assessment of grey matter contraction in amyotrophic lateral sclerosis: A tensor based morphometry study. *Amyotroph. Lateral Scler.* 10:168-74.
- Agosta F, Rocca MA, Valsasina P, et al. (2009b) A longitudinal diffusion tensor MRI study of the cervical cord and brain in amyotrophic lateral sclerosis patients. *J. Neurol. Neurosurg. Psychiatry* 80:53-5.
- Agosta F, Pagani E, Petrolini M, et al. (2010a) Assessment of white matter tract damage in patients with amyotrophic lateral sclerosis: a diffusion tensor MR imaging tractography study. *AJNR Am. J. Neuroradiol.* 31:1457-61.
- Agosta F, Pagani E, Petrolini M, et al. (2010b) MRI predictors of long-term evolution in amyotrophic lateral sclerosis. *Eur. J. Neurosci.* 32:1490-6.
- Agosta F, Chio A, Cosottini M, et al. (2010c) The Present and the Future of Neuroimaging in Amyotrophic Lateral Sclerosis. *AJNR Am. J. Neuroradiol.* 31:1769-77

- Agosta F, Valsasina P, Absinta M, et al. (2011) Sensorimotor functional connectivity changes in amyotrophic lateral sclerosis. *Cereb. Cortex* 21:2291-8.
- Alstott J, Breakspear M, Hagmann P, Cammoun L, Sporns O. (2009) Modeling the impact of lesions in the human brain. *PLoS Comput. Biol.* 5:e1000408.
- Andersson JL, Skare S. (2002) A model-based method for retrospective correction of geometric distortions in diffusion-weighted EPI. *NeuroImage* 16:177-99.
- Andersson JL, Skare S, Ashburner J. (2003) How to correct susceptibility distortions in spin-echo echo-planar images: application to diffusion tensor imaging. *NeuroImage* 20:870-88.
- Aoki S, Iwata NK, Masutani Y, et al. (2005) Quantitative evaluation of the pyramidal tract segmented by diffusion tensor tractography: feasibility study in patients with amyotrophic lateral sclerosis. *Radiat. Med.* 23:195-9.
- Armon C. (2010) Is the lithium-for-ALS genie back in the bottle?: Not quite. *Neurology* 75:586-7.
- Ashburner J, Friston KJ. (2000) Voxel-based morphometry--the methods. *NeuroImage* 11:805-21.
- Atassi N, Ratai EM, Greenblatt DJ, et al. (2010) A phase I, pharmacokinetic, dosage escalation study of creatine monohydrate in subjects with amyotrophic lateral sclerosis. *Amyotroph. Lateral Scler.* 11:508-13.
- Bakkour A, Morris JC, Dickerson BC. (2009) The cortical signature of prodromal AD: regional thinning predicts mild AD dementia. *Neurology* 72:1048-55.
- Barkhof F, Simon JH, Fazekas F, et al. (2011) MRI monitoring of immunomodulation in relapse-onset multiple sclerosis trials. *Nat. Rev. Neurol.* 8:13-21.
- Barkovich AJ. (2005) Magnetic resonance techniques in the assessment of myelin and myelination. *J. Inherit. Metab. Dis.* 28:311-43.
- Bartels C, Mertens N, Hofer S, et al. (2008) Callosal dysfunction in amyotrophic lateral sclerosis correlates with diffusion tensor imaging of the central motor system. *Neuromuscul. Disord.* 18:398-407.
- Basser PJ, Mattiello J, LeBihan D. (1994) Estimation of the effective self-diffusion tensor from the NMR spin echo. *J. Magn. Reson. B* 103:247-54.
- Basser PJ, Pierpaoli C. (1996) Microstructural and physiological features of tissues elucidated by quantitative-diffusion-tensor MRI. *J. Magn. Reson.* 111:209-19.
- Basser PJ, Pajevic S, Pierpaoli C, Duda J, Aldroubi A. (2000) In vivo fiber tractography using DT-MRI data. *Magn. Reson. Med.* 44:625-32.
- Bassett DS, Bullmore ET, Meyer-Lindenberg A, Apud JA, Weinberger DR, Coppola R. (2009) Cognitive fitness of cost-efficient brain functional networks. *Proc. Natl. Acad. Sci. U. S. A.* 106:11747-52.
- Bassett DS, Greenfield DL, Meyer-Lindenberg A, Weinberger DR, Moore SW, Bullmore ET. (2010) Efficient physical embedding of topologically complex information processing networks in brains and computer circuits. *PLoS Comput. Biol.* 6:e1000748.
- Beaulieu C, Allen PS. (1994a) Determinants of anisotropic water diffusion in nerves. *Magn. Reson. Med.* 31:394-400.

References

- Beaulieu C, Allen PS. (1994b) Water diffusion in the giant axon of the squid: implications for diffusion-weighted MRI of the nervous system. *Magn. Reson. Med.* 32:579-83.
- Beaulieu C. (2002) The basis of anisotropic water diffusion in the nervous system - a technical review. *NMR Biomed.* 15:435-55.
- Becker JA, Hedden T, Carmasin J, et al. (2011) Amyloid-beta associated cortical thinning in clinically normal elderly. *Ann. Neurol.* 69:1032-42.
- Beckmann CF, DeLuca M, Devlin JT, Smith SM. (2005) Investigations into resting-state connectivity using independent component analysis. *Philos. Trans. R. Soc. Lond. B. Biol. Sci.* 360:1001-13.
- Behrens TE, Woolrich MW, Jenkinson M, et al. (2003) Characterization and propagation of uncertainty in diffusion-weighted MR imaging. *Magn. Reson. Med.* 50:1077-88.
- Bensimon G, Lacomblez L, Meininger V. (1994) A controlled trial of riluzole in amyotrophic lateral sclerosis. ALS/Riluzole Study Group. *N. Engl. J. Med.* 330:585-91.
- Bian Q, Shi T, Chuang DM, Qian Y. (2007) Lithium reduces ischemia-induced hippocampal CA1 damage and behavioral deficits in gerbils. *Brain Res.* 1184:270-6.
- Biswal B, Yetkin FZ, Haughton VM, Hyde JS. (1995) Functional connectivity in the motor cortex of resting human brain using echo-planar MRI. *Magn. Reson. Med.* 34:537-41.
- Blain CR, Williams VC, Johnston C, et al. (2007) A longitudinal study of diffusion tensor MRI in ALS. *Amyotroph. Lateral Scler.* 8:348-55.
- Block W, Karitzky J, Traber F, et al. (1998) Proton magnetic resonance spectroscopy of the primary motor cortex in patients with motor neuron disease: subgroup analysis and follow-up measurements. *Arch. Neurol.* 55:931-6.
- Block W, Traber F, Flacke S, Jessen F, Pohl C, Schild H. (2002) In-vivo proton MR-spectroscopy of the human brain: assessment of N-acetylaspartate (NAA) reduction as a marker for neurodegeneration. *Amino Acids* 23:317-23.
- Bouwman CJ, Wilmink JT, Mess WH, Backes WH. (2008) Spinal cord functional MRI at 3 T: gradient echo echo-planar imaging versus turbo spin echo. *NeuroImage* 43:288-96.
- Bowen BC, Pattany PM, Bradley WG, et al. (2000) MR imaging and localized proton spectroscopy of the precentral gyrus in amyotrophic lateral sclerosis. *AJNR Am. J. Neuroradiol.* 21:647-58.
- Bowen DM, Procter AW, Mann DM, et al. (2008) Imbalance of a serotonergic system in frontotemporal dementia: implication for pharmacotherapy. *Psychopharmacology* 196:603-10.
- Bowser R, Turner MR, Shefner J. (2011) Biomarkers in amyotrophic lateral sclerosis: opportunities and limitations. *Nat. Rev. Neurol.* 7:631-8.
- Braak H, Braak E, Bohl J. (1993) Staging of Alzheimer-related cortical destruction. *Eur. Neurol.* 33:403-8.
- Bradley WG, Bowen BC, Pattany PM, Rotta F. (1999) 1H-magnetic resonance spectroscopy in amyotrophic lateral sclerosis. *J. Neurol. Sci.* 169:84-6.
- Brooks BR, Sufit RL, DePaul R, Tan YD, Sanjak M, Robbins J. (1991) Design of clinical therapeutic trials in amyotrophic lateral sclerosis. *Adv. Neurol.* 56:521-46.

- Brooks BR. (1991) The role of axonal transport in neurodegenerative disease spread: a meta-analysis of experimental and clinical poliomyelitis compares with amyotrophic lateral sclerosis. *Can. J. Neurol. Sci.* 18:435-8.
- Brooks BR, Miller RG, Swash M, Munsat TL, World Federation of Neurology Research Group on Motor Neuron Diseases. (2000) El Escorial revisited: revised criteria for the diagnosis of amyotrophic lateral sclerosis. *Amyotroph. Lateral Scler.* 1:293-9.
- Brooks JC, Beckmann CF, Miller KL, et al. (2008) Physiological noise modelling for spinal functional magnetic resonance imaging studies. *NeuroImage* 39:680-92.
- Brownell B, Oppenheimer DR, Hughes JT. (1970) The central nervous system in motor neurone disease. *J. Neurol. Neurosurg. Psychiatry* 33:338-57.
- Budde MD, Kim JH, Liang HF, et al. (2007) Toward accurate diagnosis of white matter pathology using diffusion tensor imaging. *Magn. Reson. Med.* 57:688-95.
- Budde MD, Kim JH, Liang HF, Russell JH, Cross AH, Song SK. (2008) Axonal injury detected by in vivo diffusion tensor imaging correlates with neurological disability in a mouse model of multiple sclerosis. *NMR Biomed.* 21:589-97.
- Bullmore E, Sporns O. (2009) Complex brain networks: graph theoretical analysis of structural and functional systems. *Nat. Rev.* 10:186-98.
- Caldero J, Brunet N, Tarabal O, et al. (2010) Lithium prevents excitotoxic cell death of motoneurons in organotypic slice cultures of spinal cord. *Neuroscience* 165:1353-69.
- Canu E, Agosta F, Riva N, et al. (2011) The topography of brain microstructural damage in amyotrophic lateral sclerosis assessed using diffusion tensor MR imaging. *AJNR Am. J. Neuroradiol.* 32:1307-14.
- Carew JD, Nair G, Andersen PM, et al. (2011a) Presymptomatic spinal cord neurometabolic findings in SOD1-positive people at risk for familial ALS. *Neurology* 77:1370-5.
- Carew JD, Nair G, Pineda-Alonso N, Usher S, Hu X, Benatar M. (2011b) Magnetic resonance spectroscopy of the cervical cord in amyotrophic lateral sclerosis. *Amyotroph. Lateral Scler.* 12:185-91.
- Carrara G, Carapelli C, Venturi F, et al. (2012) A distinct MR imaging phenotype in amyotrophic lateral sclerosis: correlation between T1 magnetization transfer contrast hyperintensity along the corticospinal tract and diffusion tensor imaging analysis. *AJNR Am. J. Neuroradiol.* 33:733-9.
- Carvalho MD, Swash M. (2009) Awaji diagnostic algorithm increases sensitivity of El Escorial criteria for ALS diagnosis. *Amyotroph. Lateral Scler.* 10:53-7.
- Cauchemez S, Bhattarai A, Marchbanks TL, et al. (2011) Role of social networks in shaping disease transmission during a community outbreak of 2009 H1N1 pandemic influenza. *Proc. Natl. Acad. Sci. U. S. A.* 108:2825-30.
- Cedarbaum JM, Stambler N, Malta E, et al. (1999) The ALSFRS-R: a revised ALS functional rating scale that incorporates assessments of respiratory function. BDNF ALS Study Group (Phase III). *J. Neurol. Sci.* 169:13-21.
- Chang JL, Lomen-Hoerth C, Murphy J, et al. (2005a) A voxel-based morphometry study of patterns of brain atrophy in ALS and ALS/FTLD. *Neurology* 65:75-80.

References

- Chang LC, Jones DK, Pierpaoli C. (2005b) RESTORE: robust estimation of tensors by outlier rejection. *Magn. Reson. Med.* 53:1088-95.
- Charil A, Corbo M, Filippi M, et al. (2009) Structural and metabolic changes in the brain of patients with upper motor neuron disorders: a multiparametric MRI study. *Amyotroph. Lateral Scler.* 10:269-79.
- Chen G, Ward BD, Xie C, et al. (2011) Classification of Alzheimer Disease, Mild Cognitive Impairment, and Normal Cognitive Status with Large-Scale Network Analysis Based on Resting-State Functional MR Imaging. *Radiology* 259:213-21.
- Chen Z, Ma L. (2010) Grey matter volume changes over the whole brain in amyotrophic lateral sclerosis: A voxel-wise meta-analysis of voxel based morphometry studies. *Amyotroph. Lateral Scler.* 11:549-54.
- Chen ZJ, He Y, Rosa-Neto P, Germann J, Evans AC. (2008) Revealing modular architecture of human brain structural networks by using cortical thickness from MRI. *Cereb. Cortex* 18:2374-81.
- Chio A, Logroscino G, Hardiman O, et al. (2009) Prognostic factors in ALS: A critical review. *Amyotroph. Lateral Scler.* 10:310-23.
- Chio A, Borghero G, Calvo A, et al. (2010) Lithium carbonate in amyotrophic lateral sclerosis: Lack of efficacy in a dose-finding trial. *Neurology* 75:619-25.
- Chio A, Calvo A, Moglia C, Mazzini L, Mora G, PARALS study group. (2011a) Phenotypic heterogeneity of amyotrophic lateral sclerosis: a population based study. *J. Neurol. Neurosurg. Psychiatry* 82:740-6.
- Chio A, Canosa A, Gallo S, et al. (2011b) ALS clinical trials: do enrolled patients accurately represent the ALS population? *Neurology* 77:1432-7.
- Choi JK, Kustermann E, Dedeoglu A, Jenkins BG. (2009) Magnetic resonance spectroscopy of regional brain metabolite markers in FALS mice and the effects of dietary creatine supplementation. *Eur. J. Neurosci.* 30:2143-50.
- Choi JK, Dedeoglu A, Jenkins BG. (2010) Longitudinal monitoring of motor neuron circuitry in FALS rats using in-vivo phMRI. *Neuroreport* 21:157-62.
- Chou SM, Norris FH. (1993) Amyotrophic lateral sclerosis: lower motor neuron disease spreading to upper motor neurons. *Muscle Nerve* 16:864-9.
- Chuang DM, Chen RW, Chalecka-Franaszek E, et al. (2002) Neuroprotective effects of lithium in cultured cells and animal models of diseases. *Bipolar Disord.* 4:129-36.
- Ciccarelli O, Behrens TE, Altmann DR, et al. (2006) Probabilistic diffusion tractography: a potential tool to assess the rate of disease progression in amyotrophic lateral sclerosis. *Brain* 129:1859-71.
- Ciccarelli O, Behrens TE, Johansen-Berg H, et al. (2009) Investigation of white matter pathology in ALS and PLS using tract-based spatial statistics. *Hum. Brain Mapp.* 30:615-24.
- Clare S, Jezzard P. (2001) Rapid T(1) mapping using multislice echo planar imaging. *Magn. Reson. Med.* 45:630-4.
- Clavaguera F, Bolmont T, Crowther RA, et al. (2009) Transmission and spreading of tauopathy in transgenic mouse brain. *Nat. Cell Biol.* 11:909-13.
- Cohen-Adad J, Descoteaux M, Rossignol S, Hoge RD, Deriche R, Benali H. (2008) Detection of multiple pathways in the spinal cord using q-ball imaging. *NeuroImage* 42:739-49.

- Cordes D, Haughton VM, Arfanakis K, et al. (2000) Mapping functionally related regions of brain with functional connectivity MR imaging. *AJNR Am. J. Neuroradiol.* 21:1636-44.
- Cordes D, Haughton VM, Arfanakis K, et al. (2001) Frequencies contributing to functional connectivity in the cerebral cortex in "resting-state" data. *AJNR Am. J. Neuroradiol.* 22:1326-33.
- Cosottini M, Giannelli M, Siciliano G, et al. (2005) Diffusion-tensor MR imaging of corticospinal tract in amyotrophic lateral sclerosis and progressive muscular atrophy. *Radiology* 237:258-64.
- Cosottini M, Giannelli M, Vannozzi F, et al. (2010) Evaluation of corticospinal tract impairment in the brain of patients with amyotrophic lateral sclerosis by using diffusion tensor imaging acquisition schemes with different numbers of diffusion-weighting directions. *J. Comput. Assist. Tomogr.* 34:746-50.
- Cosottini M, Pesaresi I, Piazza S, et al. (2012) Structural and functional evaluation of cortical motor areas in Amyotrophic Lateral Sclerosis. *Exp. Neurol.* 234:169-80.
- Cudkowicz ME, Katz J, Moore DH, et al. (2010) Toward more efficient clinical trials for amyotrophic lateral sclerosis. *Amyotroph. Lateral Scler.* 11:259-65.
- Cwik VA, Hanstock CC, Allen PS, Martin WR. (1998) Estimation of brainstem neuronal loss in amyotrophic lateral sclerosis with in vivo proton magnetic resonance spectroscopy. *Neurology* 50:72-7.
- da Rocha AJ, Maia AC, Jr, Nogueira RG, Lederman HM. (1999) Magnetic resonance findings in amyotrophic lateral sclerosis using a spin echo magnetization transfer sequence. Preliminary report. *Arq. Neuropsiquiatr.* 57:912-5.
- da Rocha AJ, Oliveira AS, Fonseca RB, Maia AC, Jr, Buainain RP, Lederman HM. (2004) Detection of corticospinal tract compromise in amyotrophic lateral sclerosis with brain MR imaging: relevance of the T1-weighted spin-echo magnetization transfer contrast sequence. *AJNR Am. J. Neuroradiol.* 25:1509-15.
- da Rocha AJ, Maia AC, Jr, Valerio BC. (2012) Corticospinal tract MR signal-intensity pseudonormalization on magnetization transfer contrast imaging: a potential pitfall in the interpretation of the advanced compromise of upper motor neurons in amyotrophic lateral sclerosis. *AJNR Am. J. Neuroradiol.* 33:E79-80.
- Dadon-Nachum M, Melamed E, Offen D. (2011) The "dying-back" phenomenon of motor neurons in ALS. *J. Mol. Neurosci.* 43:470-7.
- Dalakas MC, Hatazawa J, Brooks RA, Di Chiro G. (1987) Lowered cerebral glucose utilization in amyotrophic lateral sclerosis. *Ann. Neurol.* 22:580-6.
- Damoiseaux JS, Rombouts SA, Barkhof F, et al. (2006) Consistent resting-state networks across healthy subjects. *Proc. Natl. Acad. Sci. U. S. A.* 103:13848-53.
- Damoiseaux JS, Beckmann CF, Arigita EJ, et al. (2008) Reduced resting-state brain activity in the "default network" in normal aging. *Cereb. Cortex* 18:1856-64.
- Daoud H, Valdmanis PN, Kabashi E, et al. (2009) Contribution of TARDBP mutations to sporadic amyotrophic lateral sclerosis. *J. Med. Genet.* 46:112-4.
- DeFelipe J, Arellano JI, Gomez A, Azmitia EC, Munoz A. (2001) Pyramidal cell axons show a local specialization for GABA and 5-HT inputs in monkey and human cerebral cortex. *J. Comp. Neurol.* 433:148-55.

References

- DeJesus-Hernandez M, Mackenzie IR, Boeve BF, et al. (2011) Expanded GGGGCC hexanucleotide repeat in noncoding region of C9ORF72 causes chromosome 9p-linked FTD and ALS. *Neuron* 72:245-56.
- del Aguila MA, Longstreth WT, Jr, McGuire V, Koepsell TD, van Belle G. (2003) Prognosis in amyotrophic lateral sclerosis: a population-based study. *Neurology* 60:813-9.
- Deng HX, Zhai H, Bigio EH, et al. (2010) FUS-immunoreactive inclusions are a common feature in sporadic and non-SOD1 familial amyotrophic lateral sclerosis. *Ann. Neurol.* 67:739-48.
- Deng HX, Chen W, Hong ST, et al. (2011) Mutations in UBQLN2 cause dominant X-linked juvenile and adult-onset ALS and ALS/dementia. *Nature* 477:211-5.
- Deoni SC. (2010) Quantitative relaxometry of the brain. *Top. Magn. Reson. Imaging* 21:101-13.
- Desikan RS, Segonne F, Fischl B, et al. (2006) An automated labeling system for subdividing the human cerebral cortex on MRI scans into gyral based regions of interest. *NeuroImage* 31:968-80.
- Dickerson BC, Stoub TR, Shah RC, et al. (2011) Alzheimer-signature MRI biomarker predicts AD dementia in cognitively normal adults. *Neurology* 76:1395-402.
- Ding XQ, Kollewé K, Blum K, et al. (2011) Value of quantitative analysis of routine clinical MRI sequences in ALS. *Amyotroph. Lateral Scler.* 12:406-13.
- Douaud G, Filippini N, Knight S, Talbot K, Turner MR. (2011) Integration of structural and functional magnetic resonance imaging in amyotrophic lateral sclerosis. *Brain* 134:3470-9.
- Dula AN, Asche EM, Landman BA, et al. (2011) Development of chemical exchange saturation transfer at 7 T. *Magn. Reson. Med.* 66:831-8.
- Eisele YS, Obermüller U, Heilbronner G, et al. (2010) Peripherally applied Abeta-containing inoculates induce cerebral beta-amyloidosis. *Science* 330:980-2.
- Eisen A, Swash M. (2001) Clinical neurophysiology of ALS. *Clin. Neurophysiol.* 112:2190-201.
- Eisen A, Weber M. (2001) The motor cortex and amyotrophic lateral sclerosis. *Muscle Nerve* 24:564-73.
- Eisen A. (2009) Amyotrophic lateral sclerosis-Evolutionary and other perspectives. *Muscle Nerve* 40:297-304.
- Eisen A, Kuwabara S. (2012) The split hand syndrome in amyotrophic lateral sclerosis. *J. Neurol. Neurosurg. Psychiatry* 83:399-403.
- Elamin M, Phukan J, Bede P, et al. (2011) Executive dysfunction is a negative prognostic indicator in patients with ALS without dementia. *Neurology* 76:1263-9.
- Ellis CM, Simmons A, Andrews C, Dawson JM, Williams SC, Leigh PN. (1998) A proton magnetic resonance spectroscopic study in ALS: correlation with clinical findings. *Neurology* 51:1104-9.
- Ellis CM, Simmons A, Jones DK, et al. (1999) Diffusion tensor MRI assesses corticospinal tract damage in ALS. *Neurology* 53:1051-8.
- Ellis CM, Suckling J, Amaro E, Jr, et al. (2001) Volumetric analysis reveals corticospinal tract degeneration and extramotor involvement in ALS. *Neurology* 57:1571-8.
- Evans MC, MODO M, Talbot K, Sibson N, Turner MR. (2012) Magnetic resonance imaging of pathological processes in rodent models of amyotrophic lateral sclerosis. *Amyotroph. Lateral Scler.* 13:288-301.

- Eyler LT, Prom-Wormley E, Panizzon MS, et al. (2011) Genetic and Environmental Contributions to Regional Cortical Surface Area in Humans: A Magnetic Resonance Imaging Twin Study. *Cereb. Cortex* 21:2313-21.
- Fatouros PP, Marmarou A. (1999) Use of magnetic resonance imaging for in vivo measurements of water content in human brain: method and normal values. *J. Neurosurg.* 90:109-15.
- Feng HL, Leng Y, Ma CH, Zhang J, Ren M, Chuang DM. (2008) Combined lithium and valproate treatment delays disease onset, reduces neurological deficits and prolongs survival in an amyotrophic lateral sclerosis mouse model. *Neuroscience* 155:567-72.
- Figley CR, Stroman PW. (2009) Development and validation of retrospective spinal cord motion time-course estimates (RESPITE) for spin-echo spinal fMRI: Improved sensitivity and specificity by means of a motion-compensating general linear model analysis. *NeuroImage* 44:421-7.
- Filippi M, Agosta F, Abrahams S, et al. (2010) EFNS guidelines on the use of neuroimaging in the management of motor neuron diseases. *Eur. J. Neurol.* 17:526-e20.
- Filippini N, Douaud G, Mackay CE, Knight S, Talbot K, Turner MR. (2010) Corpus callosum involvement is a consistent feature of amyotrophic lateral sclerosis. *Neurology* 75:1645-52.
- Fischl B, Sereno MI, Dale AM. (1999) Cortical surface-based analysis. II: Inflation, flattening, and a surface-based coordinate system. *NeuroImage* 9:195-207.
- Fischl B, Dale AM. (2000) Measuring the thickness of the human cerebral cortex from magnetic resonance images. *Proc. Natl. Acad. Sci. U. S. A.* 97:11050-5.
- Fischl B, van der Kouwe A, Destrieux C, et al. (2004) Automatically parcellating the human cerebral cortex. *Cereb. Cortex* 14:11-22.
- Fornai F, Longone P, Cafaro L, et al. (2008) Lithium delays progression of amyotrophic lateral sclerosis. *Proc. Natl. Acad. Sci. U. S. A.* 105:2052-7.
- Fornito A, Zalesky A, Bullmore ET. (2010) Network scaling effects in graph analytic studies of human resting-state FMRI data. *Front. Syst. Neurosci.* 4:22.
- Foulds P, McAuley E, Gibbons L, et al. (2008) TDP-43 protein in plasma may index TDP-43 brain pathology in Alzheimer's disease and frontotemporal lobar degeneration. *Acta Neuropathol.* 116:141-6.
- Foulds PG, Davidson Y, Mishra M, et al. (2009) Plasma phosphorylated-TDP-43 protein levels correlate with brain pathology in frontotemporal lobar degeneration. *Acta Neuropathol.* 118:647-58.
- Freund PA, Dalton C, Wheeler-Kingshott CA, et al. (2010) Method for simultaneous voxel-based morphometry of the brain and cervical spinal cord area measurements using 3D-MDEFT. *J. Magn. Reson. Imaging* 32:1242-7.
- Friston KJ, Frith CD, Liddle PF, Frackowiak RS. (1993) Functional connectivity: the principal-component analysis of large (PET) data sets. *J. Cereb. Blood Flow Metab.* 13:5-14.
- Frost B, Diamond MI. (2010) Prion-like mechanisms in neurodegenerative diseases. *Nat. Rev. Neurosci.* 11:155-9.

References

- Fujimura-Kiyono C, Kimura F, Ishida S, et al. (2011) Onset and spreading patterns of lower motor neuron involvements predict survival in sporadic amyotrophic lateral sclerosis. *J. Neurol. Neurosurg. Psychiatry* 82:1244-9.
- Garbuzova-Davis S, Saporta S, Haller E, et al. (2007) Evidence of compromised blood-spinal cord barrier in early and late symptomatic SOD1 mice modeling ALS. *PLoS ONE* 2:e1205.
- Gargiulo-Monachelli GM, Janota F, Bettini M, Shoosmith CL, Strong MJ, Sica RE. (2012) Regional spread pattern predicts survival in patients with sporadic amyotrophic lateral sclerosis. *Eur. J. Neurol.* 19:834-41.
- Geser F, Stein B, Partain M, et al. (2011) Motor neuron disease clinically limited to the lower motor neuron is a diffuse TDP-43 proteinopathy. *Acta Neuropathol.* 121:509-17.
- Ghidoni R, Benussi L, Glionna M, Franzoni M, Binetti G. (2008) Low plasma progranulin levels predict progranulin mutations in frontotemporal lobar degeneration. *Neurology* 71:1235-9.
- Giordana MT, Ferrero P, Grifoni S, Pellerino A, Naldi A, Montuschi A. (2011) Dementia and cognitive impairment in amyotrophic lateral sclerosis: a review. *Neurol. Sci.* 32:9-16.
- Giroud M, Walker P, Bernard D, et al. (1996) Reduced brain N-acetyl-aspartate in frontal lobes suggests neuronal loss in patients with amyotrophic lateral sclerosis. *Neurol. Res.* 18:241-3.
- Glasser MF, Van Essen DC. (2011) Mapping human cortical areas in vivo based on myelin content as revealed by T1- and T2-weighted MRI. *J. Neurosci.* 31:11597-616.
- Goldstein LH, Newsom-Davis IC, Bryant V, Brammer M, Leigh PN, Simmons A. (2011) Altered patterns of cortical activation in ALS patients during attention and cognitive response inhibition tasks. *J. Neurol.* 258:2186-98.
- Gordon PH, Cheng B, Katz IB, et al. (2006) The natural history of primary lateral sclerosis. *Neurology* 66:647-53.
- Gordon PH, Goetz RR, Rabkin JG, et al. (2010) A prospective cohort study of neuropsychological test performance in ALS. *Amyotroph. Lateral Scler.* 11:312-20.
- Govindaraju V, Young K, Maudsley AA. (2000) Proton NMR chemical shifts and coupling constants for brain metabolites. *NMR Biomed.* 13:129-53.
- Graham JM, Papadakis N, Evans J, et al. (2004) Diffusion tensor imaging for the assessment of upper motor neuron integrity in ALS. *Neurology* 63:2111-9.
- Gredal O, Rosenbaum S, Topp S, Karlsborg M, Strange P, Werdelin L. (1997) Quantification of brain metabolites in amyotrophic lateral sclerosis by localized proton magnetic resonance spectroscopy. *Neurology* 48:878-81.
- Greenberg SM, Vernooij MW, Cordonnier C, et al. (2009) Cerebral microbleeds: a guide to detection and interpretation. *Lancet Neurol.* 8:165-74.
- Greicius M. (2008) Resting-state functional connectivity in neuropsychiatric disorders. *Curr. Opin. Neurol.* 21:424-30.
- Greicius MD, Krasnow B, Reiss AL, Menon V. (2003) Functional connectivity in the resting brain: a network analysis of the default mode hypothesis. *Proc. Natl. Acad. Sci. U. S. A.* 100:253-8.

- Greicius MD, Supekar K, Menon V, Dougherty RF. (2008) Resting-State Functional Connectivity Reflects Structural Connectivity in the Default Mode Network. *Cereb. Cortex* 19:72-8.
- Groeneveld GJ, Veldink JH, van der Tweel I, et al. (2003) A randomized sequential trial of creatine in amyotrophic lateral sclerosis. *Ann. Neurol.* 53:437-45.
- Groeneveld GJ, van der Tweel I, Wokke JH, van den Berg LH. (2004) Sequential designs for clinical trials in amyotrophic lateral sclerosis. *Amyotroph. Lateral Scler.* 5:202-7.
- Groeneveld GJ, Graf M, van der Tweel I, van den Berg LH, Ludolph AC. (2007) Alternative trial design in amyotrophic lateral sclerosis saves time and patients. *Amyotroph. Lateral Scler.* 8:266-9.
- Grosskreutz J, Kaufmann J, Fradrich J, Dengler R, Heinze HJ, Peschel T. (2006) Widespread sensorimotor and frontal cortical atrophy in Amyotrophic Lateral Sclerosis. *BMC Neurol.* 6:17.
- Grosskreutz J, Peschel T, Unrath A, Dengler R, Ludolph AC, Kassubek J. (2008) Whole brain-based computerized neuroimaging in ALS and other motor neuron disorders. *Amyotroph. Lateral Scler.* 9:238-48.
- Grossman M, Anderson C, Khan A, Avants B, Elman L, McCluskey L. (2008) Impaired action knowledge in amyotrophic lateral sclerosis. *Neurology* 71:1396-401.
- Guo W, Chen Y, Zhou X, et al. (2011) An ALS-associated mutation affecting TDP-43 enhances protein aggregation, fibril formation and neurotoxicity. *Nat. Struct. Mol. Biol.* 18:822-30.
- Gurney ME, Pu H, Chiu AY, et al. (1994) Motor neuron degeneration in mice that express a human Cu,Zn superoxide dismutase mutation. *Science* 264:1772-5.
- Hagmann P, Kurrant M, Gigandet X, et al. (2007) Mapping human whole-brain structural networks with diffusion MRI. *PLoS ONE* 2:e597.
- Hagmann P, Cammoun L, Gigandet X, et al. (2008) Mapping the Structural Core of Human Cerebral Cortex. *PLoS biology* 6:e159.
- Han J, Ma L. (2006) Functional magnetic resonance imaging study of the brain in patients with amyotrophic lateral sclerosis. *Chin. Med. Sci. J.* 21:228-33.
- Han J, Ma L. (2010) Study of the features of proton MR spectroscopy (¹H-MRS) on amyotrophic lateral sclerosis. *J. Magn. Reson. Imaging* 31:305-8.
- Hanstock CC, Cwik VA, Martin WR. (2002) Reduction in metabolite transverse relaxation times in amyotrophic lateral sclerosis. *J. Neurol. Sci.* 198:37-41.
- Hardiman O, van den Berg LH, Kiernan MC. (2011) Clinical diagnosis and management of amyotrophic lateral sclerosis. *Nat. Rev. Neurol.* 7:639-49.
- Henkelman RM, Stanisz GJ, Graham SJ. (2001) Magnetization transfer in MRI: a review. *NMR Biomed.* 14:57-64.
- Honey CJ, Kotter R, Breakspear M, Sporns O. (2007) Network structure of cerebral cortex shapes functional connectivity on multiple time scales. *Proc. Natl. Acad. Sci. U. S. A.* 104:10240-5.
- Honey CJ, Sporns O, Cammoun L, et al. (2009) Predicting human resting-state functional connectivity from structural connectivity. *Proc. Natl. Acad. Sci. U. S. A.* 106:2035-40.

References

- Hughes JT. (1982) Pathology of amyotrophic lateral sclerosis. *Adv. Neurol.* 36:61-74.
- Huisman MH, de Jong SW, van Doormaal PT, et al. (2011) Population based epidemiology of amyotrophic lateral sclerosis using capture-recapture methodology. *J. Neurol. Neurosurg. Psychiatry* 82:1165-70.
- Hutton C, Draganski B, Ashburner J, Weiskopf N. (2009) A comparison between voxel-based cortical thickness and voxel-based morphometry in normal aging. *NeuroImage* 48:371-80.
- Ikedo K, Akiyama H, Arai T, Ueno H, Tsuchiya K, Kosaka K. (2002) Morphometrical reappraisal of motor neuron system of Pick's disease and amyotrophic lateral sclerosis with dementia. *Acta Neuropathol.* 104:21-8.
- Ince PG, Lowe J, Shaw PJ. (1998) Amyotrophic lateral sclerosis: current issues in classification, pathogenesis and molecular pathology. *Neuropathol. Appl. Neurobiol.* 24:104-17.
- Ince PG, Evans J, Knopp M, et al. (2003) Corticospinal tract degeneration in the progressive muscular atrophy variant of ALS. *Neurology* 60:1252-8.
- Ince PG, Highley JR, Kirby J, et al. (2011) Molecular pathology and genetic advances in amyotrophic lateral sclerosis: an emerging molecular pathway and the significance of glial pathology. *Acta Neuropathol.* 122:657-71.
- Ioannidis JP. (2008) Why most discovered true associations are inflated. *Epidemiology* 19:640-8.
- Iwanaga K, Hayashi S, Oyake M, et al. (1997) Neuropathology of sporadic amyotrophic lateral sclerosis of long duration. *J. Neurol. Sci.* 146:139-43.
- Iwata NK, Aoki S, Okabe S, et al. (2008) Evaluation of corticospinal tracts in ALS with diffusion tensor MRI and brainstem stimulation. *Neurology* 70:528-32.
- Iwata NK, Kwan JY, Danielian LE, et al. (2011) White matter alterations differ in primary lateral sclerosis and amyotrophic lateral sclerosis. *Brain* 134:2642-55.
- Jelsone-Swain LM, Fling BW, Seidler RD, Hovatter R, Gruis K, Welsh RC. (2010) Reduced Interhemispheric Functional Connectivity in the Motor Cortex during Rest in Limb-Onset Amyotrophic Lateral Sclerosis. *Front. Syst. Neurosci.* 4:158.
- Johnstone D, Milward EA. (2010) Molecular genetic approaches to understanding the roles and regulation of iron in brain health and disease. *J. Neurochem.* 113:1387-402.
- Jones AP, Gunawardena WJ, Coutinho CM, Gatt JA, Shaw IC, Mitchell JD. (1995) Preliminary results of proton magnetic resonance spectroscopy in motor neurone disease (amyotrophic lateral sclerosis). *J. Neurol. Sci.* 129S:85-9.
- Jones CK, Polders D, Hua J, et al. (2012) In vivo three-dimensional whole-brain pulsed steady-state chemical exchange saturation transfer at 7 T. *Magn. Reson. Med.* 67:1579-89.
- Jones DK, Horsfield MA, Simmons A. (1999) Optimal strategies for measuring diffusion in anisotropic systems by magnetic resonance imaging. *Magn. Reson. Med.* 42:515-25.
- Jones DK. (2004) The effect of gradient sampling schemes on measures derived from diffusion tensor MRI: a Monte Carlo study. *Magn. Reson. Med.* 51:807-15.

- Jucker M, Walker LC. (2011) Pathogenic protein seeding in Alzheimer disease and other neurodegenerative disorders. *Ann. Neurol.* 70:532-40.
- Kabashi E, Valdmanis PN, Dion P, et al. (2008) TARDBP mutations in individuals with sporadic and familial amyotrophic lateral sclerosis. *Nat. Genet.* 40:572-4.
- Kahkonen S, Ilmoniemi RJ. (2004) Transcranial magnetic stimulation: applications for neuropsychopharmacology. *J. Psychopharmacol.* 18:257-61.
- Kaiser M. (2011) A tutorial in connectome analysis: Topological and spatial features of brain networks. *NeuroImage* 57:892-907.
- Kalra S, Cashman NR, Genge A, Arnold DL. (1998) Recovery of N-acetylaspartate in corticomotor neurons of patients with ALS after riluzole therapy. *Neuroreport* 9:1757-61.
- Kalra S, Hanstock CC, Martin WR, Allen PS, Johnston WS. (2006a) Detection of cerebral degeneration in amyotrophic lateral sclerosis using high-field magnetic resonance spectroscopy. *Arch. Neurol.* 63:1144-8.
- Kalra S, Tai P, Genge A, Arnold DL. (2006b) Rapid improvement in cortical neuronal integrity in amyotrophic lateral sclerosis detected by proton magnetic resonance spectroscopic imaging. *J. Neurol.* 253:1060-3.
- Kanouchi T, Ohkubo T, Yokota T. (2012) Can regional spreading of amyotrophic lateral sclerosis motor symptoms be explained by prion-like propagation? *J. Neurol. Neurosurg. Psychiatry* 83:739-45.
- Karandreas N, Papadopoulou M, Kokotis P, Papapostolou A, Tsivgoulis G, Zambelis T. (2007) Impaired interhemispheric inhibition in amyotrophic lateral sclerosis. *Amyotroph. Lateral Scler.* 8:112-8.
- Kasai T, Tokuda T, Ishigami N, et al. (2009) Increased TDP-43 protein in cerebrospinal fluid of patients with amyotrophic lateral sclerosis. *Acta Neuropathol.* 117:55-62.
- Kassubek J, Unrath A, Huppertz HJ, et al. (2005) Global brain atrophy and corticospinal tract alterations in ALS, as investigated by voxel-based morphometry of 3-D MRI. *Amyotroph. Lateral Scler.* 6:213-20.
- Kato S. (2008) Amyotrophic lateral sclerosis models and human neuropathology: similarities and differences. *Acta Neuropathol.* 115:97-114.
- Kato Y, Matsumura K, Kinoshita Y, Narita Y, Kuzuhara S, Nakagawa T. (1997) Detection of pyramidal tract lesions in amyotrophic lateral sclerosis with magnetization-transfer measurements. *AJNR Am. J. Neuroradiol.* 18:1541-7.
- Kaufmann P, Pullman SL, Shungu DC, et al. (2004) Objective tests for upper motor neuron involvement in amyotrophic lateral sclerosis (ALS). *Neurology* 62:1753-7.
- Kew JJ, Goldstein LH, Leigh PN, et al. (1993) The relationship between abnormalities of cognitive function and cerebral activation in amyotrophic lateral sclerosis. A neuropsychological and positron emission tomography study. *Brain* 116:1399-423.
- Kew JJ, Brooks DJ, Passingham RE, Rothwell JC, Frackowiak RS, Leigh PN. (1994) Cortical function in progressive lower motor neuron disorders and amyotrophic lateral sclerosis: a comparative PET study. *Neurology* 44:1101-10.

References

- Kiernan JA, Hudson AJ. (1991) Changes in sizes of cortical and lower motor neurons in amyotrophic lateral sclerosis. *Brain* 114 (Pt 2):843-53.
- Kiernan MC, Vucic S, Cheah BC, et al. (2011) Amyotrophic lateral sclerosis. *Lancet* 377:942-55.
- Kim JH, Loy DN, Liang HF, Trinkaus K, Schmidt RE, Song SK. (2007) Noninvasive diffusion tensor imaging of evolving white matter pathology in a mouse model of acute spinal cord injury. *Magn. Reson. Med.* 58:253-60.
- Kirsch W, McAuley G, Holshouser B, et al. (2009) Serial Susceptibility Weighted MRI Measures Brain Iron and Microbleeds in Dementia. *J. Alzheimers Dis.* 17:599-609.
- Kollewe K, Munte TF, Samii A, Dengler R, Petri S, Mohammadi B. (2011) Patterns of cortical activity differ in ALS patients with limb and/or bulbar involvement depending on motor tasks. *J. Neurol.* 258:804-10.
- Konrad C, Henningsen H, Bremer J, et al. (2002) Pattern of cortical reorganization in amyotrophic lateral sclerosis: a functional magnetic resonance imaging study. *Exp. Brain Res.* 143:51-6.
- Konrad C, Jansen A, Henningsen H, et al. (2006) Subcortical reorganization in amyotrophic lateral sclerosis. *Exp. Brain Res.* 172:361-9.
- Kornelsen J, Stroman PW. (2004) fMRI of the lumbar spinal cord during a lower limb motor task. *Magn. Reson. Med.* 52:411-4.
- Korner S, Kollewe K, Fahlbusch M, et al. (2011) Onset and spreading patterns of upper and lower motor neuron symptoms in amyotrophic lateral sclerosis. *Muscle Nerve* 43:636-42.
- Kriz J, Gowing G, Julien JP. (2003) Efficient three-drug cocktail for disease induced by mutant superoxide dismutase. *Ann. Neurol.* 53:429-36.
- Kuiperij HB, Abdo WF, van Engelen BG, Schelhaas HJ, Verbeek MM. (2010) TDP-43 plasma levels do not differentiate sporadic inclusion body myositis from other inflammatory myopathies. *Acta Neuropathol.* 120:825-6.
- Kunst CB. (2004) Complex genetics of amyotrophic lateral sclerosis. *Am. J. Hum. Genet.* 75:933-47.
- Lacomblez L, Bensimon G, Leigh PN, Guillet P, Meininger V. (1996a) Dose-ranging study of riluzole in amyotrophic lateral sclerosis. Amyotrophic Lateral Sclerosis/Riluzole Study Group II. *Lancet* 347:1425-31.
- Lacomblez L, Bensimon G, Leigh PN, et al. (1996b) A confirmatory dose-ranging study of riluzole in ALS. ALS/Riluzole Study Group-II. *Neurology* 47:S242-50.
- Lanctot KL, Herrmann N, Ganjavi H, et al. (2007) Serotonin-1A receptors in frontotemporal dementia compared with controls. *Psychiatry Res.* 156:247-50.
- Langkammer C, Enzinger C, Quasthoff S, et al. (2010) Mapping of iron deposition in conjunction with assessment of nerve fiber tract integrity in amyotrophic lateral sclerosis. *J. Magn. Reson. Imaging* 31:1339-45.
- Latora V, Marchiori M. (2001) Efficient behavior of small-world networks. *Physical review letters* 87:198701.
- Leemans A, Jones DK. (2009) The B-matrix must be rotated when correcting for subject motion in DTI data. *Magn. Reson. Med.* 61:1336-49.

- Li J, Pan P, Song W, Huang R, Chen K, Shang H. (2012) A meta-analysis of diffusion tensor imaging studies in amyotrophic lateral sclerosis. *Neurobiol. Aging* 33:1833-8.
- Li S, Chen Q, Yu B, et al. (2009a) Structural and functional changes mapped in the brains of amyotrophic lateral sclerosis patients with/without dysphagia: A pilot study. *Amyotroph Lateral Scler.* 1-9.
- Li Y, Liu Y, Li J, et al. (2009b) Brain anatomical network and intelligence. *PLoS Comput. Biol.* 5:e1000395.
- Lillo P, Garcin B, Hornberger M, Bak TH, Hodges JR. (2010) Neurobehavioral features in frontotemporal dementia with amyotrophic lateral sclerosis. *Arch. Neurol.* 67:826-30.
- Liu Y, Liang M, Zhou Y, et al. (2008) Disrupted small-world networks in schizophrenia. *Brain* 131:945-61.
- Lloyd CM, Richardson MP, Brooks DJ, Al-Chalabi A, Leigh PN. (2000) Extramotor involvement in ALS: PET studies with the GABA(A) ligand [(11)C]flumazenil. *Brain* 123:2289-96.
- Logroscino G, Traynor BJ, Hardiman O, et al. (2008) Descriptive epidemiology of amyotrophic lateral sclerosis: new evidence and unsolved issues. *J. Neurol. Neurosurg. Psychiatry* 79:6-11.
- Lombardo F, Frijia F, Bongioanni P, et al. (2009) Diffusion tensor MRI and MR spectroscopy in long lasting upper motor neuron involvement in amyotrophic lateral sclerosis. *Arch. Ital. Biol.* 147:69-82.
- Lowe MJ, Beall EB, Sakaie KE, et al. (2008) Resting state sensorimotor functional connectivity in multiple sclerosis inversely correlates with transcallosal motor pathway transverse diffusivity. *Human Brain Mapp.* 29:818-27.
- Lowe MJ, Dzemidzic M, Lurito JT, Mathews VP, Phillips MD. (2000) Correlations in low-frequency BOLD fluctuations reflect cortico-cortical connections. *NeuroImage* 12:582-7.
- Ludolph AC, Elger CE, Bottger IW, Kuttig AG, Lottes G, Brune GG. (1989) N-isopropyl-p-123I-amphetamine single photon emission computer tomography in motor neuron disease. *Eur. Neurol.* 29:255-60.
- Ludolph AC, Langen KJ, Regard M, et al. (1992) Frontal lobe function in amyotrophic lateral sclerosis: a neuropsychological and positron emission tomography study. *Acta Neurol. Scand.* 85:81-9.
- Lule D, Diekmann V, Anders S, et al. (2007a) Brain responses to emotional stimuli in patients with amyotrophic lateral sclerosis (ALS). *J. Neurol.* 254:519-27.
- Lule D, Diekmann V, Kassubek J, et al. (2007b) Cortical plasticity in amyotrophic lateral sclerosis: motor imagery and function. *Neurorehabil. Neural Repair* 21:518-26.
- Lule D, Diekmann V, Muller HP, Kassubek J, Ludolph AC, Birbaumer N. (2010) Neuroimaging of multimodal sensory stimulation in amyotrophic lateral sclerosis. *J. Neurol. Neurosurg. Psychiatry* 81:899-906.
- Mackenzie IR, Feldman HH. (2005) Ubiquitin immunohistochemistry suggests classic motor neuron disease, motor neuron disease with dementia, and frontotemporal dementia of the motor neuron disease type represent a clinicopathologic spectrum. *J. Neuropathol. Exp. Neurol.* 64:730-9.
- Mackenzie IR, Rademakers R, Neumann M. (2010) TDP-43 and FUS in amyotrophic lateral sclerosis and frontotemporal dementia. *Lancet Neurol.* 9:995-1007.

References

- Mandl RC, Schnack HG, Zwiers MP, van der Schaaf A, Kahn RS, Hulshoff Pol HE. (2008) Functional diffusion tensor imaging: measuring task-related fractional anisotropy changes in the human brain along white matter tracts. *PLoS ONE* 3:e3631.
- Mandl RC, Schnack HG, Luigjes J, et al. (2010) Tract-based Analysis of Magnetization Transfer Ratio and Diffusion Tensor Imaging of the Frontal and Frontotemporal Connections in Schizophrenia. *Schizophr. Bull.* 36:778-87.
- Martinez-Vicente M, Cuervo AM. (2007) Autophagy and neurodegeneration: when the cleaning crew goes on strike. *Lancet Neurol.* 6:352-61.
- Mezzapesa DM, Ceccarelli A, Dicuonzo F, et al. (2007) Whole-brain and regional brain atrophy in amyotrophic lateral sclerosis. *AJNR Am. J. Neuroradiol.* 28:255-9.
- Miller R, Bradley W, Cudkovic M, et al. (2007) Phase II/III randomized trial of TCH346 in patients with ALS. *Neurology* 69:776-84.
- Miller RG, Moore DH, Forshef DA, et al. (2011) Phase II screening trial of lithium carbonate in amyotrophic lateral sclerosis: Examining a more efficient trial design. *Neurology* 77:973-9.
- Minnerop M, Specht K, Ruhlmann J, Grothe C, Wullner U, Klockgether T. (2009) In vivo voxel-based relaxometry in amyotrophic lateral sclerosis. *J. Neurol.* 256:28-34.
- Mitsumoto H, Ulug AM, Pullman SL, et al. (2007) Quantitative objective markers for upper and lower motor neuron dysfunction in ALS. *Neurology* 68:1402-10.
- Mohammadi B, Kollwe K, Samii A, Krampfl K, Dengler R, Munte TF. (2009a) Changes of resting state brain networks in amyotrophic lateral sclerosis. *Exp. Neurol.* 217:147-53.
- Mohammadi B, Kollwe K, Samii A, Krampfl K, Dengler R, Munte TF. (2009b) Decreased brain activation to tongue movements in amyotrophic lateral sclerosis with bulbar involvement but not Kennedy syndrome. *J. Neurol.* 256:1263-9.
- Mohammadi B, Kollwe K, Samii A, Dengler R, Munte TF. (2011) Functional neuroimaging at different disease stages reveals distinct phases of neuroplastic changes in amyotrophic lateral sclerosis. *Hum. Brain Mapp.* 32:750-8.
- Moll NM, Rietsch AM, Thomas S, et al. (2011) Multiple sclerosis normal-appearing white matter: pathology-imaging correlations. *Ann. Neurol.* 70:764-73.
- Morgan VL, Mishra A, Newton AT, Gore JC, Ding Z. (2009) Integrating functional and diffusion magnetic resonance imaging for analysis of structure-function relationship in the human language network. *PLoS ONE* 4:e6660.
- Mori S, Crain BJ, Chacko VP, van Zijl PC. (1999) Three-dimensional tracking of axonal projections in the brain by magnetic resonance imaging. *Ann. Neurol.* 45:265-9.
- Mori S, Kaufmann WE, Davatzikos C, et al. (2002) Imaging cortical association tracts in the human brain using diffusion-tensor-based axonal tracking. *Magn. Reson. Med.* 47:215-23.
- Mori S, van Zijl PC. (2002) Fiber tracking: principles and strategies - a technical review. *NMR Biomed.* 15:468-80.

- Mougin OE, Coxon RC, Pitiot A, Gowland PA. (2010) Magnetization transfer phenomenon in the human brain at 7 T. *NeuroImage* 49:272-81.
- MPS Research Unit. (2000) PEST 4: operating manual.
- Muller HP, Unrath A, Huppertz HJ, Ludolph AC, Kassubek J. (2012) Neuroanatomical patterns of cerebral white matter involvement in different motor neuron diseases as studied by diffusion tensor imaging analysis. *Amyotroph. Lateral Scler.* 13:254-64.
- Munch C, O'Brien J, Bertolotti A. (2011) Prion-like propagation of mutant superoxide dismutase-1 misfolding in neuronal cells. *Proc. Natl. Acad. Sci. U. S. A.* 108:3548-53.
- Nair G, Carew JD, Usher S, Lu D, Hu XP, Benatar M. (2010) Diffusion tensor imaging reveals regional differences in the cervical spinal cord in amyotrophic lateral sclerosis. *Neuroimage* 53:576-83.
- Neary D, Snowden JS, Mann DM, Northen B, Goulding PJ, Macdermott N. (1990) Frontal lobe dementia and motor neuron disease. *J. Neurol. Neurosurg. Psychiatry* 53:23-32.
- Neary D, Snowden JS, Gustafson L, et al. (1998) Frontotemporal lobar degeneration: a consensus on clinical diagnostic criteria. *Neurology* 51:1546-54.
- Neema M, Stankiewicz J, Arora A, et al. (2007) T1- and T2-based MRI measures of diffuse gray matter and white matter damage in patients with multiple sclerosis. *J. Neuroimaging* 17S:16S-21S.
- Nelles M, Block W, Traber F, Wullner U, Schild HH, Urbach H. (2008) Combined 3T Diffusion Tensor Tractography and 1H-MR Spectroscopy in Motor Neuron Disease. *AJNR Am. J. Neuroradiol.* 29:1708-14.
- Neumann M, Sampathu DM, Kwong LK, et al. (2006) Ubiquitinated TDP-43 in frontotemporal lobar degeneration and amyotrophic lateral sclerosis. *Science* 314:130-3.
- Ng MC, Ho JT, Ho SL, et al. (2008) Abnormal diffusion tensor in nonsymptomatic familial amyotrophic lateral sclerosis with a causative superoxide dismutase 1 mutation. *J. Magn. Reson. Imaging* 27:8-13.
- Ngai S, Tang YM, Du L, Stuckey S. (2007) Hyperintensity of the precentral gyral subcortical white matter and hypointensity of the precentral gyrus on fluid-attenuated inversion recovery: variation with age and implications for the diagnosis of amyotrophic lateral sclerosis. *AJNR Am. J. Neuroradiol.* 28:250-4.
- Nicaise C, Mitrecic D, Demetter P, et al. (2009) Impaired blood-brain and blood-spinal cord barriers in mutant SOD1-linked ALS rat. *Brain Res.* 1301:152-62.
- Nickerson DA, Tobe VO, Taylor SL. (1997) PolyPhred: automating the detection and genotyping of single nucleotide substitutions using fluorescence-based resequencing. *Nucleic Acids Res.* 25:2745-51.
- Norris F, Shepherd R, Denys E, et al. (1993) Onset, natural history and outcome in idiopathic adult motor neuron disease. *J. Neurol. Sci.* 118:48-55.
- Noto Y, Shibuya K, Sato Y, et al. (2011) Elevated CSF TDP-43 levels in amyotrophic lateral sclerosis: Specificity, sensitivity, and a possible prognostic value. *Amyotroph. Lateral Scler.* 12:140-3.
- Ordidge RJ, Gibbs P, Chapman B, Stehling MK, Mansfield P. (1990) High-speed multislice T1 mapping using inversion-recovery echo-planar imaging. *Magn. Reson. Med.* 16:238-45.
- Palmieri A, Naccarato M, Abrahams S, et al. (2010) Right hemisphere dysfunction and emotional processing in ALS: an fMRI study. *J. Neurol.* 257:1970-8.

References

- Paone JF, Waalkes TP, Baker RR, Shaper JH. (1980) Serum UDP-galactosyl transferase as a potential biomarker for breast carcinoma. *J. Surg. Oncol.* 15:59-66.
- Paus T, Collins DL, Evans AC, Leonard G, Pike B, Zijdenbos A. (2001) Maturation of white matter in the human brain: a review of magnetic resonance studies. *Brain Res. Bull.* 54:255-66.
- Penfield W, Rasmussen T. (1968) The cerebral cortex of man: A clinical study of localization of function.
- Pereira JB, Ibarretxe-Bilbao N, Marti MJ, et al. (2011) Assessment of cortical degeneration in patients with parkinson's disease by voxel-based morphometry, cortical folding, and cortical thickness. *Hum. Brain Mapp.* Sep 6. [Epub ahead of print]
- Philips T, Robberecht W. (2011) Neuroinflammation in amyotrophic lateral sclerosis: role of glial activation in motor neuron disease. *Lancet Neurol.* 10:253-63.
- Phukan J, Pender NP, Hardiman O. (2007) Cognitive impairment in amyotrophic lateral sclerosis. *Lancet Neurol.* 6:994-1003.
- Piao YS, Wakabayashi K, Kakita A, et al. (2003) Neuropathology with clinical correlations of sporadic amyotrophic lateral sclerosis: 102 autopsy cases examined between 1962 and 2000. *Brain Pathol.* 13:10-22.
- Piepers S, Veldink JH, de Jong SW, et al. (2009) Randomized sequential trial of valproic acid in amyotrophic lateral sclerosis. *Ann. Neurol.* 66:227-34.
- Pierpaoli C, Jezzard P, Basser PJ, Barnett A, Di Chiro G. (1996) Diffusion tensor MR imaging of the human brain. *Radiology* 201:637-48.
- Pierpaoli C, Barnett A, Pajevic S, et al. (2001) Water diffusion changes in Wallerian degeneration and their dependence on white matter architecture. *NeuroImage* 13:1174-85.
- Pioro EP, Antel JP, Cashman NR, Arnold DL. (1994) Detection of cortical neuron loss in motor neuron disease by proton magnetic resonance spectroscopic imaging in vivo. *Neurology* 44:1933-8.
- Pioro EP, Majors AW, Mitsumoto H, Nelson DR, Ng TC. (1999) 1H-MRS evidence of neurodegeneration and excess glutamate + glutamine in ALS medulla. *Neurology* 53:71-9.
- Pizzasegola C, Caron I, Daleno C, et al. (2009) Treatment with lithium carbonate does not improve disease progression in two different strains of SOD1 mutant mice. *Amyotroph. Lateral Scler.* 10:221-8.
- Pocock SJ, Simon R. (1975) Sequential treatment assignment with balancing for prognostic factors in the controlled clinical trial. *Biometrics* 31:103-15.
- Pohl C, Block W, Karitzky J, et al. (2001a) Proton magnetic resonance spectroscopy of the motor cortex in 70 patients with amyotrophic lateral sclerosis. *Arch. Neurol.* 58:729-35.
- Pohl C, Block W, Traber F, et al. (2001b) Proton magnetic resonance spectroscopy and transcranial magnetic stimulation for the detection of upper motor neuron degeneration in ALS patients. *J. Neurol. Sci.* 190:21-7.
- Polders DL, Leemans A, Hendrikse J, Donahue MJ, Luijten PR, Hoogduin JM. (2011) Signal to noise ratio and uncertainty in diffusion tensor imaging at 1.5, 3.0, and 7.0 Tesla. *J. Magn. Reson. Imaging* 33:1456-63.

- Polymenidou M, Cleveland DW. (2011) The seeds of neurodegeneration: prion-like spreading in ALS. *Cell* 147:498-508.
- Poujois A, Schneider FC, Faillenot I, et al. (2012) Brain plasticity in the motor network is correlated with disease progression in amyotrophic lateral sclerosis. *Hum. Brain Mapp.* Mar 28. [Epub ahead of print]
- Pyra T, Hui B, Hanstock C, et al. (2010) Combined structural and neurochemical evaluation of the corticospinal tract in amyotrophic lateral sclerosis. *Amyotroph. Lateral Scler.* 11:157-65.
- Querbes O, Aubry F, Pariente J, et al. (2009) Early diagnosis of Alzheimer's disease using cortical thickness: impact of cognitive reserve. *Brain* 132:2036-47
- Raaphorst J, de Visser M, Linsen WH, de Haan RJ, Schmand B. (2010) The cognitive profile of amyotrophic lateral sclerosis: A meta-analysis. *Amyotroph. Lateral Scler.* 11:27-37.
- Raj A, Kuceyeski A, Weiner M. (2012) A Network Diffusion Model of Disease Progression in Dementia. *Neuron* 73:1204-15.
- Rametti A, Esclaire F, Yardin C, Cogne N, Terro F. (2008) Lithium down-regulates tau in cultured cortical neurons: A possible mechanism of neuroprotection. *Neurosci. Lett.* 434:93-8.
- Ravits J, Laurie P, Fan Y, Moore DH. (2007a) Implications of ALS focality: rostral-caudal distribution of lower motor neuron loss postmortem. *Neurology* 68:1576-82.
- Ravits J, Paul P, Jorg C. (2007b) Focality of upper and lower motor neuron degeneration at the clinical onset of ALS. *Neurology* 68:1571-5.
- Ravits JM, La Spada AR. (2009) ALS motor phenotype heterogeneity, focality, and spread: deconstructing motor neuron degeneration. *Neurology* 73:805-11.
- Reijneveld JC, Ponten SC, Berendse HW, Stam CJ. (2007) The application of graph theoretical analysis to complex networks in the brain. *Clin. Neurophysiol.* 118:2317-31.
- Renton AE, Majounie E, Waite A, et al. (2011) A hexanucleotide repeat expansion in C9ORF72 is the cause of chromosome 9p21-linked ALS-FTD. *Neuron* 72:257-68.
- Ringholz GM, Appel SH, Bradshaw M, Cooke NA, Mosnik DM, Schulz PE. (2005) Prevalence and patterns of cognitive impairment in sporadic ALS. *Neurology* 65:586-90.
- Rivara CB, Sherwood CC, Bouras C, Hof PR. (2003) Stereologic characterization and spatial distribution patterns of Betz cells in the human primary motor cortex. *Anat. Rec. A. Discov. Mol. Cell. Evol. Biol.* 270:137-51.
- Roccatagliata L, Bonzano L, Mancardi G, Canepa C, Caponnetto C. (2008) Detection of motor cortex thinning and corticospinal tract involvement by quantitative MRI in amyotrophic lateral sclerosis. *Amyotroph. Lateral Scler.* 1-6.
- Roche JC, Rojas-Garcia R, Scott KM, et al. (2012) A proposed staging system for amyotrophic lateral sclerosis. *Brain* 135:847-52.
- Rogers J, Kochunov P, Lancaster J, et al. (2007) Heritability of brain volume, surface area and shape: an MRI study in an extended pedigree of baboons. *Hum. Brain Mapp.* 28:576-83.
- Rohrer JD, Warren JD, Modat M, et al. (2009) Patterns of cortical thinning in the language variants of frontotemporal lobar degeneration. *Neurology* 72:1562-9.

References

- Rohrer JD, Lashley T, Schott JM, et al. (2011) Clinical and neuroanatomical signatures of tissue pathology in frontotemporal lobar degeneration. *Brain* 134:2565-81.
- Rooney WD, Miller RG, Gelinas D, Schuff N, Maudsley AA, Weiner MW. (1998) Decreased N-acetylaspartate in motor cortex and corticospinal tract in ALS. *Neurology* 50:1800-5.
- Rosas HD, Salat DH, Lee SY, et al. (2008) Cerebral cortex and the clinical expression of Huntington's disease: complexity and heterogeneity. *Brain* 131:1057-68.
- Rose S, Pannek K, Bell C, et al. (2012) Direct evidence of intra- and interhemispheric corticomotor network degeneration in amyotrophic lateral sclerosis: an automated MRI structural connectivity study. *NeuroImage* 59:2661-9.
- Rosen DR. (1993) Mutations in Cu/Zn superoxide dismutase gene are associated with familial amyotrophic lateral sclerosis. *Nature* 364:362.
- Rothstein JD. (2009) Current hypotheses for the underlying biology of amyotrophic lateral sclerosis. *Ann. Neurol.* 65S:S3-9.
- Rubinov M, Sporns O. (2010) Complex network measures of brain connectivity: uses and interpretations. *NeuroImage* 52:1059-69.
- Rule RR, Suhy J, Schuff N, Gelinas DE, Miller RG, Weiner MW. (2004) Reduced NAA in motor and non-motor brain regions in amyotrophic lateral sclerosis: a cross-sectional and longitudinal study. *Amyotroph. Lateral Scler.* 5:141-9.
- Rule RR, Schuff N, Miller RG, Weiner MW. (2010) Gray matter perfusion correlates with disease severity in ALS. *Neurology* 74:821-7.
- Sach M, Winkler G, Glauche V, et al. (2004) Diffusion tensor MRI of early upper motor neuron involvement in amyotrophic lateral sclerosis. *Brain* 127:340-50.
- Sage CA, Peeters RR, Gorner A, Robberecht W, Sunaert S. (2007) Quantitative diffusion tensor imaging in amyotrophic lateral sclerosis. *NeuroImage* 34:486-99.
- Sage CA, Van Hecke W, Peeters R, et al. (2009) Quantitative diffusion tensor imaging in amyotrophic lateral sclerosis: revisited. *Hum. Brain Mapp.* 30:3657-75.
- Salvador R, Martinez A, Pomarol-Clotet E, Sarro S, Suckling J, Bullmore E. (2007) Frequency based mutual information measures between clusters of brain regions in functional magnetic resonance imaging. *Neuroimage* 35:83-8.
- Sandyk R. (2006) Serotonergic mechanisms in amyotrophic lateral sclerosis. *Int. J. Neurosci.* 116:775-826.
- Sarchielli P, Pelliccioli GP, Tarducci R, et al. (2001) Magnetic resonance imaging and 1H-magnetic resonance spectroscopy in amyotrophic lateral sclerosis. *Neuroradiology* 43:189-97.
- Sarkar S, Rubinsztein DC. (2006) Inositol and IP3 levels regulate autophagy: biology and therapeutic speculations. *Autophagy* 2:132-4.
- Sarro L, Agosta F, Canu E, et al. (2011) Cognitive Functions and White Matter Tract Damage in Amyotrophic Lateral Sclerosis: A Diffusion Tensor Tractography Study. *AJNR Am. J. Neuroradiol.* 32:1866-72.

- Sato K, Aoki S, Iwata NK, et al. (2010) Diffusion tensor tract-specific analysis of the uncinate fasciculus in patients with amyotrophic lateral sclerosis. *Neuroradiology* 52:729-33.
- Saute JA, Valler L, Schestatsky P. (2010) The role of lithium in ALS remains unknown. *Amyotroph. Lateral Scler.* 11:574.
- Schimrigk SK, Bellenberg B, Schluter M, et al. (2007) Diffusion tensor imaging-based fractional anisotropy quantification in the corticospinal tract of patients with amyotrophic lateral sclerosis using a probabilistic mixture model. *AJNR Am. J. Neuroradiol.* 28:724-30.
- Schoenfeld DA, Cudkowicz M. (2008) Design of phase II ALS clinical trials. *Amyotroph. Lateral Scler.* 9:16-23.
- Schoenfeld MA, Tempelmann C, Gaul C, et al. (2005) Functional motor compensation in amyotrophic lateral sclerosis. *J. Neurol.* 252:944-52.
- Schrooten M, Smetcoren C, Robberecht W, Van Damme P. (2011) Benefit of the awaji diagnostic algorithm for amyotrophic lateral sclerosis: A prospective study. *Ann. Neurol.* 70:79-83.
- Schuff N, Rooney WD, Miller R, et al. (2001) Reanalysis of multislice (1)H MRSI in amyotrophic lateral sclerosis. *Magn. Reson. Med.* 45:513-6.
- Seeley WW, Crawford RK, Zhou J, Miller BL, Greicius MD. (2009) Neurodegenerative diseases target large-scale human brain networks. *Neuron* 62:42-52.
- Senda J, Ito M, Watanabe H, et al. (2009) Correlation between pyramidal tract degeneration and widespread white matter involvement in amyotrophic lateral sclerosis: A study with tractography and diffusion-tensor imaging. *Amyotroph. Lateral Scler.* 10:288-94.
- Senda J, Kato S, Kaga T, et al. (2011) Progressive and widespread brain damage in ALS: MRI voxel-based morphometry and diffusion tensor imaging study. *Amyotroph. Lateral Scler.* 12:59-69.
- Sharma KR, Saigal G, Maudsley AA, Govind V. (2011) 1H MRS of basal ganglia and thalamus in amyotrophic lateral sclerosis. *NMR Biomed.* 24:1270-6.
- Shaw P, Lerch JP, Pruessner JC, et al. (2007) Cortical morphology in children and adolescents with different apolipoprotein E gene polymorphisms: an observational study. *Lancet Neurol.* 6:494-500.
- Sigmund EE, Suero GA, Hu C, et al. (2012) High-resolution human cervical spinal cord imaging at 7 T. *NMR Biomed.* 25:891-9.
- Sivak S, Bittsansky M, Kurca E, et al. (2010) Proton magnetic resonance spectroscopy in patients with early stages of amyotrophic lateral sclerosis. *Neuroradiology* 52:1079-85.
- Skotland T. (2012) Molecular imaging: challenges of bringing imaging of intracellular targets into common clinical use. *Contrast Media Mol. Imaging* 7:1-6.
- Smith MC. (1960) Nerve Fibre Degeneration in the Brain in Amyotrophic Lateral Sclerosis. *J. Neurol. Neurosurg. Psychiatry* 23:269-82.
- Smith SM, Fox PT, Miller KL, et al. (2009) Correspondence of the brain's functional architecture during activation and rest. *Proc. Natl. Acad. Sci. U. S. A.* 106:13040-5.
- Sperfeld AD, Bretschneider V, Flaith L, et al. (2005) MR-pathologic comparison of the upper spinal cord in different motor neuron diseases. *Eur. Neurol.* 53:74-7.

References

- Sporns O, Zwi JD. (2004) The small world of the cerebral cortex. *Neuroinformatics* 2:145-62.
- Sporns O. (2006) Small-world connectivity, motif composition, and complexity of fractal neuronal connections. *Bio Systems* 85:55-64.
- Sporns O. (2011) The human connectome: a complex network. *Ann. N. Y. Acad. Sci.* 1224:109-25.
- Sreedharan J, Blair IP, Tripathi VB, et al. (2008) TDP-43 mutations in familial and sporadic amyotrophic lateral sclerosis. *Science* 319:1668-72.
- Staekenborg SS, Koedam EL, Henneman WJ, et al. (2009) Progression of mild cognitive impairment to dementia: contribution of cerebrovascular disease compared with medial temporal lobe atrophy. *Stroke* 40:1269-74.
- Stam CJ. (2004) Functional connectivity patterns of human magnetoencephalographic recordings: a 'small-world' network? *Neurosci. Lett.* 355:25-8.
- Stam CJ, Reijneveld JC. (2007) Graph theoretical analysis of complex networks in the brain. *Nonlinear Biomed. Phys.* 1:3.
- Stam CJ, de Haan W, Daffertshofer A, et al. (2009) Graph theoretical analysis of magnetoencephalographic functional connectivity in Alzheimer's disease. *Brain* 132:213-24.
- Stanisz GJ, Kecojevic A, Bronskill MJ, Henkelman RM. (1999) Characterizing white matter with magnetization transfer and T(2). *Magn. Reson. Med.* 42:1128-36.
- Stanton BR, Shinhar D, Turner MR, et al. (2009) Diffusion tensor imaging in sporadic and familial (D90A SOD1) forms of amyotrophic lateral sclerosis. *Arch. Neurol.* 66:109-15.
- Stanton BR, Williams VC, Leigh PN, et al. (2007a) Cortical activation during motor imagery is reduced in Amyotrophic Lateral Sclerosis. *Brain Res.* 1172:145-51.
- Stanton BR, Williams VC, Leigh PN, et al. (2007b) Altered cortical activation during a motor task in ALS. Evidence for involvement of central pathways. *J. Neurol.* 254:1260-7.
- Steinacker P, Hendrich C, Sperfeld AD, et al. (2008) TDP-43 in cerebrospinal fluid of patients with frontotemporal lobar degeneration and amyotrophic lateral sclerosis. *Arch. Neurol.* 65:1481-7.
- Sudharshan N, Hanstock C, Hui B, Pyra T, Johnston W, Kalra S. (2011) Degeneration of the mid-cingulate cortex in amyotrophic lateral sclerosis detected in vivo with MR spectroscopy. *AJNR Am. J. Neuroradiol.* 32:403-7.
- Suh J, Miller RG, Rule R, et al. (2002) Early detection and longitudinal changes in amyotrophic lateral sclerosis by (1)H MRSI. *Neurology* 58:773-9.
- Takahashi H, Snow BJ, Bhatt MH, Peppard R, Eisen A, Calne DB. (1993) Evidence for a dopaminergic deficit in sporadic amyotrophic lateral sclerosis on positron emission scanning. *Lancet* 342:1016-8.
- Talbot PR, Goulding PJ, Lloyd JJ, Snowden JS, Neary D, Testa HJ. (1995a) Inter-relation between "classic" motor neuron disease and frontotemporal dementia: neuropsychological and single photon emission computed tomography study. *J. Neurol. Neurosurg. Psychiatry* 58:541-7.
- Talbot PR, Snowden JS, Lloyd JJ, Neary D, Testa HJ. (1995b) The contribution of single photon emission tomography to the clinical differentiation of degenerative cortical brain disorders. *J. Neurol.* 242:579-86.

- Tanabe JL, Vermathen M, Miller R, Gelinus D, Weiner MW, Rooney WD. (1998) Reduced MTR in the corticospinal tract and normal T2 in amyotrophic lateral sclerosis. *Magn. Reson. Imaging* 16:1163-9.
- Tanaka M, Kondo S, Hirai S, Sun X, Yamagishi T, Okamoto K. (1993) Cerebral blood flow and oxygen metabolism in progressive dementia associated with amyotrophic lateral sclerosis. *J. Neurol. Sci.* 120:22-8.
- Tartaglia MC, Rowe A, Findlater K, Orange JB, Grace G, Strong MJ. (2007) Differentiation between primary lateral sclerosis and amyotrophic lateral sclerosis: examination of symptoms and signs at disease onset and during follow-up. *Arch. Neurol.* 64:232-6.
- Terao S, Sobue G, Yasuda T, Kachi T, Takahashi M, Mitsuma T. (1995) Magnetic resonance imaging of the corticospinal tracts in amyotrophic lateral sclerosis. *J. Neurol. Sci.* 133:66-72.
- Tessitore A, Esposito F, Monsurro MR, et al. (2006) Subcortical motor plasticity in patients with sporadic ALS: An fMRI study. *Brain Res. Bull.* 69:489-94.
- The PLoS Medicine Editors. (2008) It's the network, stupid: why everything in medicine is connected. *PLoS Med.* 5:e71.
- Thivard L, Pradat PF, Lehericy S, et al. (2007) Diffusion tensor imaging and voxel based morphometry study in amyotrophic lateral sclerosis: relationships with motor disability. *J. Neurol. Neurosurg. Psychiatry* 78:889-92.
- Ticozzi N, LeClerc AL, van Blitterswijk M, et al. (2011) Mutational analysis of TARDBP in neurodegenerative diseases *Neurobiol. Aging* 32:2096-9.
- Tofts PS, Steens CA, van Buchem MA. (2003) Quantitative MRI of the Brain: Measuring Changes Caused by Disease. 258-98.
- Toosy AT, Werring DJ, Orrell RW, et al. (2003) Diffusion tensor imaging detects corticospinal tract involvement at multiple levels in amyotrophic lateral sclerosis. *J. Neurol. Neurosurg. Psychiatry* 74:1250-7.
- Traynor BJ, Zhang H, Shefner JM, Schoenfeld D, Cudkovicz ME, NEALS Consortium. (2004) Functional outcome measures as clinical trial endpoints in ALS. *Neurology* 63:1933-5.
- Tsujimoto M, Senda J, Ishihara T, et al. (2011) Behavioral changes in early ALS correlate with voxel-based morphometry and diffusion tensor imaging. *J. Neurol. Sci.* 307:34-40.
- Turner MR, Cagnin A, Turkheimer FE, et al. (2004) Evidence of widespread cerebral microglial activation in amyotrophic lateral sclerosis: an [11C](R)-PK11195 positron emission tomography study. *Neurobiol. Dis.* 15:601-9.
- Turner MR, Hammers A, Al-Chalabi A, et al. (2005a) Distinct cerebral lesions in sporadic and 'D90A' SOD1 ALS: studies with [11C]flumazenil PET. *Brain* 128:1323-9.
- Turner MR, Gerhard A, Al-Chalabi A, et al. (2005b) Mills' and other isolated upper motor neurone syndromes: in vivo study with 11C-(R)-PK11195 PET. *J. Neurol. Neurosurg. Psychiatry* 76:871-4.
- Turner MR, Rabiner EA, Hammers A, et al. (2005c) 11C]-WAY100635 PET demonstrates marked 5-HT1A receptor changes in sporadic ALS. *Brain* 128:896-905.

References

- Turner MR, Hammers A, Allsop J, et al. (2007) Volumetric cortical loss in sporadic and familial amyotrophic lateral sclerosis. *Amyotroph. Lateral Scler.* 8:343-7.
- Turner MR, Kiernan MC, Leigh PN, Talbot K. (2009) Biomarkers in amyotrophic lateral sclerosis. *Lancet Neurol.* 8:94-109.
- Turner MR, Grosskreutz J, Kassubek J, et al. (2011a) Towards a neuroimaging biomarker for amyotrophic lateral sclerosis. *Lancet Neurol.* 10:400-3.
- Turner MR, Wicks P, Brownstein CA, et al. (2011b) Concordance between site of onset and limb dominance in amyotrophic lateral sclerosis. *J. Neurol. Neurosurg. Psychiatry* 82:853-4.
- Turner MR. (2011) MRI as a frontrunner in the search for amyotrophic lateral sclerosis biomarkers? *Biomark. Med.* 5:79-81.
- Turner MR, Kiernan MC. (2012) Does interneuronal dysfunction contribute to neurodegeneration in amyotrophic lateral sclerosis? *Amyotroph. Lateral Scler.* 13:245-50.
- Turner MR, Agosta F, Bede P, Govind V, Lule D, Verstraete E. (2012) Neuroimaging in amyotrophic lateral sclerosis. *Biomark. Med.* 6:319-37.
- Underwood CK, Kurniawan ND, Butler TJ, Cowin GJ, Wallace RH. (2011) Non-invasive diffusion tensor imaging detects white matter degeneration in the spinal cord of a mouse model of amyotrophic lateral sclerosis. *NeuroImage* 55:455-61.
- Unrath A, Ludolph AC, Kassubek J. (2007) Brain metabolites in definite amyotrophic lateral sclerosis. A longitudinal proton magnetic resonance spectroscopy study. *J. Neurol.* 254:1099-106.
- Unrath A, Muller HP, Riecker A, Ludolph AC, Sperfeld AD, Kassubek J. (2010) Whole brain-based analysis of regional white matter tract alterations in rare motor neuron diseases by diffusion tensor imaging. *Hum. Brain Mapp.* 31:1727-40.
- Usman U, Choi C, Camicioli R, et al. (2011) Mesial prefrontal cortex degeneration in amyotrophic lateral sclerosis: a high-field proton MR spectroscopy study. *AJNR Am. J. Neuroradiol.* 32:1677-80.
- Valsasina P, Agosta F, Benedetti B, et al. (2007) Diffusion anisotropy of the cervical cord is strictly associated with disability in amyotrophic lateral sclerosis. *J. Neurol. Neurosurg. Psychiatry* 78:480-4.
- Van den Berg-Vos RM, Visser J, Kalmijn S, et al. (2009) A long-term prospective study of the natural course of sporadic adult-onset lower motor neuron syndromes. *Arch. Neurol.* 66:751-7.
- van den Heuvel MP, Stam CJ, Boersma M, Hulshoff Pol HE. (2008a) Small-world and scale-free organization of voxel-based resting-state functional connectivity in the human brain. *NeuroImage* 43:528-39.
- van den Heuvel MP, Mandl RC, Luijckes J, Hulshoff Pol HE. (2008b) Microstructural organization of the cingulum tract and the level of default mode functional connectivity. *J. Neurosci.* 28:10844-51.
- van den Heuvel MP, Mandl RC, Kahn RS, Hulshoff Pol HE. (2009) Functionally linked resting-state networks reflect the underlying structural connectivity architecture of the human brain. *Hum. Brain Mapp.* 30:3127-41.
- van den Heuvel MP, Stam CJ, Kahn RS, Hulshoff Pol HE. (2009) Efficiency of functional brain networks and intellectual performance. *J. Neurosci.* 29:7619-24.

- van den Heuvel MP, Hulshoff Pol HE. (2010) Exploring the brain network: a review on resting-state fMRI functional connectivity. *Eur. Neuropsychopharmacol.* 20:519-34.
- van den Heuvel MP, Mandl RC, Stam CJ, Kahn RS, Hulshoff Pol HE. (2010) Aberrant frontal and temporal complex network structure in schizophrenia: a graph theoretical analysis. *J. Neurosci.* 30:15915-26.
- van den Heuvel MP, Sporns O. (2011) Rich-club organization of the human connectome. *J. Neurosci.* 31:15775-86.
- van der Graaff MM, Sage CA, Caan MW, et al. (2011) Upper and extra-motoneuron involvement in early motoneuron disease: a diffusion tensor imaging study. *Brain* 134:1211-28.
- van der Schot AC, Vonk R, Brans RG, et al. (2009) Influence of genes and environment on brain volumes in twin pairs concordant and discordant for bipolar disorder. *Arch. Gen. Psychiatry* 66:142-51.
- van Eimeren T, Monchi O, Ballanger B, Strafella AP. (2009) Dysfunction of the default mode network in Parkinson disease: a functional magnetic resonance imaging study. *Arch. Neurol.* 66:877-83.
- Van Zandijcke M, Casselman J. (1995) Involvement of corpus callosum in amyotrophic lateral sclerosis shown by MRI. *Neuroradiology* 37:287-8.
- van Zijl PC, Yadav NN. (2011) Chemical exchange saturation transfer (CEST): what is in a name and what isn't? *Magn. Reson. Med.* 65:927-48.
- Veldink JH, Kalmijn S, Groeneveld GJ, Titulaer MJ, Wokke JH, van den Berg LH. (2005) Physical activity and the association with sporadic ALS. *Neurology* 64:241-5.
- Verstraete E, Veldink JH, van den Berg LH. (2010) Would riluzole be efficacious in the new ALS trial design? *Lancet Neurol.* 9:949,50; author reply 950-1.
- Verstraete E, van den Heuvel MP, Veldink JH, et al. (2010) Motor network degeneration in amyotrophic lateral sclerosis: a structural and functional connectivity study. *PLoS ONE* 5:e13664.
- Verstraete E, Veldink JH, Mandl RC, van den Berg LH, van den Heuvel MP. (2011) Impaired structural motor connectome in amyotrophic lateral sclerosis. *PLoS ONE* 6:e24239.
- Verstraete E, Veldink JH, Hendrikse J, Schelhaas HJ, van den Heuvel MP, van den Berg LH. (2012) Structural MRI reveals cortical thinning in amyotrophic lateral sclerosis. *J. Neurol. Neurosurg. Psychiatry* 83:383-8.
- Visser J, van den Berg-Vos RM, Franssen H, et al. (2007) Disease course and prognostic factors of progressive muscular atrophy. *Arch. Neurol.* 64:522-8.
- Visser J, de Jong JM, de Visser M. (2008) The history of progressive muscular atrophy: syndrome or disease? *Neurology* 70:723-7.
- Vrenken H, Geurts JJ, Knol DL, et al. (2006) Whole-brain T1 mapping in multiple sclerosis: global changes of normal-appearing gray and white matter. *Radiology* 240:811-20.
- Vucic S, Nicholson GA, Kiernan MC. (2008) Cortical hyperexcitability may precede the onset of familial amyotrophic lateral sclerosis. *Brain* 131:1540-50.
- Vucic S, Cheah BC, Kiernan MC. (2009) Defining the mechanisms that underlie cortical hyperexcitability in amyotrophic lateral sclerosis. *Exp. Neurol.* 220:177-82.

References

- Wahl M, Lauterbach-Soon B, Hattingen E, et al. (2007) Human motor corpus callosum: topography, somatotopy, and link between microstructure and function. *J. Neurosci.* 27:12132-8.
- Wang S, Poptani H, Bilello M, et al. (2006a) Diffusion tensor imaging in amyotrophic lateral sclerosis: volumetric analysis of the corticospinal tract. *AJNR Am. J. Neuroradiol.* 27:1234-8.
- Wang S, Poptani H, Woo JH, et al. (2006b) Amyotrophic lateral sclerosis: diffusion-tensor and chemical shift MR imaging at 3.0 T. *Radiology* 239:831-8.
- Waragai M. (1997) MRI and clinical features in amyotrophic lateral sclerosis. *Neuroradiology* 39:847-51.
- Weiller C, May A, Sach M, Buhmann C, Rijntjes M. (2006) Role of functional imaging in neurological disorders. *J. Magn. Reson. Imaging* 23:840-50.
- Whitehead J. (1997) *The Design and Analysis of Sequential Clinical Trials, Revised, 2nd Edition.* 328.
- Wicks P, Abrahams S, Papps B, et al. (2009) SOD1 and cognitive dysfunction in familial amyotrophic lateral sclerosis. *J. Neurol.* 256:234-41.
- Wicks P, Vaughan TE, Massagli MP, Heywood J. (2011) Accelerated clinical discovery using self-reported patient data collected online and a patient-matching algorithm. *Nat. Biotechnol.* 29:411-4.
- Wijesekera LC, Mathers S, Talman P, et al. (2009) Natural history and clinical features of the flail arm and flail leg ALS variants. *Neurology* 72:1087-94.
- Wilson JM, Petrik MS, Grant SC, Blackband SJ, Lai J, Shaw CA. (2004) Quantitative measurement of neurodegeneration in an ALS-PDC model using MR microscopy. *NeuroImage* 23:336-43.
- Winkler AM, Kochunov P, Blangero J, et al. (2010) Cortical thickness or grey matter volume? The importance of selecting the phenotype for imaging genetics studies. *NeuroImage* 53:1135-46.
- Winner B, Jappelli R, Maji SK, et al. (2011) In vivo demonstration that alpha-synuclein oligomers are toxic. *Proc. Natl. Acad. Sci. U. S. A.* 108:4194-9.
- Wittstock M, Wolters A, Benecke R. (2007) Transcallosal inhibition in amyotrophic lateral sclerosis. *Clin. Neurophysiol.* 118:301-7.
- Won Seo S, Hwa Lee B, Kim EJ, et al. (2007) Clinical significance of microbleeds in subcortical vascular dementia. *Stroke* 38:1949-51.
- Wong JC, Concha L, Beaulieu C, Johnston W, Allen PS, Kalra S. (2007) Spatial profiling of the corticospinal tract in amyotrophic lateral sclerosis using diffusion tensor imaging. *J. Neuroimaging* 17:234-40.
- Wu T, Wang L, Chen Y, Zhao C, Li K, Chan P. (2009) Changes of functional connectivity of the motor network in the resting state in Parkinson's disease. *Neurosci. Lett.* 460:6-10.
- Wu Y, Le W, Jankovic J. (2011) Preclinical biomarkers of Parkinson disease. *Arch. Neurol.* 68:22-30.
- Yamauchi H, Fukuyama H, Ouchi Y, et al. (1995) Corpus callosum atrophy in amyotrophic lateral sclerosis. *J. Neurol. Sci.* 134:189-96.
- Yin H, Lim CC, Ma L, et al. (2004) Combined MR spectroscopic imaging and diffusion tensor MRI visualizes corticospinal tract degeneration in amyotrophic lateral sclerosis. *J. Neurol.* 251:1249-54.
- Zalesky A. (2008) DT-MRI fiber tracking: a shortest paths approach. *IEEE Trans. Med. Imaging* 27:1458-71.

- Zalesky A, Fornito A, Bullmore ET. (2010) Network-based statistic: identifying differences in brain networks. *NeuroImage* 53:1197-207.
- Zalesky A, Fornito A, Seal ML, et al. (2011) Disrupted axonal fiber connectivity in schizophrenia. *Biol. Psychiatry* 69:80-9.
- Zarei M, Johansen-Berg H, Jenkinson M, Ciccarelli O, Thompson AJ, Matthews PM. (2007) Two-dimensional population map of cortical connections in the human internal capsule. *J. Magn. Reson. Imaging* 25:48-54.
- Zhai P, Pagan F, Statland J, Butman JA, Floeter MK. (2003) Primary lateral sclerosis: A heterogeneous disorder composed of different subtypes? *Neurology* 60:1258-65.
- Zhang Y, Schuff N, Woolley SC, et al. (2011) Progression of white matter degeneration in amyotrophic lateral sclerosis: A diffusion tensor imaging study. *Amyotroph. Lateral Scler.* 12:421-9.
- Zhong Z, Deane R, Ali Z, et al. (2008) ALS-causing SOD1 mutants generate vascular changes prior to motor neuron degeneration. *Nat. Neurosci.* 11:420-2.
- Zhou J, Payen JF, Wilson DA, Traystman RJ, van Zijl PC. (2003) Using the amide proton signals of intracellular proteins and peptides to detect pH effects in MRI. *Nat. Med.* 9:1085-90.
- Zhou J, Greicius MD, Gennatas ED, et al. (2010) Divergent network connectivity changes in behavioural variant frontotemporal dementia and Alzheimer's disease. *Brain* 133:1352-67.
- Zhou J, Gennatas ED, Kramer JH, Miller BL, Seeley WW. (2012) Predicting Regional Neurodegeneration from the Healthy Brain Functional Connectome. *Neuron* 73:1216-27.

References

Summary



Amyotrophic lateral sclerosis (ALS) is a neurodegenerative disease involving both upper motor neurons in the brain and lower motor neurons in the spinal cord. The clinical hallmark of ALS is progressive muscle weakness, mostly with a focal onset, e.g. in one arm or leg, and subsequent spread of symptoms to other parts of the body. ALS can occur at any age during adulthood. Patients generally die due to respiratory failure only three to five years after onset of symptoms. Onset and disease course in ALS are heterogeneous as each patient has a unique combination of upper and lower motor neuron involvement, site of onset and symptom development. ALS is part of the spectrum of motor neuron diseases (MND), which also includes primary lateral sclerosis (PLS), with only upper motor neuron involvement, and progressive muscular atrophy (PMA), with only lower motor neuron involvement. In addition to motor symptoms, a subgroup of patients with ALS develops cognitive deficits. A minority of this subgroup is even diagnosed with frontotemporal dementia (FTD), a type of dementia characterized by behavioural problems.

This thesis is entitled ‘Traces of disease in amyotrophic lateral sclerosis’, reflecting the search for a good biomarker by exploring both neuroimaging techniques and measurements in biological samples (**part 2: Biomarkers**). In addition, it looks at the spread of disease; does the disease propagate in a predictable way, following a certain path or ‘trace’ (**part 1: Spread of disease**)? The third section of this thesis is about clinical trials in which we depend on measureable markers (or traces) of disease to assess efficacy of the drug undergoing study or intervention (**part 3: Clinical trials**).

Neuroimaging using MRI is the most important research tool applied in this thesis. It allows both structural and functional examination of the brain in a non-invasive and radiation-free way. In addition, advanced software applications enable automated measurements whereby detailed data on brain structures or brain activity are acquired, which allow for subsequent comparison between patients and healthy controls. **Chapter 2** considers the full range of neuroimaging techniques applied to ALS, the biomarkers they have revealed and future developments.

Part I: Spread of disease

ALS is characterized by gradual progression of disease. The underlying mechanisms which cause this clinical deterioration are, however, largely unknown. Insight into how clinical symptoms spread throughout the body and into the parallel changes occurring in the brain might help elucidate the underlying mechanisms. Knowledge about the

spread of disease might provide new leads for future therapeutic targets to slow disease progression.

In **chapter 3** we used a questionnaire to investigate how motor symptoms (e.g. weakness, difficulty swallowing) developed over time in patients with MND (ALS, PLS and PMA). We found symptoms spread preferably from one arm to the contralateral arm and from one leg to the contralateral leg. This observation was consistent among the different MND phenotypes. In the brain, left and right motor areas are connected by the corpus callosum. Our findings suggest interhemispheric spread of disease potentially guided by this major interconnecting white matter tract. In conclusion, this study showed non-random distribution of symptoms in MND with symptoms spreading preferably to the contralateral limb.

In **chapters 4, 5 and 6** we examined the changes in the brain or – more specifically – the brain network in patients with ALS using MRI. First, we studied the structural and functional changes within the motor network (**chapter 4**). Using ‘diffusion tensor imaging’ (DTI) to assess the integrity of the white matter connections, we found a reduced structural integrity of the corpus callosum. Based on functional MRI, however, functional connectivity between the right and left primary motor cortices was found to be preserved. Interestingly, we even observed a positive correlation between functional connectivity and the rate of disease progression. This seemingly contradictory finding might support a role of the corpus callosum as an intermediate in spread of disease. On the basis of these results, we arrived at the hypothesis that the disease process in ALS might spread through the connections within the motor network.

The changes occurring outside the motor network, in the rest of the brain network, were explored in **chapters 5 and 6**. We reconstructed the structural brain network by dividing the cortical surface into a number of regions and subsequently determined if and how strong these regions are interconnected. The white matter connections were again reconstructed using DTI. The integrity of the brain network was then compared between patients and healthy controls (**chapter 5**), in addition, longitudinal changes in patients were assessed (**chapter 6**). This study revealed a subnetwork of impaired connectivity in ALS with a central role for the primary motor regions and impaired connections to other (frontal, parietal and temporal) brain regions. In addition, we found a significant overlap between brain regions included in this impaired subnetwork and the regions connected to the primary motor regions in healthy controls. We concluded that ALS not only affects the connections within the primary motor system, but also the connections between motor regions and the rest of the brain.



In order to assess longitudinal brain network changes, we compared the reconstructed brain network of patients at two time-points (a baseline measure and after an average of five months) with that of healthy controls. This analysis resulted in a growing subnetwork of impaired white matter connections including more direct and indirect motor connections in ALS. The initially impaired connections did not show progressive impairment. These findings might suggest the disease process follows the connections of the brain network.

To summarize, we found indications for spread of disease in ALS guided by the brain's network structure. This finding is of importance as it may provide new leads for therapeutic targets to slow disease progression.

Part II: Biomarkers

As described above, there is great variation among ALS patients regarding the extent of involvement of upper and lower motor neurons, but also the extent to which other brain regions are involved. Alongside the clinical examination of patients, electromyography (EMG) allows objective assessment of lower motor neuron involvement. A similar objective assessment of the upper motor neuron or extra-motor brain involvement is currently lacking but would improve the diagnosis of ALS. In addition, an objective upper motor neuron marker might be of importance for prognosis or evaluation of (experimental) treatment.

In **chapter 7** we report on an imaging study measuring whole brain cortical thickness in 45 patients with ALS compared to a group of healthy controls. We found convincing cortical thinning in the primary motor regions (motor cortex) in ALS, suggesting this measure might be an objective marker for upper motor neuron involvement. A subset of patients was re-examined after several months revealing no progressive changes with time. It was hypothesized that the cortical thinning had occurred before onset of symptoms or that it may be a risk factor for ALS. Future studies should aim to assess the diagnostic potential of this measure, it being vital to establish the discriminating power between ALS and its mimics.

In **chapters 8 and 9** we explored newly developed acquisition sequences on ultra-high field MRI for their potential in ALS. This 7T MRI has an increased sensitivity enabling detection of specific tissue changes such as, for example, increased iron content. In previous chapters we used DTI to study the integrity of white matter. It is not, however, fully understood

what kind of changes in the brain tissue cause the effects found with DTI. In **chapter 8** we examined whether other MRI contrasts can provide more insight into the underlying tissue changes, the results suggested an increased liquid fraction within the affected white matter. This could mean that the effects found with DTI might be caused by alterations in the supportive tissue (e.g. proliferation of glial cells and extracellular matrix expansion). Demyelination seems less likely to be the primary cause of these effects. In **chapter 9** we assessed the presence of cerebral microbleeds in sporadic ALS cases using a technique highly sensitive to iron accumulation. This study, in contrast to previous results in the mouse model for ALS, did not reveal any microbleeds in patients.

The final chapter (**chapter 10**) of this part on biomarkers describes the findings following TDP-43 protein measures in blood. The TDP-43 protein has been identified as a key player in ALS pathology since accumulations containing this protein are found in the brain tissue of virtually all patients. Blood measurements show that this protein is slightly but significantly raised compared to healthy controls. Future research should aim to establish the relation between the TDP-43 protein blood concentration and the cerebral accumulations.

Based on the biomarker studies in this thesis, cortical thickness of the motor cortex is the most promising measurement as objective marker for upper motor neuron involvement in ALS. In the future this measurement might become a part of the diagnostic workup.



Part III: Clinical trials

Improving treatment of ALS or finding a cure is the ultimate goal of all research activities. Performing a clinical trial is a crucial step towards reaching this goal and should, therefore, be carried out with great care. A false positive or false negative outcome is detrimental for patients, as well as for progress in the field. In 2008, there was a report on lithium and its potential to slow disease progression and increase survival in ALS mice and also in a small group of patients (n=44) (Fornai et al. PNAS 2008). The hypothesized mode of action is promoting cellular protein clearance of misfolded or defective proteins. More research was needed to establish the true effects of lithium on the disease course of ALS.

In **chapter 11** we performed a randomized, placebo-controlled, double-blind trial studying the effect of lithium on survival and functional decline in patients with ALS. The study

Summary

data were analyzed sequentially to permit discontinuation as soon as enough evidence for a treatment effect or lack thereof was obtained. This method of analysis minimizes the burden for patients participating in clinical trials and prevents unnecessary delay should a novel therapy prove effective. After two and a half years and 133 participating patients, it turned out that lithium (unfortunately) did not have a beneficial effect on survival in ALS. Nor did secondary outcome measurements differ between patients treated with lithium or placebo. This study has effectively ruled out a beneficial effect of lithium on the disease course in ALS.

We conclude from a randomized, placebo-controlled, double-blind trial that lithium has no beneficial effect on the disease course in ALS.

Samenvatting (Summary in Dutch)



Amyotrofische laterale sclerose (ALS) is een aandoening waarbij er verlies is van motorische zenuwcellen in de hersenen (centraal motorische neuronen) en het ruggenmerg (perifeer motorische neuronen). De ziekte kenmerkt zich door toenemende spierzwakte, meestal beginnend in één lichaamsdeel, bijvoorbeeld een arm of been, waarna de klachten zich uitbreiden naar de rest van het lichaam. ALS kan op elke volwassen leeftijd ontstaan. Patiënten overlijden doorgaans aan zwakte van de ademhalingsspieren na een gemiddelde overleving van slechts vijf jaar. Het ziektebeloop is bij elke patiënt anders, onder andere door verschil in de mate waarin het centraal en perifeer motorisch neuron betrokken is, de lichaamsregio waarin de ziekteverschijnselen beginnen en hoe de symptomen zich ontwikkelen in de tijd. ALS behoort tot het spectrum van motor neuron ziekten, samen met primaire laterale sclerose (PLS) waarbij enkel het centraal motorisch neuron betrokken is en progressieve spinale spieratrofie (PSMA) waarbij enkel het perifeer motorisch neuron betrokken is. Naast de motorische problemen ontwikkelt een gedeelte van de patiënten met ALS problemen in 'het denken'. Hierbij is er in een minderheid van de gevallen zelfs sprake van frontotemporale dementie (FTD), een type dementie dat gekenmerkt wordt door gedragsveranderingen.

Dit proefschrift draagt de titel 'Sporen van ziekte bij amyotrofische laterale sclerose', waarmee verwezen wordt naar de zoektocht naar een goede biomarker voor de ziekte (**deel II: Biomarkers**). Daarnaast verwijst de titel naar de verspreiding van de ziekte; verspreidt het ziekteproces zich op een voorspelbare manier, volgens een bepaald 'spoor' (**deel I: Verspreiding van ziekte**)? Het derde deel van dit proefschrift gaat over klinisch geneesmiddelenonderzoek waarbij het effect van de interventie wordt beoordeeld aan de hand van meetbare uitkomstmaten (of sporen van ziekte) (**deel III: Klinisch geneesmiddelenonderzoek**).

Beeldvorming van de hersenen middels MRI is het belangrijkste onderzoeksinstrument geweest in dit proefschrift. Deze techniek maakt het mogelijk – op niet-invasieve wijze en zonder gebruik van straling – zowel structuur als functie van de hersenen te onderzoeken. Bovendien is het door nieuwe softwaretoepassingen mogelijk geautomatiseerde metingen uit te voeren. Hierbij worden gedetailleerde gegevens verkregen over hersenstructuren of hersenactiviteit die vervolgens vergeleken kunnen worden tussen patiënten met ALS en gezonde controlepersonen. In **hoofdstuk 2** worden de verschillende MRI-technieken besproken. Tevens wordt er een overzicht gegeven van wat er tot op heden gevonden is bij ALS en welke kansen er liggen voor de toekomst.

Deel I: Verspreiding van ziekte

ALS kenmerkt zich door geleidelijke ziekteprogressie, waarbij echter niet goed bekend is waardoor de klinische achteruitgang wordt veroorzaakt. Inzicht in hoe het ziekteproces zich verspreidt in het lichaam en de veranderingen die parallel hieraan optreden in de hersenen kunnen helpen de onderliggende mechanismen te begrijpen. Als er meer duidelijk is over hoe de ziekte zich verspreidt biedt dit mogelijk aangrijpingspunten voor nieuwe geneesmiddelen of behandelingen die het ziektebeloop vertragen.

In **hoofdstuk 3** hebben we door middel van vragenlijstonderzoek onder patiënten met motor neuron ziekten (ALS, PLS en PSMA) geïnventariseerd hoe klachten van spierzwakte zich ontwikkelden in de tijd. Dit onderzoek laat zien dat symptomen vaker verspreiden van de ene arm naar de andere arm of van het ene been naar het andere been dan bijvoorbeeld van een arm naar een been. Deze observatie was eenduidig bij elk type motor neuron ziekte. In de hersenen zijn de motorische gebieden links en rechts verbonden via het corpus callosum (hersenspleet). Onze resultaten ondersteunen de mogelijkheid dat het ziekteproces zich via deze verbinding verspreidt. Wij hebben kunnen vaststellen dat de verspreiding van symptomen niet willekeurig is, maar dat er voorkeur is voor verspreiding van arm naar arm en been naar been.

In **hoofdstuk 4, 5 en 6** is onderzocht welke veranderingen optreden in de hersenen of – meer specifiek – in het breinnetwerk van patiënten met ALS met behulp van MRI-technieken. Allereerst hebben we onderzocht welke structurele en functionele veranderingen optreden binnen het motorische netwerk in het brein (**hoofdstuk 4**). Met behulp van ‘diffusion tensor imaging’ (DTI), een techniek waarmee de kwaliteit van de witte stofverbindingen onderzocht kan worden, werden aanwijzingen gevonden voor aantasting van het corpus callosum bij patiënten met ALS. Echter, op basis van functionele MRI waren er aanwijzingen dat de informatie uitwisseling binnen het motorisch netwerk (functionele connectiviteit) niet verminderd was. Interessant was dat een hoge functionele connectiviteit zelfs in relatie stond met een snelle achteruitgang door de ziekte. Op basis van deze bevinding kwamen wij tot de hypothese dat het ziekteproces bij ALS zich mogelijk verspreidt via de verbindingen binnen het motorische netwerk.

De veranderingen die optreden buiten het motorisch netwerk, in de rest van het breinnetwerk, zijn onderzocht in **hoofdstuk 5 en 6**. In dit onderzoek hebben we het breinnetwerk gereconstrueerd door de hersenschors op te delen in kleine gebiedjes en vervolgens te kijken óf en hoe sterk deze gebiedjes met elkaar verbonden zijn. Voor de reconstructie



van de witte stofverbindingen is wederom gebruik gemaakt van DTI. De kwaliteit van het breinnetwerk is vervolgens vergeleken tussen patiënten en gezonde controlepersonen (**hoofdstuk 5**) en er is gekeken naar veranderingen bij patiënten in de tijd (**hoofdstuk 6**). Dit onderzoek laat zien dat een gedeelte van het breinnetwerk, een subnetwerk, is aangetast bij ALS. In dit subnetwerk is er een centrale rol voor de primaire motorische gebieden met aantasting van verbindingen naar andere (frontale, pariëtale en temporale) hersengebieden. Er blijkt een grote overlap te zijn tussen de hersengebieden die deel uitmaken van het aangetaste subnetwerk en de hersengebieden waarmee primaire motorische gebieden bij gezonde controlepersonen verbonden zijn. Op basis van dit onderzoek hebben we geconcludeerd dat ALS niet alleen de verbindingen binnen het primaire motorische systeem aantast, maar ook de verbindingen met de motorische gebieden en de rest van het brein.

Om te kijken hoe een en ander zich ontwikkelt in de tijd hebben we het breinnetwerk van patiënten op twee momenten (een uitgangsmeting en na ongeveer 5 maanden) vergeleken met een groep gezonde controlepersonen. Dit onderzoek toont een groeiend subnetwerk van aangetaste witte stofverbindingen dat een toenemend aantal hersengebieden omvat die direct of indirect met de motorische gebieden verbonden zijn. We hebben geen aanwijzingen gevonden voor verder verval van reeds aangedane verbindingen. Deze bevindingen suggereren uitbreiding van het ziekteproces bij ALS via de verbindingen van het breinnetwerk.

Samenvattend hebben we aanwijzingen gevonden voor verspreiding van het ziekteproces bij ALS via de verbindingen van het breinnetwerk. Deze bevinding is relevant aangezien dit mogelijk aangrijpingspunten biedt voor de ontwikkeling van nieuwe geneesmiddelen die het ziektebeloop kunnen vertragen.

Deel II: Biomarkers

Zoals hierboven reeds beschreven, is er veel variatie tussen patiënten met ALS in de mate waarin het centraal en perifeer motorisch neuron betrokken is, maar ook in de mate waarin andere hersengebieden worden aangetast door de ziekte. Naast het klinisch neurologisch onderzoek kan met elektromyografisch (EMG) onderzoek op objectieve wijze betrokkenheid van het perifeer motorisch neuron vastgesteld worden. Een dergelijke objectieve meting is voor het centraal motorisch neuron of andere hersengebieden op dit moment

(nog) niet beschikbaar. Zo'n meting zou wel van meerwaarde zijn in het diagnostische traject, zowel voor het bepalen van de prognose als voor het evalueren van het effect van een behandeling.

In **hoofdstuk 7** beschrijven we MRI-onderzoek waarbij de dikte van de hersenschors (cortex) werd gemeten over het gehele hersenoppervlak bij 45 patiënten met ALS in vergelijking met een groep gezonde controlepersonen. Uit dit onderzoek blijkt dat de hersenschors in de motorische gebieden (motor cortex) dunner is bij ALS. Op basis van deze resultaten concludeerden wij dat de dikte van de motor cortex mogelijk een objectieve marker zou kunnen zijn voor betrokkenheid van het centraal motorisch neuron. Een gedeelte van de patiënten is op een later tijdstip nogmaals onderzocht, hierbij werden geen veranderingen waargenomen in de motorische hersenschors. Op basis hiervan is het niet ondenkbaar dat de veranderingen reeds opgetreden waren voordat patiënten überhaupt klachten hadden ontwikkeld of dat het hier zelfs een risicofactor betreft. Toekomstig onderzoek zal de diagnostische meerwaarde van corticale diktemetingen bij de diagnostiek van ALS moeten vaststellen. Essentieel hierbij is of deze meting onderscheid kan maken tussen ALS en aandoeningen die zich kunnen presenteren zoals ALS ('ALS mimics').

In **hoofdstuk 8 en 9** hebben we nieuwe toepassingen op een ultra-hoog veld MRI onderzocht op hun meerwaarde bij ALS. Deze 7 Tesla MRI kent een grotere gevoeligheid om bepaalde veranderingen op weefselniveau te detecteren zoals bijvoorbeeld ophopingen van ijzer. In voorgaande hoofdstukken is gebruik gemaakt van DTI om de kwaliteit van de witte stof te beoordelen, het is echter niet goed bekend welke veranderingen in het hersenweefsel aan deze DTI-effecten ten grondslag liggen. In **hoofdstuk 8** hebben we onderzocht of andere MRI-contrasten meer inzicht kunnen geven in de onderliggende weefselveranderingen. De resultaten van dit onderzoek suggereren dat de vrije waterfractie is toegenomen in de aangetaste witte stof. Dit zou kunnen betekenen dat de effecten gevonden bij DTI verklaard worden door veranderingen in het steunweefsel (glia-cellen en/of extracellulaire matrix). Demyelinisatie (= verlies van isolatie rondom zenuwuitlopers) is met deze bevindingen minder waarschijnlijk geworden. In **hoofdstuk 9** hebben we gezocht naar microbloedingen in het hersenweefsel bij ALS met een techniek die bijzonder gevoelig is voor ijzerophopingen die hierbij optreden. Dit onderzoek laat, in tegenstelling tot eerder onderzoek bij muizen met ALS, geen aanwijzingen zien voor de aanwezigheid van deze microbloedingen.



Het laatste hoofdstuk (**hoofdstuk 10**) in dit deel van het proefschrift over biomarkers beschrijft de bevindingen naar aanleiding van TDP-43 eiwitmetingen in bloed. Aangezien bij bijna alle patiënten ophopingen van dit eiwit in het hersenweefsel worden gevonden, wordt het TDP-43 eiwit als een centrale speler in het ziekteproces bij ALS gezien. De metingen in het bloed laten zien dat de concentratie TDP-43 in patiënten licht maar significant verhoogd is ten opzichte van controlepersonen. Toekomstig onderzoek zal moeten uitwijzen of de TDP-43 bloedwaarden in relatie staan met de ophopingen in het hersenweefsel.

Op basis van het biomarkeronderzoek in dit proefschrift is de dikte van de motorische hersenschors het meest kansrijk als objectieve marker voor betrokkenheid van het centraal motorisch neuron bij ALS. In de toekomst zou deze meting een onderdeel kunnen gaan vormen van het diagnostische traject.

Deel III: Klinisch geneesmiddelenonderzoek

Het ultieme doel van al het onderzoek naar ALS is om tot genezing of een betere behandeling te komen. Het klinisch geneesmiddelenonderzoek is een cruciale stap op weg naar dit doel. Middelen die mogelijk effectief zijn dienen op zorgvuldige wijze onderzocht te worden aangezien fout-positieve of fout-negatieve uitkomsten schadelijk zijn voor patiënten en de wetenschappelijke vooruitgang. In 2008 verscheen onderzoek (Fornai et al. PNAS 2008) waarin gerapporteerd werd dat lithium in het muismodel voor ALS alsook in een kleine groep patienten (n=44) het ziekteproces kon vertragen. Het veronderstelde werkingsmechanisme betrof het stimuleren van autofagie, oftewel het geheel aan processen in een cel dat ervoor zorgt dat defecte of beschadigde eiwitten worden opgeruimd. Meer onderzoek was nodig om vast te stellen of lithium werkelijk een gunstig effect had op het beloop van ALS.

In **hoofdstuk 11** is in een gerandomiseerde, dubbelblinde, placebo-gecontroleerde studie het effect van lithium op de overleving en functionele achteruitgang bij patiënten met ALS onderzocht. De resultaten zijn sequentieel geanalyseerd, dit betekent dat er tussentijds gekeken is of er een verschil ontstond tussen de placebo- en de lithiumgroep. Deze manier van analyseren voorkomt dat een effectief middel onnodig lang in de onderzoeksfase blijft en dat een niet-effectief middel onnodig lang aan patiënten gegeven wordt. Na ruim twee en een half jaar en 133 deelnemende patiënten bleek dat lithium (helaas) geen gunstig effect had op de overleving bij ALS. Ook andere uitkomstmaten waren niet verschillend

tussen patiënten behandeld met lithium of placebo. Door dit onderzoek is er duidelijkheid gekomen over het effect van lithium op het ziektebeloop bij ALS.

Op basis van een gerandomiseerde, dubbelblinde, placebo-gecontroleerde studie kan geconcludeerd worden dat lithium geen gunstig effect heeft op het ziektebeloop bij ALS.



Samenvatting (Summary in Dutch)

Dankwoord



Gedurende mijn promotietraject heb ik veel geleerd over de specifieke onderwerpen die in dit proefschrift aan bod komen, over de wetenschappelijke wereld en over mezelf. Ik ben dankbaar voor alles wat het me heeft gebracht en voor de hulp en steun van iedereen die hieraan heeft bijgedragen. Een aantal mensen wil ik hier in het bijzonder bedanken.

Allereerst, alle kleurrijke **patiënten met ALS** die kostbare tijd hebben vrijgemaakt voor het onderzoek, mijn dank en waardering hiervoor is groot. Naast deze essentiële bijdrage ben ik een aantal patiënten heel dankbaar dat ik kennis heb mogen maken met hun bewonderenswaardige levensinstelling.

Mijn promotor, **Prof. dr. L.H. van den Berg**.

Beste Leonard, als je het mij vraagt, vind ik dat een goed leider op de éérste plaats een inspirator moet zijn en dat ben je voor mij. Op de poli vond ik het bijzonder om te zien hoe je patiënten met mogelijk een dodelijke ziekte binnen enkele minuten op hun gemak stelde en een luchtige draai wist te geven aan de beladen situatie. In het onderzoek vond ik het opvallend om te zien hoe je mensen als vanzelfsprekend voor je weet te winnen en altijd oog houdt voor wat, wanneer prioriteit heeft. Jouw grootse ambitie (die soms wat weg heeft van een ‘reality distortion field’ zoals Steve Jobs dat ook kon hebben) in combinatie met een flinke dosis creativiteit gaan ongetwijfeld nog veel betekenen voor patiënten met ALS.

Mijn co-promotoren, **Dr. M.P. van den Heuvel** en **Dr. J.H. Veldink**.

Martijn, hoe anders zou dit boekje eruit gezien hebben als ik niet op een willekeurige dag jouw kamer was binnengewandeld... Ik heb grote bewondering voor hoe je simultaan je Mac's weet te hanteren en die vaardigheid combineert met een ongelooflijke dosis creativiteit waarmee je écht nieuwe concepten op neurowetenschappelijk gebied weet neer te zetten. Diezelfde creativiteit en het vermogen in mogelijkheden te denken maakte dat onze overlegmomenten zich al snel ontwikkelden in ideeënstromen vol positieve energie. Deze ‘creatieve flow’ heb ik als heel bijzonder ervaren. Daarbij heb je sturing gegeven aan mijn promotietraject en me gemotiveerd het beste in mezelf naar boven te halen. Jouw coachende vaardigheden in combinatie met een hoge mate van wetenschappelijke creativiteit moeten wel gaan leiden tot een bijzondere plek in de wetenschappelijke wereld.

Jan, jouw statistische kennis is van grote waarde geweest voor mij en ik weet dat dit voor mijn collega onderzoekers niet anders is. Bijzonder om – zo'n beetje – te allen tijde een 'hulplijn' te kunnen raadplegen om toch die deadline te kunnen halen. Bedankt voor de fijne samenwerking al die jaren (en natuurlijk alle lithiumspiegels die je doorgedoseerd hebt).

Mijn opleiders, **Prof. dr. J. van Gijn** en **Prof. dr. J.H.J. Wokke**.

Beste professor van Gijn, u was mijn opleider in mijn eerste opleidingsjaar. Ik heb groot respect voor alles wat u bereikt heeft als dokter voor patiënten, hoofd van de afdeling neurologie en als wetenschapper. U bent voor mij in veel opzichten een rolmodel.

Beste professor Wokke, ik wil u danken voor de mooie opleiding die ik mag genieten in Utrecht. Uw inspanningen voor onderwijs en opleidingsvernieuwing zijn goed merkbaar. In het bijzonder waardeer ik de ruimte die u geeft voor differentiatie, zoals in mijn geval het ontwikkelen van bestuurlijke vaardigheden.

Leden van de beoordelingscommissie.

Geachte **prof. dr. P.R. Luijten**, **dr. M.R. Turner**, **prof. dr. G.J. Biessels**, **prof. dr. H.E. Hulshoff Pol**, **prof. dr. J.P.H. Burbach**, hartelijk dank dat ik u mijn proefschrift ter beoordeling mocht voorleggen.

Dr. M.R. Turner. Dear Martin, it is an honour to me that you are willing to attend the defense of my thesis. The discussions we had at meetings the past years on ALS and the brain have been inspiring to me. I am looking forward to further collaboration in the future.

Prof. dr. G.J. Biessels. Beste Geert-Jan, allereerst heb ik veel respect voor jouw kwaliteiten als supervisor, recht door zee en je bent er écht als het nodig is. Ook waar we samengewerkt hebben in het onderzoek heb ik jouw mentaliteit van 'aanpakken' mogen ervaren, waarvoor dank.

De mensen van het ALS-onderzoek.

Inge van Beilen, mijn steun en toeverlaat tijdens de lithium trial... Jouw praktische, oplossingsgerichte instelling heb ik altijd als heel prettig ervaren. **Mark Huisman**, bedankt dat je samen met mij patiënten wilde zien voor de lithium trial, zonder jou was dit proefschrift aanzienlijk dunner geweest. Dankzij jou en Inge heb ik een onbezorgde tijd gehad rondom de geboorte van Lise, heel erg bedankt daarvoor! **Nienke de Goeijen**, 'de spil van



het ALS-centrum, wat fijn dat patiënten, maar ook dokters en verpleegkundigen op jou kunnen terugvallen met hun vragen.

Alle andere mensen die ondersteunend/faciliterend zijn geweest, **Petra Berk, Hermieneke Vergunst** en voorgangers, heel veel dank!

De onderzoekers in het AMC, **Prof. dr. M. de Visser, dr. A.J. van der Kooi** en **Dorien Standaar** en in het UMC St. Radboud **dr. H.J. Schelhaas, Martha Huvenaars, Lotte Knapen** en **Tim Draak**. Beste Marianne, Anneke en Jurgen, heel veel dank voor jullie bijdragen als lokale hoofdonderzoekers van de lithium trial. Zonder de inspanningen en toewijding van jullie allemaal, waren we nu nog niet klaar geweest...

Maar ook alle andere mensen die op de achtergrond het lithium onderzoek mogelijk gemaakt hebben, zoals in de eerste plaats **Ingeborg van der Tweel** en de leden van de Data Safety and Monitoring Board. Beste Ingeborg, jouw zuivere, statistische blik was onmisbaar op meerdere momenten gedurende het onderzoek, ontzettend bedankt daarvoor. Mijn dank ook voor de ondersteuning door de mensen van de apotheek en het laboratorium, waaronder **Esther Uijtendaal**. Alsook voor de service en persoonlijke aanpak door **Bram Dijker** van Research Online en onze monitor **Jacobien Vermande** vanuit Julius Clinical Research. **Bart van der Worp**, veel dank dat je wederom onafhankelijk arts wilde zijn bij een ALS trial.

Lieve paranimfen, **Elisabeth Cats** en **Liza Cornet**.

Elies je ging mij voor in zwangerschappen en promotie. Bijzonder om zoveel met je te hebben kunnen delen tijdens onze onderzoeks- en opleidingstijd.

Liza, aangezien onze mannen over het algemeen veel te bespreken hebben is het erg prettig dat ook wij de nodige raakvlakken hebben. Bedankt voor je interesse in alles en de leuke gesprekken!

Alle labmaatjes, **Michael, Christiaan, Paul, Hylke, Elies, Ewout, Sanne, Frank, Marka, Lotte, Renske, Max** en **Femke**, bedankt voor de gezellige koffie- en lunchpauzes en alle gesprekken over belangrijke en vooral ook minder belangrijke zaken. Toen ik het lab voor het eerst zag had ik nooit kunnen denken dat het zo'n fijne werkplek is. **Peter Sodaar**, bedankt voor je hulp en ondersteuning bij het verwerken en opslaan van serum en plasma, RNA isolatie en het doen van celkweken. Ik heb veel geleerd, maar helaas is het nooit echt tot een succesvol labexperiment gekomen, aan jou heeft het niet gelegen.

Andere NMZ-onderzoekers, **Nadia, Sonja, Jan, Nora, Mark, Dirk, Perry** en **Meinie**, bedankt voor het verzamelen van patiëntgegevens en natuurlijk dat ik ook bij jullie (op kamer 4) taart mocht komen eten.

Mijn ‘opvolgers’, **Renée Walhout** en **Henk-Jan Westeneng**.

Ik heb het vaker gezegd, ik ben stiekem een beetje jaloers op de hoeveelheid data waarmee jullie van start gaan. Het is een boeiend onderzoeksveld met veel beloften voor de toekomst. Ik heb er alle vertrouwen in dat jullie samen met Martijn een belangrijke bijdrage gaan leveren aan de rol van beeldvorming bij ALS in de toekomst.

Renée, ik vond het heel leuk om je als student te begeleiden met als hoogtepunt onze trip naar Jena! Ik heb het eerder gezegd, je bent ontzettend goed in het stellen van kritische vragen, een heel belangrijke eigenschap om een goed onderzoeker én neuroloog te worden.

Collega onderzoekers/mede-auteurs.

Daniel Polders, bedankt voor al je inspanningen om ons 7T experiment tot een succes te maken!

René Mandl, jouw ‘voorwerk’ was voor een aantal van de studies in dit proefschrift onmisbaar, bedankt daarvoor.

Bea Kuiperij, bedankt voor het uitvoeren van de ELISA's en je geduld bij het schrijven van ons artikel.

Afdeling radiologie UMC-Utrecht.

Jeroen Hendrikse, Anneke Hamersma, Niels Blanken en alle MRI laboranten bedankt voor jullie hulp en de fijne samenwerking. Niels, jouw hulp bij het opstarten van de studie was bijzonder welkom en het scannen op zaterdag was eigenlijk best gezellig.

De 7T groep, in het bijzonder **Fredy Visser** en **Hans Hoogduin**, bedankt voor het meedenken over mogelijke toepassingen van de 7 Tesla MRI bij ALS en alle praktische ondersteuning die ik hierbij heb gekregen.

Colleagues of the **NISALS** network.

Thanks for the inspiring meetings. I am confident that this collaboration will make the MRI scanner a vital part of the ALS diagnostic workup in the future!



Collega a(n)ios in het UMC-Utrecht.

Bedankt voor jullie collegialiteit en gezelligheid! Mede door het uitgebreide sociale programma zijn we een hechte groep waarbij collegialiteit altijd prevaleert boven competitiviteit (behalve bij karaoke natuurlijk). Collega mama's, **Elies, Sanne, Manon, Sefanja**, bijzonder prettig om af en toe met jullie de uitdagingen rondom moederschap/werk/promotie te kunnen bespreken! En niet te vergeten, bedankt dat ik gebruik kon maken van een bijzonder uitgebreide positiemode garderobe. Mooi dat de 'neuro-kledingdoos' een begrip is geworden, 'who's next?'

Alle mensen die me in het verleden enthousiast gemaakt hebben.

Elske Hoitsma, jouw succesvolle promotietraject en de kans hieraan bij te dragen hebben ongetwijfeld een rol gespeeld in de keuzes die ik gemaakt heb.

Maatschap neurologie in Roermond, het eerste jaar dokteren bij jullie was onvergetelijk en achteraf nog specialer dan ik me toen realiseerde.

Lieve **pap** en **mam**, 'zonder een goed fundament kun je niet bouwen'. Dank voor alles wat jullie mij hebben gegeven en nog steeds geven, waarvan onvoorwaardelijke liefde en een veilige thuishaven de allerbelangrijkste zijn. **Stan**, broer, door jou ben ik vast zo'n doorbijter geworden, 'bloed, zweet en tranen...' volgende keer ga ik mee naar Ajax!

Lieve **Tjeu, Marlies, Harm** en **Jos Rietjens**, ook bij jullie ben ik thuis en dat vind ik heel bijzonder.

Mijn sociale netwerk.

Ondanks dit proefschrift is mijn sociale netwerk toch nog te uitgebreid om hier iedereen afzonderlijk te bedanken. De mensen in dit netwerk vormen een belangrijke bron van inspiratie. Sommigen zie ik maar enkele malen per jaar, maar desondanks krijg ik veel positieve energie van deze ontmoetingen! Een paar mensen wil ik nog even in het bijzonder noemen.

Lieve **Tamara, Anke** en **Ilse**, vriendinnetjes van het eerste uur, bedankt voor jullie interesse en begrip. Dankzij het steevast en tijdig plannen van leuke dingen heb ik, vaker dan met sommige anderen, alles even 'de boel, de boel gelaten' om er met jullie op uit te gaan. Het was het steeds waard!

Inger, jouw kritische vragen houden me vaak nog lang bezig. Bedankt voor de bijzondere vriendschap die ik met je heb.

Martijn en Marjolein, Tristan en Maartje dank voor jullie gezelligheid met pannenkoeken/frietjes-avonden. Onze groeiende gezinnen vormen samen een gezellige bende!

Lieve **Lise** en **Hanna**, meisjes van me, jullie komst en het promoveren zullen in mijn herinnering verbonden blijven. Gelukkig heeft een mens de eerste bewuste herinneringen vanaf ongeveer driejarige leeftijd, wat mij in de gelegenheid stelt een ander beeld in te prenten dan ‘mama achter de computer’.

Tijs, lief, wat te zeggen, je bent en blijft mijn roze bril!

Kus.



Dankwoord

About the author



CURRICULUM VITAE

Esther Verstraete werd geboren op 19 juni 1981 te Gent (België). In 1999 behaalde zij haar VWO-diploma aan Stedelijke scholengemeenschap 'De Rede' te Terneuzen (*cum laude*). Aansluitend begon zij met de studie geneeskunde aan de Universiteit Maastricht. Vanaf 2001 werkte zij als student-assistent op de afdeling Klinische Neurofysiologie van het Maastrichts Universitair Medisch Centrum, destijds onder leiding van prof. dr. F. Spaans, waar haar interesse voor de neurologie werd gewekt. Vanuit deze functie was zij verbonden aan het promotieonderzoek van Elske Hoitsma naar dunne vezelneuropathie bij sarcoïdose wat heeft geresulteerd in mede-auteurschap bij twee wetenschappelijke publicaties. Voor een keuzestage kindergeneeskunde is zij in 2002 naar Blantyre, Malawi gegaan en in 2005 sloot zij haar opleiding af met een co-schap KNO op Aruba. Na het verkrijgen van de artsenbul heeft zij ervaring opgedaan als arts (niet in opleiding tot specialist) op de afdeling neurologie van het Laurentius ziekenhuis te Roermond. In 2006 werd zij aangenomen voor de opleiding neurologie in het Universitair Medisch Centrum Utrecht (opleiders: prof. dr. J. van Gijn en prof. dr. J.H.J. Wokke). In 2008 begon zij aan haar promotieonderzoek onder leiding van prof. dr. L.H. van den Berg waar dit proefschrift uit voortgekomen is. Van 2007 tot 2010 is zij bestuurslid geweest bij De Jonge Orde, de belangenvereniging voor artsen (niet in opleiding tot specialist en was zij initiatiefneemster van de landelijke Opleidingsprijs. Eind 2011 is zij voorgedragen om zitting te nemen in de projectgroep Medisch Specialist 2015 waaruit in 2012 een visiedocument is voortgekomen over de toekomst van de medisch specialistische zorg in Nederland. Naar verwachting zal zij in 2016 de opleiding tot neuroloog afronden. Esther is getrouwd met Tijs en zij hebben samen twee dochters.

LIST OF PUBLICATIONS

1. Verstraete E*, Kuiperij HB*, van Blitterswijk MM, Veldink JH, Schelhaas HJ, van den Berg LH#, Verbeek MM#. (2012) TDP-43 plasma levels are higher in amyotrophic lateral sclerosis. *Amyotroph Lateral Scler.* 13:446-51.
2. Turner MR, Agosta F, Bede P, Govind V, Lule D, Verstraete E. (2012) Neuroimaging in amyotrophic lateral sclerosis. *Biomark Med.* 6:319-37.
3. Verstraete E, Veldink JH, Huisman MH, Draak T, Uijtendaal EV, van der Kooi AJ, Schelhaas HJ, de Visser M, van der Tweel I, van den Berg LH. (2012) Lithium lacks effect on survival in amyotrophic lateral sclerosis: a phase IIb randomised sequential trial. *J. Neurol. Neurosurg. Psychiatry.* 83:557-64.
4. Verstraete E, Veldink JH, Hendrikse J, Schelhaas HJ, van den Heuvel MP*, van den Berg LH*. (2012) Structural MRI reveals cortical thinning in amyotrophic lateral sclerosis. *J. Neurol. Neurosurg. Psychiatry.* 83:383-8.
5. Verstraete E, Veldink JH, Mandl RC, van den Berg LH*, van den Heuvel MP*. (2011) Impaired structural motor connectome in amyotrophic lateral sclerosis. *PLoS One* 6:e24239.
6. Verstraete E*, van den Heuvel MP*, Veldink JH, Blanken N, Mandl RC, Hulshoff Pol HE, van den Berg LH. (2010) Motor network degeneration in amyotrophic lateral sclerosis: a structural and functional connectivity study. *PLoS One* 5:e13664.
7. Verstraete E, Veldink JH, van den Berg LH. (2010) Would riluzole be efficacious in the new ALS trial design? *Lancet Neurol.* 9:949,50; author reply 950-1.
8. Verstraete E, Biessels GJ, van den Heuvel MP, Visser F, Luijten PR, van den Berg LH. (2010) No evidence of microbleeds in ALS patients at 7 Tesla MRI. *Amyotroph Lateral Scler.* 11:555-7.
9. Verstraete E, van Domburg P, Twijnstra A. (2007) Leptomeningeale metastasen als eerste uiting van een maligniteit. *Tijdschrift voor Neurologie en Neurochirurgie* 4:181-7
10. Hoitsma E, Drent M, Verstraete E, Faber CG, Troost J, Spaans F, Reulen JP. (2003) Abnormal warm and cold sensation thresholds suggestive of small-fibre neuropathy in sarcoidosis. *Clin. Neurophysiol.* 114:2326-33.



List of publications

11. Reulen JP, Lansbergen MD, Verstraete E, Spaans F. (2003) Comparison of thermal threshold tests to assess small nerve fiber function: limits vs. levels. *Clin. Neurophysiol.* 114:556-63.

Submitted/in preparation

1. Polders D*, Verstraete E*, Mandl RCW, van den Heuvel MP, Veldink JH, Lijten P, van den Berg LH, Hoogduin J. Multimodal tract-based analysis in ALS patients at 7T.
2. Verstraete E, Veldink JH, van den Berg LH#, van den Heuvel MP#. Structural brain network imaging shows progressive disconnection of the motor system in ALS.
3. Walhout R*, Verstraete E*, van den Heuvel MP, Veldink JH, van den Berg LH. Symptom development in patients with motor neuron disease.

*# These authors contributed equally to the manuscript

Just imagine...

2030

'Every newborn is genetically screened for the risk of developing a number of diseases during lifetime, including ALS. This screening program has followed the heel prick and is based on the same principles. About 2.5% of the population turns out to be at risk for ALS, but only about 10% of this subpopulation will actually develop clinical symptoms and it is not known at what age the disease will manifest. Fortunately, there is an effective and non-invasive screening method available, advanced MRI-imaging of the brain, to evaluate the cortical surface in order to detect (focal) abnormalities (chapter 7). People at risk are screened starting at 18 years of age. If a focal, cortical abnormality or disease focus is found, this is usually an asymptomatic focus which is too small to cause symptoms, but which has the potential to spread throughout the brain and lead to progressive neurodegeneration. Which clinical phenotype will develop, bulbar or spinal onset, depends on the location of the disease focus. The organisation or architecture of the individual brain network has a role in the spread of disease e.g. the connectedness of a brain region will largely determine which brain region(s) will be involved next (chapters 5 and 6) and how fast other regions will become affected (chapter 4). However, before the disease develops and spreads further, the disease focus is irradiated, thereby impeding the development of clinical symptoms.

The ability to screen for ALS at an early stage – as, for example, is common for many years in breast cancer – and subsequently give focal treatment, has led to a significantly reduced mortality rate due to ALS. In addition, for the patients who still develop ALS, either because they were not at risk and therefore not included in the screening programme, or because they presented with a disseminated disease, survival has improved due to new disease-modifying drugs (e.g. by slowing disease spread). New potential treatments are effectively tested in worldwide trials facilitated by online data acquisition and using the sequential trial design (chapters 11 and 12).'

We are still far from the scenario as described above and the actual future will always be different from what we imagine it to be. However, a (dream) scenario like this greatly motivated us in performing the studies we did. Time will tell if any of our findings turn out to be of relevance for patients with ALS in the future. But just imagine...